

**LITHOSTRATIGRAPHIC ANALYSIS AND PALAEOENVIRONMENTAL
INTERPRETATION OF THE LATE TERTIARY AND QUATERNARY SED-
IMENTS OF THE NAKURU, ELMENTAITA AND NAIVASHA BASINS."**

By

Benson Gingo O. Mboya.

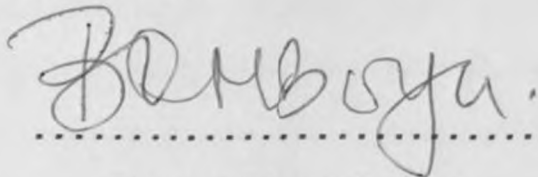
**A thesis submitted for the degree of Doctor of Philosophy
(Geology) in the University of Nairobi.**

December, 1993.

Nairobi.

DECLARATION

This thesis is my original work and has not been presented for a degree in any other other University.

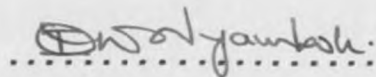
.....

Benson Gingo O. Mboya

Department of Geology

University of Nairobi.

This thesis has been submitted for examination with my knowledge as the University supervisor.

.....

Professor Isaac O. Nyambok

Professor of Geology

University of Nairobi

ABSTRACT

The objective of this study is to provide a better understanding and appreciation of the importance of the life cycle and business life cycle. This research was carried out in the form of a descriptive study. The study involved both field and laboratory work. In the field, data were collected through observation, interviews, and questionnaires. In the laboratory, data were collected through experiments and analysis. The results of the study show that the life cycle and business life cycle are closely related and have a significant impact on the success of a business. The study also found that the life cycle and business life cycle can be used as a tool for strategic planning and decision-making. The study concludes that the life cycle and business life cycle are essential for the success of a business and should be given more attention by researchers and practitioners.

**This thesis is dedicated to my beloved wife Eunice, daughter
Judy, sons Kelvin and Bryan and sister Risanael.**

ABSTRACT

The objective of this thesis is to provide a better understanding and correlation of the lacustrine palaeoenvironments of the late Tertiary and Quaternary rift sediments within the basins of Lakes Nakuru, Elmentaita and Naivasha. The study involved both field and laboratory investigations. In the field, detailed geological mapping, description, stratigraphic measurements and interpretation of rock outcrops were undertaken. Collected samples were subsequently subjected to petrographic and geochemical laboratory analyses. Both the field data and laboratory results were further subjected to computer analysis and results presented as maps, stratigraphic sections, tables, graphics, triangular plots and correlation fence diagrams. A survey of the strata within these basins yielded localised composite fluviatile deposits of mainly alluvio-lacustrine stratified tuffs and relatively thin diatomaceous beds. Over 50m thick diatomaceous lacustrine deposits at Kariandusi diatomite mine formed in an extensive lake on the rift floor and is an obvious evidence of an extensive old lake formation on the rift floor. The lake beds formed thick tabular sediments on unstable faulted rift floor and were later incised by rivers which are then infilled by high energy polymictic volcanoclastics fluviatile conglomerates. The erosional contact separating the fluviatile and lacustrine lithofacies provide useful marker for intra-basinal correlations. Stratigraphic sections of thick diatomaceous beds at Soysambu mine document another extensive

(i)

shallow palaeo-lake on the contemporary divide plain between the basins of Lakes Nakuru and Naivasha.

The stratigraphic data, sedimentology and lithofacies established correlative lithological sequences within the sedimentary basins in the area. The results convincingly indicate significant differences between basins and largely support the occurrence of distinct but possibly contemporaneously evolved depositional environments. Lithofacies were uniquely diagnostic of specific depositional environments, and often reflected the physical sedimentation processes. The findings hence highlight descriptive framework of the sub-environments, their sedimentology, lithofacies evolution and variations within the basins. Over 95 percent of the sedimentary infill of the basins are mainly volcanoclastic detritals of alluvial and fluvial origin which were formed in fault-controlled traps associated with the Plio-Pleistocene evolution of the rift floor. Less than 5 percent of the clastics constitute lacustrine deposits.

Despite the thick recent alluvium cover, numerous Pleistocene grid faulting and discontinuous sediment outcrops, the geochemical results indicate the existence of several isolated and distinct depositional lakes and non-lacustrine environments. These results further confirm that statistical data manipulation may be useful in the understanding of the relatively scattered lake sedimentations within the Kenya rift valley.

ACKNOWLEDGEMENTS

The accomplishment of a project of this nature calls for the cooperation and goodwill of many people, all to whom I owe sincere appreciation. I particularly thank my supervisor Professor Isaac O. Nyambok for his constructive discussions, reviews and guidance in the preparation of the thesis.

Discussions with Dr. Mario Fay formerly of University of Dar es Salaam were useful and encouraging. I also thank the Department of Geology for supporting this research. The Mines and Geology Department allowed me free access and use of their sedimentology laboratory and I gratefully acknowledge the generous assistance. I also thank Mr. Muli of the National Museums of Kenya, Gilbert Minya of the British Institute in Eastern Africa, and George Openji of Enduro L.T.D Ceramics and Sanitary Wares for field assistance.

The Deans' Committee, University of Nairobi provided an advance loan for commencing the field reconnaissance. This research was financially supported by D.A.A.D. German Academic Exchange Service grant and the National Council for Science grant and their assistance is gratefully acknowledged.

CONTENTS

	Page
ABSTRACT	(i)
ACKNOWLEDGEMENTS	(iii)
LIST OF FIGURES	(vii)
LIST OF PLATES	(xiii)
LIST OF TABLES	(xv)
CHAPTER 1 - INTRODUCTION	1
1.1 Introduction	1
1.2 Location and drainage network of the basins	2
1.3 Scope and objectives of the study	7
1.4 Previous geological work	8
1.5 Methods of investigation	11
1.5.1 Basis of palaeoenvironmental interpretation	11
1.5.2 Field techniques	13
1.5.3 Laboratory analysis	15
1.5.3.1 Petrographic investigation	15
1.5.3.2 Geochemical investigation	17
CHAPTER 2 - GEOLOGY AND TECTONIC EVOLUTION.	21
2.1 Origin and evolution of the basins	21
2.1.1 Faulted landforms	26
2.1.2 Tectonic grabens	35
2.2 Pliocene-lower Pleistocene geology	36
2.3 Middle Pleistocene and Recent volcanics	41

2.4	Pleistocene - Holocene sedimentary formations	43
2.4.1	Kariandusi and Soysambu Formations	43
2.4.2	Enderit and Ronda Formations	57
CHAPTER 3 - MEASURED STRATIGRAPHIC SECTIONS		61
3.1	Measured stratigraphic sections.	61
3.2	Use of measured stratigraphic sections	63
3.3	Notes on lithological symbols for the sections	64
3.4	Sequence of the measured sections	68
3.4.1	Kariandusi Formation	68
3.4.2	Soysambu Formation	76
3.4.3	Enderit Formation	82
3.4.3.1	Makalia Beds	96
3.4.4	Ronda Formation	99
CHAPTER 4 - PETROLOGY AND GEOCHEMISTRY OF THE SEDIMENTARY ROCKS.		106
4.1	Petrology of the sedimentary formations	106
4.1.1	Grain-size distribution	111
4.3	Geochemical Data	119
CHAPTER 5 - LITHOSTRATIGRAPHIC FORMATIONS.		142
5.1	Lithofacies Associations	142
5.2	Kariandusi Formation	144
5.2.1	Lacustrine facies	144

5.2.2	Deltaic - littoral facies	147
5.2.3	Fluvial facies	150
5.3	Enderit Formation	151
5.3.1	Lacustrine facies	154
5.3.2	Lake margin facies	157
5.3.3	Alluvial fan facies	159
5.3.4	Eolian facies	160
5.3.5	Fluvial facies	162
5.4	Ronda Formation	163
5.4.1	Deltaic - littoral facies	163
5.4.2	Fluvial - lacustrine facies	164
5.5	Soysambu Formation	167
5.5.1	Lacustrine facies	167
5.5.2	Deltaic - littoral facies	170
CHAPTER 6 - ENVIRONMENTS AND SEDIMENTARY PROCESSES		173
6.1	Depositional Environments	173
6.1.1	Piedmont environment	173
6.1.2	Alluvial fan environment	175
6.1.3	Fluvial environment	178
6.1.4	Alluvial plain environment	180
6.1.5	Lacustrine environment	182
6.1.6	Palaeontology and archaeological evidence	185
6.1.7	Provenance of clastic deposits	186

CHAPTER 7 -CORRELATION	191
7.1 Chronostratigraphic correlation	191
7.2 Lithostratigraphic correlation of measured sections	193
7.2.1 Enderit Formation	195
7.2.1.1 Makalia Beds	207
7.2.2 Ronda Formation	207
7.2.3 Soysambu Formation	215
7.2.4 Kariandusi Formation	219
7.3 Geochemical correlation	226
7.3.1 Sediment chemistry variation trends	227
7.3.2 Discriminant factor correlation	247
CHAPTER 8 - SUMMARY AND CONCLUSIONS	265
8.1 Lithostratigraphic correlations	265
8.2 Major element variation trends	267
8.2.1 Q-mode analyses	268
8.3 Depositional Systems	269
8.4 Conclusions	273
REFERENCES	275

LIST OF FIGURES

Fig. 1.1	Location of the study area	3
Fig. 1-2	Drainage network of Lakes Nakuru, Elmenteita and Naivasha Basins	4
Fig. 2-1	Location of the E-W transects across the basins	27
Fig. 2-2	Geological cross section showing types of sedimentary basins in the area south of Gilgil-Elmenteita	28
Fig. 2-3	West-East sections (a) north of Nakuru Town (b) a cross Lake Nakuru	28
Fig. 2-4	Geological cross sections a cross Lake Nakuru	29
Fig. 2-5	West-East sections a cross (a) Lake Nakuru (b) Lake Elmenteita and Kariandusi	30
Fig. 2-6	West-East sections (a) a cross Lake Elmenteita (b) south of Lake Elmenteita	32
Fig. 2-7	West-East cross sections to the south of Lake Elmenteita	33
Fig. 2-8	Geology of the Pleistocene-Holocene sediments and volcanics of the Nakuru, Elmenteita and Naivasha graben	37
Fig. 2-9	Schematic diagram showing stratigraphy of the Pleistocene sediments of the Nakuru, Elmenteita and Naivasha graben	38
Fig. 3-1	Geological symbols for the measured lithostratigraphic sections	65
Fig. 3-2	Field locations of measured lithostratigraphic sections	66
Fig. 3-3	Data point linkages for the correlated lithostratigraphic sections	67
Fig. 3-4	Lithostratigraphic section of the Kariandusi Formation at the diatomite mine	69

Fig. 3-5	Measured lithostratigraphic sections on the east face of the Kariandusi Diatomite Mine	70
Fig. 3-6	Lithostratigraphic sections, north-east of Kariandusi Mine extending to the Prehistoric site	71
Fig. 3-7	Lithostratigraphic sections, south of Karaindusi Diatomite mine	72
Fig. 3-8	Lithostratigraphic sections north-west of the Kariandusi Mine	73
Fig. 3-9	Lithostratigraphic section on the Nakuru-Naivasha road cut.	74
Fig. 3-10	Lithostratigraphic sections of the Soysambu Diatomite Mine	77
Fig. 3-11	Lithostratigraphic sections along a west-east transect from the edge of Lake Nakuru basin to the Soysambu Mine	78
Fig. 3-12	Lithostratigraphic sections along west-east transect of the Soysambu Mine	79
Fig. 3-13	Lithostratigraphic sections along River Enderit on the south of the Drift	84
Fig. 3-14	Lithostratigraphic sections along River Enderit	85
Fig. 3-15	Lithostratigraphic sections, Enderit River Drift	86
Fig. 3-16	Lithostratigraphic sections, along River Enderit	87
Fig. 3-17	Lithostratigraphic sections, River Enderit	88
Fig. 3-18	Lithostratigraphic sections Enderit River Drift	89
Fig. 3-19	Lithostratigraphic sections north of Enderit Drift	90
Fig. 3-20	Lithostratigraphic sections, along River Enderit north of the Drift	91

Fig. 3-21	Lithostratigraphic sections, Enderit Drift	92
Fig. 3-22	Lithostratigraphic sections west of the River Makalia Valley	97
Fig. 3-23	Lithostratigraphic sections along the eastern bank of River Makalia	98
Fig. 3-24	Lithostratigraphic sections, north eastern edge Lake Nakuru park	100
Fig. 3-25	Lithostratigraphic sections in the Ronda sand quarry	101
Fig. 3-26	Lithostratigraphic sections, eastern face of Ronda sand quarry	102
Fig. 3-27	Lithostratigraphic sections, along River Njoro	103
Fig. 4-1	TiO ₂ -K ₂ O-Al ₂ O ₃ ternary plots of the (i) Soysambu and (ii) Enderit Formations	128
Fig. 4-1A	TiO ₂ -K ₂ O-Al ₂ O ₃ ternary plots of the (i) Kariandusi Formation and (ii) Makalia Beds	129
Fig. 4-1B	TiO ₂ -K ₂ O-Al ₂ O ₃ ternary plot of the Ronda Formation	130
Fig. 4-2A	MgO-Al ₂ O ₃ -CaO ternary plot of the (i) Makalia Beds and (ii) Enderit Formation	131
Fig. 4-2B	MgO-Al ₂ O ₃ -CaO ternary plot of the (i) Ronda Formation and (ii) Soysambu Formation	132
Fig. 4-2C	MgO-Al ₂ O ₃ -CaO ternary plot of the Kariandusi Formation	133
Fig. 4-3A	K ₂ O-Mg + Fe - Al ₂ O ₃ ternary plot of the (i) Soysambu Formation and (ii) Enderit Formation	134
Fig. 4-3B	K ₂ O-Mg + Fe - Al ₂ O ₃ ternary plot of the (i) Kariandusi Formation and (ii) Makalia Beds	135
Fig. 4-3C	K ₂ O-Mg + Fe - Al ₂ O ₃ ternary plot of the Ronda Formation	136
Fig. 4-4A	SiO ₂ -Al ₂ O ₃ -Na + K ternary plot of the (i) Makalia Beds and (ii) Kariandusi Formation	137

Fig. 4-4B	SiO ₂ -Al ₂ O ₃ - Na + K ternary plot of the (i) Ronda Formation and (ii) Enderit Formation	138
Fig. 4-5A	Al ₂ O ₃ -MgO-Fe ₂ O ₃ ternary plot of the (i) Ronda Formation and (ii) Kariandusi Formation	139
Fig. 4-5B	Al ₂ O ₃ -MgO-Fe ₂ O ₃ ternary plot of the (i) Soysambu Formation and (ii) Enderit Formation	140
Fig. 5-1	Correlated stratigraphic sections and lithologic facies at Karindusi Mine extending to the prehistoric site	145
Fig. 5-2A	Correlated stratigraphic sections and lithologic facies south-north along River Enderit	152
Fig. 5-2B	Correlated stratigraphic sections and lithologic facies in East-West transect of River Enderit	153
Fig. 5-3	Correlated stratigraphic sections and lithologic facies in the Nakuru National Park, Ronda sand quarry and Lamuriak River valley	168
Fig. 5-4	Correlated stratigraphic sections and lithologic facies at the Soysambu Diatomite Mine, extended westward to the eastern edge of Lake Nakuru	169
Fig. 7-3-BO	Correlated lithostratigraphic sections, River Enderit	196
Fig. 7-3-1A	Correlated lithostratigraphic sections along River Enderit	197
Fig. 7-3-1B	Correlated lithostratigraphic sections along River Enderit	198
Fig. 7-3-1C	Correlated lithostratigraphic section, Enderit River Drift	199
Fig. 7-3-1D	Correlated lithostratigraphic sections, north of Enderit Drift	200
Fig. 7-3-S1	Correlated lithostratigraphic section, west Enderit Drift	201
Fig. 7-1C4	Correlated lithostratigraphic section, Enderit River	202

Fig. 7-1B2	Correlated lithostratigraphic section, Enderit River	203
Fig. 7-NK-1A	Correlated lithostratigraphic sections, north of Enderit River	204
Fig. 7-3-2	Correlated lithostratigraphic section along River Makalia	206
Fig. 7-3-3A	Correlated lithostratigraphic sections eastern face of Ronda sand quarry	208
Fig. 7-3-3B	Correlated lithostratigraphic sections along River Njoro	209
Fig. 7-3-3C	Correlated lithostratigraphic sections, along River Njoro	210
Fig. 7-3-C	Correlated lithostratigraphic sections along River Njoro	211
Fig. 7-3-3D	Correlated lithostratigraphic sections, north-eastern edge of Lake Nakuru game park	212
Fig. 7-3-D	Correlated lithostratigraphic sections on River Lamuriak	213
Fig. 7-3-4	Correlated lithostratigraphic sections at the Soysambu Diatomite mine	216
Fig. 7-3-4A	Lithostratigraphic sections west of the Soysambu Diatomite Mine	217
Fig. 7-3-4B	Lithostratigraphic sections on the western bounding edge of the Soysambu Basin	218
Fig. 7-3-5A	Correlated lithostratigraphic sections south of the Kariandusi	220
Fig. 7-3-5B	Correlated lithostratigraphic sections north of Kariandusi Diatomite Mine	221
Fig. 7-3-5C	Correlated lithostratigraphic sections northwest of Kariandusi Diatomite Mine	222
Fig. 7-3-5D	Correlated lithostratigraphic sections north-east Karaindusi Mine extending to the Prehistoric Site	223

Fig. 7-8C	Bivariate discriminant diagrams of Enderit vs Makalia deposits	252
Fig. 7-9B	Bivariate discriminant plots of Enderit vs Ronda	
Fig. 7-1A	K ₂ O and Al ₂ O ₃ variation in sediments from (i) Soysambu and (ii) Kariandusi	230
Fig. 7-1B	K ₂ O and Al ₂ O ₃ variation in sediments from (i) Enderit and (ii) Makalia	231
Fig. 7-1C	K ₂ O and Al ₂ O ₃ variation in sediments from Ronda	232
Fig. 7-2A	Al ₂ O ₃ and SiO ₂ variation of sediments from (i) Kariandusi and (ii) Soysambu	233
Fig. 7-2B	Al ₂ O ₃ and SiO ₂ variation of sediments from (i) Enderit and (ii) Makalia	234
Fig. 7-3A	Fe ₂ O ₃ and Al ₂ O ₃ variation of sediments from (i) Soysambu and (ii) Kariandusi	236
Fig. 7-3B	Fe ₂ O ₃ and Al ₂ O ₃ variation of sediments from (i) Makalia and (ii) Enderit	237
Fig. 7-3C	Fe ₂ O ₃ and Al ₂ O ₃ variation in sediments from Ronda	238
Fig. 7-4A	Na ₂ O and SiO ₂ variation of sediments from Ronda	239
Fig. 7-4B	Na ₂ O and SiO ₂ variation of sediments from Ronda	240
Fig. 7-5A	Na ₂ O and K ₂ O variation in sediment from (i) Soysambu and (ii) Kariandusi	242
Fig. 7-5B	Na ₂ O and K ₂ O variation of sediments from (i) Enderit and (ii) Makalia	243
Fig. 7-6A	MgO and Al ₂ O ₃ variation of sediments from (i) Makalia and (ii) Enderit	244
Fig. 7-6B	MgO and Al ₂ O ₃ variation of sediments from (i) Kariandusi and (ii) Soysambu	245
Fig. 7-6C	MgO and Al ₂ O ₃ variation of sediments from Ronda	246
Fig. 7-8A	Bivariate discriminant scores plot of Enderit (O) vs Kariandusi Formations (+)	251
Fig. 7-8B	Bivariate discriminant diagrams of Enderit vs Kariandusi Formations	252

Fig. 7-8C	Bivariate discriminant diagrams of Enderit vs Makalia deposits	253
Fig. 7-8D	Bivariate discriminant plots of Enderit vs Ronda Formations	254
Fig. 7-8E	Bivariate diagrams of Makalia vs Kariandusi Formations showing good discrimination of the deposits	255
Fig. 7-8F	Bivariate discriminant diagram of Makalia vs Ronda sediments	258
Fig. 7-8G	Bivariate discriminant diagrams of Makalia Beds vs Soysambu Formation	259
Fig. 7-8H	Bivariate discriminant diagrams of Ronda Formation vs Makalia Beds	260
Fig. 7-8J	Bivariate discriminant diagram of Soysambu vs Ronda Formations	261
Fig. 7-8K	Bivariate discriminant diagrams of Soysambu Formation vs Kariandusi Formation	262
Fig. 7-8L	Bivariate discriminant diagrams of Soysambu vs Enderit Formations	263

LIST OF PLATES

- Plate 1a: Kariandusi Formation**
Sheared fault contact of light coloured lake beds and trachyte on the Nakuru-Naivasha road cut west of the diatomite mine 44
- Plate 1b: Kariandusi Formation**
Neotectonic faulting displaced Pleistocene lake sediments and formed classic normal rift graben on either side of a road cut. Pre-Pleistocene fault down-stepped the trachyte on the foreground 45
- Plate Kariandusi Formation 2a:**
Cross-bedded pebbly cobble conglomerate infilling the diatomite bed and grades upward into clast-size sandstones 46
- Plate 2b: Kariandusi Formation**
Diatomite mined by tunnel and pillar method at Kariandusi 46
- Plate 3a: South end of Elmenteita Basin**
NE-SE Mount Eburru volcanic ridge in the horizon mark the southern extent of the basin. Foreground: the Karterit Hill cone encloses a crescent crater. On the outward face of the cone erosion incised parallel line marks 47
- Plate 3b: Trona deposits of Lake Elmenteita**
View of Lake Elmenteita from south reveal thin layer of trona crusts surrounding the lake water body perimeter. North-south grid faults delimit the western edge of the lake. On the horizon Mau escarpment mark western extent of the basin 47
- Plate 4a: Soysambu Formation**
View from north of the Soysambu open pit diatomite mine. Eburru volcano trends NE-SW on the horizon east-south-west 48
- Plate 4b: Soysambu Formation**
Stained lacustrine beds of the Soysambu Formation with mudcracks exposed on the mine floor 48

Plate 4c: Soysambu Formation
Solution generated cavern structure at the transitional contact of diatomite and tuff 49

Plate 4d: Soysambu Formation
Leached-bedded tuff sequence intercalated with caliche limestone concentration formed along desiccation cracks toward top of the formation 50

Plate 5a: Lamuriak Beds Stratified pyroclastic tuffs and ashes sequence form the lowermost unit of Ronda Formation at the mouth of River Lamuriak gorge 51

Plate 5b: Ronda Formation
View of modern coalesced alluvial fan being deposited outward from active fault scarp in response to active tectonic subsidence 52

Plate 5c: Ronda Formation
A high angle cross stratified lenticular fluvio-deltaic Ronda Formation. Repeated light coloured silts alternate with coarse pumicious tuffs at the sand quarry 52

Plate 6a: Enderit Formation
Massive fluvio-fanglomerate with deltaic-lacustrine silt intercalation at base and top of the formation at Enderit drift 53

Plate 6b: Enderit Formation
Close-up view of the fanglomerate reveal large tuffaceous clast inclusions and sharp contact at the base with laminated lacustrine beds 40

Plate 6c: Enderit Formation
Close-up view of (i) large tuffaceous clast fanglomerate overlies (ii) fine laminated silts exposed in trench transect at Enderit River drift 54

Plate 7: Makalia Beds
Laminated Makalia member of Enderit Formation 55

LIST OF TABLES

Table 2-1	Schematic sequence of Quaternary sedimentary formations in the Nakuru and Elmenteita Basins	59
Table 4A	Calculated values for mean, sorting, kurtosis, skewness measured on Phi scale	113
Table 4B	Calculated values for mean, sorting, kurtosis, skewness measured on Phi scale	114
Table 4C	Calculated values for mean, sorting, kurtosis, skewness measured on Phi scale	115
Table 4-1A	Major oxide composition of Kariandusi sediments	120
Table 4-1B	Major oxide composition of Kariandusi sediments	121
Table 4-2	Major oxide composition of Soysambu sediments	122
Table 4-3	Major oxide composition of Enderit sediments	123
Table 4-4	Major oxide composition of Ronda sediments	124
Table 4-5	Major oxide composition of Makalia sediments	125
Table 6	Discriminant factor analysis (F-test)	249

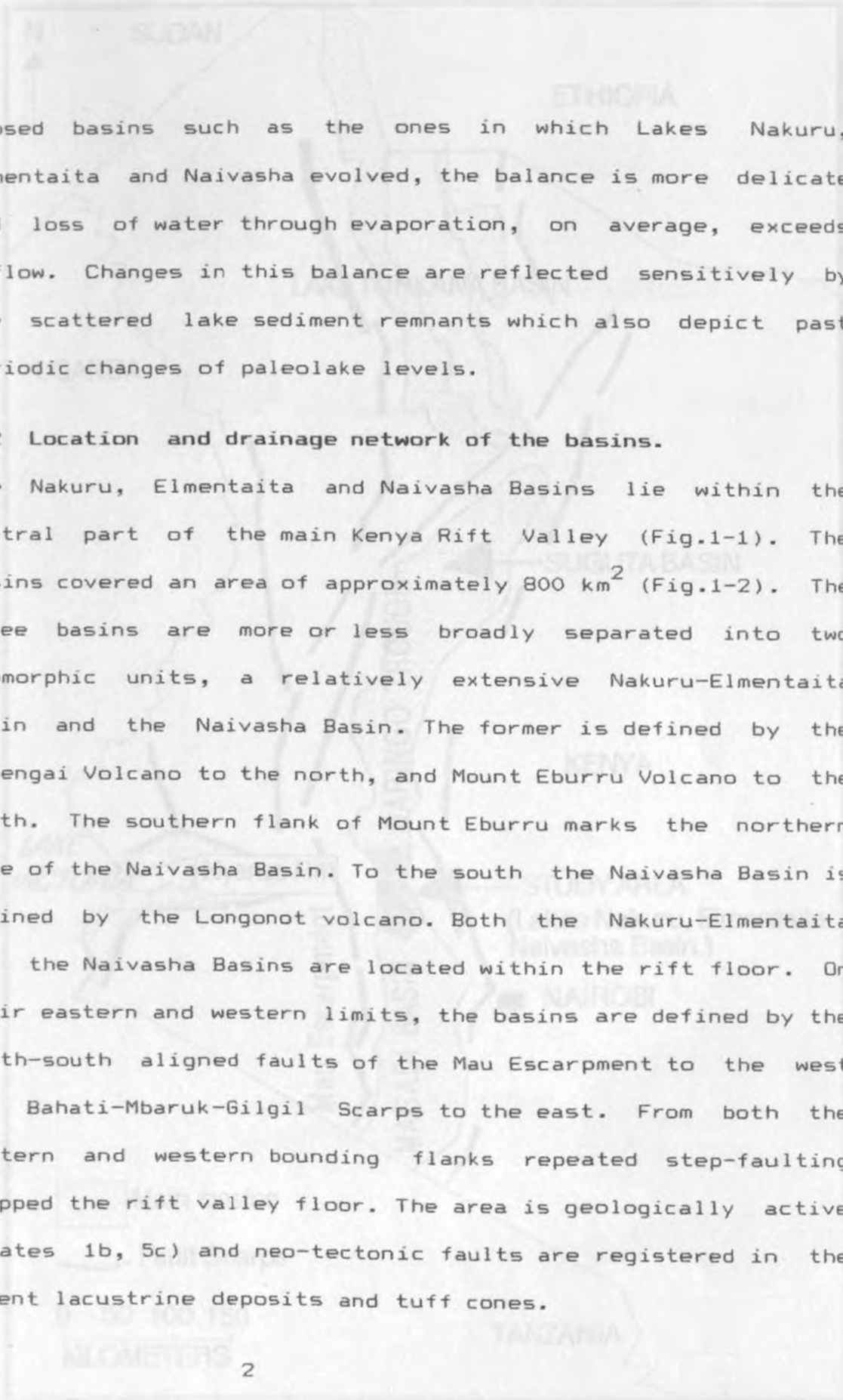
CHAPTER 1

INTRODUCTION

1.1 Introduction

Lake deposits contain detailed record of local climatic, hydrologic, sedimentologic, tectonic, geochemical and biochemical conditions which provides an invaluable guide to the understanding of the continental environments and their evolution in geological times. Apart from interest based on economic factors related to the associated diatomites, brines and evaporites, Kenya rift lake sediments have not attracted detailed sedimentological studies although they are obvious natural archives for processes in non-marine environments. They provide potential field laboratories where geologists may be able to define the nature of the lake formational processes, their evolution through time and their link with the deposits.

Local tectonic and associated volcanicity have important consequences for lacustrine sedimentation within the Kenya Rift Valley at any particular geological time. Lakes with permanent outlets, would normally have stable shorelines hence inflow plus precipitation on the lake surface is balanced by evaporation plus outflow. Commonly sediment formations in such lakes are dominated by river-born clastics whereas in situation where basins are protected from such input, chemical and biochemical sediments may become dominant. In hydrological



closed basins such as the ones in which Lakes Nakuru, Elmentaita and Naivasha evolved, the balance is more delicate and loss of water through evaporation, on average, exceeds inflow. Changes in this balance are reflected sensitively by the scattered lake sediment remnants which also depict past periodic changes of paleolake levels.

1.2 Location and drainage network of the basins.

The Nakuru, Elmentaita and Naivasha Basins lie within the central part of the main Kenya Rift Valley (Fig.1-1). The basins covered an area of approximately 800 km² (Fig.1-2). The three basins are more or less broadly separated into two geomorphic units, a relatively extensive Nakuru-Elmentaita Basin and the Naivasha Basin. The former is defined by the Menengai Volcano to the north, and Mount Eburru Volcano to the south. The southern flank of Mount Eburru marks the northern edge of the Naivasha Basin. To the south the Naivasha Basin is defined by the Longonot volcano. Both the Nakuru-Elmentaita and the Naivasha Basins are located within the rift floor. On their eastern and western limits, the basins are defined by the north-south aligned faults of the Mau Escarpment to the west and Bahati-Mbaruk-Gilgil Scarps to the east. From both the eastern and western bounding flanks repeated step-faulting dropped the rift valley floor. The area is geologically active (Plates 1b, 5c) and neo-tectonic faults are registered in the recent lacustrine deposits and tuff cones.

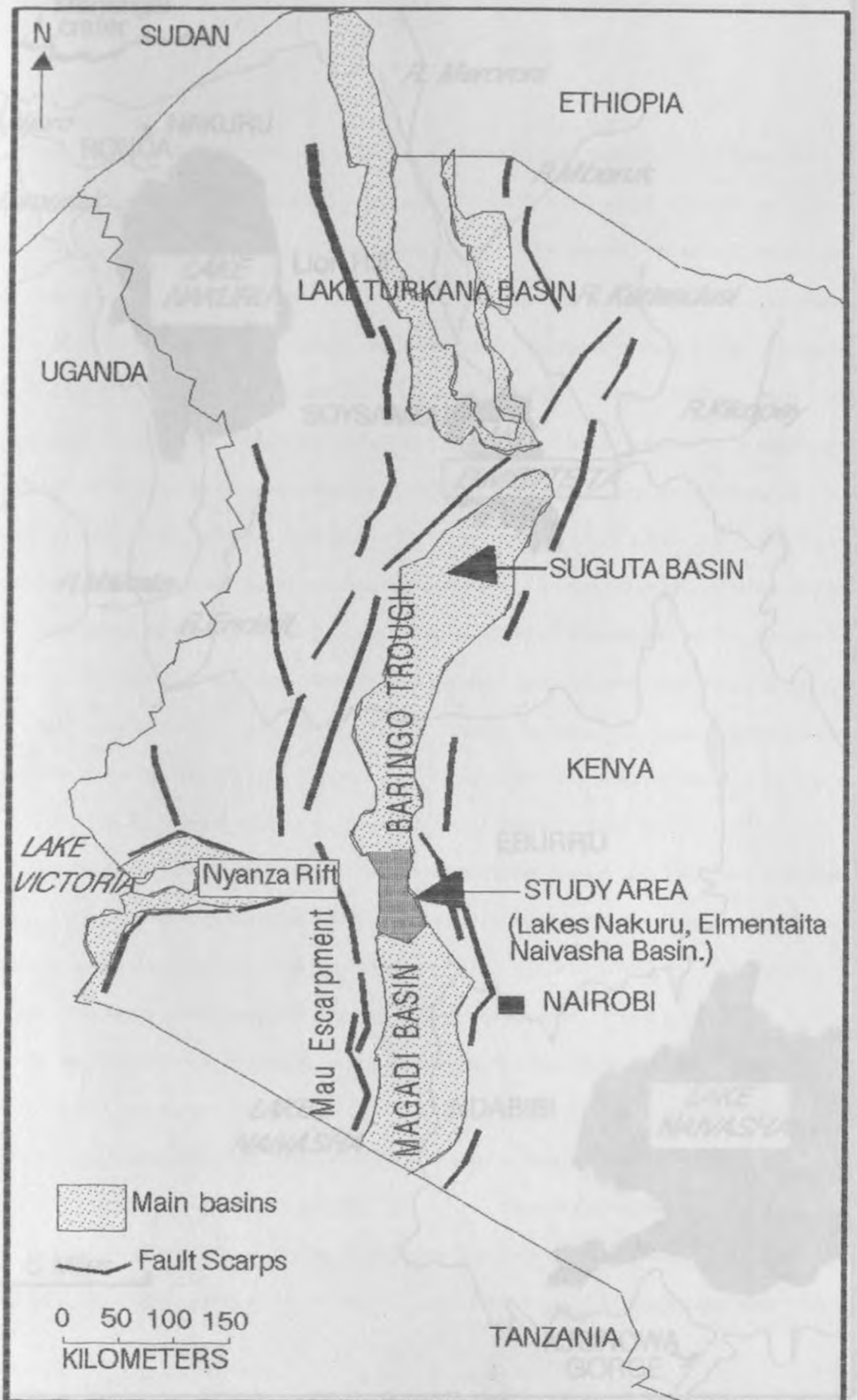


FIG. 1 - 1 Location of the study area

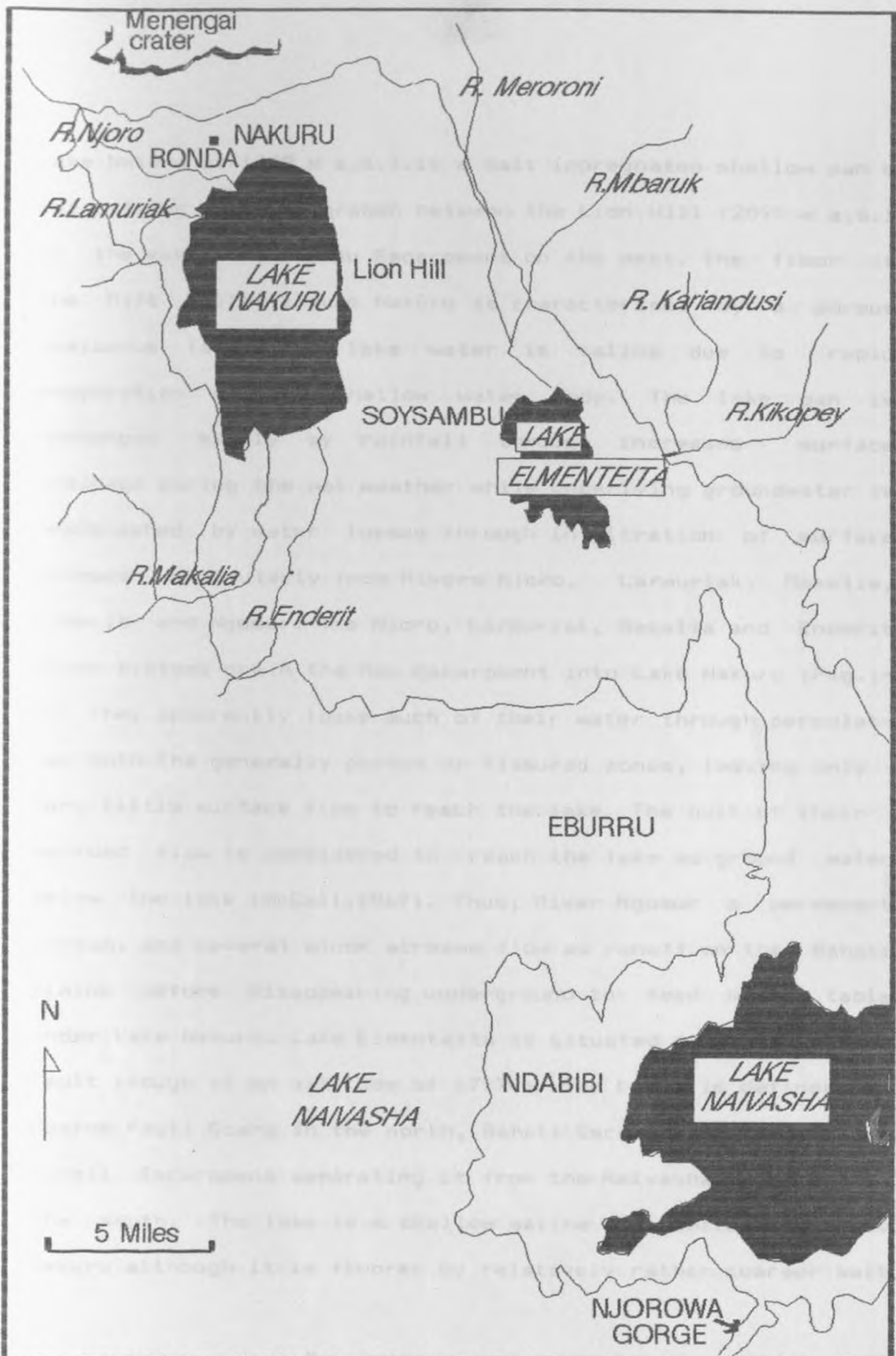


FIG. 1 - 2 Drainage network of Lakes Nakuru Elmenteita and Naivasha Basins

Lake Nakuru at 1758 m a.s.l. is a salt impregnated shallow pan of water lying in fault graben between the Lion Hill (2097 m a.s.l. in the east and the Mau Escarpment on the west. The floor of the Rift Valley around Nakuru is characterised by a porous pumiceous lava. The lake water is saline due to rapid evaporation of the shallow water body. The lake pan is recharged mainly by rainfall through increased surface drainage during the wet weather while underlying groundwater is replenished by water losses through infiltration of surface streams particularly from Rivers Njoro, Larmuriak, Makalia, Enderit and Ngosur. The Njoro, Larmuriak, Makalia and Enderit river systems drain the Mau Escarpment into Lake Nakuru (Fig.1-2). They apparently lose much of their water through percolation into the generally porous or fissured zones, leaving only very little surface flow to reach the lake. The bulk of their accrued flow is considered to reach the lake as ground water below the lake (McCall, 1967). Thus, River Ngosur a permanent stream, and several minor streams flow as runoff on the Bahati plains before disappearing underground to feed water table under Lake Nakuru. Lake Elmentaita is situated within a complex fault trough at an altitude of 1777 m. The basin is defined by Mbaruk Fault Scarp in the north, Bahati Escarpment and the low Gilgil Escarpment separating it from the Naivasha basin into the south. The lake is a shallow saline pan similar to Lake Nakuru although it is floored by relatively rather coarser salt

impregnated sedimentary material than Lake Nakuru. Its surface water is recharged by the Rivers Meroroni, Mbaruk and Kariandusi and like Nakuru it is also fed from the water tables. Evaporation accounts for its high salinity. The Meroroni, Mbaruk and Kariandusi Rivers flow southward from the Bahati Escarpment into Lake Elmentaita. Like almost all streams in the Nakuru - Elmentaita and Naivasha Basins, these rivers taper as a result of considerable decrease through underground loss and consequently the amount of water reaching the lake is greatly reduced. River Kariandusi is over the years largely fed by quite constant hot springs on the Bahati Escarpment. These hot springs are probably fed by deep water bodies (McCall, 1967).

Unlike the relatively saline Lakes Nakuru and Elmentaita, Lake Naivasha is a fresh water lake. The Lake Naivasha Basin formed in a trough defined by the northern edge of an eastward sloping Mau Escarpment in the west, the Longonot Volcano in the south and the eastern extent is marked by the Kinangop-Kedong scarps of the Njabini Escarpment. An almost complete absence of thick sedimentary sequence in both surface sections and borehole record within the basin suggests that the lake is a contemporary feature on the Rift Valley floor. The lake is fed by the permanent Rivers Malewa and Turasha. River Malewa drains the Sattima Escarpment and has cut a steep walled gorge along its course into the lake. The river cuts across the lower Malewa

Gorge along a fault line to its confluence with River Turasha. River Turasha drains the Kinangop Plateau collecting tributaries from the forested massif of Kipiripiri. The river also has excavated a deep steep wall cut several hundred feet deep into the flat topped tuff plateau and its tributaries are similarly incised. The steep walled incisions of these river valleys appear to be due to sudden lowering of the base level in the floor of the Rift Valley consequent on major fault movements of the Pliocene period. The two streams are united into a single flow southward to feed Lake Naivasha.

1.3 Scope and objectives of the study.

The primary objectives and scope of this research were first to establish the lithostratigraphic sequence of lacustrine deposits within the basins of Lakes Nakuru, Elmentaita and Naivasha and associated sedimentary environments. The initial and most essential task therefore involved working out the lithostratigraphy, that is subdividing the vertical and lateral successions and finding marker beds for correlating sediments within the three basins. Secondly, the investigation aimed to establish some basic stratigraphic correlation framework within and between the three basins. The third and final goal of this research was to identify and attempt a reconstruction of the depositional history of the deposits in this central sector of the Kenya Rift Valley.

1.4 Previous geological work

Thompson (1885) made the first mention of the faulted landscape of the rift valley around Lakes Nakuru and Elmentaita basins following his brief tour of the area. However, the earliest description and subsequent publication of the geology of Kenya Rift Valley can only be attributed to Gregory (Gregory, 1896,1921) who reported evidence for former larger lakes in the central part of the Kenya Rift Valley. He suggested that the palaeolake represented two important periods of lacustrine deposition within the rift. The widely separated and scattered sediment remnants of Kamasia Beds in the Baringo Basin, Kariandusi sediments of Lakes Nakuru-Elmentaita Basins, and the Njorowa Gorge deposits to the south of Lake Naivasha were considered to be evidence of Gregory's larger lower Miocene "Lake Kamasia". It was incorrectly perceived that the northern limit of the vast rift lake was located near Baringo and extended south to form Lake Suess around Suswa and Longonot in the Naivasha Basin. Lacustrine sediments in the region were therefore considered to represent a single depositional episode which according to Gregory fitted into the geological sequence established for East Africa.

The idea of lacustrine sedimentation in an extensive palaeolake in the Nakuru, Elmentaita and Naivasha Basins received intense criticism (Cooke, 1957; Flint, 1959) but ironically was to influence and find stronger support in Leakey's later archaeological field expeditions in the area (Leakey, 1931). Leakey's excursions were primarily of archaeological concern although to considerable extent, the investigations covered sediments and shorelines of the former lakes Nakuru, Elmentaita and Naivasha Basins. On the basis of the archaeological artefacts within some of these deposits, Leakey assigned the sediments a date of Lower Pleistocene.

Nilsson mapped the shoreline features of lakes Nakuru, Elmentaita and Naivasha basins (Nilsson, 1931 and 1940). The goal of his work was to use the sediment sections in the area to correlate climatic phases with moraine deposits on Mount Kenya. In search of evidence for higher lake levels in the area, he described numerous shoreline features including river sections at Enderit and Makalia areas which he considered to represent particular lake level fluctuations. Nilsson's results have been heavily criticised as most of his sections arose from tectonic processes rather than lake level fluctuations. Again his argument that both the Enderit and Makalia sediments were of lacustrine origin has been disproved by this author. While undertaking a purely geomorphological

study in the Lakes Nakuru and Elmentaita Basins, Cilia Nyamweru pointed out that the earlier correlations advanced by Leakey and others were based on discontinuous sections. Nyamweru further argued that the altitudes of these sediments were not accurately measured (Nyamweru, 1966). Hence her work in the Nakuru-Elmentaita basin primarily dealt with measurement of lake level fluctuation in the area, out of which she questioned Nilsson's attempt to interpret the complex Enderit Drift in terms of lake level fluctuations.

Shackleton (1955) gave a generalised account of the rift sediments of Kariandusi which he unfortunately referred to as the Kanjeran. A name Leakey used to imply a correlation of the Lakes Nakuru-Elmentaita deposits with similar sediments at Kanjera on Lake Victoria. Shackleton's view that sediments in the rift formed when the scarp was already in existence is also supported by McCall, Baker and Wash (1967). In his geological survey report of the Nakuru-Elmentaita Basins, McCall (1967) attempted to relate the Plio-Pleistocene sediments in the area with episodes of faulting and volcanicity of the Rift Valley.

In their geological report of the Naivasha Area, Thompson and Dodson (1963) never contributed any new knowledge to the sediments of the area. They, instead, adopted with no supportive field evidence the Gamblian, Makalian and Nakuran subdivisions of the sediments by Leakey and Nilsson (Leakey 1931).

1.5 Methods of investigation.

1.5.1 Basis of palaeoenvironmental interpretation

Description of the measured sections (Chapter 4) allows interpretation of sedimentary facies in terms of their environment of deposition. Certain diagnostic parameters resulting from operation of specific processes or conditions within the sedimentary environment were distinguished and divided into four sub-environments:

a. Internal organisation

Structure within the sediment reflect the hydrological conditions at deposition or structures resulting from organic activity within the sedimentary environment.

b. Grain Size

A simple classification of sedimentary grains into four classes include coarse sand, medium sand, silt and clay grades. These classes also reflect the hydrological conditions at deposition.

c. Faunal assemblage

Although not particularly pursued in this study the distribution of animals living in the lacustrine environments today is assumed to reflect in broad sense the distribution of their Plio-Pleistocene ancestors. Molluscs are considered with a few exceptions to have lived in the lake. The vertebrates are considered as terrestrial, amphibious or lacustrine. Though the possibility of burial outside the habitat of the animal is admitted, it is assumed that the commonest occurrence of fossils in the group above is in their normal habitat.

d. Chemical factors

Unlike the other three parameters, chemical activity will often occur as post-deposition phenomena. It is usually not possible to observe their formative processes on the depositional surface. However, chemical activity does appear to vary significantly between environments and are useful diagnostic parameters. Except in one case none of the parameters are unique to a specific sedimentary environment. For example diagnostic parameter (desiccation cracks) is most important in the alluvial valley delta plain and less important in the alluvial valley and coastal plains. The parameter does not occur in lacustrine environment.

The diagnostic parameters are usually not going to allow separation of the alluvial environment but will separate alluvial from lacustrine environments. The diagnostic parameters are used to make direct interpretations of the sedimentary environments from facies on the measured sections. Some segments of measured sections will, however still be incompletely interpreted owing to either insufficient information from the facies or through lack of record due to non-exposure. After correlation has been established (Chapter 5) it is possible to assess the environments of such missing segments from the known environmental relationships that surrounded them. These assessments are termed broad sedimentary environments to distinguish them from the direct interpretation.

A second category of information dependent on the correlation but independent of environmental interpretations is the sedimentary thickness data which can provide good indication of tectonism in the study area. Although there is no guarantee that the maximum thickness of preserved sediments (depocentre) coincides with the maximum basin subsidence in practical terms it can be assumed to give a good indication of the tectonics in the study area. Clearly the subsidence will, in part have controlled sedimentation and therefore the location of environments

The history of the sedimentation in the area studied must be based on the mutually consistent fusing of basin tectonics and the spatial distribution of the sedimentary environments.

1.5.2 Field techniques.

In order to fulfil the above objectives both field and laboratory investigations were designed and some basic stratigraphic methods of investigations undertaken by the author. The field work entailed locating and mapping sedimentary rock outcrops located mostly along road cuts (Plates 1a, 1b), river valleys (Plates 5a, 6a, 6c), sand quarries (Plate 5b), diatomite mines (Plates 2a, 2b; 4a-4d) and also in trenches. This was carried out hand-in-hand with detailed measurement and description of the lithological properties of natural surface exposures of the sediments as well as physical lateral correlation of the beds. At each locality of exposed sedimentary deposits, sections were described and stratum thickness measured using Jacobstuff Abney level. The obvious lithological attributes of individual beds noted and recorded included the upper contact, bed geometry, lithology, grain size, colour, chemical properties and fossil contents. Lithological units were recognised to form laterally continuous beds on evidence of lithological homogeneity together with related geomorphic expression. Representative but homogeneous beds were selectively sampled in plastic sample bags for later

laboratory analysis to supplement and also verify the field observations where uncertainty existed.

The lateral correlation of the sections relied heavily on the distinctive lithological units within a given locality. However due to the discontinuous nature of outcrops in the area, the stratigraphic columns were pieced together as composites of local sections. Once composite stratigraphic sections were established marker horizons or lithological units were selected and used in the tracing of lateral continuity of the strata. It is upon the lithological elements that the vertical and horizontal relationships within the sediment body and the various facies associations were recognised and subsequently their palaeoenvironmental interpretations made. The resultant maps illustrate both the lithological variations and changes of geometric patterns of the sediments along transects.

1.5.3 Laboratory analysis.

Basin analyses and palaeoenvironmental studies can successfully be accomplished without the inclusion of secondary laboratory investigations component (Miall, 1986) since facies interpretations are often entirely based on the primary field

data. However, in this investigation, laboratory studies of the rift valley sediments were later undertaken essentially to supplement the field observations and also partly to provide an additional line of evidence for the stratigraphical correlations and palaeoenvironmental interpretations. Hence the investigations were of two main types, petrographic and geochemical analyses.

1.5.3.1 Petrographic investigation.

Samples of sandstones, coarser siltstones, volcanic ashes and soils, were subjected to a standard grain size analysis. A set of 8 - inch diameter A.S.T.M. sieves which were in the best condition and which would give a good spread of grain sizes were used. The grain size study used A.S.T.M. sieves #5, #16, #30, #60, #140 and #200 (apertures: 3.40, 1.19, 0.59, 0.25, 0.105, 0.074 mm respectively), and a bottom pan to trap the finest material. Size analysis on the finer sediment samples and the first size fraction, using particle settling rates through water columns, were not undertaken as time could not allow.

Approximately 50 g of sediment were weighed on balance to 0.01 g and put into 500 ml beakers, and about 100 ml of HCl solution (10:1) were added. This HCl treatment removed most of

the excess carbonate and carbonate cement in the rocks. Desegregation of the samples was aided by a pestle and glass stirring rod. The sediments were kept in dilute HCl and repeatedly digested with fresh additional acid until all effervescence stopped, signalling removal of most of the carbonate. This took between 25 minutes to 120 minutes depending on the amount of carbonate present in the sample.

The contents of the beakers were then poured into funnels lined with filter paper, washed three times with distilled water and allowed to drain. After the liquid had dripped through, the filter paper containing the sediment was opened and spread to dry on watch glasses in 100 °C oven for about 3 hours. After cooling overnight or over the weekend the sediment was transferred from the filter paper to the pre-weighed containers, and weighed on a balance to 0.01 g, in order to determine the percentage of calcareous material that was lost. The sample was then poured into nested sieves and agitated in a Ro-Tap shaker for 10 minutes. The fraction of sediment in each sieve was carefully tapped into separate pre-weighed containers, and the weights of each was obtained to 0.01 g. Sediment lost during transfer, sieving or left on the filter paper was calculated.

After sieving and weighing, the sediment in each size fraction except for the finest, was examined through a binocular microscope. The number of grains in each of the following categories was counted: quartz, feldspar, biotite, micas, opaque minerals, aggregate grains (presumably still cemented), clay and lithic (mostly volcanic) fragments. In fractions containing little sediment, all of the grains were counted; in others, at least 300 grains were counted. Percentages of each of the categories of material were calculated for each size fraction, to provide an estimate of the composition and to provide a background to palaeoenvironmental interpretation and geochemical analysis. The data from the sieving were then plugged into a computer program designed by Davis (1986). This program computed the mean, standard deviation, skewness, and kurtosis by the method of moments for size distribution of sediments.

1.5.3.2 Geochemical investigation.

Geochemical determination of the major oxides of Si, Al, Fe, Mn, Mg, Ti, K, Na and P were carried out through bulk wet chemical method. Each sample was decomposed with acid mixtures of HCl-HF-HNO₃-HClO₄ and the solution evaporated to complete dryness to remove excess acids. Silica was then removed by volatilisation as silicon tetra fluoride (SiF₄). The paste was

dissolved in dilute nitric acid. The resultant solution was then transferred into a 5000 ml volumetric flask and diluted to the mark with distilled water. This was further diluted 20 times giving a dilution factor of 10000. The diluted samples solution were then analysed for Mg, Na, K, Fe and Mn at 285.22 μm , 589 μm , 766.5 μm , 386.0 μm and 403.1 μm respectively in an air-acetylene flame. The solution was also analysed for Ca, Al, Ti at 422.7 μm , 309.1 μm and 364.3 μm respectively in a nitrous-oxide-acetylene flame. Both potassium and sodium were determined at 766.5 μm and 589.0 μm respectively. Phosphorous and titanium in the solution were determined by calometric method.

Procedure:

1. For each sample 1.000 g of finely crushed (to 100 mesh) was weighed into a tephlon beaker and 10 ml of concentrated hydrochloric acid added. The sample was the covered with a watch glass, transferred to a hot plate and evaporated to complete dryness.
2. The above procedure was repeated with 10 ml of concentrated nitric acid.
3. A mixture of 10 ml of perchloric acid and evaporated to copious fumes of perchloric acid and eventually to complete dryness. The evaporation was repeated with 10 ml of

concentrated hydrofluoric acid to complete dryness to ensure that all the silica was completely removed by volatilisation as SiF₄.

4. The heater was removed and walls rinsed with some water. The solution was evaporated to dryness on hot plate. The heater and its content was allowed to cool at room temperature then the total weight of the heater and its content recorded. The loss in weight represent the silica content of the sample volatilised as SiF₄ ($\text{SiO}_2 + 4\text{HF} = \text{SiF}_4 + 2\text{H}_2\text{O}$).

5. The salts left in the heater are dissolved in dilute nitric acid. The resultant solution is analysed for the elements outlined above.

CHAPTER 2

TECTONIC EVOLUTION AND GEOLOGY.

2.1. Origin and evolution of the rift basins.

The tectonic evolution, volcanism and geology, of the Main Rift Valley and westward bifurcating Nyanza Rift Valley have been subjects of several studies (Baker 1970, 1986; Baker et al., 1972, 1978; Baker and Wohlenberg, 1971; McKenzie et al. 1970; McConnell 1972, Williams 1970, 1978; Fairhead et al. 1972, 1986; King and Chapman 1972; Baker and Michell 1976; King and Williams 1976; King 1978; Jones and Lippard 1979; Nyambok 1985, Williams et al. 1983; Mboya 1983), partly in the quest to understand the geology of continental rifts and partly due to interest generated by the concept of plate tectonics. Arising from the investigations the linear though sometimes diffuse, topographic configuration (Fig.1-1) of the rift system in Kenya is well known. The main Kenya rift valley which extends from Turkana depression in northern Kenya to central Tanzania plateau in the south covers a distance of over 900 km. The combined effects of greater uplift and volcanism in the rift valley has developed over the last 30 Ma (Bellieni et al. 1981). The rift formation was initiated by broad initial downwarping giving rise to a depression in the north. The depression was progressively deepened during 16 to 7 Ma, when it was apparently faulted on its western side and monoclinally

downflexed on its eastern side. Subsidence of a graben only became dominant tectonic process during the last 4 Ma. The topographic expression of the rift was controlled by opposing effects of subsidence and volcanism.

The rift tectonic development both in the north and south of the Kenya Rift started with gentle downwarping followed by repeated flooding of the depression with lavas. Volcanism, tectonic and evolution of the rift system and its initial plate movements were preceded by crustal thinning, and formation of depression in the present site of the Rift Valley. The rifting apparently began with the uplift in the Ethiopia-Arabian region during the late Eocene (Baker et al. 1972; Nyambok 1985). Early Miocene dominal upwarping propagated rifting southward into both Ethiopia and Kenya. The resulting triangular Turkana depression was partially filled with Miocene (17.2 + 1.8 M.B.P) to Pliocene ignimbrite, basal lavas and minor sedimentary intercalations (Fitch and Miller, 1976). Late Miocene and Pliocene faulting defined the principal elements of eastern rift in the northern Kenya. Volcanism in the southern sector of the Kenya Rift Valley began at 15 Ma. The eruption was later succeeded by faulting at 7 Ma which led to the formation of half graben on the western rift flank. By 4 Ma the flexed eastern margin of the depression was faulted and a graben formed. Subsequent faulting and volcanism migrated

inwards creating step-fault platforms.

In the Nakuru, Elementaita and Naivasha sector, voluminous trachytic volcanism completely filled the inner rift depression at intervals between 6 and 2 Ma. The inner graben was dissected by dense swarms of minor faults from about 2 Ma that continued into the last 0.5 Ma. At the last stages of the period a series of trachytic caldera volcanoes were built axially in the inner graben. Sedimentary lake basins formed into local closed structural basins where volcanic damming also formed lakes in the graben floor.

The elliptical shape of the Kenya dome was created by gentle upwarping of the rift shoulders accompanied by sagging of the central rift floor (Baker and Wohlenberg 1971). The uplift reached a maximum of 1.7 km. (Saggerson and Baker 1965). The faulting of the rift floor around the Nakuru region exhibits symmetry (Figs. 2-3 to 2-8). It is within the area that large volumes of volcanic rocks were reported and the elevation of the rift flank and depression of its subvolcanic floor considered greatest (Baker et al. 1972).

During the Plio-Pleistocene times eruption of voluminous phonolitic and trachytic and ash flow tuffs locally filled the rift and overflowed its flanks (Williams et al. 1983). Volcanism in the southern rift began at 15 Ma (Crossley 1980. Crossley and Knight 1981). In the central sector of the rift a

half-graben was filled by upto 2.5 km of basaltic and phonolitic lavas between 15 and 7 Ma and some of these lavas spilled over both shoulders of the rift (Williams et al. 1983)

By 7 Ma. the Nguruman Fault had formed creating a half-graben in the southern rift. The northern part of the central rift was already filled by trachytic and phonolitic lavas that overflowed eastwards in the Nairobi region. The large Aberdare volcanic complex and other smaller volcanoes on eastern shoulder of the rift formed between 6 and 3 Ma. On the western side of the rift valley continued movements on the marginal faults accompanied by volcanism were taking place within the deepening half-graben

In the central sector (Naivasha and Gilgil) explosive volcanic eruptions formed a widespread series of lavas and trachytic tuffs between 6 and 2 Ma, filling the central part of the rift and covering both its flanks. This was accompanied and followed by the collapse of the rift floor to form a graben for the first time. Between 3 and 1.7 Ma several outpourings of basaltic and trachytic lavas covered the rift floor, accompanied by the collapse of the inner graben leaving normal step-fault platforms at its sides (Baker and Mitchell 1976). Several central volcanoes were built during the interval and project above the successive flood lavas. Subsequent volcanic

and tectonic activities were confined to the floor of the inner graben. These consisted of several phases of basaltic and trachytic volcanism accompanied by several closely developed swarms of closely spaced faults. In the last 0.7 Ma., volcanism has been confined to building a more or less linear salic caldera volcanoes axially in the floor of the inner graben, including the Suswa, Longonot, Eburru, and Menengai volcanoes and localised basaltic and rhyolitic eruptions. The north-south lined caldera volcanoes and associated faults divided the narrow inner graben into separate sedimentary basins seen in the present day. The volcanoes in addition built up thick pyroclastic ash on the floor and over the flanks of the central rift. The structural evolution of the southern part began at about 7 Ma passing through an initial half-graben phase, and developing into a graben between 4 and 3 Ma. The zones of active volcanism have tended to narrow with time and the spacings between the faults have narrowed. The central rift was repeatedly completely filled with volcanic deposits which overspilled its shoulders. The earlier structures of the central rift are largely obscured by later volcanic deposits. However, from landsat immageries and aerial photos the faulting pattern tends to be concentrated on the rift floor. The tectonic depressions become relatively smaller and more numerous towards the rift floor away from the flanks.

2.1.1 Faulted Landforms .

The topographic diversity of the area is attributed primarily to the tectonic and volcanic processes. Faulting in the area has fragmented the landscape into numerous troughs and ridges (Figs.2-1 to 2-7). The general terrain is aligned in a north-south direction in the same trend as the faults in the area. Both tectonics and volcanic activity in the area resulted into voluminous build up of thick volcanic masses and the creation of separate tectonic basins. The processes of rift fragmentation and volcanic eruptions had apparently occurred in phases resulting into complex rift morphology as reflected by the serrated topography in the area. The rift tectonic terrains contrast in age, size and type. The outer bounding rift margins are marked by antithetic tilted large blocks. These major tectonic units slope gently away from the uplifted rift centre (Figs. 2-3 and 2-4) and were followed by a second order tectonic phase which formed a relatively narrow graben. As the focus of faulting shifted inward, stepped ramps and step-fault platforms developed at rift margins.

The third order tectonic features comprise the intensely faulted inner graben floor where the spacing of faults averages 1.5 km. The structural framework consists of graben and step platforms. The bounding faults and ramp structures evolved through termination of *en chelon* major faults. On both its down-throw and upthrow sides the Mau Faults are connected by

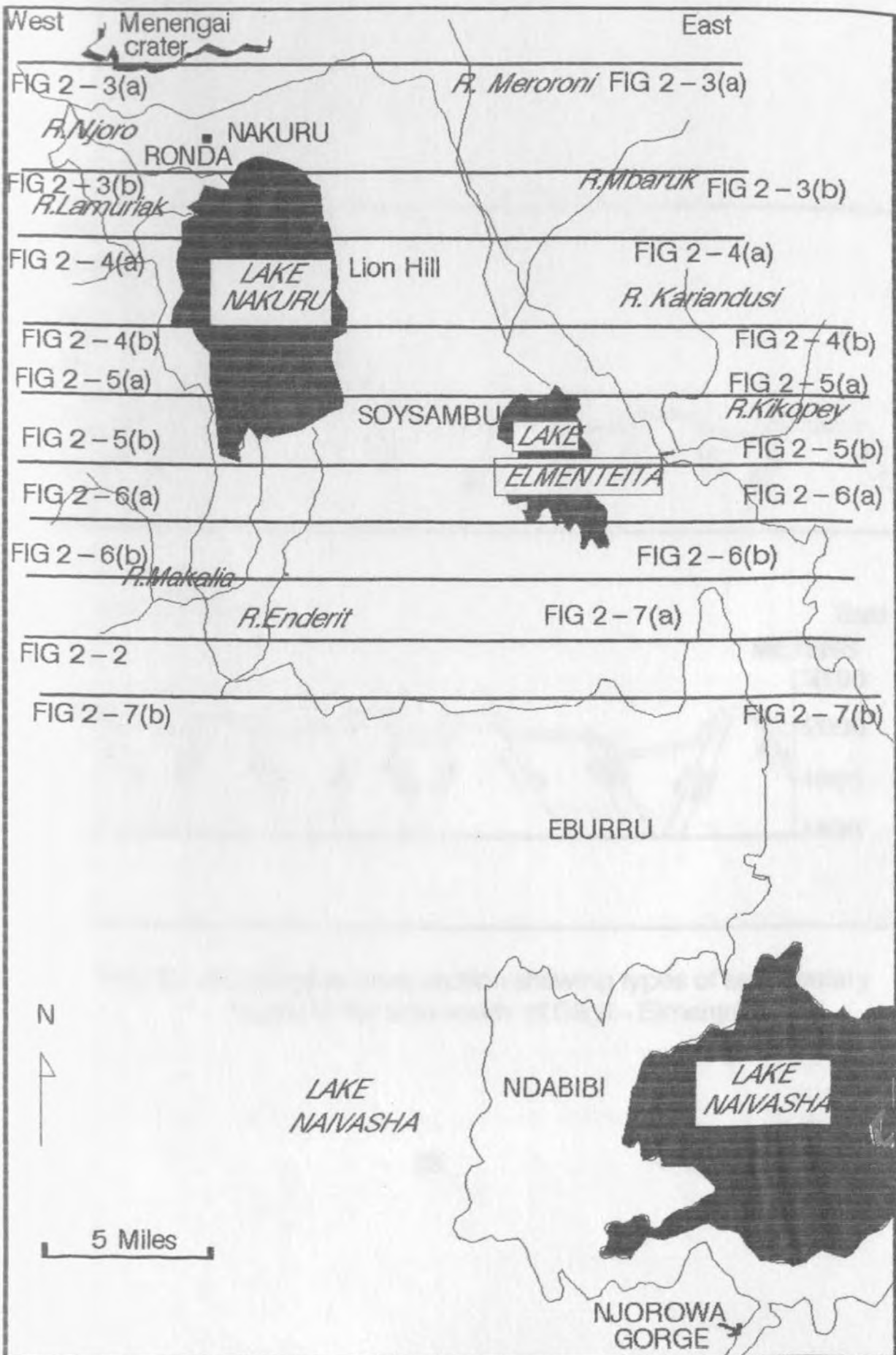


FIG. 2-1 Location of W-E transect cross sections.

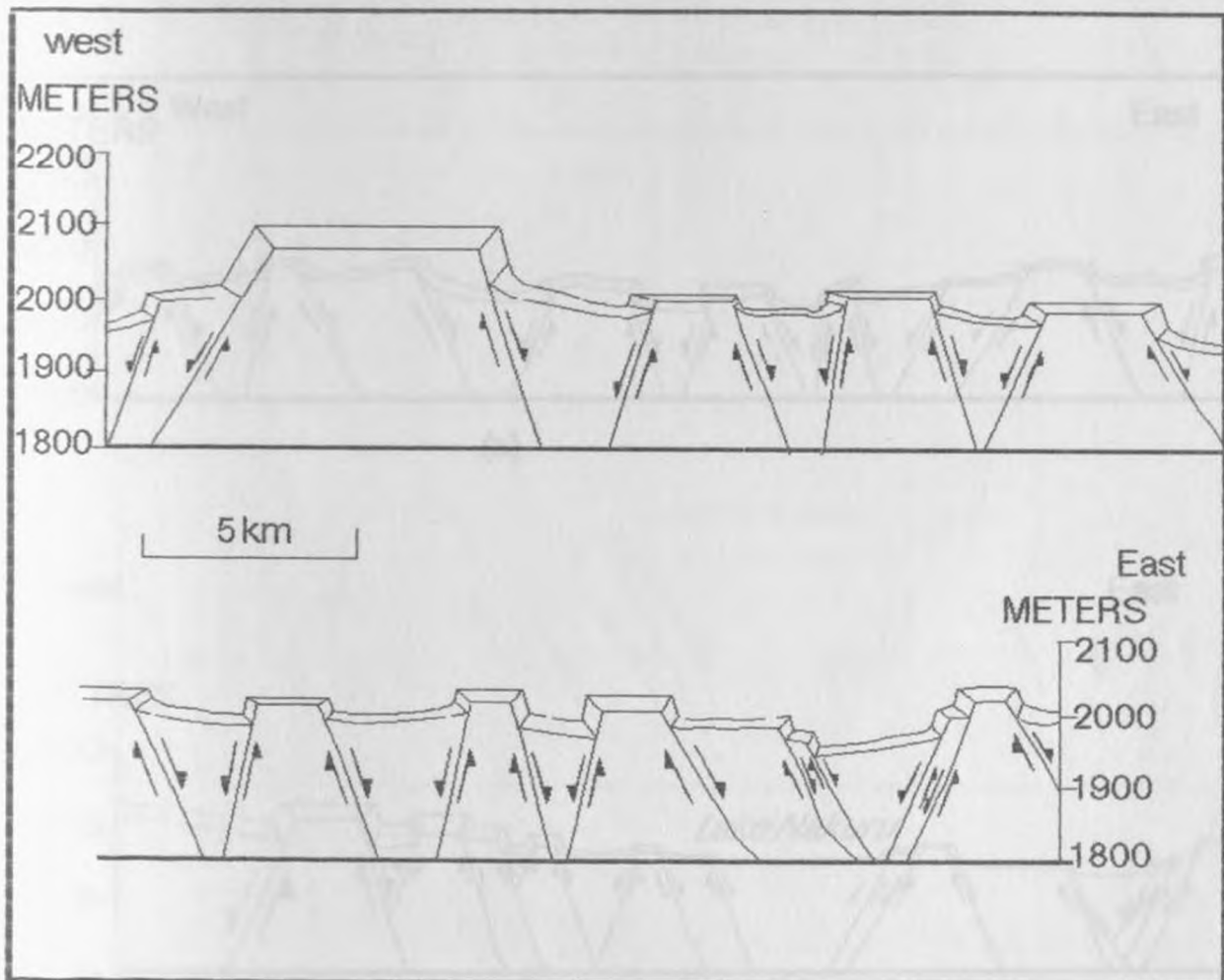


FIG. 2-2 Geological cross section showing types of sedimentary basins in the area south of Gilgil - Elmenteita.

(a) West - East sections (a) north of Nakuru Town (b) across Lake Nakuru.

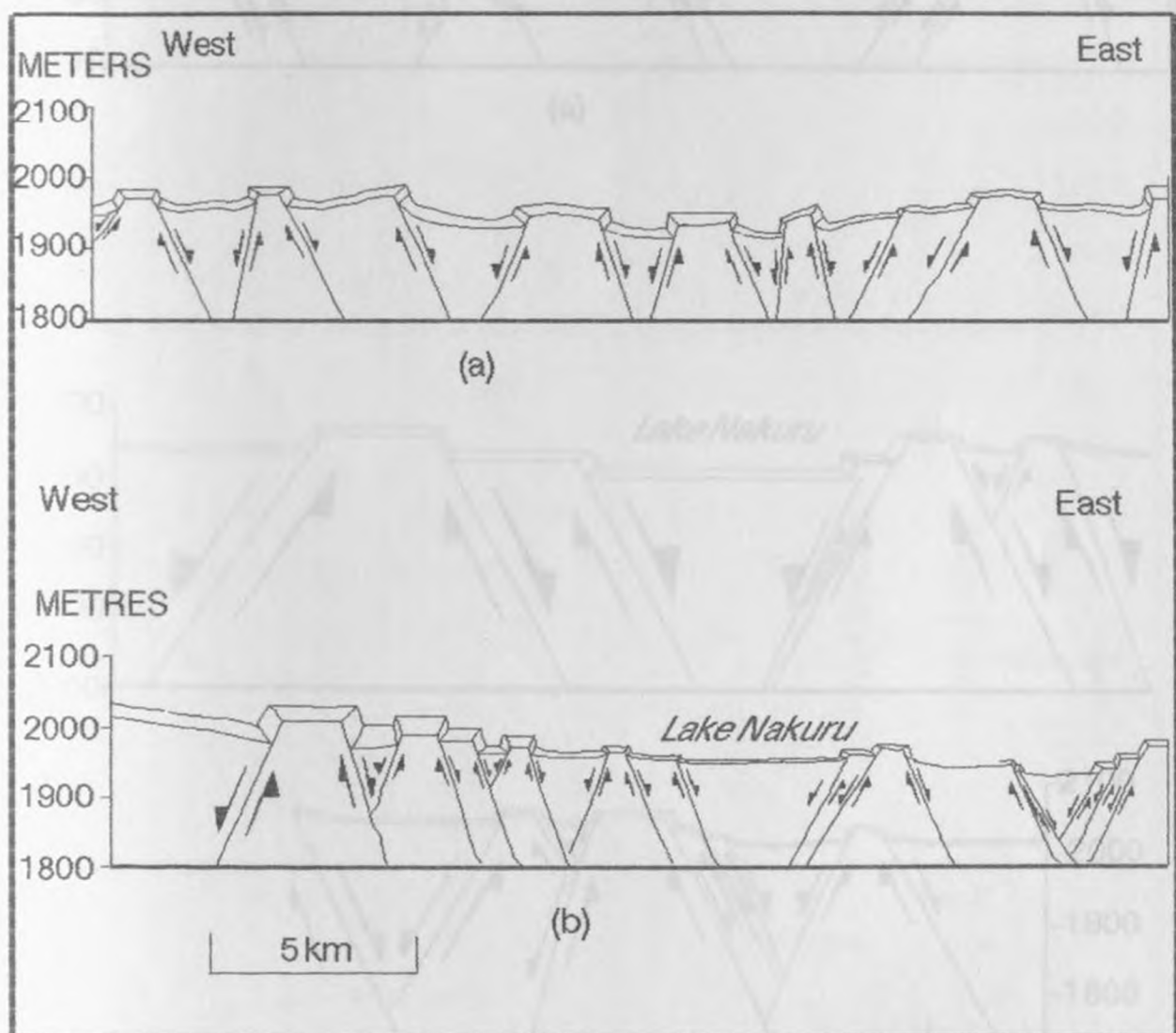


FIG. 2 - 3 West - East sections (a) north of Nakuru Town (b) across Lake Nakuru.

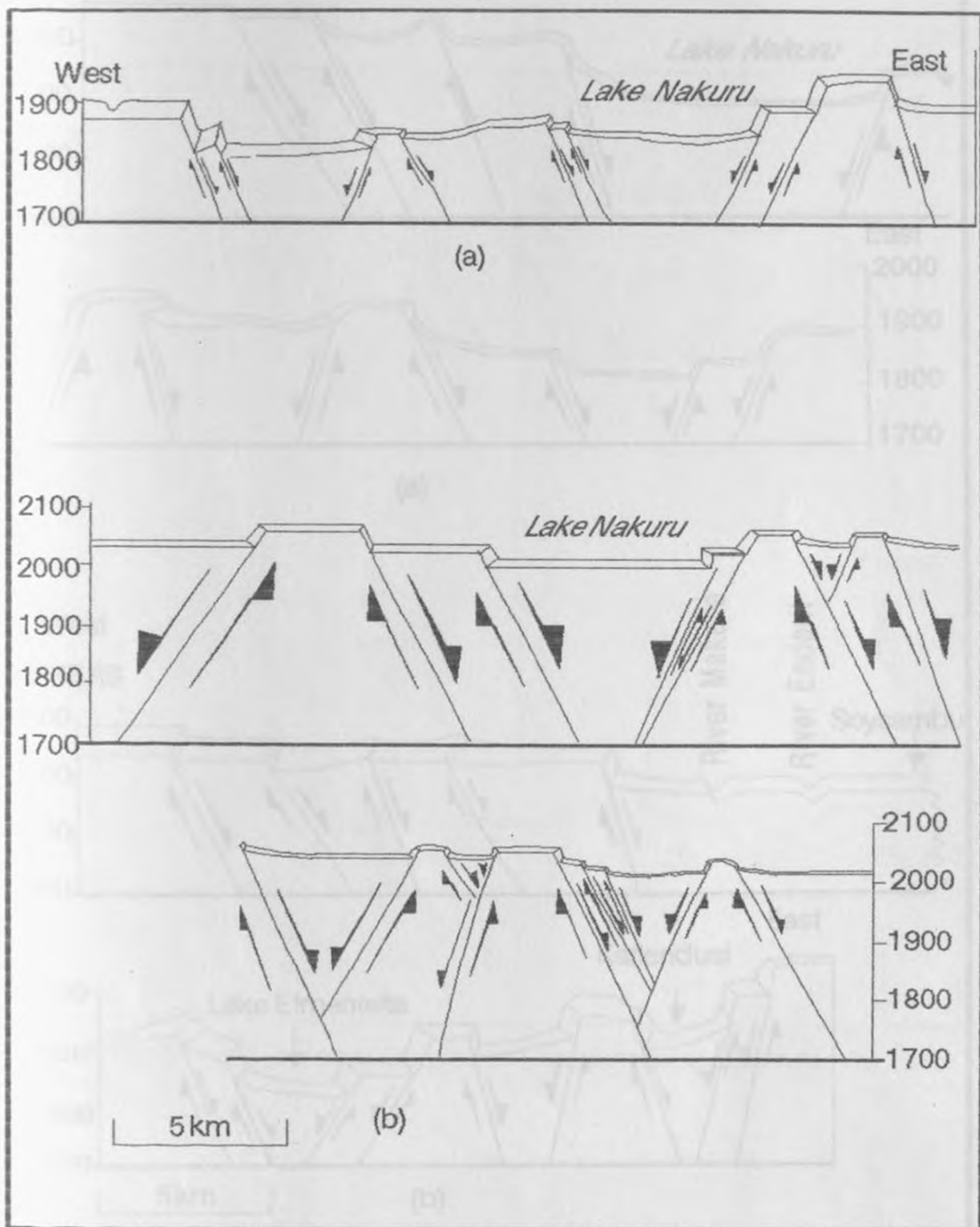


FIG. 2-4 Geological cross sections across Lake Nakuru.

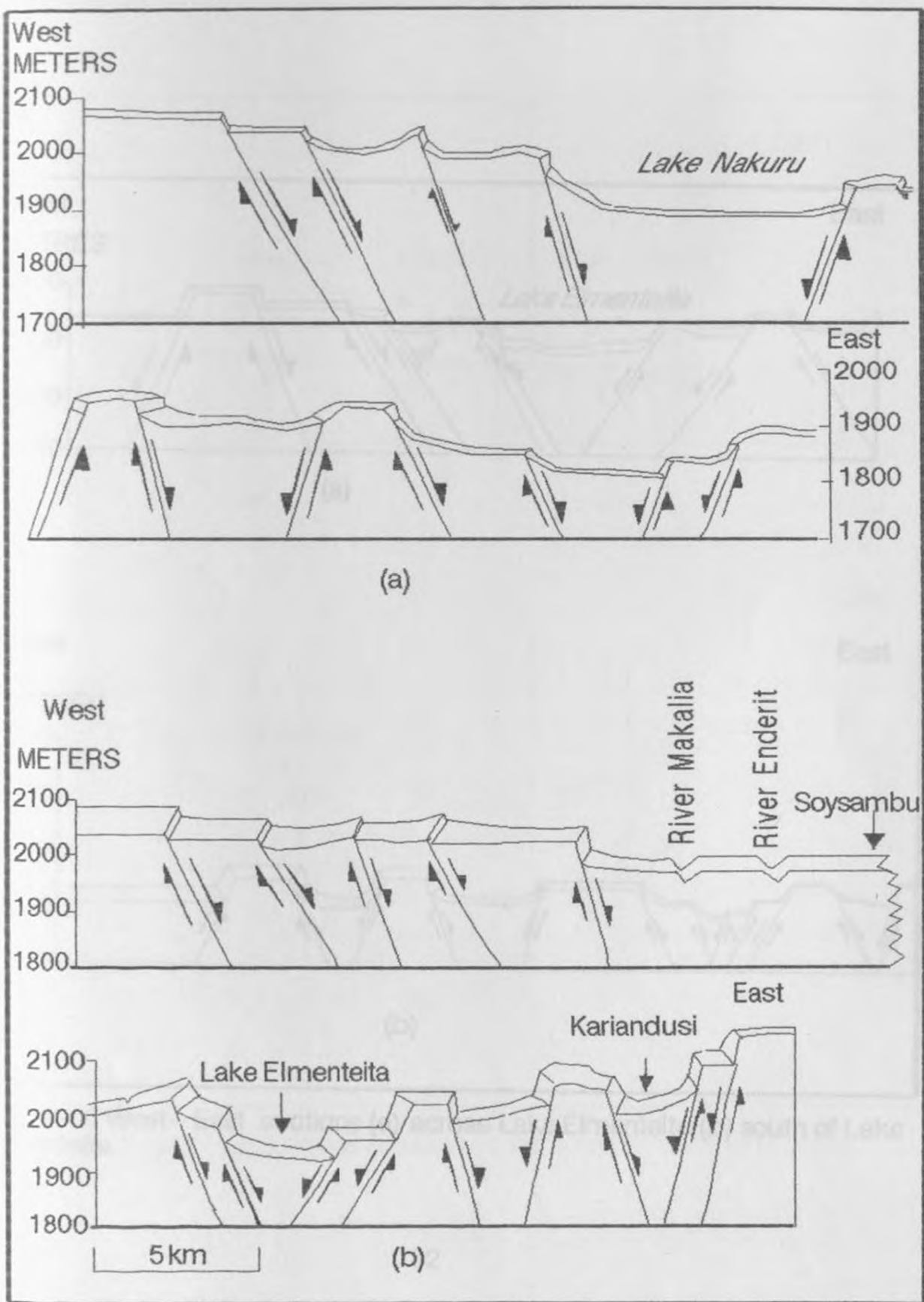


FIG. 2-5 West-East sections across (a) Lake Nakuru (b) Lake Elmenteita and Kariandusi.

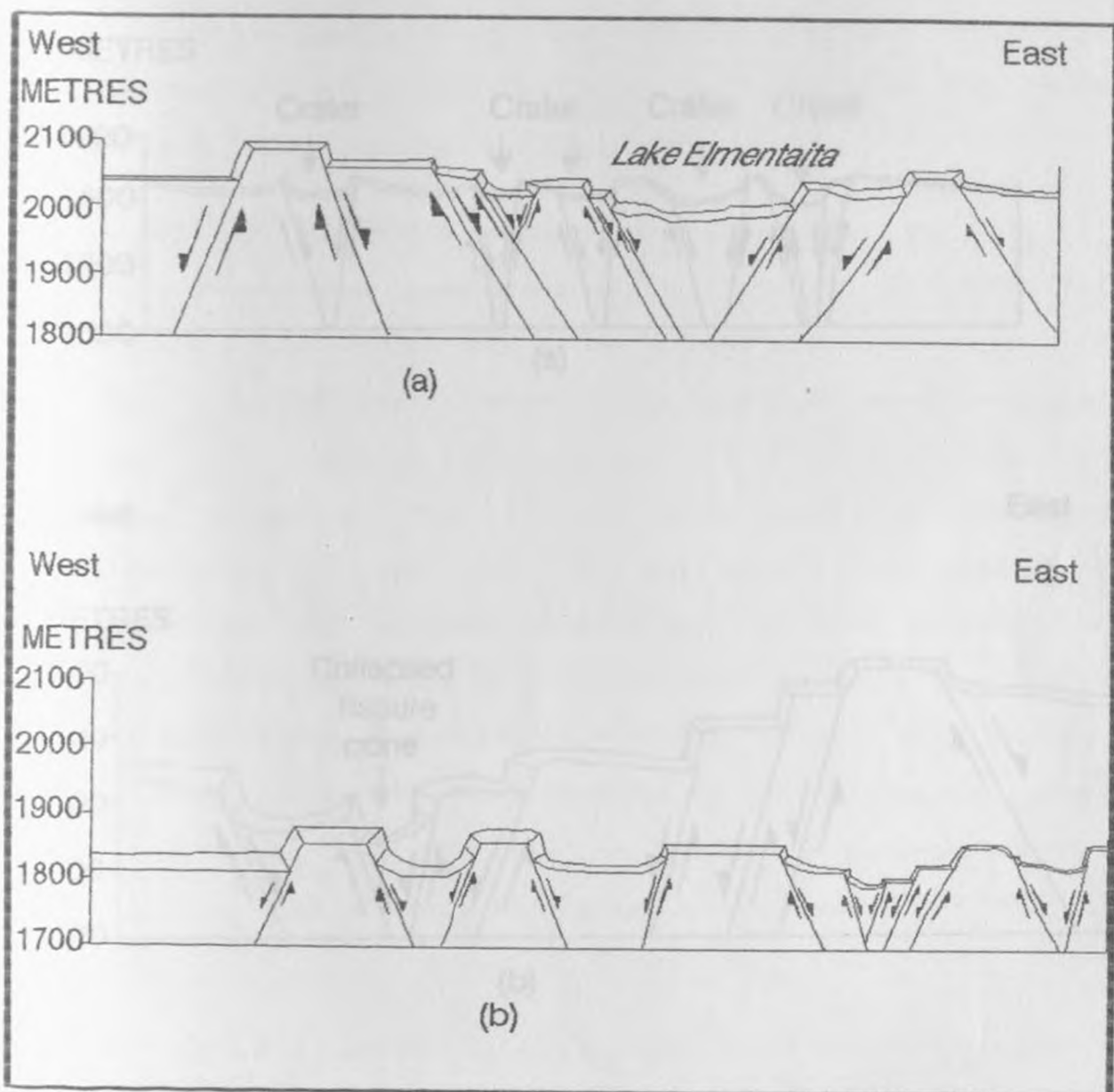


FIG. 2 - 6 West - East sections (a) across Lake Elmentaita (b) south of Lake Elmentaita.

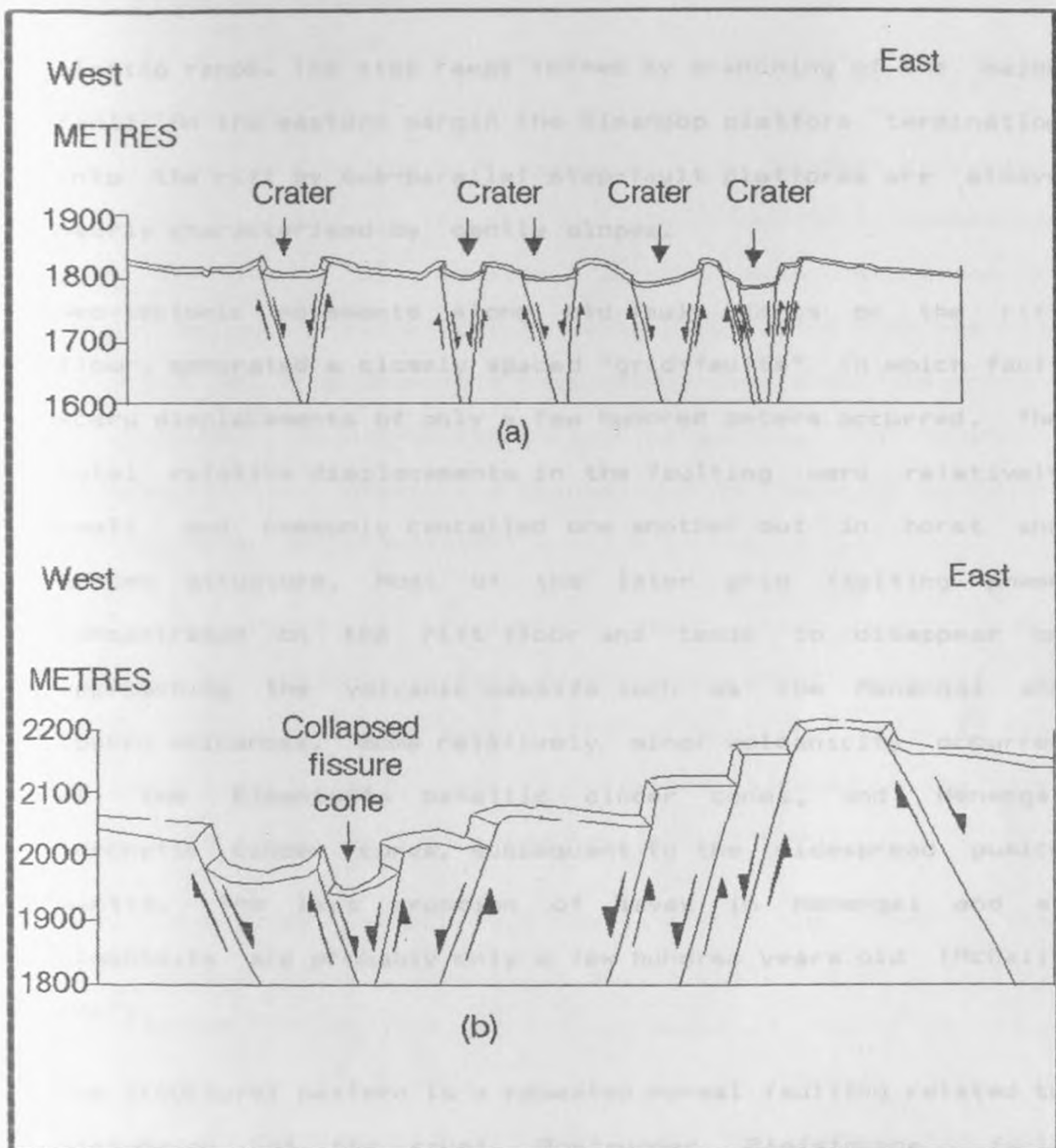


FIG. 2-7 West-East cross sections to the south of Lake Elmenteita.

sloping ramps. The step ramps formed by branching of the major fault. On the eastern margin the Kinangop platform termination into the rift by sub-parallel step-fault platforms are always nearly characterised by gentle slopes.

Neo-tectonic movements along old fault scarps on the rift floor, generated a closely spaced "grid-faults" in which fault scarp displacements of only a few hundred meters occurred. The total relative displacements in the faulting were relatively small and commonly cancelled one another out in horst and graben structure. Most of the later grid faulting phase concentrated on the rift floor and tends to disappear on approaching the volcanic massifs such as the Menengai and Eburru volcanoes. Some relatively minor volcanicity occurred at the Elmentaita basaltic cinder cones, and Menengai trachytic cinder cones, subsequent to the widespread pumice mantle. The last eruption of lavas in Menengai and at Elmentaita are probably only a few hundred years old (McCall, 1967).

The structural pattern is a repeated normal faulting related to distension of the crust. Post-upper Pleistocene fault movements extend through Nakuru, Elmentaita and Naivasha areas are represented by shear cliffs free of screes and vegetation. The fault planar are near vertical, which are characterised by very small throws.

2.1.2 Tectonic Grabens

The floor of the lake basins are extensively concealed underneath mantles of different volcanic rocks, which makes the history of the Rift Valley in this sector remarkably complex. Faulting in the north of the Kenya Rift associated with downwarping of the valley in the south, eruptions of phonolites and trachytes from central volcanoes such as the Menengai, and from depressed fissure sources formed the present rift valley. In the Naivasha-Elmentaita area, the movements of basaltic lavas possibly originating from fissures succeeded the trachytes and phonolites.

The main types of sedimentary basin traps created and structural volcanic effect in the area occur variously as graben, step fault platform, inner graben and volcanic dam. Numerous small graben and half-graben basins found in the inner graben are less than 2 Ma. (Strecker, et al. 1990).

The contemporary sedimentary basins within the inner graben contain Lakes Nakuru, Elmentaita and Naivasha basins (Fig.1-2). The basins are on flat lying flood lavas of the rift floor which have been subsequently faulted during the last 2 Ma. The basins are structurally controlled and the lakes on the rift floor were apparently, occasionally, dammed by volcanic cones. Lakes Nakuru and Naivasha, for example, were partially ponded by the Menengai crater and the Longonot-Olkaria volcanic

complex respectively. The Soysambu Basin fault formed on a volcanic platform east of Lake Nakuru whereas the Kariandusi Graben is a fault slope basin which owes its existence to the gentle eastward tilt of the Mbaruk fault.

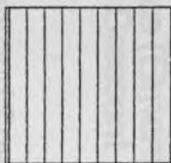
The continuous tectonic movement created numerous small short lived basins in the main graben. The tendency for basins to fragment due to subsequent faulting resulted into complex stratigraphic relations and extremely rapid variation of the sediment types in response to changes in the topography. Growth faults are common and the relative effects of fault displacements, erosion and volcanism have varied greatly in time and space and have caused frequent changes in the sedimentary environments.

2.2 Pliocene-Lower Pleistocene Geology.

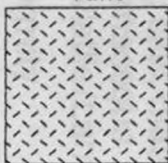
The rock formations within the central part of the Kenya Rift are predominantly Plio-Pleistocene volcanic, discontinuous Pleistocene - Holocene sediments and relatively widespread Recent alluvial volcanic cover (Figs.2-8, 2-9). The Cenozoic volcanic are of interest in this study as the source of clastic sediments in the Lakes Nakuru, Elmentaita and Naivasha Basins. These lavas occur as fissure flows and central volcanoes (Plate 3a).

EXPLANATION

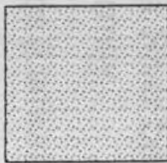
Basalt



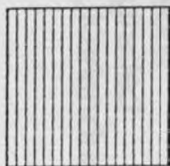
Agglomeratic
Tuffs



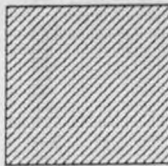
Sediments



Undifferentiated
lava



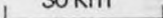
Phonolite



Lakes



30 km



N



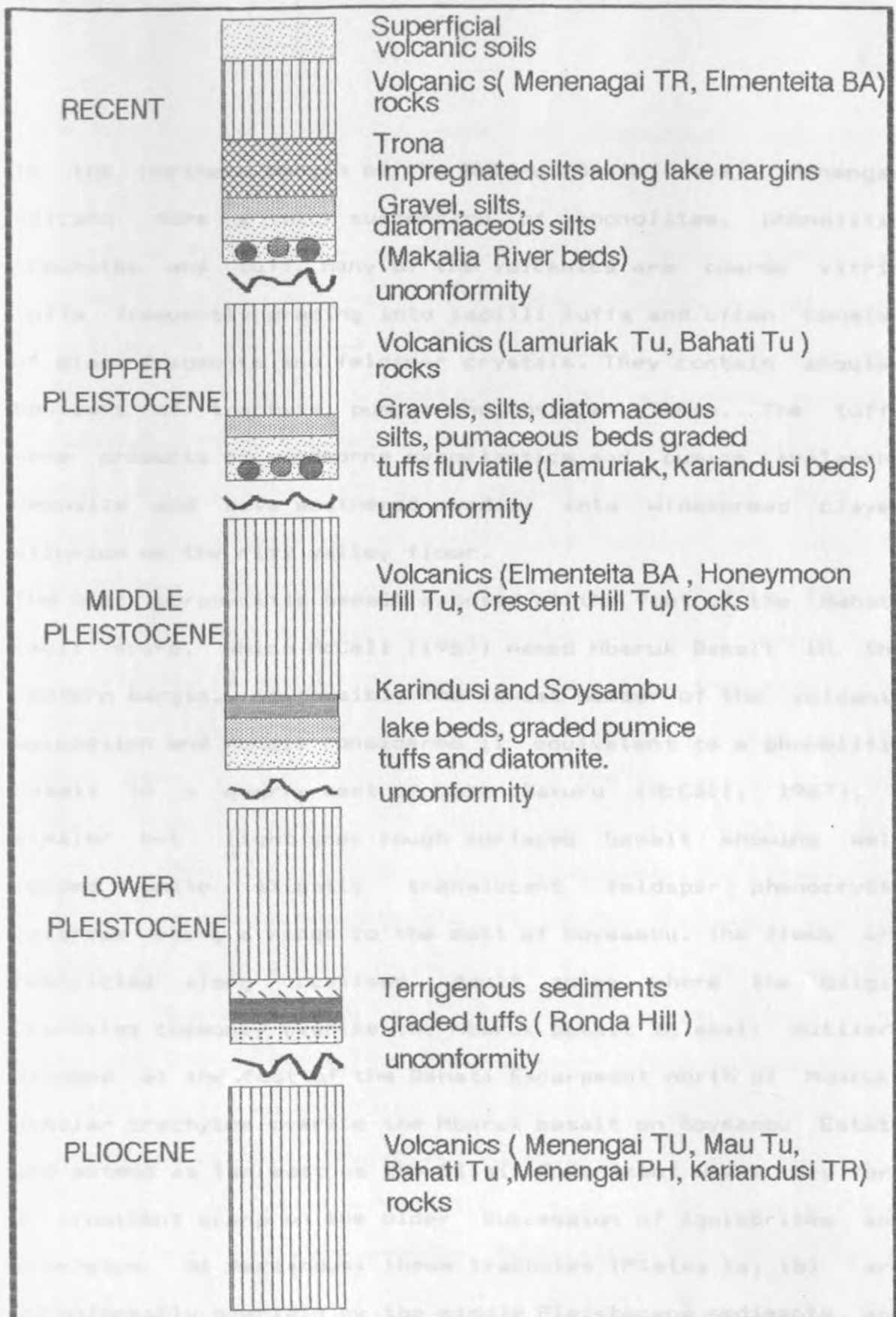


FIG. 2-9 Schematic diagram showing stratigraphy of the Pleistocene sediments and volcanics of the Nakuru, Elmenteita and Naivasha graben. (BA basalt, TR trachyte, TU tuff, PH phonolite)

In the northern margin of the Nakuru Basin, the Menengai Volcano form a thick succession of phonolites, phonolitic trachytes and tuff. Many of the volcanics are coarse vitric tuffs frequently grading into lapilli tuffs and often consist of glass fragments and feldspar crystals. They contain angular boulders of trachyte, pumice and obsidian lamps. The tuffs were products of windborne pyroclastics and pumice avalanche deposits and have weathered readily into widespread clayey alluvium on the rift valley floor.

The black porphyritic basalt exposed at the foot of the Bahati Fault scarp, which McCall (1967) named Mbaruk Basalt in the eastern margin, is possibly the lowest member of the volcanic succession and McCall considered it equivalent to a phonolitic basalt in a quarry west of Lake Nakuru (McCall, 1967). A similar but light grey rough surfaced basalt showing well formed white slightly translucent feldspar phenocrysts outcrops along a ridge to the east of Soysambu. The flows are restricted along localised fault zones where the Gilgil trachytes commonly overlie the Mbaruk basalt in small outliers exposed at the foot of the Bahati Escarpment north of Mbaruk. Similar trachytes overlie the Mbaruk basalt on Soysambu Estate and extend as far east as the Gilgil Escarpment where they form a prominent scarp on the older succession of ignimbrites and trachytes. At Kariandusi these trachytes (Plates 1a, 1b) are unconformably overlain by the middle Pleistocene sediments and

form a faulted trough in which the Kariandusi lacustrine sediments formed.

Along the fault scarps to the west of Lake Nakuru basin are exposed fissile and banded trachytes which overlain by phonolites characterised by dark nepheline, anorthoclase and pyroxene phenocrysts. A basalt flow with prominent pyroxene phenocrysts form the escarpment west of Lake Nakuru. The southern part of the Lake in the Makalia Gorge is underlain by phonolitic trachytes which McCall reported to be possible equivalent of the Ronda lavas (McCall, 1967). The north eastern edge of the basin is underlain by coarse, obsidian, pumice tuff and sediments in the Bahati area. On the cliffs immediately to the west of Lake Nakuru are exposed dark lavas similar to the Mbaruk Basalt in the south of Gilgil and Kariandusi on the eastern edge of the Lake Elmentaita area. The lavas along the Gilgil old road include trachytes, agglomeratic ridges and basalts, welded siltstone tuffs and coarse columnar jointed ignimbrites and limited pumice tuffs. At Gilgil the trachytes underlie ignimbrite on the Gilgil Escarpment below the diatomite. The trachytes at Kariandusi are heterogeneous quartz trachytes that show faint to pronounced laminar flow and enclaves of lithic fragments. At Mbaruk in the immediate northern part of Lake Elmentaita a dark phonolite unit on the west of lake Nakuru is overlain by basalt along the bounding fault scarp.

2.3 Middle Pleistocene and Recent volcanics.

Late Pleistocene and Recent volcanic rocks in the area formed tuff cones to the south of Lake Elmentaita and also form the Honeymoon Hill on the immediate north of Lake Nakuru. The cones transected by neo-tectonic median grabens are composed of steep dipping stratified light coloured tuffs and commonly contain boulders of lavas. The Honeymoon tuffs consist of basaltic and trachytic boulders, agglomerates, and fragments torn-off the underlying lava formations. McCall reported the stratified tuffs of the cones south of Lake Elmentaita to be the same age and continuous laterally with the Kariandusi Formation (McCall, 1957, 1967). The observation was most probably partly based on the questionable evidence for shorelines (Nyamweru, 1969) reported by Nilsson (Leakey, 1931) as one of the Gamblian (Upper Pleistocene) series on the faults of the two larger cones south of Lake Elmentaita. However, from the geological investigations conducted by the author there is no field evidence in the area supporting a stratigraphical or chronological contemporaneity between the Kariandusi Formation and volcanic tuff cones to the south of Lake Elmentaita. Although from the recent radiometric calibration of Recent basalt flows in the area (Strecker, personal communication.) which dates .4 Ma. in the area and Kariandusi trachyte .7 Ma., the Kariandusi Formation would appear relatively older.

Tuff cones to the south of Lake Elmentaita area are generally composed of spongy yellowish glass in which are set fragments of lava and crystals. The presence of plagioclase mineral in the rock may be attributed to basaltic tuff origin which was reported to be compositionally similar to the older basalts (McCall, 1967) but also indistinguishable from the younger basalts. In the area along the western shore and immediately south of Lake Elmentaita, Holocene (?) olivine basalt form a broken sparsely vegetated lava terrain. The main body of these flows are unfaulted although a similar basalt unit is exposed by the low fault ridges. On the basis of sparse vegetation cover over of the basaltic flows the lavas are reported to be considerably recent in age (McCall, 1967; Nyamweru, 1969) and possible contemporaneous with the recent glassy trachytic scoria of the Menengai Caldera.

The basaltic cinder cones to the south of Lake Elmentaita in the rift floor are considered intimately connected with the flows and probably represent the vents from which they were derived. Since the flows consistently slope evenly northwards to Lake Elmentaita, it is predictable the source of the basalt is possibly concealed within the lava (McCall, 1967). The widespread pumice deposit which cover large areas of the rift floor to the south and west of the Menengai consist of coarse agglomeratic beds. They are possibly part of the lapilli tuffs associated with the upper Pleistocene sediments of the Nakuru

Basin. These sediments are composed of coarse crudely stratified deposits up to 15 m thick composed of light coloured well sorted fragments of reworked pumice debris. Obsidian, trachyte and syenite fragments have all been noted in the pumice, but the pumice comprise over 90% of siliciclastic deposits. Many of the lacustrine tuffs are finely stratified water lain pumice glass particles. Though much finer, the particles are essentially similar to the clastic fragments.

2.4 Pleistocene - Holocene sedimentary formations

The Pleistocene - Holocene sedimentary formations in the study area commonly occur as localised patches within fault-controlled basins. Modern deposits associated with contemporary rift lakes occur intermittently as thin apron along the lake margins (Plate 3b). However, in both the modern and ancient deposits, two principal types of sediments recognised in the study area are either lacustrine deposits typically represented by the Kariandusi (Plates 2a-2b) and Soysambu (Plates 4, 4B) Formations or the relatively complex mixtures of alluvial (Plates 5c, 6a, 6b), fluvial and limited deltaic, infra-lacustrine (Plates 5b, 7) sedimentary formations of Enderit and Ronda.

2.4.1 Kariandusi and Soysambu Formations.

The Kariandusi and Soysambu Formations were deposited in separate basins on a surface of considerable relief. Sediments



Plate 1a Kariandusi Formation
Sheared fault contact of light coloured lake beds and trachyte
on the Nakuru – Naivasha road cut west of the diatomite mine.



Plate 1b Kariandusi Formation

Neotectonic faulting displaced Pleistocene lake sediments and formed classic normal rift graben on either side of a road-cut. Pre-Pleistocene fault down-stepped the trachyte on the foreground.



Plate 2a Kariandusi Formation

Cross – bedded pebbly cobble conglomerate infilling the diatomite bed and grades upward into clast – size sand – stones.



Plate 2b Kariandusi Formation

Diatomite mined by tunnel and pillar method at Kariandusi.



Plate 3a South end of the Elmenteita Basin.

NE – SE Mount Eburru volcanic ridge in the horizon mark the southern extent of the basin. Foreground: the Karterit Hill cone encloses a crescent crater. On the outward face of the cone erosion incised parallel line marks.



Plate 3b Trona deposits of Lake Elmenteita.

View of Lake Elmenteita from south reveal thin layer of trona crusts surrounding the lake water body perimeter. North – south grid faults delimit the western edge of the lake. On the horizon Mau escarpment mark western extent of the basin.



Plate 4a Soysambu Formation.

View from north of the Soysambu open pit diatomite mine. Eburru volcano trends NE – SW on the horizon teast south – west.



Plate 4b Soysambu Formation

Stained lacustrine beds of the Soysambu Formation measures 7 meters thick with recent mudcracks exposed on the mine floor.

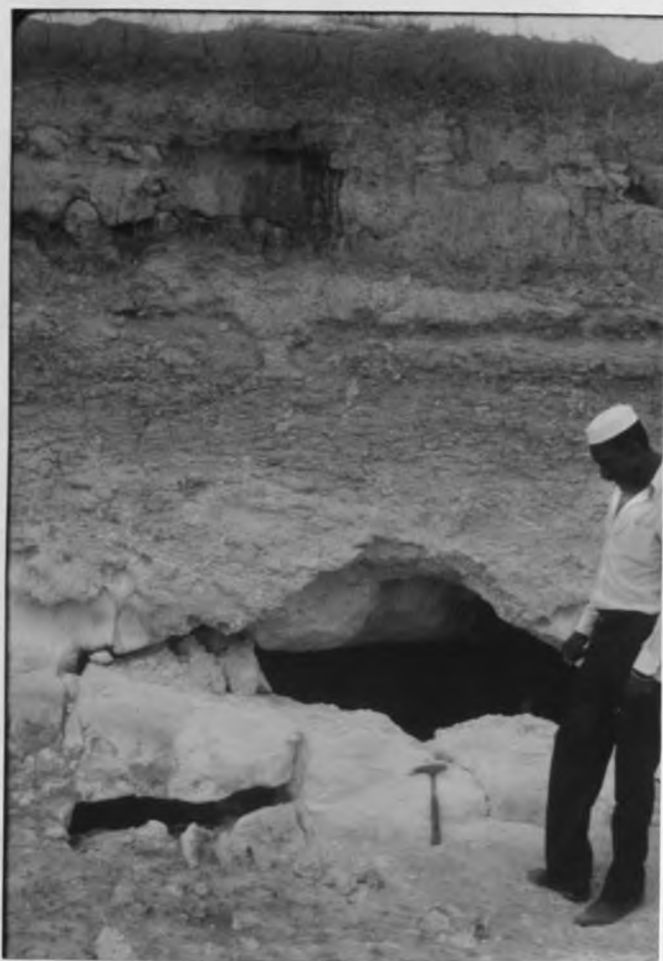


Plate 4c Soysambu Formation.

Solution generated cavern structure at the transitional contact of diatomite and tuff.

Small irregularly shaped caverns with circular limestone concretions formed along desiccation cracks toward top of the formation.

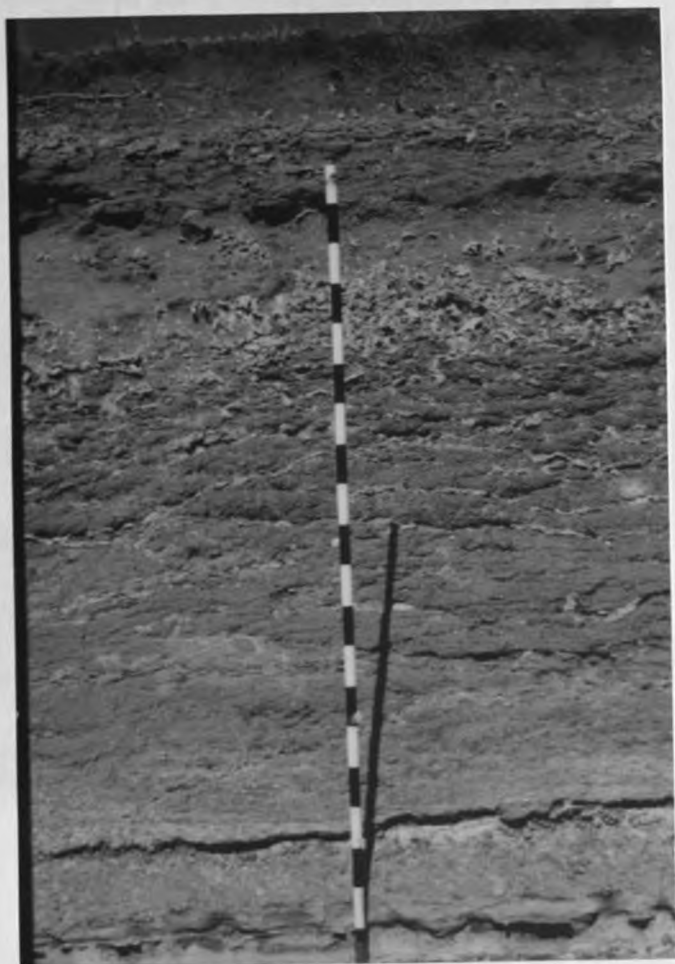


Plate 4d Soysambu Formation

Leached – bedded tuff sequence intercalated with caliche limestone concentration formed along desiccation cracks toward top of the formation



Plate 5a Lamuriak Beds.

Stratified pyroclastic tuffs and ashes sequence form the lowermost unit of Ronda Formation at the mouth of River Lamuriak gorge.



Plate 5c Ronda Formation

View of modern coalesced alluvial fan being deposited outward from active fault scarp in response to active tectonic subsidence.



Plate 5b Ronda Formation

A high angle cross stratified lenticular fluvio-deltaic Ronda Formation. Repeated light coloured silts alternate with coarse pumiceous tuffs at the sand quarry.



Plate 6a Enderit Formation

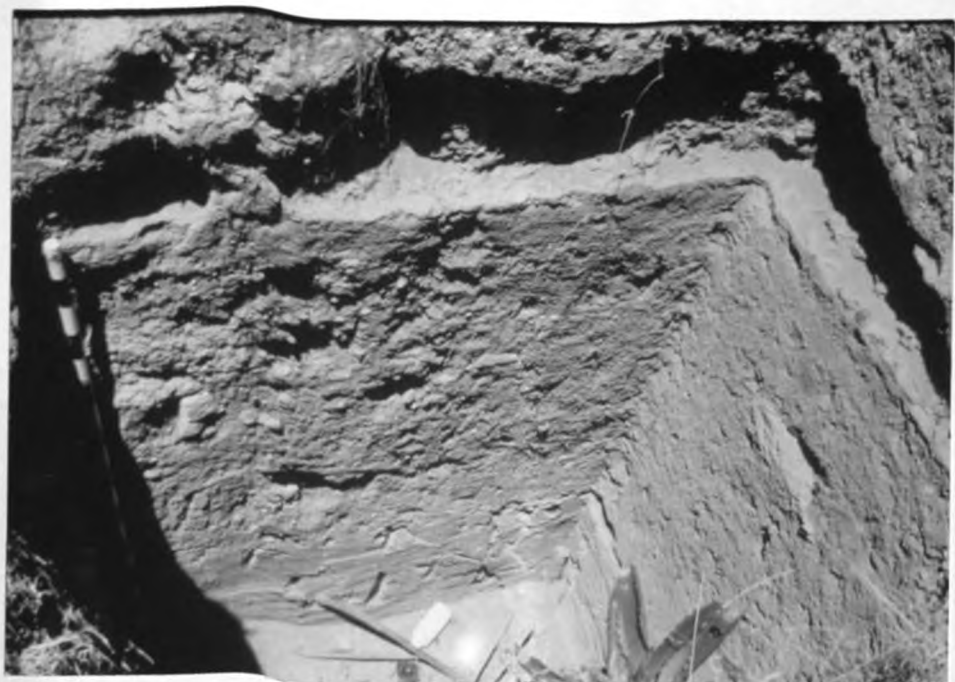
Massive fluvio – fanglomerate with deltaic – lacustrine silt inter –
calation at the base and top of the Formation at Enderit drift.



Plate 6b Enderit Formation.

Close – up view of the fanglomerate reveal large tuffaceous
clast inclusions and sharp contact at the base with laminated
lacustrine beds.

(i)



(ii)



Plate 6c Enderit Formation.

Close-up view of (i) large tuffaceous clast fan conglomerate
overlie (ii) fine laminated silts exposed in trench transects
at Enderit River drift.

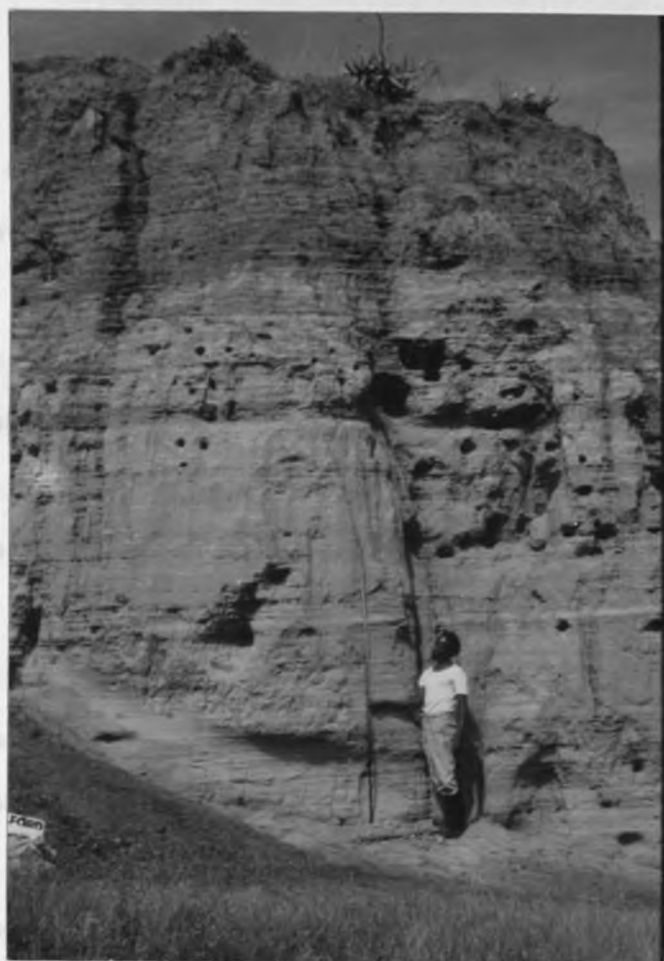


Plate 7 Makalia Beds

Laminated Makalia member of Enderit Formation.

exposed at Kariandusi Diatomite Mine are principally diatomaceous beds which measures up to 30 m at the mine (Plate 2b). Here the sequence was formed in a shallow lake of about 10 km in diameter underlain by trachytes. The Kariandusi Formation is subdivided into two mappable units, a lacustrine diatomite at the base and a fluvial pumice conglomerate towards the top. Like the unconformably superimposed post-lacustrine fluvial deposits the lake sediments pitch out both in the northward and south directions. At the base, the unit is agglomeratic with sparse obsidian fragments. The lower part of the Kariandusi Formation consist of dirty white greyish diatomite. The dirty white colour is attributed to volcanic ash which form discontinuous pumice patches. The diatomite formation is filler variety referred to as F.B1 or white diatomite at the higher levels at the Mine. Occasionally thin blue volcanic ash intercalation occur intermittently within the diatomites which formed directly on a faulted and eroded trachytes. The sediments are often thicker within the troughs but wedges out on raised ridges. The relatively scattered widespread tuffs locally serve as marker beds for correlating Bed 1. The basin was faulted on its western margin during the deposition of lower section of the Bed 1. The unit is subdivided into five lithofacies, which comprise the Lake deposits, lake-margin terrain, an alluvial fan and alluvial plain.

2.4.2 Enderit and Ronda Formations

At the southern end of Lake Nakuru, fluvial, and deltaic deposits in the Enderit River pass upwards into alluvial fan conglomerates. Further west in the Makalia area, lacustrine deposits are overlain conformably by black tuffs. The same tuff is noted at Ronda and also forms a thin layer on top of the Soysambu Formation. Thus despite geographic isolation of the depositional centres there could well be some limited overlap in the ages of sedimentation in the Nakuru and Soysambu Basins.

The Ronda Formation in the north-west of Lake Nakuru consists primarily of less than 10 metres of stratified pumice tuffs. The tuff beds occasionally intercalated with thin and discontinuous diatomite beds exposed at Ronda in the sand quarry. Most of the deposits are weathered volcanoclastic debris though often truncated with thin lacustrine surfaces. A lower Pleistocene or Lower Middle Pleistocene age has been proposed for these sediments (Leakey, 1931; McCall, 1967), on the basis that the Mbaruk basalt which predates the deposits is considered not to be very much older than the Gilgil trachyte, which appears to have immediately preceded the upper Middle Pleistocene Kariandusi sediments (McCall, 1967).

Within the Lamuriak River bank, the Ronda sediments consist of coarse yellowish stratified tuffs (Plate 5b). The lower unit of these sediments are dominantly pumiceous scoria which are

Table 2:1 Stratigraphic sequence of Quaternary sedimentary
apparently stratigraphically much older than the deposits at
the main Ronda sand quarry sections. Eastwards along River
Njoro these sediments underly unconformably the overlying Ronda
quarry deposits. North of the sand quarry, the older sediments
are faulted and warped, possibly from the effects of a strongly
developed fault that deformed exposure to the north of
Honeymoon sand quarry.

The geochronological subdivision of the Pleistocene rift
sediments are not very clearly defined owing to lack of fossil
evidence. The much older sequence located in the eastern gully
of River Lamuriak obviously represent no lacustrine deposition
It possibly preceded the third and last major faulting of the
Rift valley floor which formed the grid structures. McCall's
view that the early lake occupied the Nakuru-Elmentaita basin,
which was already formed by tectonic events was confirmed
during this study as lacustrine sedimentation was evidently
localised with the earliest formation probably taking place
contemporaneously at Kariandusi and Soysambu which was later
followed by Enderit Formation and finally the Ronda Formation
(Table 2:1). The author's finding is also in agreement with
McCall's (1967) observation that the tectonic episodes
subsequent to the lacustrine deposition in the basin were very
minor (Plate 1b) and insufficient to radically alter the
outlines of the basin. The widespread Recent alluvium cover of

Table 2:1 Schematic sequence of Quaternary sedimentary formations in Nakuru and Elmentaita Basins

McCall's (1967) Sequence		Proposed Sequence	
Formation	Locality		
Makalia beds (Epi - Pleistocene) Upper Sequence	Makalia River Enderit River	Holocene Alluvium	
Lamudiak sediments (Gamblian beds) Middle Sequence	Makalia River Enderit River North and West of Lake Nakuru	Ronda Beds Lamudiak Beds Enderit Beds Makalia Beds	<div style="display: flex; align-items: center;"> <div style="border-left: 1px solid black; border-right: 1px solid black; height: 20px; margin-right: 5px;"></div> <div style="margin-right: 5px;">}</div> <div>Ronda Formation</div> </div> <div style="display: flex; align-items: center; margin-top: 5px;"> <div style="border-left: 1px solid black; border-right: 1px solid black; height: 20px; margin-right: 5px;"></div> <div style="margin-right: 5px;">}</div> <div>Enderit Formation</div> </div>
Kariandusi silts Upper Pleistocene	Mbaruk Kariandusi	Soysambu Beds Kariandusi Beds	<div style="display: flex; align-items: center;"> <div style="border-left: 1px solid black; border-right: 1px solid black; height: 40px; margin-right: 5px;"></div> <div style="margin-right: 5px;">}</div> <div>Kariandusi & Soysambu Formations</div> </div>
Kariandusi Lake Beds (Kanjeran)	Kariandusi		
Soysambu (Middle Pleistocene)	Soysambu		

major sediment displacement in the area possibly led Leakey and Solomon (Leakey, 1931) to the conclusion that the Nakuru and Naivasha basins were never affected by faulting, hence the upper Pleistocene lakes sediments and non-lacustrine contemporary deposits in the area are reported to be extremely well preserved, unfaulted shoreline features previously regarded to extend from the Baringo Basin in the north to the Naivasha Basin in the south. In the central sector of the Nakuru-Naivasha Basin, Nilsson (1935, 1940) identified seven distinct lake levels. The author, however established most of the graded sediments in the area are not necessarily lacustrine. Thus, although stratified pyroclastic tuffs which are closely similar to lacustrine deposits are common in the area they are lithologically different from lake sediments. The rounded fragments suggest transport by water but do not necessarily reflect beach sedimentation associated directly with lacustrine origin. The finer and well stratified units are certainly variable between lake and eolian deposits. They often consist of particles of glass derived from disintegrated pumice.

CHAPTER 3

MEASURED LITHOSTRATIGRAPHIC SECTIONS

3.1 Measured Stratigraphic sections.

The upper Cenozoic strata of the central Kenya Rift lake basins were formally established by lithostratigraphic field analysis. The investigation involved detailed measurement and description of exposures and subsequently their physical field correlation. Due to the discontinuous nature of the outcrops and abundant faulting in the area the stratigraphic columns could only be pieced together as composites of local sections at Ronda, Lamuriak, Enderit, Makalia, Soysambu and Kariandusi. The stratigraphic sections were measured using Jacob's staff and Abney level. The method described by Kottowski (1965) is particularly useful when carefully used on surfaces which were originally deposited as approximately planar horizontal sediments. The measured stratigraphic sections are all illustrated using the same format, a constant vertical scale of 1cm : 1m and depict the various lithological variations. The scale is in meters. Zero meters coincide with the base of the section and the values increase upward. Where measured section is continued from column to column the scale is continuous. The location is given for the area where section measurement was recorded. The capital letters A, B, C or Roman numerals i, ii, iii and iv etc. differentiate where more than one

section is present. The stratigraphic columns were recognised in the field on the identification of sub-environments and geological events such as major erosion surfaces, transgressions, regressions and possible trends in environmental change. In some sections where broad sedimentary environments are recognised their interpretation based on field resolution were later used in the synthesis of the history of sedimentation.

Grain-size is shown for four grades, clay, silt, sand and tuff/tuffaceous sediments. Where mixed grades are shown in the measured sections, the lithology is represented as the dominant grade. The sedimentary environments and the corresponding lithofacies associations recognised in this study comprise the following:

Depositional Environments		Lithofacies association
Lacustrine prodelta (Lacustrine low energy)	1	Laminated siltstone association
Lacustrine littoral (Lacustrine high energy)	2	Arenaceous (bioclastics)
Deltaic distributary channel and interdistributary floodplain (Alluvial coastal plain)	3	Lenticular fine grain and lenticular siltstone association
Fluvial floodplain Fluvial channel (Alluvial valley plain)	4	Lenticular conglomerate and sandstone association
Alluvial fan	5	Interbedded conglomerate and pebbly mudstone

3.2 Use of measured stratigraphic sections.

The correlations of these local sections were based on their distinctive stratigraphic sequences. Once a composite section was established, marker horizons identified were used in assessing the lateral continuity of individual stratum based on the lithology and distinctive geomorphic expressions. The stratigraphic sections, their composites and correlations are illustrated following the establishment of vertical and horizontal relationships within the sediment body. A corresponding description of lithofacies and facies association and their palaeoenvironmental interpretations are derived from the sections. The central rift strata constitute a complex fluvio-lacustrine and aeolian units which were subdivided into four Pleistocene-Holocene formal ranks namely, the Kariandusi Formation, Soysambu Formation, Enderit Formation, and Ronda Formation (Table 2:1). In addition discontinuous Holocene lake deposits constitute the contemporary lithological facies characteristic of the formations.

3.3 Notes on the lithological symbols for the sections (Fig. 3-1).

- CL Claystones - the sediment is smooth when ground between teeth.
- SL Siltstone - If individual grains are visible with 10 X hand lens.
- SD Sand - Individual grains visible with necked eye. The sand grade is further subdivided into very fine = vf, fine = f, medium = m, coarse = c, very coarse = vc. The sand division are based on the Wentworth grade scale (Wentworth, 1922) measured on a comparison chart prepared by the author (Fig. 3-1). For the very coarse grade a written description is given e.g. coarse pumiceous sand. These grades are at times superimposed e.g. silty sand or silty clay.
- TU Tuff or ash - silt- clay grade ash
- PU Tephra - coarser than tuff
- AG Breccia - Pumice pebble gravel
- CO Conglomerates
- BA Basalt either as substrate or sediment clasts.
- PH Phonolites
- TR Trachyte
- MF Mafic
- TA Trona.
- CRS Cross stratification, small scale less than 5 cm, large scale exceed 5 cm.

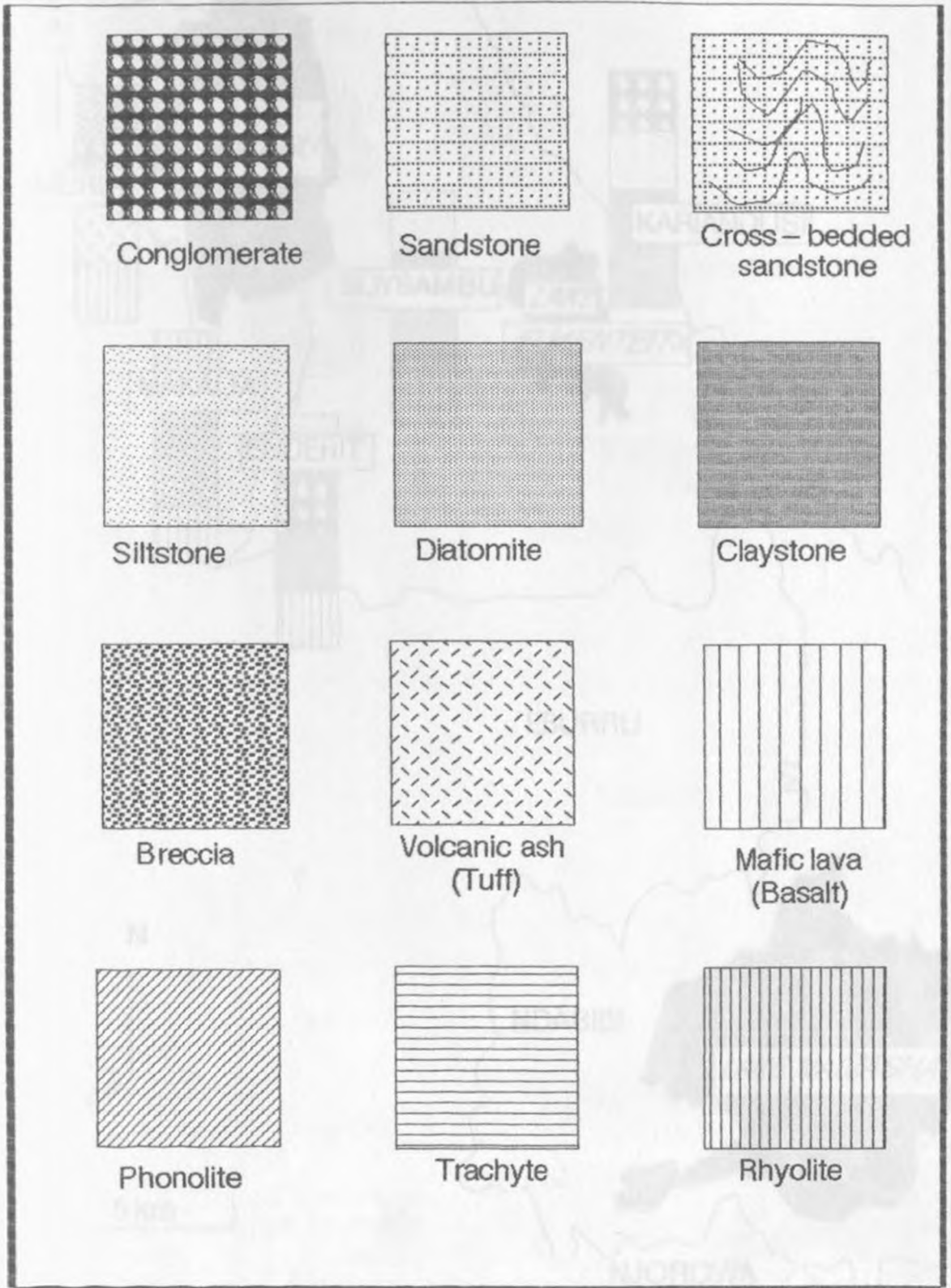


FIG. 3 – 1 Geological symbols for the measured lithostratigraphic sections.

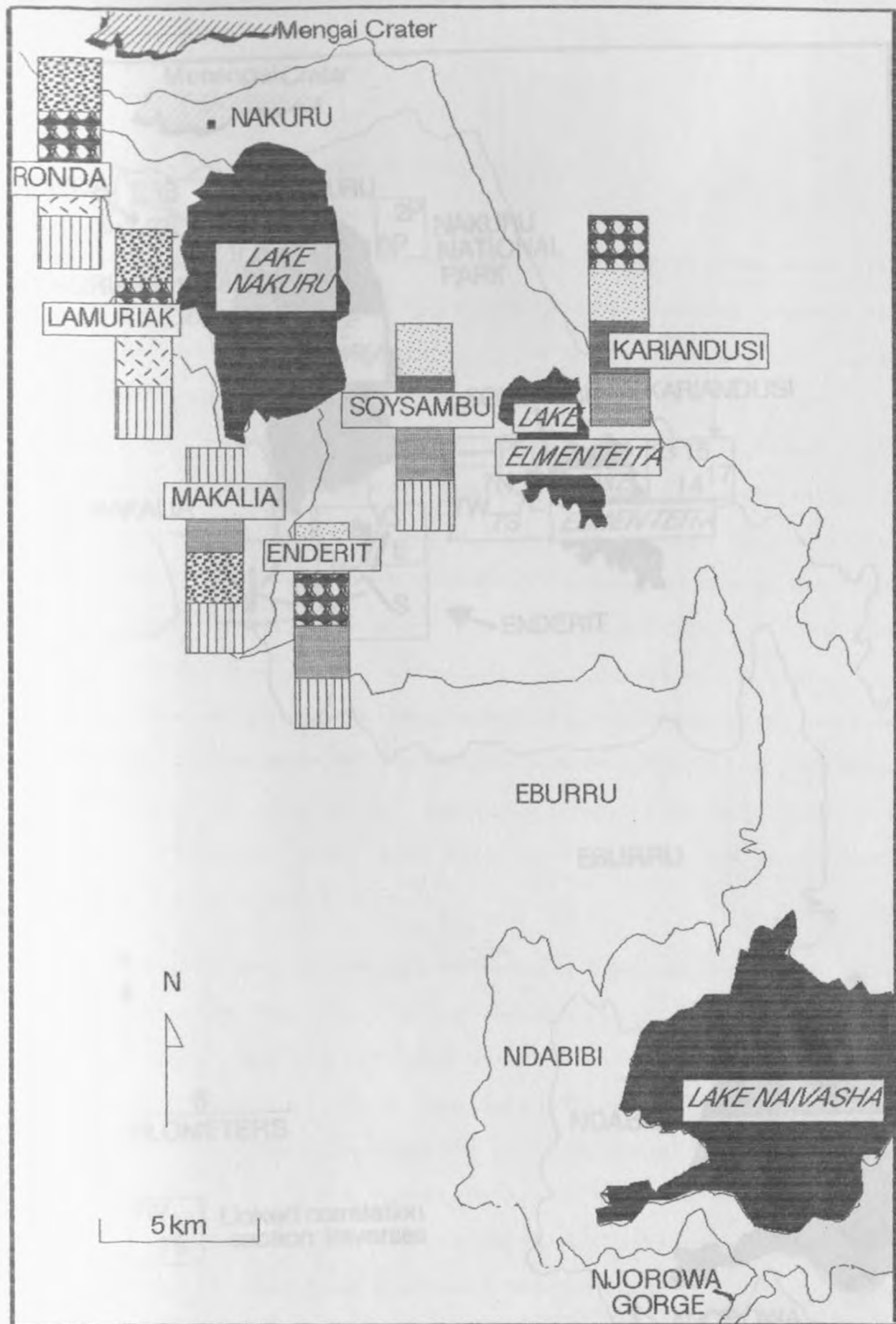


FIG. 3-2 Field locations of measured lithostratigraphic sections.



Fig. 3-3 Data point linkages for the correlated lithostratigraphic diagrams.

3.4 Sequence of the measured sections.

3.4.1 Kariandusi Formation

The Kariandusi Formation can conveniently be divided into two distinct lithological units although the boundary between the two sequences is gradational. The base of the the lower sequence exposed at the Kariandusi diatomite mine consists of a series of yellow gray (5Y7/2) claystones interbedded with olive gray 5Y4/1 siltstone. Because of poor exposure only 10 centimetres of this unit could be placed in the section. For purposes of description a boundary has been placed at the top of the diatomite. This point defines a significant transition from lacustrine to a fluvio-littoral dominated system. The lower stratum encompasses the sediments overlying this horizon and up to the base of the unconformable overlying Holocene sediments. In composite sections (Figs. 3-4 to 3-10) the entire thickness total some 30 m with 10 m in the lower unit and 20 m in the upper unit.

Exposures of the Kariandusi Formation make up the best type area for the Plio-Pleistocene and Holocene sediment in the study area. The exposure are hardly faulted and consist of numerous, repeated short sections. Although the upper top sequence is more heterogeneous than the lower unit, it does have several dominant characteristics. The most obvious of these is an almost cyclic sedimentation pattern consisting of basal rounded pumice gravels overlain by siltstones and

FIG. 3-4 Lithostratigraphic section of the Kariandusi Formation at the diatomite mine.

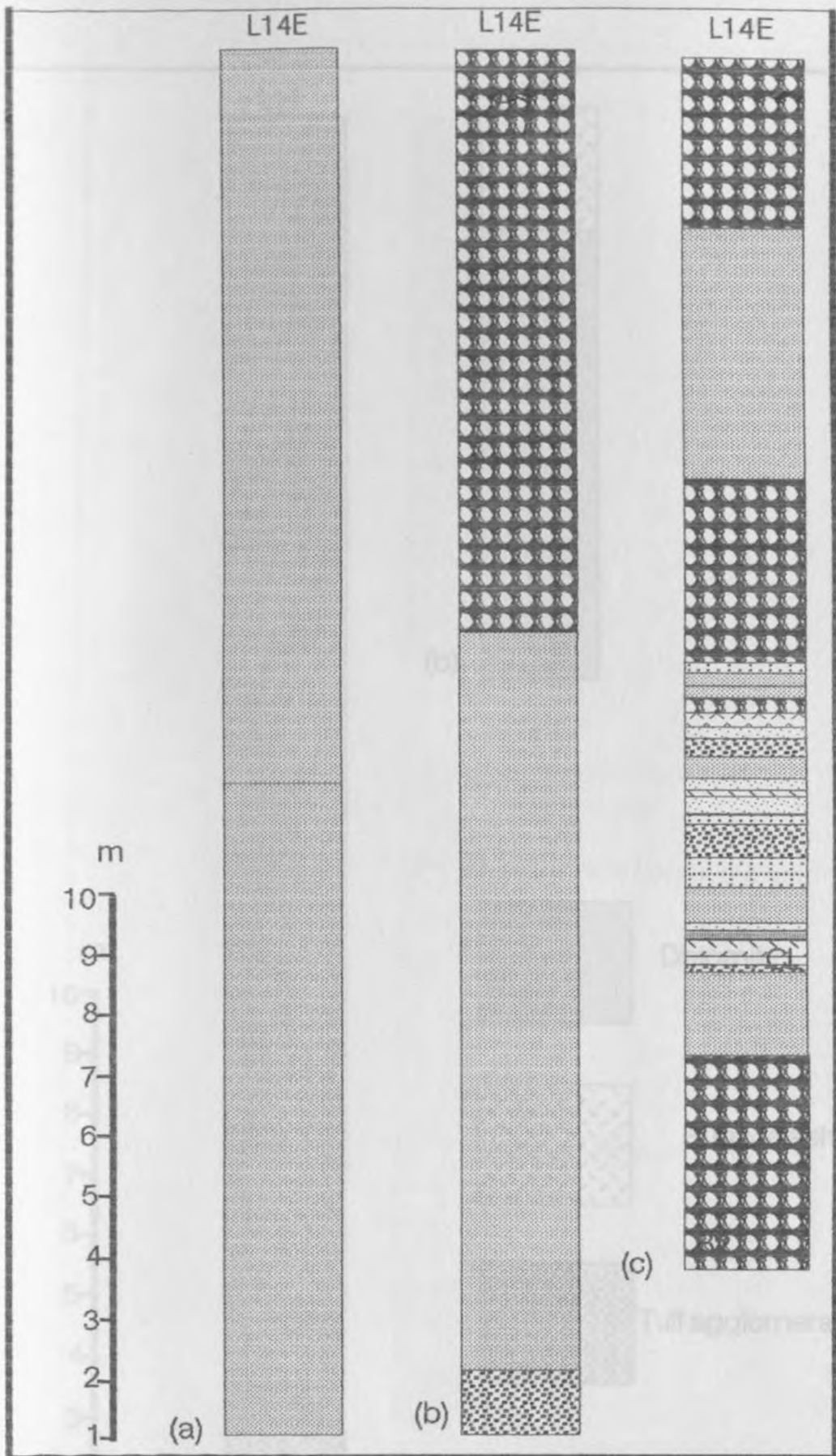


FIG. 3 – 4 Lithostratigraphic section of the Kariandusi Formation at the diatomite mine.

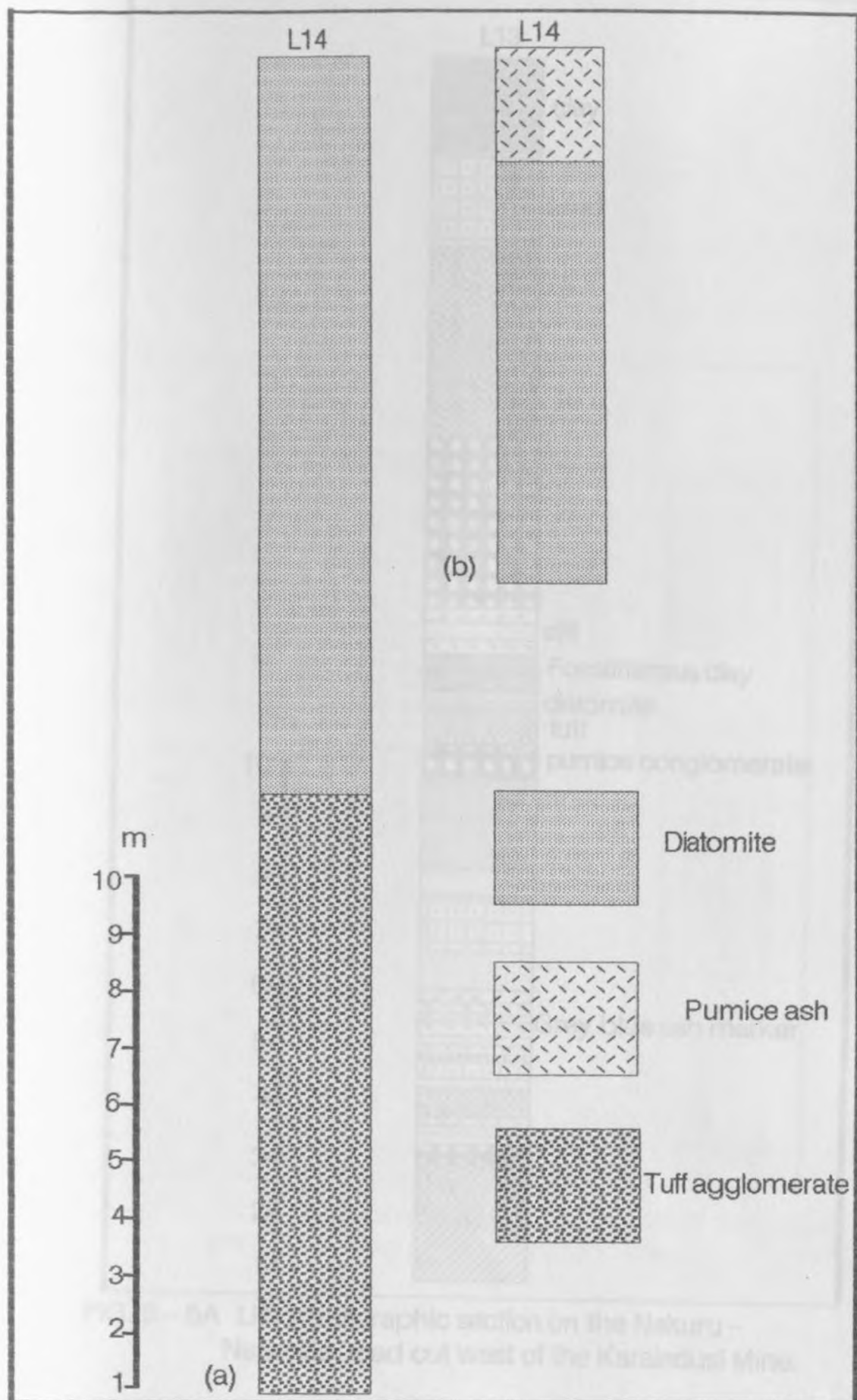


FIG. 3-5 Lithostratigraphic sections, east face of the Kariandusi Mine.

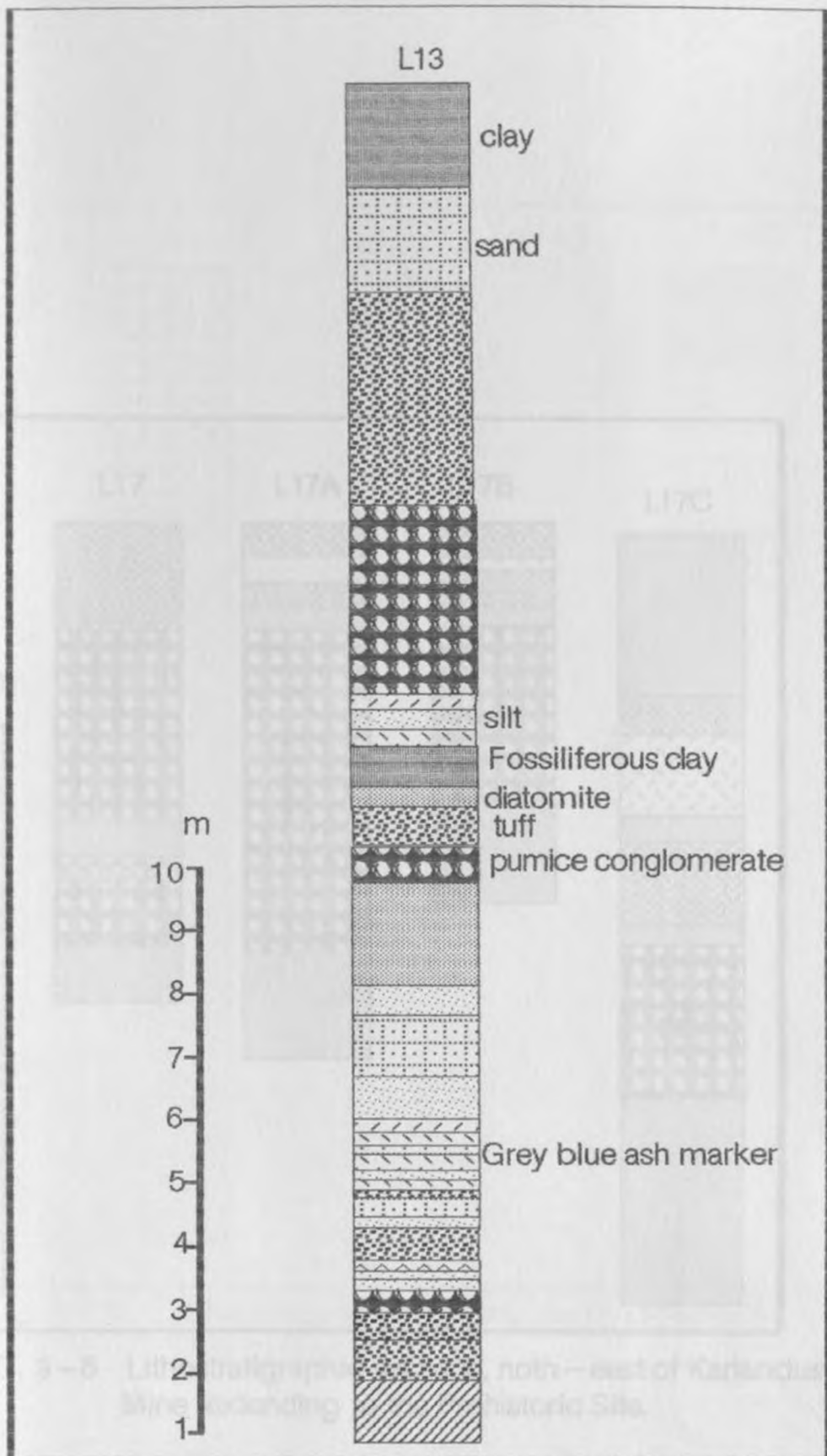


FIG. 3 - 5A Lithostratigraphic section on the Nakuru - Naivasha road cut west of the Karaindusi Mine.

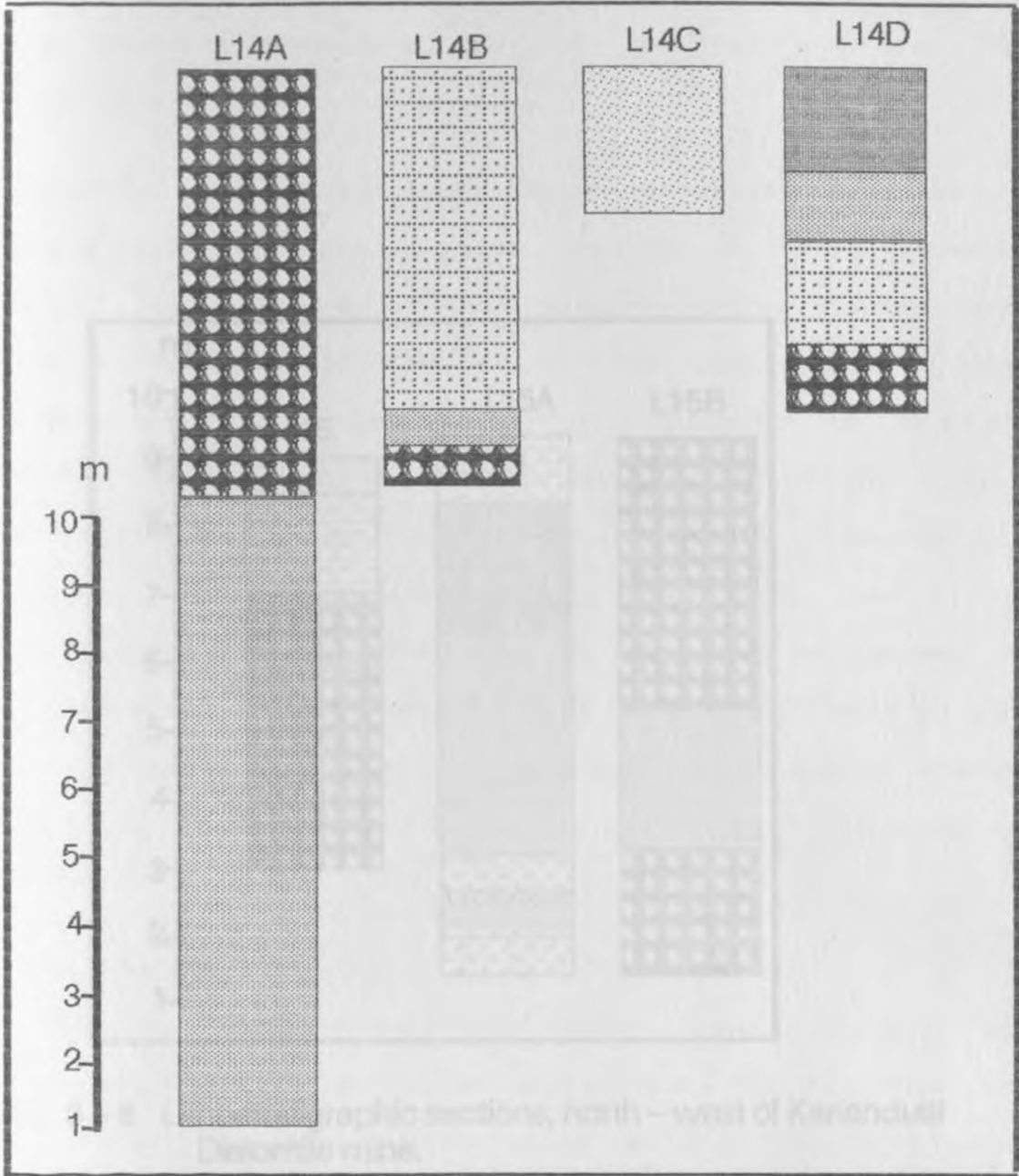


FIG. 3-7 Lithostratigraphic sections, south of Kariandusi Diatomite Mine.

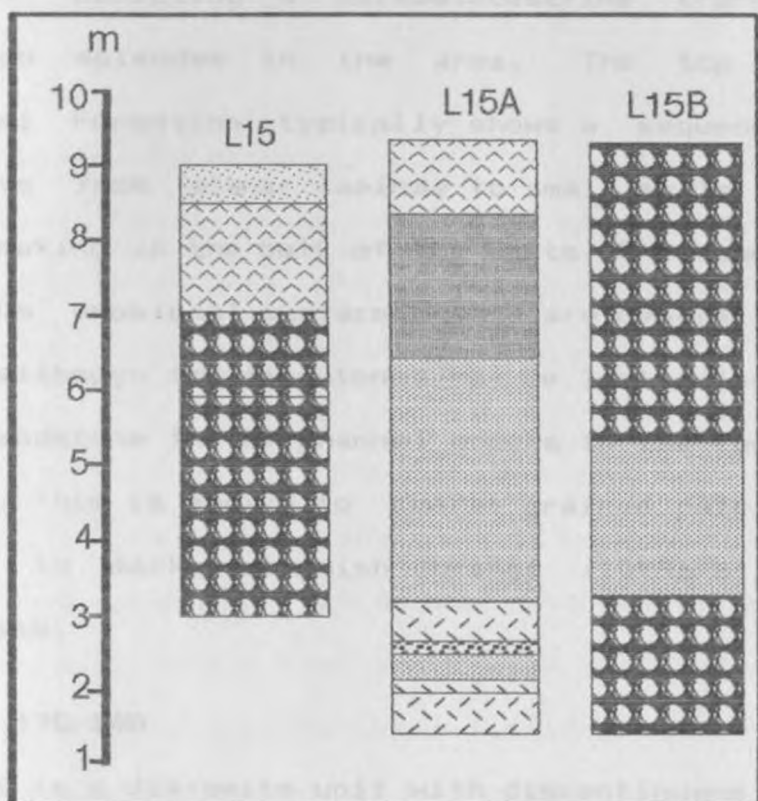


FIG. 3-8 Lithostratigraphic sections, north - west of Kariandusi Diatomite mine.

claystones which tend to coarsen upwards. The whole complex may or may not be incised by a channel. Other characteristics include abundant carbonates in form of calcrete and the apparent development of palaeosols.

The interval between the lower diatomite and the next major diatomite unit provides a good example of stratigraphic formation depicting a palaeolacustrine transgression and regression episodes in the area. The top units of the Kariandusi Formation typically shows a sequence of primary structures from planar laminae to small scale trough cross-bedding making up the bulk of the units. The base is marked by a sinuous erosional surface. These are generally tabular in nature although the sandstones may be lenticular in places. A major sandstone in the channel occurs in the lower half of the sequence. This is medium to coarse grained pale greyish orange (10YR8/4 to dark yellowish orange (10YR6/6) feldspathic litharenite.

Traverse 17C-14D

Bed 14B1 is a diatomite unit with discontinuous unstratified pumice patches of no preferred orientation. The formation is filler variety, locally referred to as F. B1 is the pure white diatomite. Blue volcanic intercalations occur within the diatomite. Deposition of the diatomite on lava was associated with intermittent pumice ash. The diatomite was directly

accumulated on a pre-faulted and erosional lava surface. It is thicker within the troughs but relatively thinner on the raised ridges. The agglomeratic base was sparsely strewn with obsidian fragments. B2 is very fine grain intercalation(s) of bluish grey ash within 13.4m thick diatomite bed. Fine grain tabular diatomite grades into B3 which is a poorly sorted pink grey angular pumice tuff, thinning 3.5 m. westward into a laminated diatomaceous clay.

3.4.2 Soysambu Formation

A detailed field study of east-west traverse of the lithostratigraphy from the Soysambu diatomite mine to the south-eastern edge of Lake Nakuru revealed numerous lithofacies associations representing varied depositional environments (Figs. 3-11, 3-12, 3-13). The strata range from pure lacustrine at the mine to alluvial fans towards Lake Nakuru. At the mine the Soysambu sequence consists essentially of lacustrine diatomite beds. Within the lake beds a tuff outcrops as a thin intercalation at a comparatively similar and distinct level to the Kariandusi Formation. The lowermost lacustrine Bed 1 at the mine, locality 7N, is underlain by interfingering sand and tough layers with repetitive laminations. The colour was however recorded when wet but was apparently ranging between yellowish brown to dirty white calcified sandy tuff. At location 7W dry land surface marked with thin ripple marks, calcareous caliche, very fine grain well sorted, upper contact

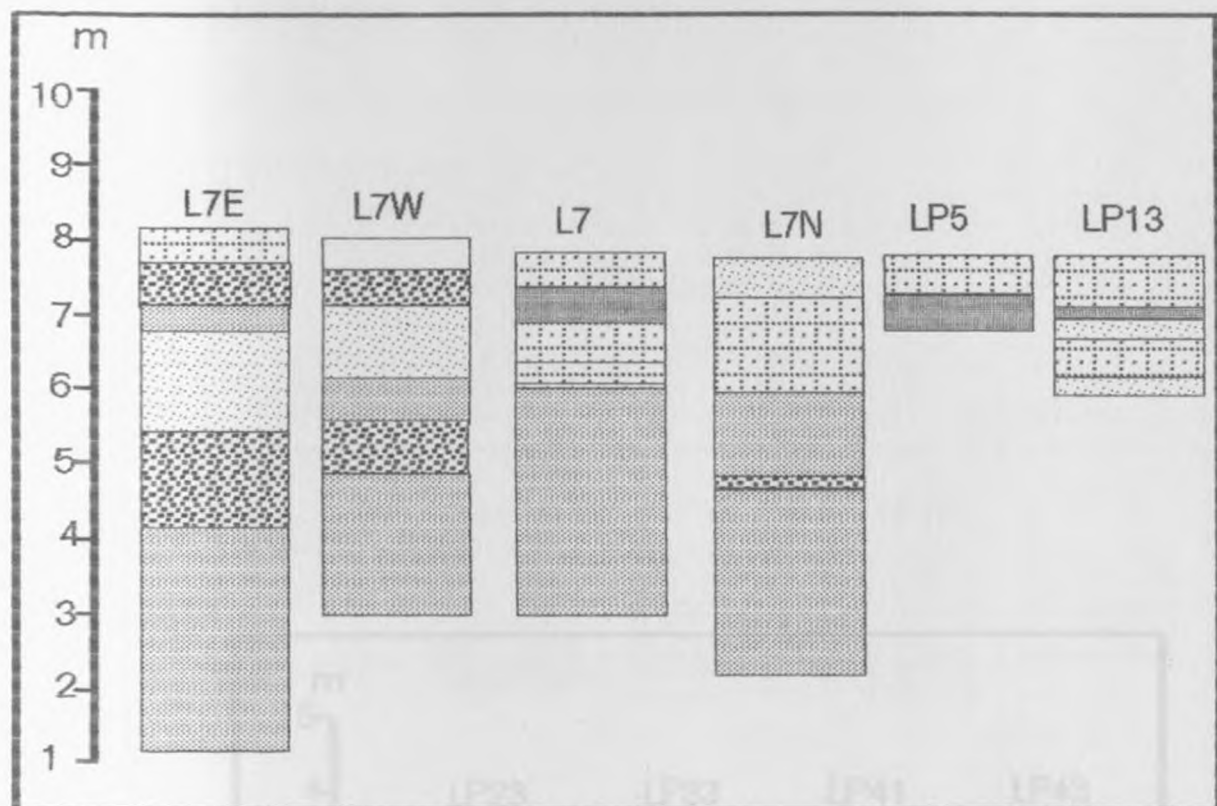


FIG. 3-10 Lithostratigraphic sections of the Soysambu Diatomite Mine.

FIG. 3-11 Lithostratigraphic sections along a west-east transect from the edge of Lake Waikare to the Soysambu Mine.

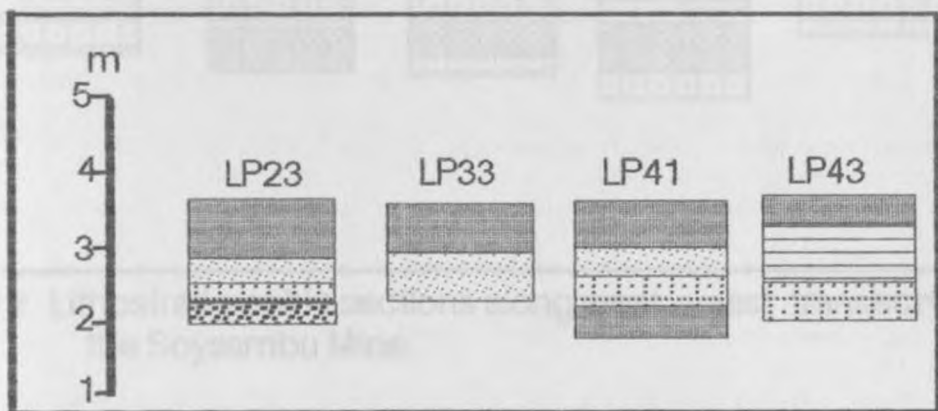


FIG. 3 – 11 Lithostratigraphic sections along a west – east transect from the edge of Lake Nakuru basin to the Soysambu Mine.

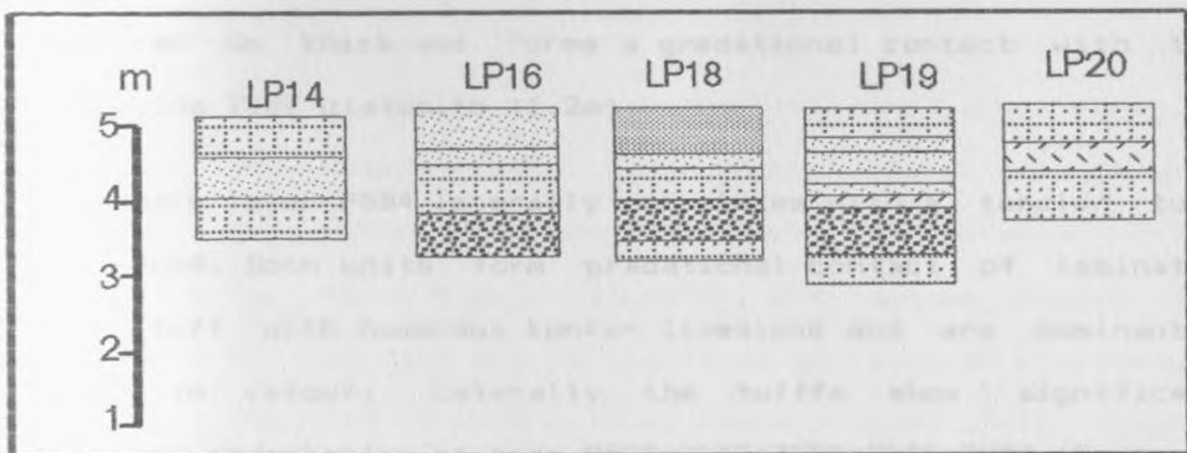


FIG. 3-12 Lithostratigraphic sections along west - east transect of the Soysambu Mine.

indicates drying diatomite-rich lake. Towards the top cm laminated pumice intercalation into diatomite proved a useful marker horizon locally. Poorly sorted lithic silty tuff palaeosol land surface was later covered with a laminated lacustrine diatomite, locally worked as BU-diatomite. Bed 1 is separated from the overlying 7NB2 by thin volcanic ash intercalation. Bed 7NB3 is well sorted laminated dirty white diatomite (D-diatomite) which formed a thick tabular bed with minor occurrences of kunkar limestone at the top of the sequence. On the quarry's eastern face 7EB1, the diatomite measured 3m thick and forms a gradational contact with the overlying 7EB2 diatomite (1.2m).

A pumice layer P5B4 laterally correlates with a tabular tuff Bed 7SB4. Both units form gradational contact of laminated fine tuff with numerous kunkar limestone and are dominantly brown in colour. Laterally the tuffs show significant physical correlation of beds P5B5=7EB5=7SB3=7NB5=7WB5 (Figs. 3-11; 7-3-4). At the mine, Bed 7WB4 characterised by a gradational calcrete horizon formed in rippled and laminated silt. The coarse sandy silt is tabular poorly sorted, laminated and occasionally grades into yellow sand. At locality 7SB2 the same unit is very fine grained, well sorted lenticular yellowish brown silt. It is immediately overlain by a moderately poorly sorted, tabular dirty white pumiceous tuff. The fine tuff show lamination with numerous kunkar limestone

sometimes forming tabular brown coloured tuff and gradually, imperceptibly grades into fine to coarse grain yellowish brown silty clay.

A traverse from the diatomite work site at Soysambu westward over a distance of 5 km to the eastern edge of Lake Nakuru revealed different types of sediments. The post lacustrine sandstone deposition in the area is dominantly volcanic-rich thinly bedded fine to coarse - grained, light gray (7N) tuff or tuffaceous sandstone with planar bedding and locally abundant rhizoliths. The basal portion consist of a massive, pale yellowish brown (10YR6/2), arenaceous claystones which contains abundant gray pumice clasts. These pumice clasts are totally altered but contain abundant feldspar phenocrysts often measuring up to 0.5 cm in diameter. The pumice clasts are concentrated near the top of the 10 cm arenaceous claystones. Overlying the unit is an erosional contact immediately covered by 1.2 m lenticular tuff and tuffaceous sandstone. Again the tuff is totally devitrified. This unit is pinkish grey (5YR8/1) to medium light grey and contains small to medium scale planar to ripple laminations with occasional small-scale trough cross-stratification. The unit fines upwards and has distinct but irregular upper contact with overlying arenaceous claystones. Towards the top of the sequence is a channel formed sand. This is a medium to coarse grained feldspathic litharenite pale

greyish orange (10YR8/4) to dark yellowish orange (10YR6/6) with well developed medium-scale trough cross-bedding.

The base of this unit is marked by 1m thick erosional contact of conglomeratic channel lags and pebbles to granule sized clasts. Laterally where the channel is absent is a coarse, dark yellowish gray (Y6/2) siltstone. A distinctive polygonal structure consisting of anastomosing veins of a much lighter coloured silty sandstone is locally present in the upper part of the siltstone. These are tectonic dykes filled with yellowish orange arenaceous silts and reworked diatomite.

3.4.3 Enderit Formation

The Enderit Formation is a complex of arenaceous agglomerate and tuffs measuring 10 m in total thickness. The outcrop at the drift show a dip slope of a portion of the units. The Formation varies laterally and vertically in Rivers Enderit and Makalia areas where the basal portion invariably consists of agglomerates, granules and rarely diatomaceous silts. Whereas the agglomerates are poorly sorted, most of the silts are often well sorted yellowish gray (5Y7/2) to greyish, orange (10Y7/4) siltstones. At the drift the silts are inclined at an angle of 2 to 5 degrees to the south-west. Above these occurs a series of laminated to thinly bedded light or olive gray (5Y6/1) siltstones and sandstones. Individual sandstone beds are 2 cm to 10 cm thick and alternate with arenaceous deposits. The

uppermost silts grade through a series of very fine laminations into the overlying units. In the Enderit River outcrop sections a cut and fill of granule units were observed repeatedly within the silts. The tuffs intercalating diatomites are fine grained very light grey tuff. It attains thickness of a few centimetres.

Traverse 8D-LB Bed1

The base of the sequence vary in thickness between 10.6 m and 3.2 m. The unit is pumiceous tuff cross channel deposit. It comprises lateritized trachytic obsidian, reworked silts, pebbles rounded to weakly subrounded, large conglomerate pebbles some measuring $10 \times 5 \text{ cm}^2$ in size. Above B1 formed a relatively more pumiceous orange yellow tuff. This lithological unit is well sorted tabular with white yellow bands. The bed is laminated yellow 5Y/V6 silt with Kunkar limestone nodules. In stratigraphic position, B1 (LBA) laterally correlates with B3(LB) where trachyte clasts of $10\text{cm} \times 9\text{cm}$ with patches of pumice ash formed trough cross bedding. The unit show gradational contact in places, vein filled with reworked diatomaceous silt. It is reddish brown, poorly sorted subrounded conglomerate clasts measuring $11\text{cm} \times 8\text{cm}$.

Traverse 8D-LB Bed2

This section predominantly consists of pumiceous yellow tuff. The units here display a well rounded granules with

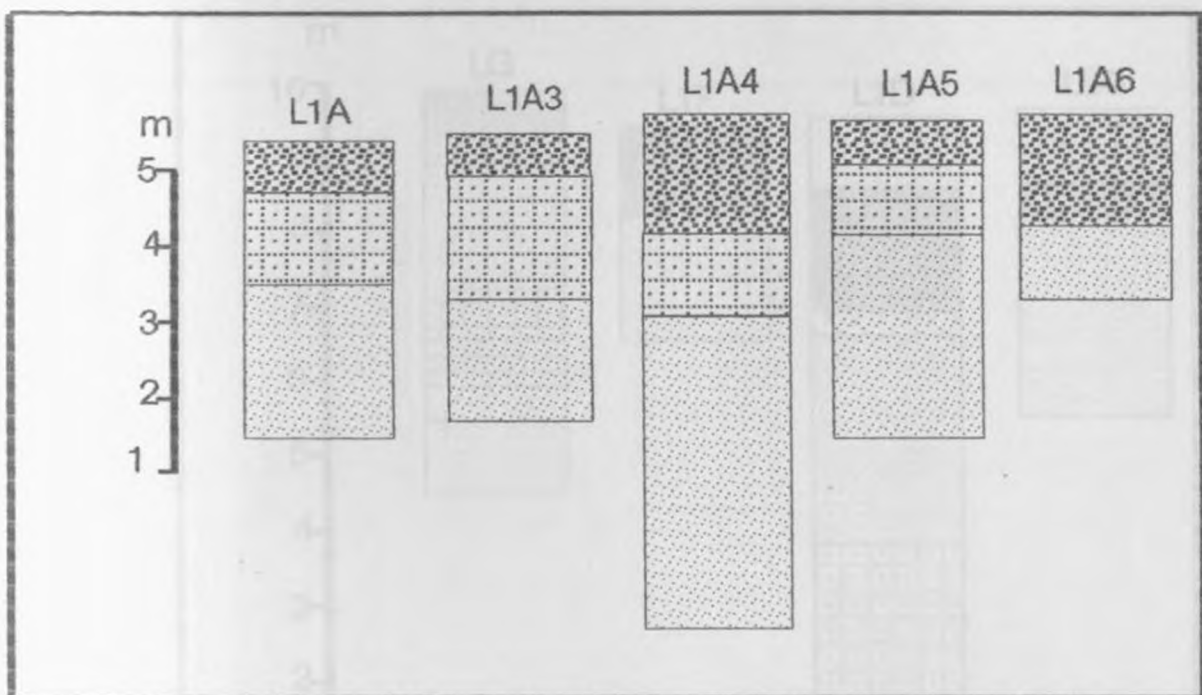


FIG. 3-13 Lithostratigraphic sections, south of River Enderit drift.

FIG. 3-14 Lithostratigraphic sections, along River Enderit.

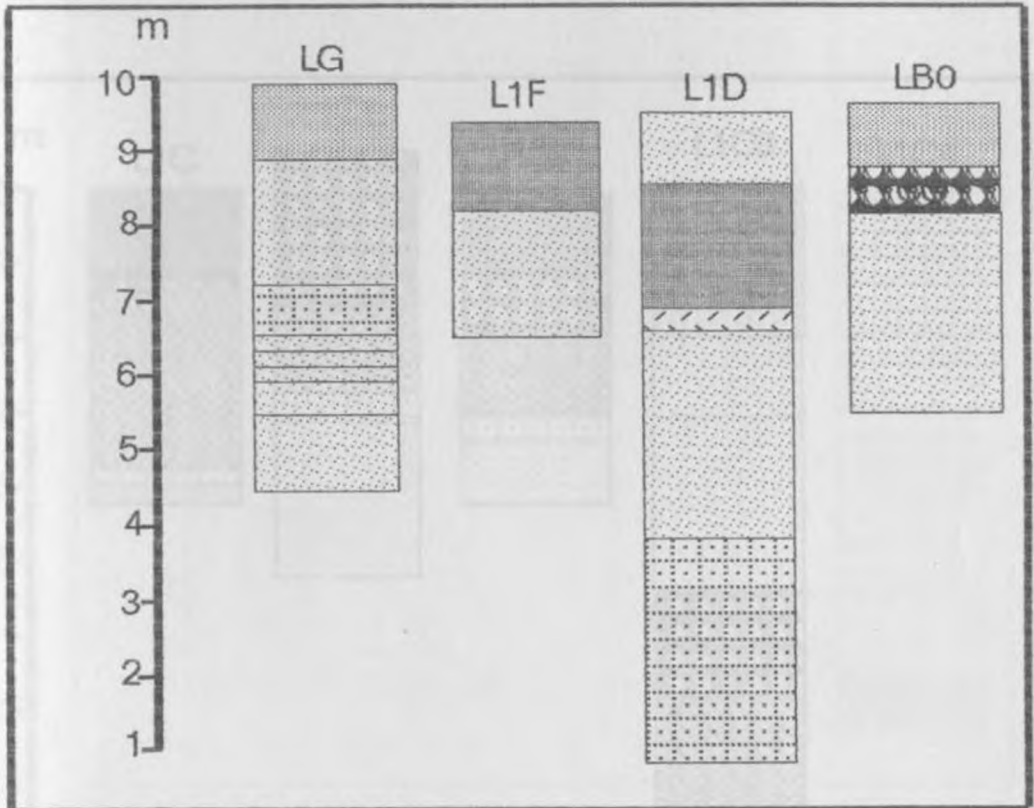


FIG. 3 – 14 Lithostratigraphic sections , along River Enderit.

3 – 15 Lithostratigraphic sections, Enderit River drift.

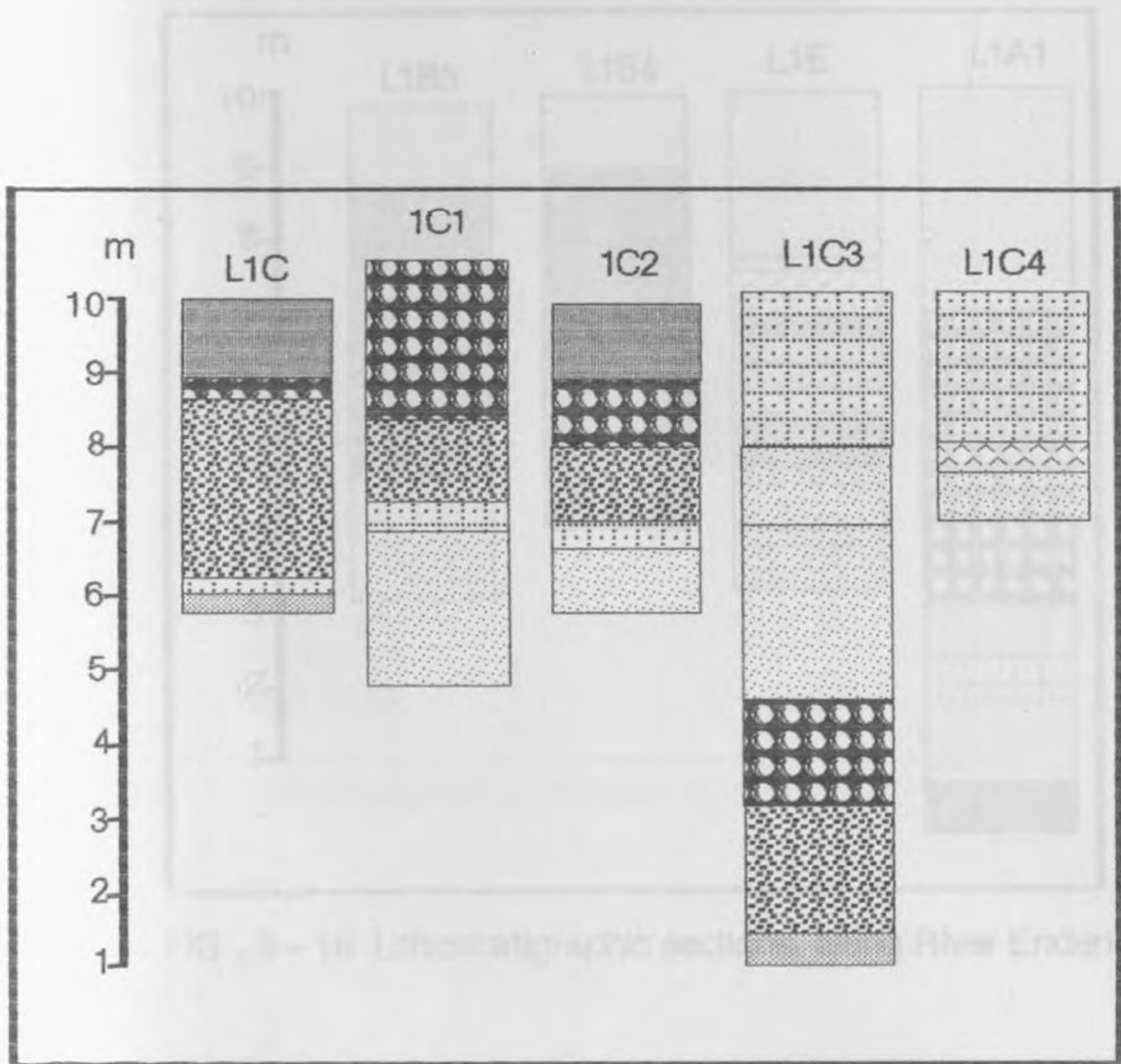


FIG. 3-15 Lithostratigraphic sections, Enderit River drift.

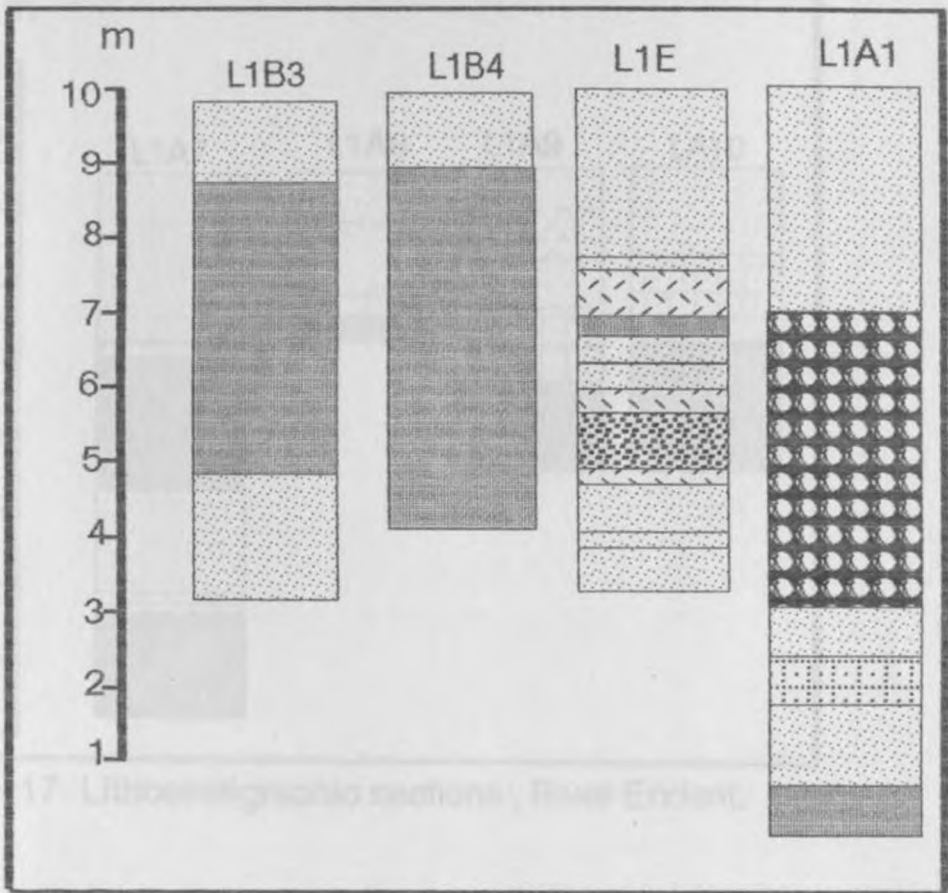


FIG . 3 – 16 Lithostratigraphic sections, along River Enderit.

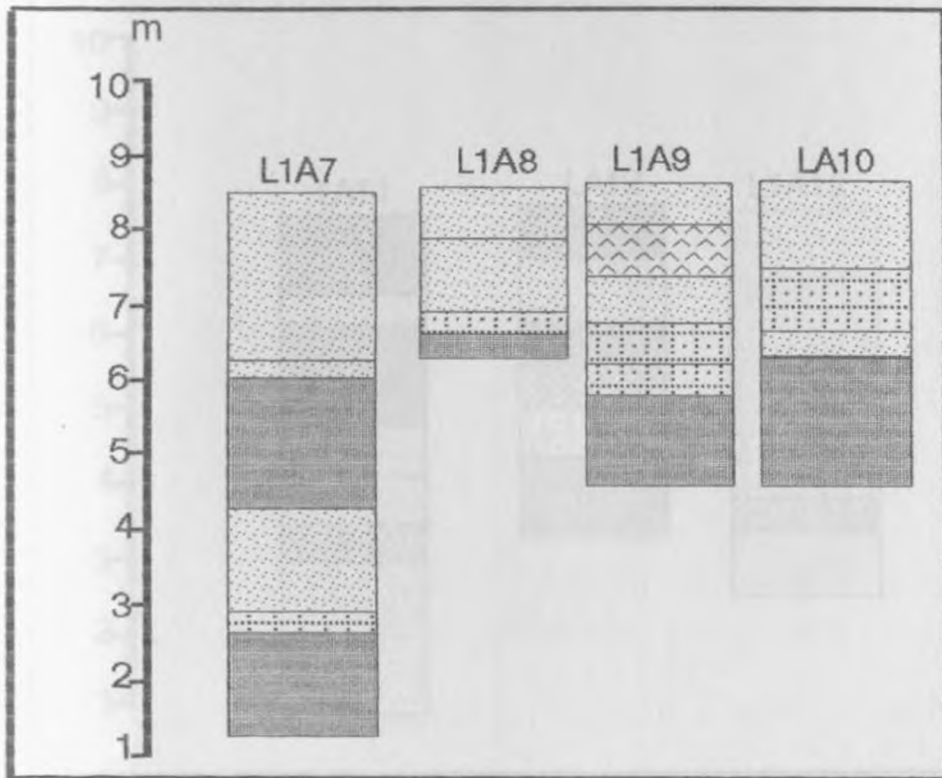


FIG. 3-17 Lithostratigraphic sections , River Enderit.

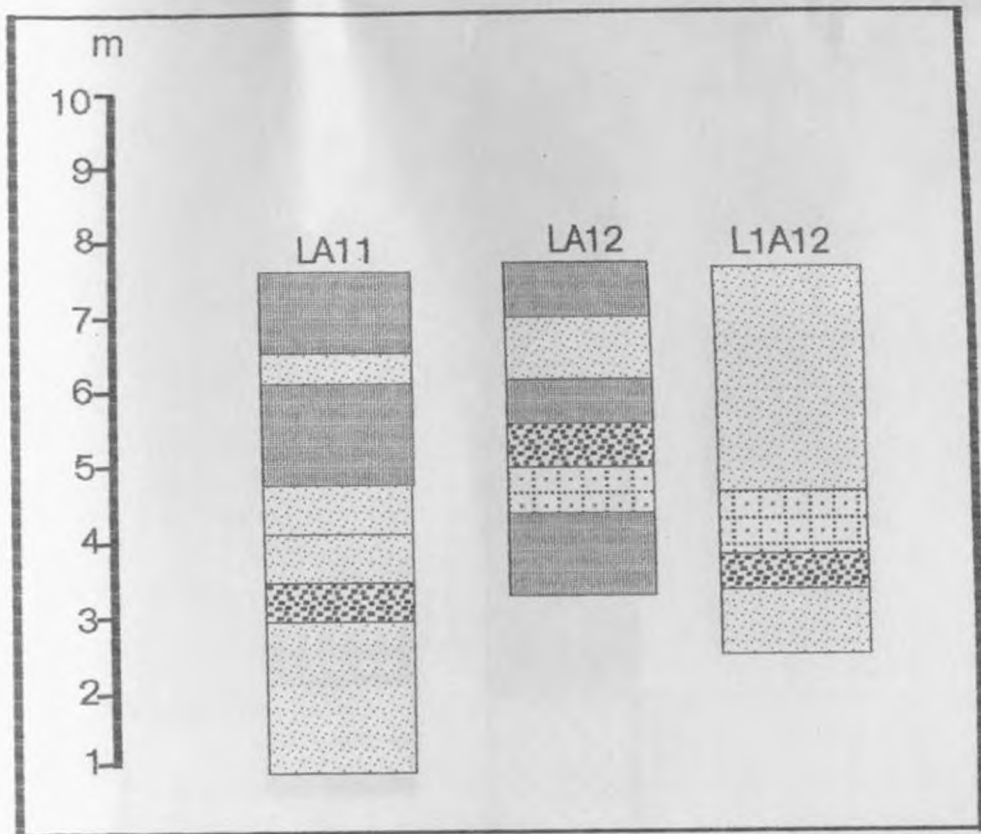


FIG. 3-18 Lithostratigraphic sections , Enderit River drift.

FIG. 3-18 Lithostratigraphic sections, Enderit River drift.

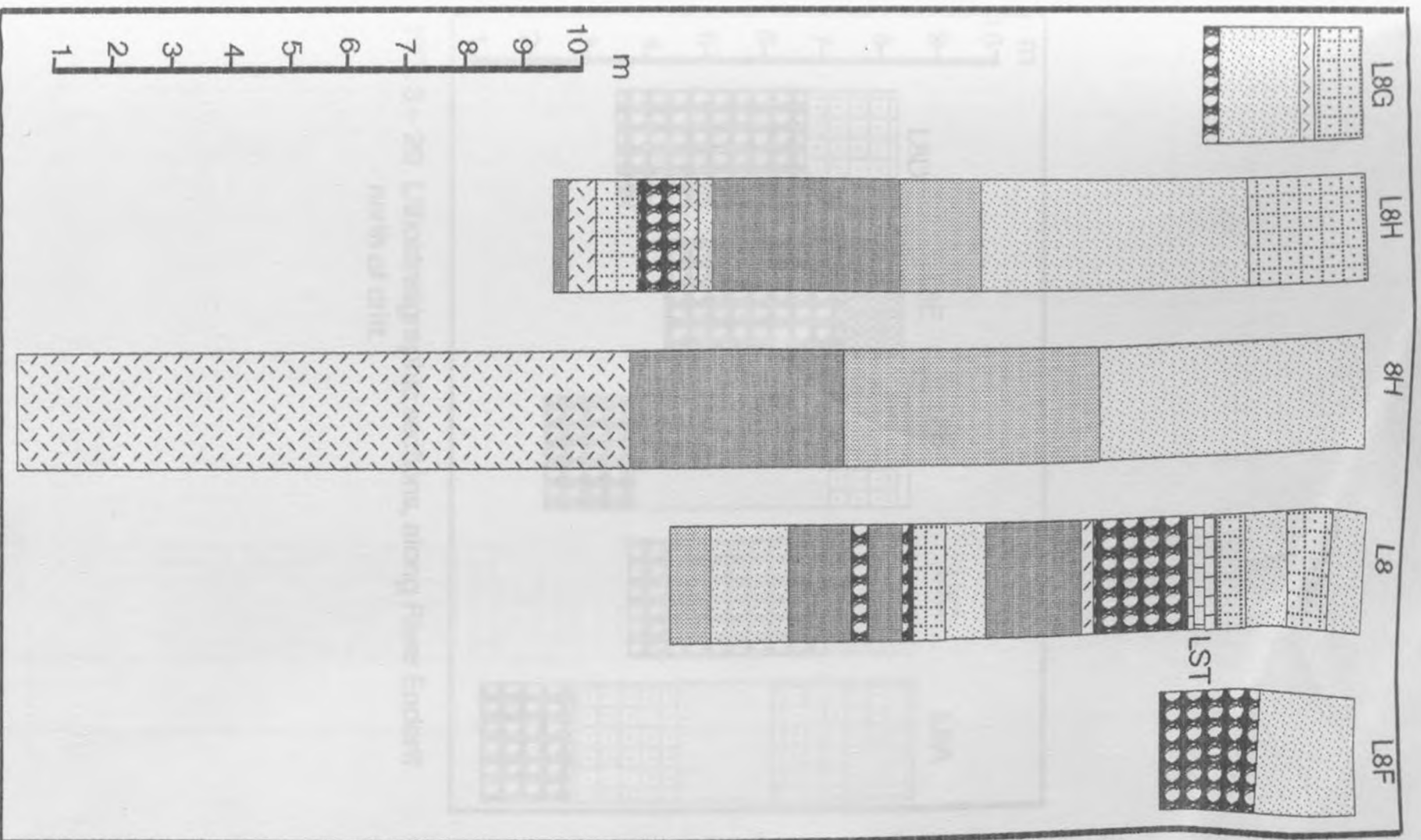


FIG. 3 – 19 Lithostratigraphic sections, north Enderit Drift.

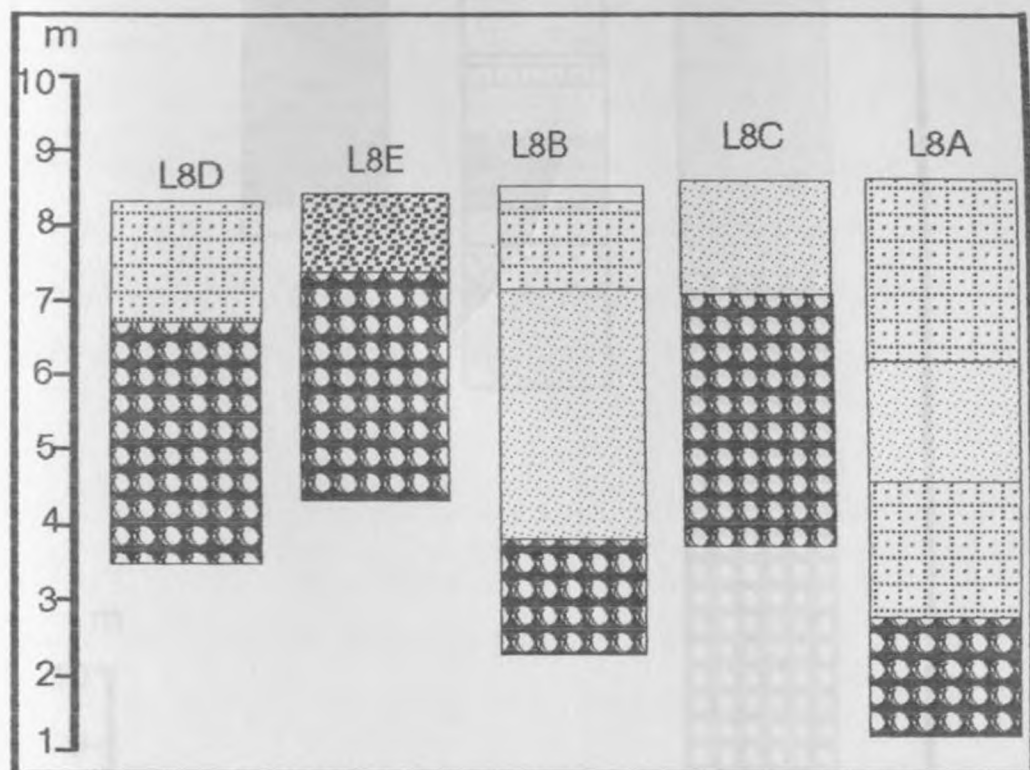


FIG. 3-20 Lithostratigraphic sections, along River Enderit north of drift.

FIG. 3-21 Lithostratigraphic sections, Enderit Drift.

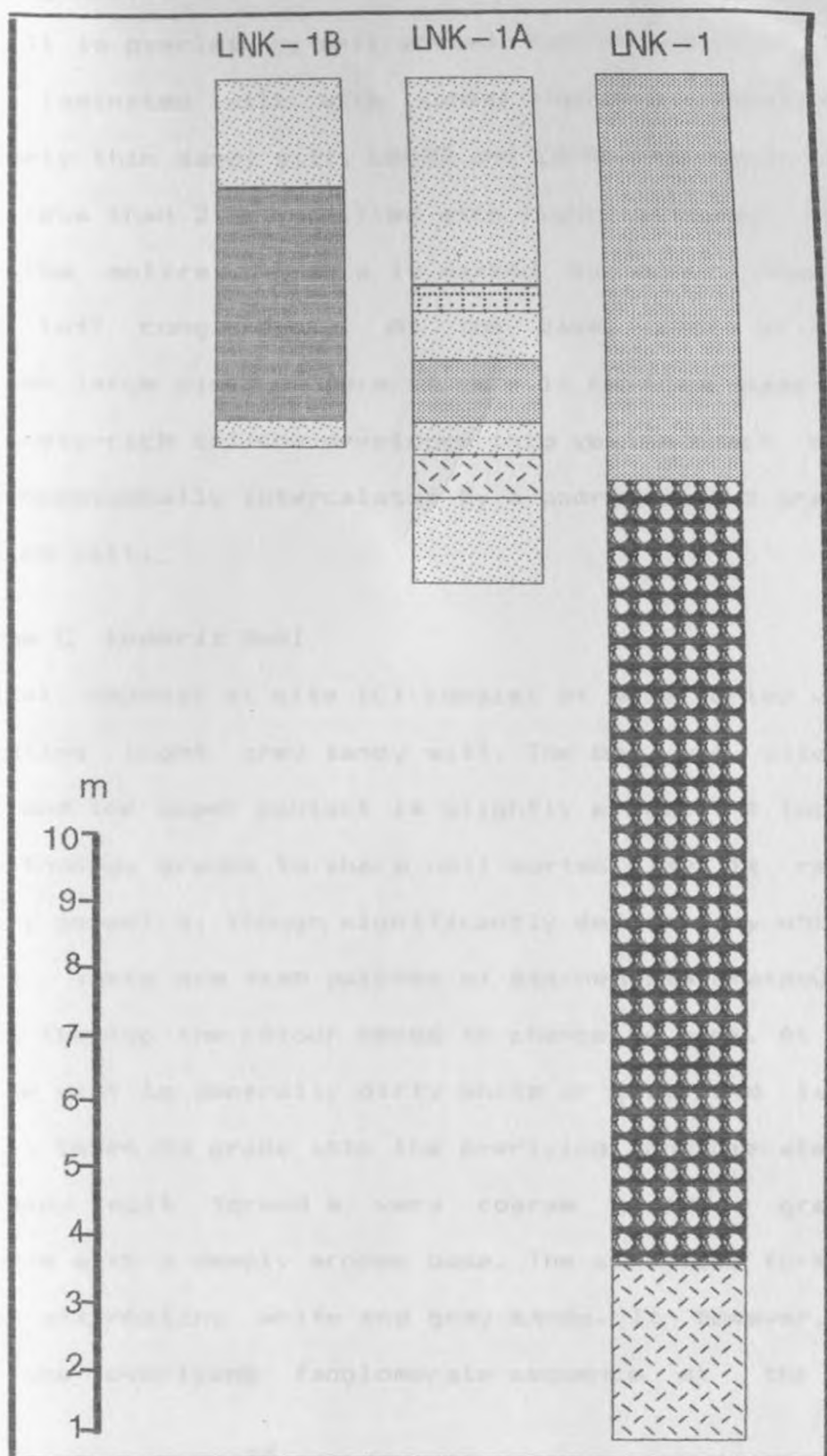


FIG . 3-21 Lithostratigraphic sections, Enderit Drift.

marked gradational contacts between laminated Bed 8CB1 and 8BB2. It is overlain by well sorted, tabular, whitish yellow 5Y/V6 laminated silt with kunkar nodules limestone. A relatively thin sandy silt, L8AB2 and L8AB3 has tectonic vein dykes less than 2 mm in filled with light coloured limonitic clay. The entire sequence is marked by minor cross-bedded pumice tuff conglomerate. At the base, L8B1 of Enderit Formation large pink boulders 15 cm x 12 cm thick base underlie a calcrete-rich caliche developed into yellow beach silt and gravel occasionally intercalated by a poorly sorted gravel rich laminated silt.

Traverse C Enderit Bed1

The basal deposit at site 1C1 consist of well sorted very fine alternating light grey sandy silt. The bed was oxidised to yellow and the upper contact is slightly eroded. At location 1C the lithology grades to sharp well sorted clay. It reveals a tabular, geometry, though significantly deformed by white root tubules. There are also patches of stained diatomaceous silt. Towards the top the colour tends to change to pink. At location 1C3 the silt is generally dirty white or grey and laminated. The unit tends to grade into the overlying fanglomerates. Above the sandy silt formed a very coarse grained gradational sandstone with a deeply eroded base. The sandstone formed cross bedded alternating white and grey bands. It however, wedges below the overlying fanglomerate sequence at the Enderit

Drift. The lithology of the fanglomerate is largely coarse sand and pebble clasts. North of the Drift the bed is poorly sorted unconsolidated conglomerate incorporating reworked diatomites. At LC3 the conglomerate consists predominantly of reworked diatomaceous pumice. On the conglomerate was deposited a well sorted laminated tabular light grey clay and at the locality L1C beds B5 and B4 were intercalated with laminated black granules.

Traverse 1A-1A13

The Traverse 1A-1A13 run east - west into the Enderit Drift and the lowermost Bed 1 measures 2.5 m from the base. It consists of white silty clay which grades into an oxidised siltstone. The white silty clay unit laterally grades into beach granule at the top. The bed increases in thickness 5.7 m towards the depocentre where it abruptly changes to yellow sand, grey pumice and poorly sorted 2.7m thick pumice gravel mixed with silt 1A4. At locality 1A5 the unit comprises a very fine sand intercalated by a thinning out silt overlain by a fairly uniform fanglomerate bed. The fanglomerate unit consists of large angular boulders measuring 20 cm x30 cm at 1A2. The fanglomerate bed is essentially thick mud slurry incorporating huge boulders. This massive fanglomerate is extremely poorly sorted with a grain size range varying between silt to large boulders. Within the same lithological

unit, beds B2, B3 and B4 belong to a single stratum which was relatively lighter in colour and shows banding of yellowish oxidised patches. The basal level of B2 is fine grained well sorted tabular silt with a colour range between slightly grey 5YR 6/1 and reddish yellow 6/6 silty tuff. The silt is intercalated with hard oxidised band forming a hard resistant tuff. The tuff bands sometimes occur in streaks although the unit is well sorted. The bed is nearly tabular in geometry with dip of 10° south towards the depocentre. The bed is pinkish white 7.5 YR 8/2 diatomaceous silt. Within the bed were preserved plant rootlets characteristic flood plain deposition. A thin laminated orange layer between B2 and B3 is marked by 3 cm and 5 cm grey silt bands at the base and top respectively.

The top of this unit (B4) is marked a sharp contact and comprise a well sorted tabular silt bed. It varies between .75m to 1 m in thickness. The unit is light reddish brown 5YR 6/3. The unit consists of minute volcanic glass mudstones, siltstones and altered small plant rootlets. The stratum is overlain by Bed B5, a laminated sandstone often intercalated with conglomerates. The thin conglomerate shows a slight sinuosity at the top and a sharp base. The conglomerate unit is made up of huge boulders with thick mud slurry matrix. It occasionally developed massive sections attributed to possible localised tectonic adjustments within the basin. The unit

measures 3 m in thickness wedging out towards the south. Lithological units B7, B8, B9 and B10 above the conglomerate are loosely lithified non-conformable yellow clay silt with columnar jointed base. The silt clay is interspersed with grey tuff of volcanic ash intercalated with yellow granules. The pumice tuff is friable, laminated and highly porous and occasionally it bears reddish brown oxidised silt.

3.4.3.1 Makalia Beds

The Makalia beds are well exposed along the River Makalia and along the ridges of the western and southern fault scarps bounding the southern margin of Lake Nakuru. The sediments vary considerably along the stream both in thickness and composition. The overall thickness ranges from less than 0.5 m at the edge of the west-north bounding fault scarp to well over 10 m in the south. The sediments can be grouped into two units, a predominantly fine grain diatomite rich intercalation with occasional sandy siltstones and coarse poorly sorted bright orange tuffs towards the top. The lower fine grained unit documents a major lacustrine transgression in the area. The upper sequence varies significantly from the northern ridge. Towards the south the strata consist of cross-bedded pumice gravels, sandstones and siltstones deposits in a dominantly fluvial environments. Along the southern ridge the sediments are generally repetitive sequence of lacustrine siltstones ,

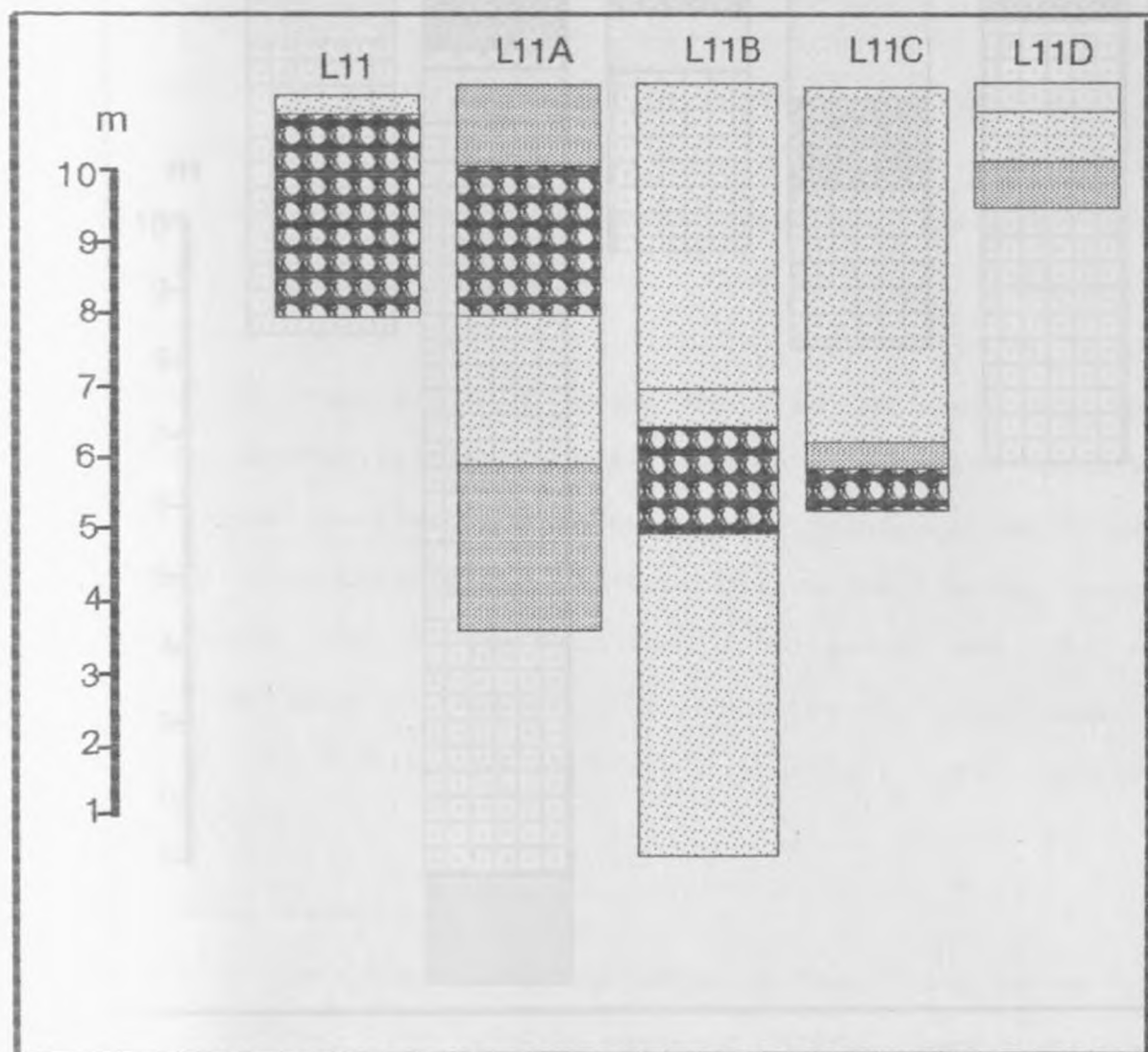


FIG. 3-22 Lithostratigraphic sections, west of the River Makalia.

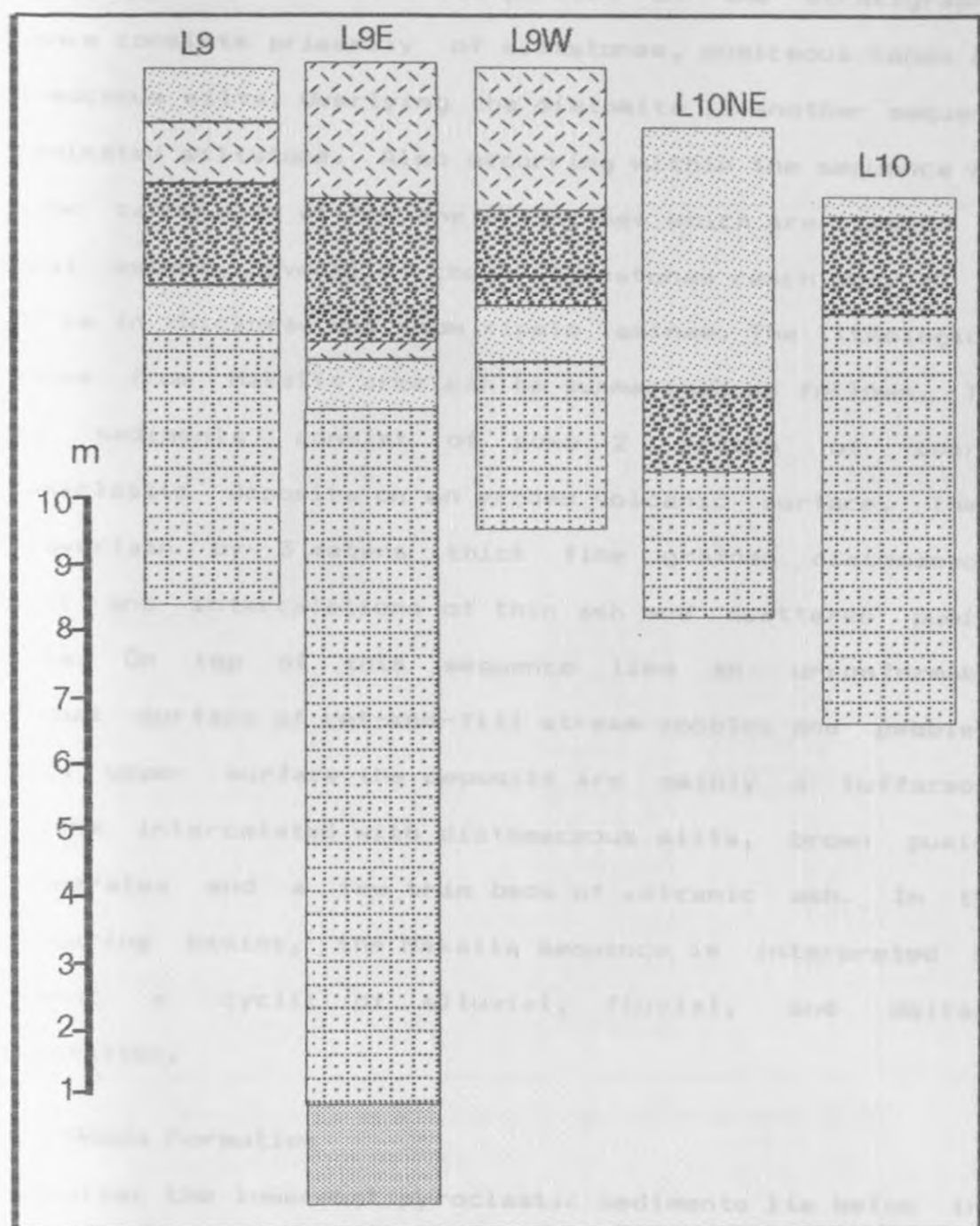


FIG. 3-23 Lithostratigraphic sections along eastern bank, River Makalia

diatomites, and fluvial pumice sandstones and siltstones (Figs. 3-22 and 3-23). This portion of the stratigraphic sequence consists primarily of siltstones, pumiceous sands and diatomaceous silts. Overlying the diatomite is another sequence of laminated siltstone. Also occurring within the sequence are caliche carbonates within the siltstones which are limited in lateral extent. Several of these limestones reach only 20 cm to 30 cm in thickness and show ripple laminae. The lithological sequence from Makalia area can be summarised as follows. The basal sediments consist of some 2 meters of coarse volcaniclastic deposits on an eroded volcanic surface. These are overlain by 3 meters thick fine grained diatomaceous deposit and intercalations of thin ash and scattered pumice gravels. On top of this sequence lies an unconformable erosional surface of cut-and-fill stream cobbles and pebbles. In its upper surface the deposits are mainly a tuffaceous sandstone intercalated with diatomaceous silts, brown pumice conglomerates and a few thin beds of volcanic ash. In the neighbouring basins, the Makalia sequence is interpreted to represent a cyclic of alluvial, fluvial, and deltaic sedimentation.

3.4.4 Ronda Formation

At Lamuriak the lowermost pyroclastic sediments lie below the Ronda Formation. The author examined these sediments and recognised that they are primarily clastic volcanogenic

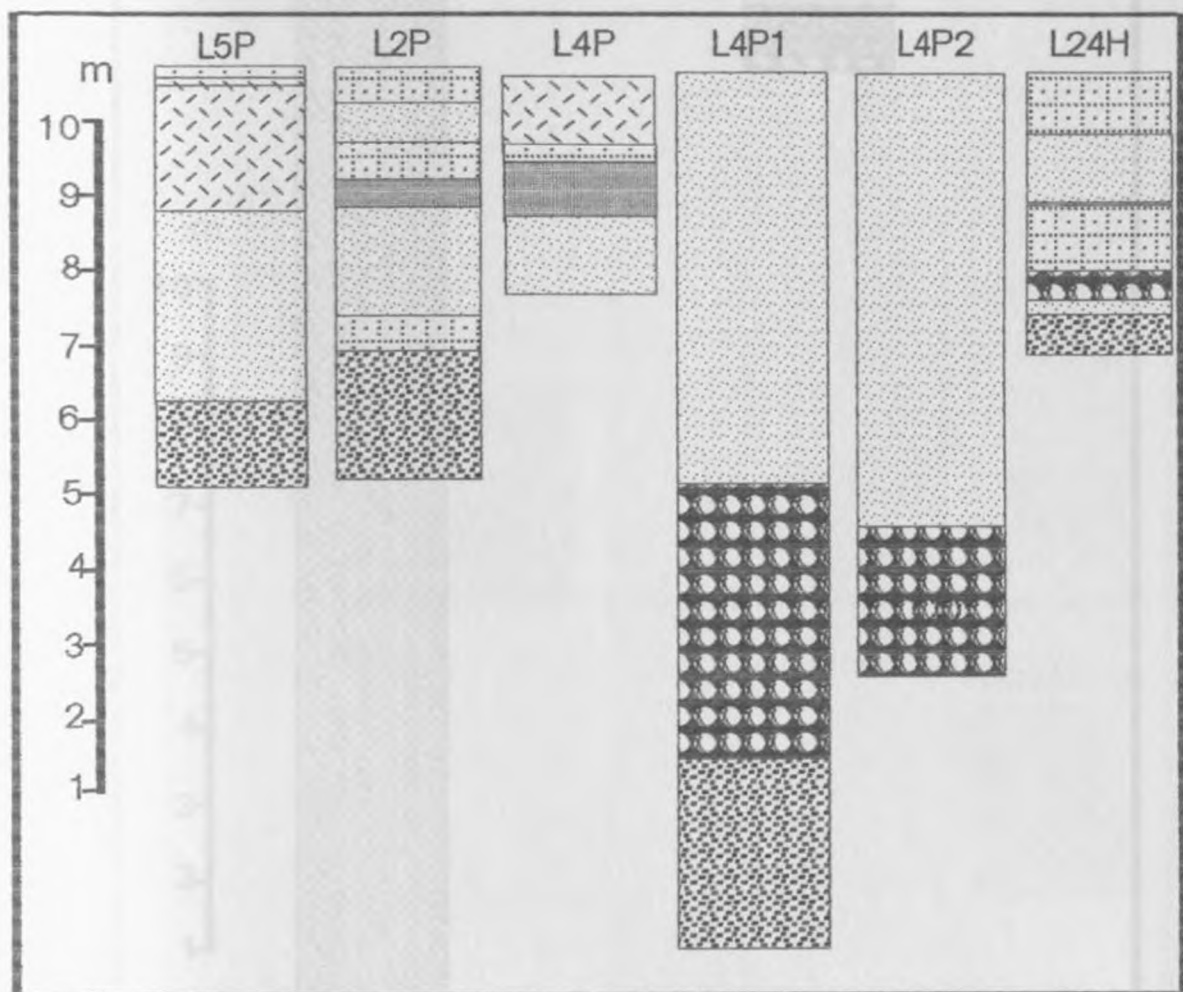


FIG.3 - 24 Lithostratigraphic sections, north eastern edge Lake Nakuru Park.

FIG. 3 - 25 Lithostratigraphic sections, in a sand quarry at Rendu.

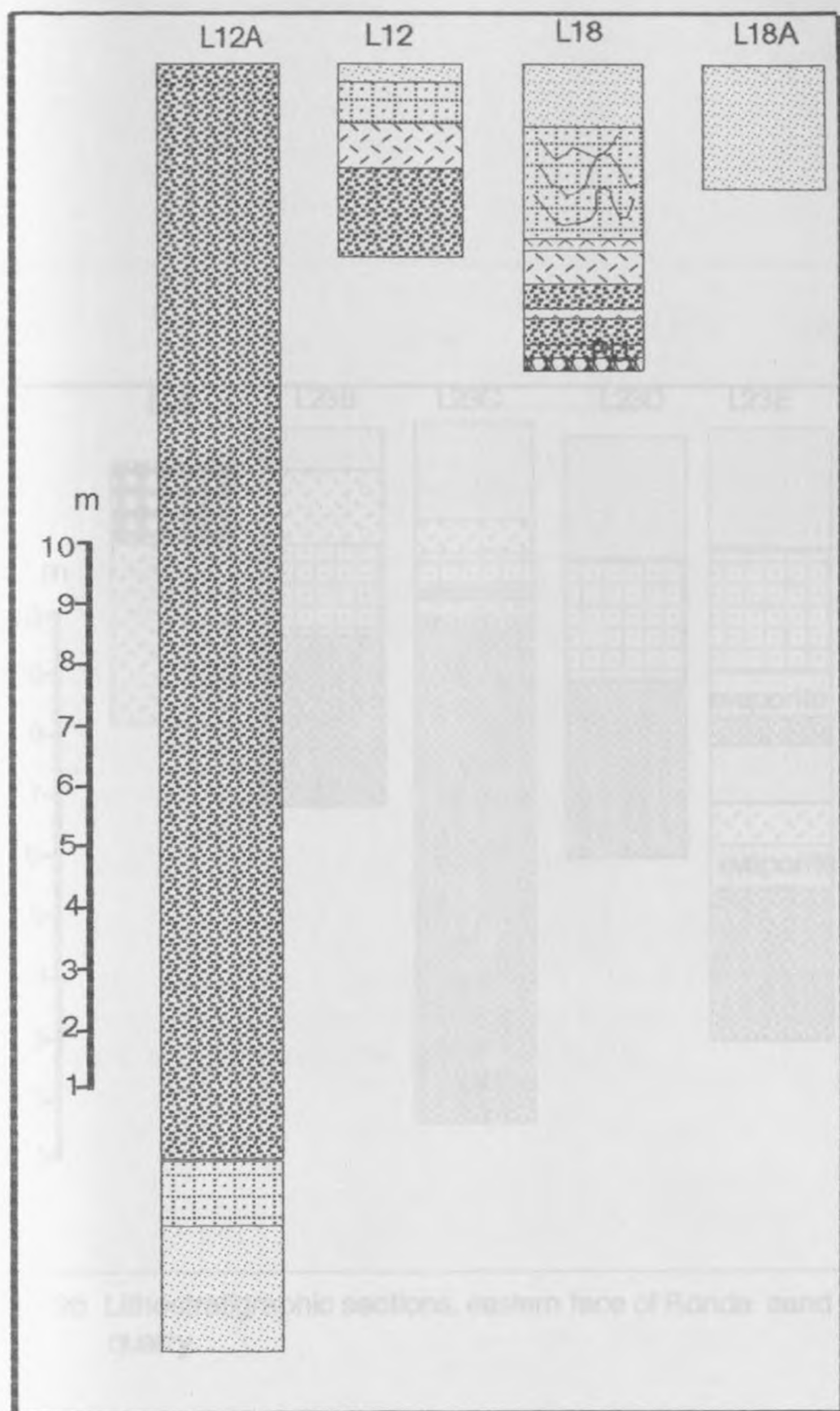


FIG. 3-25 Lithostratigraphic sections, in a sand quarry at Ronda.

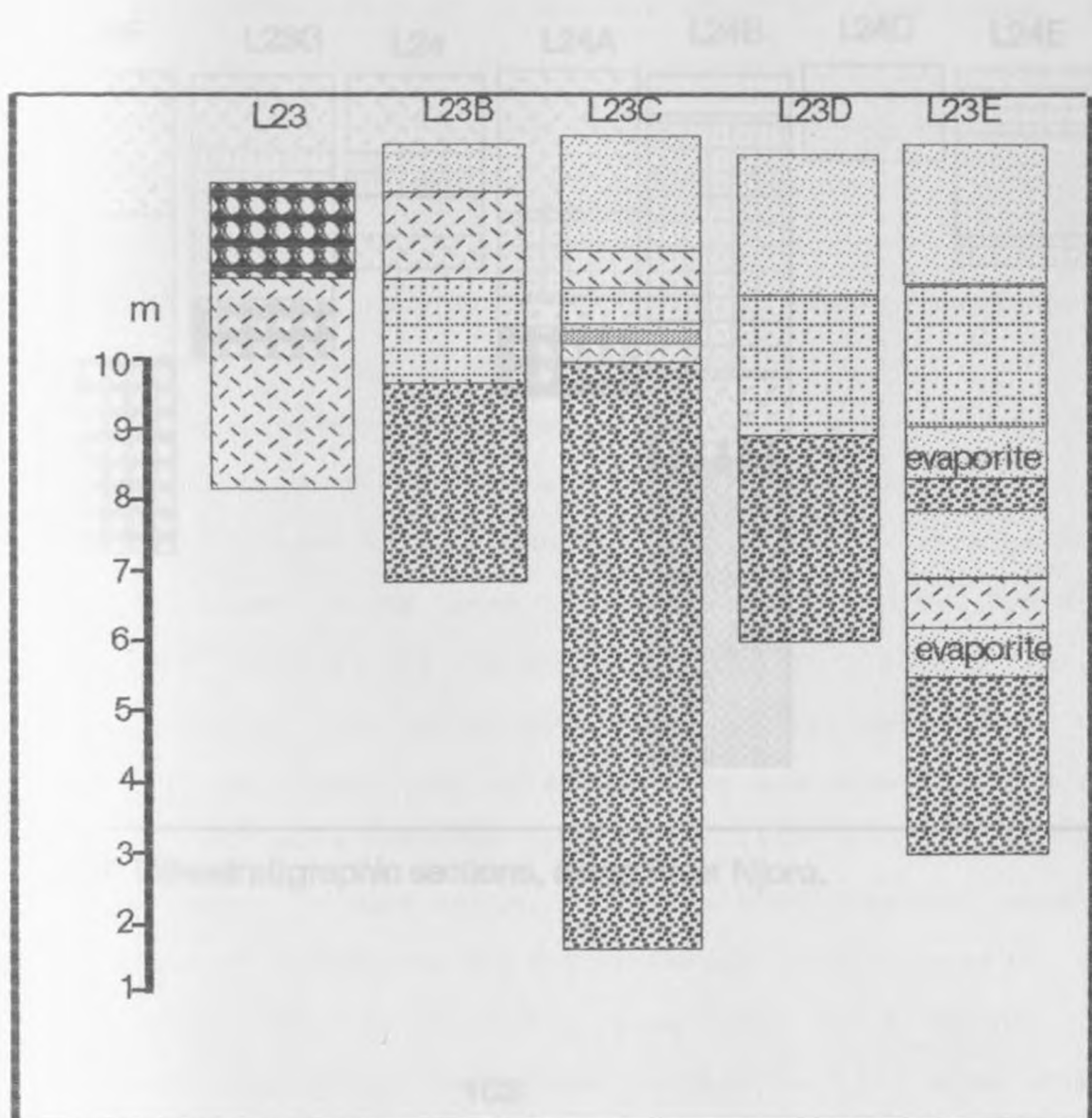


FIG. 3-26 Lithostratigraphic sections, eastern face of Ronda sand quarry.

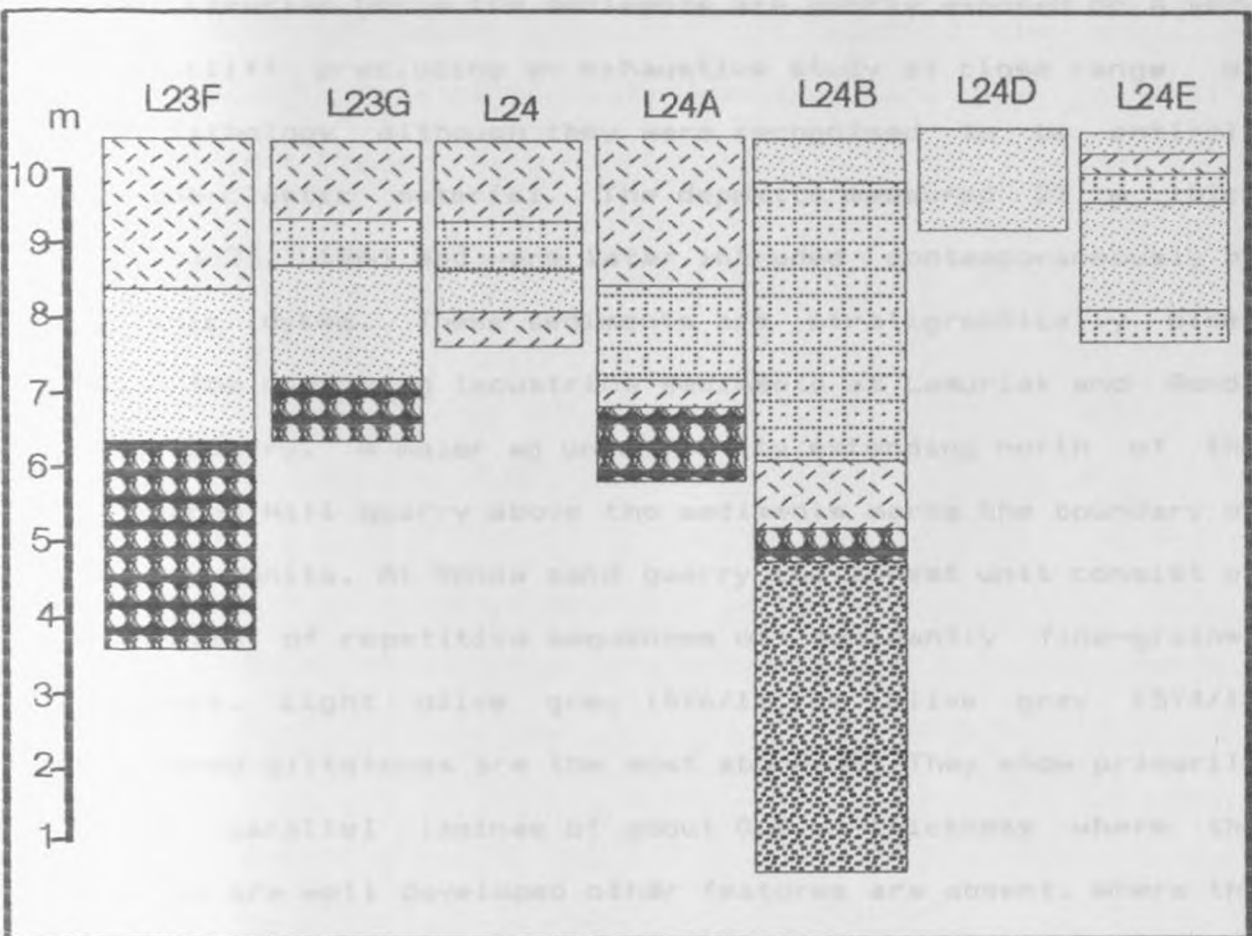


FIG. 3-27 Lithostratigraphic sections, along River Njoro.

The sandstones are dominantly subarkosic and sediments (Figs. 3-24 to 3-27) which were originally reported to be of lacustrine origin (McCall, 1967; Nyamweru 1969). They range from fine grain silts to pumice granules. Within the Lower Lamuriak Gorge the sediments are poorly exposed on a very steep cliff precluding an exhaustive study at close range of the lithology although they were recognised to be entirely volcano-clastic material. The deposits measured 25 m thick (Fig. 3-25, L12A) and were later intruded contemporaneously by volcanic dykes. These sediments are stratigraphically older than the overlying lacustrine sediments at Lamuriak and Ronda sand quarry. A major unconformity extending north of the Honeymoon Hill quarry above the sediments marks the boundary of the rock units. At Ronda sand quarry the lowest unit consist of a series of repetitive sequences of dominantly fine-grained sediment. Light olive gray (5Y6/1) to olive gray (5Y4/1) laminated siltstones are the most abundant. They show primarily planar parallel laminae of about 0.5 cm thickness where the laminae are well developed other features are absent. Where the siltstone is more massive lower limonitic concretions and caliche occur. In some units, the siltstones coarsen upwards and lenses of arenaceous siltstone become common towards the top. This may occasionally give way to a series of interbedded siltstone and fine sandstones. In most cases however, the top of siltstone unit is truncated by sharp contact with a very pale orange (10YR/2) medium grain

sandstone. The sandstones are dominantly sublitharenites and litharenites which are moderately sorted and subrounded primary structures include basal small-scale trough cross-bedding, planar cross-bedding and planar bedding. Individual sandstone units tend to become structureless towards the top. The correlations of stratigraphic sections and the composite sections are presented in chapter 5.

Individual beds and lithologies and contain stratigraphic units. These characteristics have made it possible to correlate lithostratigraphic units from various stratigraphic sections in the area. Most of the lacustrine sediments are well-sorted, silty, and normally interbedded with shales and muds. Fluvial, alluvial and lacustrine units contain significant proportions of quartz pebbles and pebbles and siltstones. Clays are readily eroded by their grey silty. Such fluctuations during sedimentation have therefore produced alternating sequences of sand layers which reflect climatic shifts caused by high level erosion. The Karanikal (Plate 2a, 2b) and the (Plate 2c, 2d) formations consist of mainly sandy silty, silty, and silty shales and muds, which are highly interbedded ranging in color from light grey to dark grey. The primary structures are well developed and parallel to the bedding planes. This is related to the concentration of cementation

CHAPTER 4

PETROLOGY AND GEOCHEMISTRY OF SEDIMENTS.

4.1 Petrology of the sedimentary formations

Late Quaternary sediments of the Central Rift consist of alternations of thick up to 11 m diatomaceous silts and thin (centimetre to decimetre) volcanic pumice ash. Individual beds have distinctive colours and lithologies and contain diagenetic assemblages. These characteristics have made it possible to develop detailed lithostratigraphy from measured stratigraphic succession in the area. Most of the lacustrine sediments are massive silty diatomite beds, commonly intercalated with clays, tuffs and sands. Fluvial, alluvial and lacustrine sediments contain significant proportions of pumice conglomerates and pyroclastic agglomerates. Clays are readily distinguished by their grey colours. Small fluctuations during the Quaternary have therefore produced alternating succession of marls and clays which reflect climatic shifts caused by high lake level cyclicity. The Kariandusi (Plates 2a,2b) and Soysambu (Plates 4a, 4b) Formations consist of mainly shallow water diatomaceous lake sediments, mainly clays and silts. They are moderately to highly indurated ranging in colour from white to light gray. Most of the deposits display primary fissility, where they tend to split or separate along relatively smooth surfaces parallel to the bedding planes. This property is related to the concentration of constituent

acted to relatively quiet environments of diminishing detrital minerals and associated quiet depositional environments. Most of these lake beds contain abundant clays and fine-sand particles of mainly quartz and feldspars which grade into siltstones. The Soysambu Formation comprises mainly of fine-grained diatomaceous siltstones, volcanic claystones, tuffs and calcrenites. The quartz is predominantly polycrystalline while the feldspars are frequently highly altered microcline.

Both Enderit and Ronda Formations reflect fluvial deltaic deposition. The conglomerate beds of the Enderit Formation are debris flow tephra. The extremely angular constituent clast of the deposits indicate provenance to be within the bounding scarp margins of the palaeobasin. The lithostratigraphic units are easily differentiated by a wide range of mineral composition both of detrital and authigenic origin. The mineral components identified in the conglomerates are quartz, potassium feldspar, plagioclase feldspar, perthite, chlorite and carbonate cement. Lake sediments are characterised by massive diatomaceous silts of lacustrine origin with pyroclastic tuff intercalations. The organic rich sediments contain large amounts of biogenic silica notably diatoms. The increased proportion of preserved lacustrine organic matter in form of siliceous microplankton are characteristic of sediments in areas of high planktonic productivity. Such sediments are

restricted to relatively quiet environments of diminishing influence of fluvial sedimentation. Toward the lake margins diatom accumulations were relatively less rapid and only thin wedging deposits recorded.

At Kariandusi a general increase in diatomite thickness occurs in southerly direction. In the same area sediments display geographic variations in diatomite content with those to the north containing 40-85 % while those to south contain less than 35 % silica. Stratigraphic sections data from the sediments demonstrate that these sediments thicken towards the depocentre and become coarser-grained towards the lake margins. The strata thickness and grain sizes variations indicate a derivation from the bounding fault margins. This conform with the relatively coarse fluvial and alluvial sediments transport pathways. Lake sediments are however, restricted to the axial parts of the basins indicating extrabasinal sources for the bulk of the deposits and constituent minerals. The differences in the diatom types was not analysed the result of which would to a lesser extent relate to provenance, lake depth variations and cyclicity although deposits of the thickest diatom sequences evidently formed in the deeper parts of the basins.

The volcanic rich sediments are best differentiated by their high aluminium and titanium contents (about 1.5 % CFB). Although the sediments are also differentiated by the major-

element compositions of the iron, magnesium, aluminium and potassium contents of the sediment groups. The increased proportion of aluminium and alkali metals in the sediments is indicative of terrestrial origin for the aluminosilicate phases of volcanic terrain of the area. In the areas where the beds are characterised by centimetres to decimetres thick basal volcanoclastic sands containing less than 20 % clay grade sands are well sorted, fine upwards and commonly laminated. Laminations are predominantly comprised of alternations of diatomite rich silts and volcanoclastic sands. The coarse sands have grains of clinopyroxene (augite) olivine and volcanic glass as the dominant phases. Secondary minerals include amphiboles (hornblende), orthopyroxene (hypersthene) epidote. More general analysis of the deposits revealed sodic pyroxene (aegerine) and some alkali feldspars (microcline, sanidine) in these beds. The chemistry of volcanic shards in the sediments indicate a trachytic-trachyandesitic composition for the parent magma. The author has observed centimetre sized pebbles of pumice. There is therefore no doubt that the deposits are derived entirely from the surrounding volcanics and consequently contain more volcanogenic and other igneous detritals than lacustrine components. The high proportion of the basic and intermediate igneous minerals clearly explain the high iron, magnesium and titanium levels in these sediments. The mineralogy and chemistry of the igneous detrital are typical of Quaternary

rift volcanics (McCall, 1967). In the Makalia river valley, the lowermost formation is underlain by coarse grained poorly sorted weathered lava. The arkosic volcanic sand is followed by predominantly medium grained well sorted yellowish white pumice sands which are weakly indurated. They are composed predominantly of silica glass and feldspar particles. The quartz particles display mostly undulatory extinction. The deposits lack cement and are very weakly consolidated. Frequently the clays are the main interstitial materials. Carbonates are present largely as calcretes. The Makalia beds of the Enderit Formation is composed of mainly of gray moderate to poorly sorted clay-rich pyroclastic tuffs. The sediments of the Enderit deposits are generally weakly indurated and they vary in mean grain-size from fine to coarse and frequently conglomeratic lithological units. The detrital particles range in shape from angular to subrounded. The modal analyses of the sediments indicate that quartz and feldspar are the dominant minerals. The quartz commonly display different degrees of undulatory extinction. Some of the sandstones are weakly welded by particle interpenetration. Frequently the clay minerals are the main interstitial materials. Again carbonate cement occur sparingly as calcretes. At Ronda, analysis of petrography indicates that quartz and feldspar are the dominant detrital particles. The quartz is occasionally monocrystalline displaying different degrees of undulatory extinction. Potassium

feldspar is the second major component and plagioclase is abundant in the arkoses than carbonate minerals (mainly calcite) are common as calcrete and they are usually coarse crystalline clays. The phyllosilicates occur as mixed layer bentonite and possibly kaolinite. The greenish and grey tinge characteristic of the clays is predominantly chlorite.

The tuffs are characterised by dark grey colour weakly indurated, poorly sorted medium to coarsely grained deposits. The detrital particles are subrounded, subangular to angular and sometimes dominantly rod-shaped. The modal analysis indicates that the tuffs are mainly felspathic with subordinate quartz and lithics. Polycrystalline quartz is abundant suggesting low sediment maturity. Potassium feldspar is usually associated with smaller amounts of perthite and plagioclase feldspar. Rock fragments are major component of the lithics detrital and they are mainly argillite volcanic rocks containing altered feldspars. The main matrix are clay minerals, sparing calcite, quartz and ferruginous material.

4.1.1 Grain-size Distribution.

Statistical grain size parameters (Tables 4A, 4B, 4C.) used for both descriptive and inferential purposes were derived from sieved data calculated according to the formula of Folk and Ward, 1957 as follows:

TABLE 4A Calculated values for mean, spring, kurtosis, skewness measured on Phi scale.

$$\text{Mean: } \bar{X} = \frac{1}{n} \sum_{i=1}^k f(x_i)x_i$$

$$\text{Standard Deviation: } s = \left[\frac{1}{n} \sum_{i=1}^k f(x_i)(x_i - \bar{x})^2 \right]^{\frac{1}{2}}$$

$$\text{Skewness: } sk = \frac{\frac{1}{2n} \sum_{i=1}^k f(x_i)(x_i - \bar{x})^3}{s^3}$$

$$\text{Kurtosis: } Ku = \frac{1}{2} \left[\frac{\sum_{i=1}^k f(x_i)(x_i - \bar{x})^4}{ns^4} - 3 \right]$$

(ϕ) = Phi were computed for the mid - points of each size class as follows:

- n = total weight of samples
- $f(x_i)$ = weight of single size class
- x_i = midpoint of same size
- k = total number of size classes

No	Description	Mean	Spring	Kurtosis	Skewness
01	MGS	.24	MS .72	PLK -1.08	-34
02	MGS	.24	MS .73	PLK +1.07	-35
03	CGS	.34	MS .97	PLK -1.08	-29
04	MGS	1.32	MS .71	PLK -.31	-50
05	MGS	1.74	MS .92	PLK +.93	-41
06	FGS	1.33	MS .95	PLK -1.21	-27
07	MGS	1.26	MS .71	PLK -1.07	-28
08	FGS	1.16	MS .71	PLK -.41	-98
09	FGS	1.20	MS .71	PLK -1.21	-25
10	FGS	1.20	MS .75	PLK -3.16	-30
11	FGS	2.75	PS 1.03	PLK -1.15	-26
12	FGS	2.18	PS 1.08	PLK -.81	-41
13	MGS	1.27	MS .72	PLK -.99	-43
14	MGS	1.53	PS 1.81	PLK -.42	-70
15	VFGS	3.46	MS .74	PLK -1.18	-18
16	MGS	1.47	PS 1.36	PLK -.77	-72
17	VFGS	3.58	MS .56	PLK -1.13	-21
18	FGS	2.77	PS 1.91	PLK 1.31	-1.41
19	MGS	1.28	MS .70	PLK -1.12	-27
20	MGS	1.28	MS .76	PLK -.58	-38
21	VFGS	3.46	MS .76	PLK -1.02	-35
22	MGS	1.28	MS .76	PLK -1.23	-22
23	FGS	2.72	PS 1.36	PLK -.89	-46
24	MGS	1.93	MS .86	PLK -.48	-74
25	VFGS	3.26	PS 1.08	PLK -.57	-1.24
26	FGS	2.86	PS 1.20	PLK -.21	-84
27	FGS	2.86	MS 1.00	PLK -1.04	-36
28	MGS	1.28	MWS .70	PLK -.32	-44
29	MGS	1.28	MS .73	PLK -1.10	-31
30	MGS	1.06	MS .77	PLK -.35	-78
31	MGS	1.24	MS .71	PLK -1.00	-37
32	FGS	2.23	PS 1.23	PLK -.84	-50
33	VFGS	3.18	MS .73	PLK -1.13	-28
34	CGS	.88	MS .80	PLK -1.11	-38
35	MGS	1.20	MS .72	PLK -1.07	-32
36	FGS	2.21	PS 1.10	PLK -.88	-48
37	FGS	3.15	MS .73	PLK -1.14	-26
38	FGS	2.63	MS .94	PLK -1.14	-23
39	VFGS	3.17	MS .75	PLK -1.20	-25

TABLE 4A Calculated values for mean, sorting, kurtosis, skewness measured on Phi scale.

Sample	Description	Mean	Sorting	Kurtosis	Skewness
PT13B1	MGS	1.22	MS .72	PLK -1.08	-.34
PT13B2	MGS	1.24	MS .73	PLK -1.07	-.36
PT13B3	CGS	.84	MS .91	PLK -1.06	-.29
PT13B4	MGS	1.32	MS .71	PLK -.91	-.50
PT13B5	MGS	1.74	MS .92	PLK -.99	-.41
PT14	FGS	2.83	MS .90	PLK -1.21	-.27
PT14B3	MGS	1.18	MS .71	PLK -1.07	-.28
PT14B4	MGS	1.26	MS .71	PLK -.41	-.98
PT16B2	FGS3	.18	MS .75	PLK -1.21	-.25
PT16B3	FGS	1.20	MS .75	PLK -1.16	-.30
PT18B5	FGS	2.75	PS 1.03	PLK -1.15	-.26
PT18B6	FGS	2.19	PS 1.09	PLK -.91	-.41
PT19B1	MGS	1.27	MS .72	PLK -.99	-.43
PT19B2	MGS	1.93	MS .84	PLK -.49	-.70
PT19B5	MGS	1.93	PS 1.61	PLK -1.19	-.18
PT19B6	VFGS	3.46	MS .74	PLK -.77	-.72
PT19B3	MGS	1.47	PS 1.35	PLK -1.13	-.21
PT19B4	VFGS	3.69	MS .58	LPK 1.31	-1.41
PT19B7	FGS	2.77	PS 1.01	PLK -1.12	-.27
PT19B8	MGS	1.26	MS .70	PLK -.98	-.39
PT20B3	MGS	1.98	PS 1.06	PLK -1.02	-.35
PT20B2	VFGS	3.16	MS .76	PLK -1.23	-.22
PT20B1	FGS	2.72	PS 1.16	PLK -.69	
PT21B1	MGS	1.93	MS .86	PLK -.48	-.74
PT21B3	VFGS	3.26	PS 1.08	LPK .67	-1.24
PT21B4	MGS	1.33	MW .70	PLK -.88	-.50
PT21B2	FGS	2.96	PS 1.20	PLK -.21	-.94
PT21B5	FGS	2.82	MS 1.00	PLK -1.04	-.36
PT23B1	MGS	1.28	MWS .70	PLK -.92	-.44
PT23B2	MGS	1.21	MS .73	PLK -1.10	-.31
PT23B4	FGS	2.06	MS .77	PLK -.35	-.79
PT23B3	MGS	1.24	MS .71	PLK -1.00	-.37
PT23B5	FGS	2.59	PS 1.23	PLK -.84	-.50
PT23B6	VFGS	3.18	MS .73	PLK -1.13	-.28
PT26B2	CGS	.68	MS .96	PLK -1.11	-.36
PT26B1	MGS	1.20	MS .72	PLK -1.07	-.32
PT26B3	FGS	2.21	PS 1.10	PLK -.88	-.46
PT26B4	FGS	3.18	MS .73	PLK -1.14	-.26
PT33B1	FGS	2.83	MS .94	PLK -1.14	-.23
PT33B2	VFGS	3.17	MS .75	PLK -1.20	-.25

Table 4B Calculated values for mean, sorting, kurtosis, skewness of Enderli sediments, measured on Phi scale.

Description	Mean	Sorting	Kurtosis	Skewness
VFGS	3.18	MS .71	PLK -1.32	-.33
VFGS	3.35	MS .75	PLK -1.09	-.55
VFGS	3.42	MS .73	PLK -.78	-.59
VFGS	3.14	MWS .70	PLK -1.34	-.25
FGS	2.52	PS 1.29	PLK -1.03	-.40
MGS	1.74	MS .93	PLK -1.00	-.42
VFGS	3.19	MS .76	PLK -1.19	-.28
VFGS	3.24	MWS .69	PLK -1.21	-.43
VFGS	3.43	MWS .57	PLK -.27	-.88
VFGS	3.05	WS .47	LPK .11	-.31
VFGS	3.78	MWS .64	PLK 1.12	-1.53
CGS	.89	MS .91	PLK -1.00	-.36
CGS	.40	PS 1.23	PL -1.19	-.24
CGS	1.20	MS .74	PLK -1.16	-.35
CGS	2.20	MS .83	PLK -.90	-.75
SILT	4.03	VWS .53	PLK -.18	-.47

Table 4B Calculated values for mean, sorting, kurtosis, skewness measured on Phi scale.

Sample	Description	Mean	Sorting	Kurtosis	Skewness
1FB5	FGS	2.30	MS .82	PLK -.96	-.31
1FB4B	VFGS	3.96	WS .38	LPK 7.29	-2.62
1FB6	VFGS	3.58	MS .71	PLK -.25	-1.04
1FB7	VFGS	3.24	MWS .67	PLK -.90	-.35
1FB8	VFGS	3.45	MWS .66	PLK -.44	-.75
S8PUM	VFGP	3.38	MS .75	PLK -.96	-.60
1GB2	MGS	1.26	MS .74	PLK -1.13	-.36
1GB1	MGS	1.21	MS .73	PLK -1.12	-.31
1GT2	VFGS	3.51	MWS .67	PLK -.25	-.90
1GPUT1	VFGP	3.61	MWS .59	LPK .51	-1.11
1GB3	VFGS	3.21	MS .76	PLK -1.19	-.30
1GB4	VFGS	3.18	MS .71	PLK -1.09	-.24
VFGS	3.20	MS .72	PLK -1.10	-.30	
FGS	2.45	VWS .26	PLK -1.15	-.33	
VFGS	3.23	MWS .76	PLK -1.20	-.36	
VFGS	3.32	MS .57	PLK -.80	-.30	
MGS	1.20	MS .71	PLK -1.04	-.33	
VFGS	3.114	MS .78	PLK -1.20	-.28	
MGS	1.19	MS .75	PLK -1.17	-.37	
VFGS	3.28	PS .77	PLK -1.20	-.78	
FGS	2.14	MWS .66	PLK -.13	-2.22	
VFGS	3.09	MWS .50	LPK -4.28	-.23	
VFGS	3.37	MS .78	PLK -1.08	-.54	

Table 4C Calculated values for mean, sorting, kurtosis, skewness of Enderit sediments, measured on Phi scale.

Sample	Description	Mean	Sorting		Kurtosis	Skewness
1CB8	VFGS	3.18	MS	.71	PLK -1.32	-.33
1CB9	VFGS	3.35	MS	.75	PLK -1.02	-.56
1CBI	VFGS	3.42	MS	.73	PLK -.78	-.69
1CBII	VFGS	3.14	MWS	.70	PLK -1.34	-.25
1D	FGS	2.52	PS	1.29	PLK -1.03	-.40
1DB	MGS	1.74	MS	.93	PLK -1.00	-.42
1DB5	VFGS	3.19	MS	.75	PLK -1.19	-.26
1DB6	VFGS	3.24	MWS	.69	PLK -1.21	-.43
1DB7	VFGS	3.43	MWS	.57	PLK -.27	-.86
23B1	VFGS	3.65	WS	.47	LPK .11	-.81
23B2	V FGS	3.76	MWS	.64	PLK 1.12	-1.55
23CB1	CGS	.92	MS	.91	PLK -1.00	-.36
23CBB	CGS	.40	PS	1.20	PL -1.10	-.24
23CB4	CGS	.86	MS	.90	PLK -1.02	-.33
23CB3	VFGS	3.21	MS	.74	PLK -1.16	-.35
23EB4	FGS	2.98	MS	.83	PLK -.90	-3.73
23FB2	SILT	4.03	VWS	.33	Plk -.18	-.47
23C	MGS	1.79	MS	.89	PLK -.87	-.93
23CA	VFGS	3.55	MS	.70	PLK -.15	-.37
24B	VFGS	3.33	MS	.73	LPK -.96	-.52
24B4	VFGS	3.25	MS	.75	PLK -1.11	-.43
24G	MGS	1.21	MS	.73	PLK -1.11	-.31
24GB3	VFGS	3.5	MS	.71	PLK -.57	-.82
NB1	VFGS	3.07	MS	.72	PLK -1.17	-.11
NB2	FGS	2.94	MS	.82	PLK -.91	-.28
DM	CGS	.87	MS	.97	PLK -.77	-.48
18P5	FGS	2.43	PS	1.37	LPK -1.22	-.39
18B1	MGS	1.19	MS	.72	PLK -1.06	-.33
18B3	MGS	1.18	MS	.71	PLK -1.07	-.28
18B4	CGS	.86	MS	.88	PLK -.98	-.27
18B5	VFGS	3.20	MS	.72	PLK -1.10	-.30
1E3	FGS	2.45	VWS	.26	PLK -1.15	-.33
1E4	VFGS	3.23	MWS	.76	PLK -1.20	-.48
1E5	VFGS	3.32	MS	.67	PLK -.80	-.30
1E7	MGS	1.20	MS	.71	PLK -1.04	-.33
E4B	VFGS	3.23	MS	.76	PLK -1.20	-.28
1FB1	MGS	1.19	MS	.75	PLK -1.17	-.37
1FB2	VFGS	3.26	PS	.77	PLK -1.20	-.79
1FB3	FGS	2.14	MWS	.68	PLK -.13	-2.22
1FB3B	VFGS	3.89	MWS	.50	LPK -4.28	-.23
1FB4	VFGS	3.37	MS	..78	PLK -1.09	-.54

Although its value remains controversial, grain-size analysis has long been a standard procedure in sedimentology since 1950s (Inman, 1952; Folk and Ward, 1957; Wentworth, 1922; Krumbein, 1935; Krumbein and Pettijohn, 1938; Friedman, 1958; Van der Pais, 1952; Griffiths, 1967). However, grain-size alone can sometimes produce ambiguous or incorrect results inspite of the fact that there still persists a general contention in sedimentology that a detailed grain size analysis can possibly indicate the environment of deposition. Hence, the adoption and application of computer programme in this study is based on this premise and indicates the importance placed on grain size analysis.

The statistical mean parameters define the central tendency of the distribution as essentially consisting of very fine grain sands to silt. The mean locate the weighted central tendency to the fines ((3.00-4.50)). The mean of the logarithmic distribution calculated is affected by weighted distribution from sieving results and is shifted slightly towards the coarser end of the distribution.

Phi sorting or standard deviation measure of scatter or dispersion seems largely related directly to the localised transporting agents of depositional environments which segregated sediment load according to size. Phi sorting frequency of the sediments broadly correlate with the mean. The coarse or fine deposits tend to have high standard deviation

and are poorly sorted whereas high degree of sorting reflect low sorting values as in sands with relatively low standard deviation (well sorted). The Central Rift sediments were both generally moderately well sorted. The poorly sorted (s.d. values greater than 1.00) is characteristic of sediments that have not undergone considerable transport. The poorly sorted are non-lacustrine terrestrial piedmont, and alluvial fan deposits.

The Phi skewness estimating non-normality or the deviation of the distribution from the normal broadly represent negative skewness coarse tail to the distribution. Thus whereas negatively skewed distribution has relatively more coarse material than would be expected in a normal distribution. The value for skewness denotes which end of the distribution has a greater proportion of sediments. The negative skewness value indicate that the finer material is more abundant and there is a tail of coarse grain. The general lack of positive value in the sediments indicate abundance of coarse material with a "tail" of fines. Hence most of the sediments in the study area were skewed to the finer material.

Though relatively abstract, Phi kurtosis measures and descriptive parameters of peakedness of the size distribution relate the rift sediments both to sorting and degree of normality of the distribution. Poorly sorted sediments tend to

have flat particle size distribution generally differ from the normal curve though showing no asymmetry (skewness). Similarly a well sorted sediment may have a more peaked distribution than normal curve. In this analysis platykurtic distribution is generally predominant although a few leptokurtic distribution occur. In most sediments the range of kurtosis varies from about 0.5 to 3.5 a normal distribution has a value of 1.0. However, in this study, because the high percentage of material is in the finest fraction, most of the sediments did show platykurtic values.

Several distinct patterns are revealed in the distribution of the grain-size parameters even within a given single sedimentary unit. These may reflect similar sediment types similar mode of deposition for different sediment types or they may be just coincidental. The high percentage of very fine sediments should be treated cautiously, for it merely reflects the lack of fine sediment analysis using settling rates in water. The presence of bimodal distribution of grains implies generally that the sediment has been transported from its place of origin and thus has undergone more than one mechanism for sorting. Apparently in the Central Rift, sediments of more distinct types were coming into one or more depositional environments. There is a normal detrital input to the lake, stream or land; there is a pyroclastic input from active volcanic vents; and there is a terreginous volcanic input from

the land to the lake or stream. Thus a bimodal or multimodal distribution of grain sizes may only reflect this plurality of sediment inputs apart from plurality of depositional environments. The author nevertheless, recognised that the sieved data from the the rift sediments do have specific meaning which may relate to their depositional environments.

4.3 Geochemical Data.

As means of relating chemical concentrations to common sediments geochemical data have previously been recognised to be of benefit in sediment correlation, such as section to section correlation, depositional environment interpretation, tectonic setting and sedimentary basin analysis (Crook, 1974, Schwab 1975, Dickson and Suczek 1979, Selley 1982, Bhatia 1983, Roser and Korch 1986, Heron 1987 Middleton 1960, Garrels and Mackenzie 1971, Pettijohn et al. 1972). Chemical studies have shown that appreciable exchanges in the contents of the mobile elements have an effect of the percentage of non-mobile elements because of the constant sum effect. This however, can be overcome if elements or oxides that are not influenced by the mobility of other elements are used for the classification and comparison between the different sedimentary formations (Hanski, 1988). The chemical composition of the rift sediments (Tables 4-1 to 4-5) generally reflect immature mineral composition in which SiO_2 is the major constituent. However

Table 4 – 1A Major oxide composition of Kariandusi sediments.

Sample number	SiO ₂	TiO ₂	Al ₂ O ₃	Fe ₂ O ₃	MnO	MgO	CaO	Na ₂ O	
17B2	45.16	.79	13.39	5.15	.15	.01	.45	2.07	4.41
17B4	56.16	.99	11.29	5.33	.00	.02	.52	2.21	3.60
15B8	39.99	.31	8.91	6.33	.12	.08	.40	2.65	3.52
15B9	45.00	.52	7.87	6.84	.07	.08	.36	1.68	3.26
15B2	43.13	.53	9.97	6.18	.14	.02	.37	2.13	4.32
15B7	44.74	.66	9.42	7.68	.64	.25	.49	1.61	3.12
15B1	45.72	.71	8.08	7.02	.00	.11	.75	1.96	3.99
15B2	42.15	.69	9.76	6.94	.13	.36	1.78	3.89	?
15B4	40.82	.56	9.54	6.49	.11	.18	.47	3.08	3.14
15B5	47.82	.29	6.66	6.04	.11	.02	.25	1.80	3.71
15B6	52.19	.00	8.51	6.17	.00	.02	.25	1.36	3.90
15B7	51.36	.65	9.23	5.58	.00	.17	.55	1.26	2.24
15B8	45.07	.79	10.78	7.07	.18	.14	.33	2.87	3.21
14B9	42.59	.00	5.77	6.10	.13	.04	.28	1.54	3.43
14B20	46.04	.00	8.35	12.00	.29	.42	2.16	2.38	3.73
14B10	49.25	.56	10.66	6.61	.07	.89	.71	1.95	2.99
14B8	42.25	.62	8.81	6.79	.18	.79	.72	2.01	3.03
14B9	38.78	.32	10.97	5.67	.06	.03	.68	2.82	4.08
14B5	46.24	.31	6.99	6.21	.06	.11	.45	1.89	3.89
14B1	37.49	1.35	9.58	7.53	.26	.18	1.14	1.86	3.79
14B11	46.19	.50	7.60	5.07	.07	.50	.57	1.63	2.79
14B16	44.91	.53	2.12	6.11	.14	.66	.67	2.30	3.22
14B22	40.75	.39	10.39	5.27	.05	.07	.55	2.96	3.79
14B2	37.39	1.33	11.32	7.13	.13	.17	.98	1.72	3.97
14B6	54.15	1.01	11.51	5.65	.00	1.82	.64	1.31	2.02
14B7	50.00	.62	7.03	6.11	.12	.06	.52	2.51	3.81
14P7A	47.27	.60	8.99	5.27	.15	.69	.58	1.67	2.72
1414B	49.80	.34	7.64	5.77	.00	.03	.28	2.72	3.89

Table 4 – 1B Major oxide composition of Kariandusi sediments.

Sample number	SiO ₂	TiO ₂	Al ₂ O ₃	Fe ₂ O ₃	MnO	MgO	CaO	Na ₂ O	
13B5	51.89	.61	6.86	6.23	.00	.26	.38	2.45	3.39
13B12	43.60	.45	6.77	5.51	.00	.12	.31	2.71	3.45
13B8B	45.33	.76	6.92	5.89	.18	.18	.32	2.67	3.64
13B8A	42.29	.69	7.87	5.95	.00	.28	.51	3.03	3.26
13B19	45.73	.55	6.24	5.30	.11	.08	.40	3.56	3.98
13B18	43.31	.92	5.14	6.75	.07	.22	.69	2.61	3.04
13B26	39.52	1.03	9.71	6.31	.20	.06	.72	2.99	4.46
13B32C	35.47	1.02	7.72	5.98	.20	.09	.50	2.64	4.18
13B30	45.11	.78	10.61	5.81	.18	.05	.54	3.91	3.83
13B28	31.72	.67	9.51	6.04	.13	.05	.73	2.85	3.76
13B22	54.76	.70	10.50	4.00	.00	.11	.29	3.32	2.53
13B17	44.04	.45	8.41	6.36	.10	.22	.48	2.60	3.04
13B16	46.56	1.14	4.31	6.19	.00	.14	.48	2.34	3.57
13B15	50.24	.71	8.07	5.80	.00	.04	.45	1.96	3.73
13B14	47.55	.69	9.63	8.74	.33	.25	.07	2.86	4.91
13B21	45.76	.76	10.76	9.11	.37	.53	.63	2.95	4.12
13B32B	57.28	.94	10.63	5.49	.18	.17	.46	2.83	4.07
13B32	39.32	.83	5.62	5.66	.13	.25	.47	3.74	3.94
13B4	47.44	.75	6.37	4.81	.00	.22	.31	2.78	2.98
13B3	43.55	.72	5.91	5.81	.10	.30	.42	3.79	3.77
13B6	54.85	.67	9.42	6.41	.00	.50	.19	2.20	3.48
13B7	47.41	.66	6.62	8.76	.17	.23	.44	4.02	4.96
13B8	46.52	.06	8.38	5.58	.34	.22	.25	2.11	3.21
13B27	42.20	.54	10.28	6.37	.21	.14	.46	2.46	4.19
13B25	53.68	.36	8.13	5.23	.00	1.25	.60	1.62	1.43
13B32A	31.76	.69	9.70	6.01	.19	.15	.51	2.66	3.83
13B9	47.28	.58	9.89	5.86	.11	.19	.43	2.73	3.78
13B29	29.02	.66	9.31	5.21	.00	.07	.55	3.72	4.51
13B31	45.28	.79	10.77	5.43	.18	.22	.36	3.71	3.66
13B33	40.09	.57	12.98	4.05	.11	.85	.24	1.57	2.90
13B2	39.32	.74	4.22	4.47	.00	.10	.26	2.11	.81

4-3 Major oxide composition of Endicott Sediments.

Table 4-2 Major oxide composition of Soysambu sediments.

Sample number	SiO ₂	TiO ₂	Al ₂ O ₃	Fe ₂ O ₃	MnO	MgO	CaO	Na ₂ O	K ₂ O
7B2	53.38	1.08	10.48	5.08	.18	.87	1.55	2.74	1.89
7B4	56.16	.51	4.35	2.30	.10	.20	25.09	.83	.74
7NB1C	52.56	1.65	14.03	7.07	1.09	1.09	4.33	2.83	.08
7NB1A	34.62	1.14	10.73	8.11	.15	.99	.95	3.06	2.60
7NB5	27.19	.90	10.23	5.41	.40	.14	2.88	3.65	2.61

Table 4-3 Major oxide composition of Florida sediments.

Table 4-3 Major oxide composition of Enderit Sediments.

Sample number	SiO ₂	TiO ₂	Al ₂ O ₃	Fe ₂ O ₃	MnO	MgO	CaO	Na ₂ O	K ₂ O
1DB6	56.15	.62	9.30	3.95	.00	.23	.59	1.16	
1CB5	53.18	.85	9.60	5.37	.07	.45	.91	1.78	1.22
1GB3	51.52	.96	10.92	6.52	.07	.40	.42	1.87	1.81
1FB7	29.16	1.82	18.33	9.01	.31	.68	2.04	6.20	4.38
1FB3B	38.83	1.01	15.23	10.07	.26	.20	.92	6.52	4.61
1FB5	25.39	2.03	13.43	7.98	.13	2.26	4.40	3.01	1.47
1E7	35.19	.74	5.55	7.77	.19	.13	.39	1.88	1.68
1E2	42.66	1.00	9.49	6.60	.13	.20	.27	1.76	1.57
1E11	46.75	1.10	4.72	7.61	.14	.44	.32	1.08	2.38
1E5	37.17	1.01	9.55	10.10	.20	.07	.52	5.50	3.29
1E9	37.67	.86	11.71	6.57	.20	.19	.42	3.48	3.23
1E4	61.02	1.28	12.45	10.98	.43	.33	.26	3.40	2.25
1CB	42.83	1.07	10.43	7.75	.06	.32	1.15	1.12	1.88
1FB4	29.77	1.48	11.16	9.02	.15	.84	1.65	2.07	1.99
1GPT1	16.29	.33	13.18	6.69	.19	.53	1.12	6.18	4.32
1CB1	59.15	.74	8.41	4.93	.22	.30	.57	4.35	1.07

Table 4-4 Major oxide composition of Ronda sediments.

Sample number	SiO ₂	TiO ₂	Al ₂ O ₃	Fe ₂ O ₃	MnO	MgO	CaO	Na ₂ O	K ₂ O
18B9	25.88	1.13	14.46	6.32	.00	.19	.74	5.50	4.50
18B10	28.90	.77	13.17	6.97	.00	.44	1.69	2.35	1.96
18B7	47.55	1.00	8.52	5.15	.09	.20	.43	3.44	1.81
18B6	26.10	1.44	13.01	5.90	.22	.31	1.08	5.22	4.15
18B3	21.09	1.17	10.30	10.01	.30	.06	.54	6.09	3.94
18B5	23.22	1.61	12.86	6.48	.29	.34	.95	4.74	4.10
18B8	9.76	1.46	12.17	7.23	.30	.30	.77	5.33	4.10
19B3	51.69	.40	4.58	2.86	.08	.32	10.68	.82	.73
19B1	49.32	1.12	12.64	6.33	.22	.26	.70	5.30	4.43
21B3	27.43	1.05	11.90	6.94	.29	.17	.73	4.61	4.01
23CB2	37.94	.73	10.28	6.37	.14	.18	.64	3.96	3.01
23CB3	39.61	.43	9.77	4.99	.00	.64	4.34	3.14	2.96
23C	26.64	1.43	18.25	6.67	.21	.45	1.20	6.36	5.43
23B2	47.34	1.56	13.22	7.33	.30	.33	1.17	5.97	4.07
23B1	35.25	1.30	11.82	6.70	.27	.31	.88	5.06	4.40
23EB4	28.20	1.38	11.14	6.57	.23	.27	.99	4.45	3.98
24GB3	37.96	1.20	10.20	10.28	.29	.09	.76	6.31	4.12
2PB	36.80	1.35	11.48	7.30	.33	.27	.99	5.32	4.27
5B3	32.77	1.11	12.91	7.05	.39	.21	.75	2.66	2.65
6B2A	42.85	1.06	10.02	6.81	.34	.28	.71	.86	1.79
24B4	52.71	1.42	12.05	5.77	.00	.24	.37	2.72	1.66
24B	30.75	1.54	13.05	7.34	.29	.22	1.11	5.17	4.62

Table 4 – 5 Major oxide composition of Makalia sediments.

Sample number	SiO ₂	TiO ₂	Al ₂ O ₃	Fe ₂ O ₃	MnO	MgO	CaO	Na ₂ O	K ₂ O
18B1	35.83	.87	11.53	6.16	.17				
8B9	35.83	.87	10.81	8.17	.19	.30	.78	1.16	2.41
8B10	27.25	1.05	11.85	7.68	.23	.42	.55	4.10	3.78
8B8	33.26	.97	10.99	6.37	.13	.21	.90	3.53	3.15
8B6	34.31	.90	12.76	8.49	.17	.25	.83	1.27	1.63
8B1	50.53	1.14	10.75	6.34	.22	.62	.72	.77	1.65
8B11	57.74	.54	4.91	4.65	.25	.50	2.37	.88	2.04
8B6C	43.33	.85	7.70	10.18	.66	.06	.50	2.47	3.07
8B6B	40.00	.92	9.49	10.04	.26	.17	.40	2.17	2.66
8B5	42.59	.74	8.41	7.47	.22	.18	.58	1.50	2.28
8B4	49.82	.92	5.45	3.85	.00	.32	1.61	1.30	1.04
8B3B	41.28	1.53	12.10	5.88	.00	.23	.67	1.48	1.87
4B ?	37.51	1.30	11.34	6.86	.12	.16	.29	2.99	2.53
4P4	32.47	.22	12.06	7.16	.82	.32	2.68	3.69	2.09
4P5	30.26	1.20	13.54	9.09	.58	.16	.63	4.35	3.67
4P2	40.86	1.20	13.54	9.09	.58	.16	.63	4.35	3.67
4P3	54.23	.20	6.79	12.45	.70	.15	.59	2.06	1.45
10NEB3	38.64	1.22	5.20	6.82	.12	.14	.29	1.49	.88
10B2	32.57	.74	6.01	6.36	.16	.13	.46	3.86	3.98
10NEB4	26.23	1.01	11.48	5.93	.13	.20	.25	1.64	1.83
10NEB1	24.61	1.09	13.16	8.71	.17	.27	.29	1.99	1.47
10NEB5	41.01	1.32	13.56	7.79	.19	.19	.20	1.16	1.04
10B1	27.13	.85	9.63	4.18	.08	.11	.29	2.40	1.07
11B1	62.52	1.04	7.85	4.01	.00	.16	.22	1.96	1.00
11B4	29.47	.86	7.55	5.09	.26	.09	.96	2.69	1.99
11B3	34.43	.55	6.98	4.64	.09	.07	.72	4.38	4.09
9WB1	70.53	1.38	12.50	6.91	.21	.19	.25	2.56	1.79
9WB2	31.42	1.37	7.79	6.77	.13	.12	.43	1.80	1.49
9WB3	36.46	1.48	12.58	7.61	.29	.21	.69	2.99	.85
9B4	15.20	1.06	11.95	7.91	.27	.49	1.18	2.29	4.26
9WB4	24.92	1.12	9.48	4.90	.11	.25	1.52	1.42	1.11
9WB5	14.12	1.46	17.21	10.01	.27	.21	.98	8.78	.30
9B5	35.56	1.08	13.65	7.43	.28	.26	.70	2.53	2.44
9EB4	25.37	1.07	14.52	8.54	.28	.14	.69	6.33	4.11

due to the low quartz, and feldspars, these rocks show dominance of SiO_2 , Al_2O_3 and Fe_2O_3 content (Figs. 5-1, 5-1D). Both the lavas and chloritic clays are important sources of Fe_2O_3 and MgO . TiO_2 is present and may possibly come from detrital ilmenite. Although the lacustrine clays are also essentially contributing to these elements. The arkoses are generally characterised by higher Na_2O and K_2O content presumably due to the more abundant feldspars (5-7E). This suggests a fairly low maturity of the arkosic deposits. However, the composition of such rocks could very well depend to a great extent on the amount and type of interstitial clay minerals. The SiO_2 - Al_2O_3 - $\text{K}_2\text{O} + \text{Na}_2\text{O}$ triangle (Figs. 5-1G, 5-1H). The K_2O versus Na_2O relationship (Figs. 5-7E) shows that the deposits are frequently characterised by higher Na_2O content possibly due to the presence of Na-plagioclase, which could be an indication of their immaturity (Pettijohn, 1975). The chemical composition of the clays and siltstones in the area are composed mainly of SiO_2 , Al_2O_3 and Fe_2O_3 . The relatively high amount of silica is contributed mainly from the quartz, whereas the aluminium originate mainly from the clay minerals and purely from feldspars. The iron may be contributed primarily by from pyrite and chlorite in the green phyllosilicates while in the red sediments iron is mainly present in the form of hematite. The potassium is possibly from clays and detrital microcline. Magnesium is derived from

chloritic clay minerals. The K_2O versus Na_2O relationship in the other formations (Figs. 5-7A, 5-7B) indicates the deposits are characterised by frequent higher content of K_2O and /or Na_2O though not as high as those of the Ronda Formation. The more K_2O in the Kariandusi Formation is partly due to the abundant clay minerals. The bulk composition of the formation (Table 8) shows that they are composed mainly of the SiO_2 , Al_2O_3 and Fe_2O_3 . The source of these oxides are the surrounding volcanics. Compositional differences between the sediment groups are apparent from the distribution depicted by plotted elements on an Al_2O_3 - MgO - Fe_2O_3 triangular diagram (Figs. 5-1I,5-1J). Volcanic sediments are here differentiated by their high iron and magnesium contents which are a consequence of higher percentages of ferromagnesium minerals. Calcareous sediments have the lowest magnesium concentration but show a wide range of iron contents (Figs. 5-1I,5-1J). The composition of the sediments are distinct from all other sediments and are distinguished by low magnesium and iron concentration relative to aluminium. Scatter on the Al_2O_3 - MgO - Fe_2O_3 plot (Figs. 5-1I,5-1J) can be attributed to the location of iron and to a lesser extent magnesium) in silicate minerals. The same group of deposits are however pieced out correctly on molecular diagram of TiO_2 - K_2O - Al_2O_3 (Figs. 4-1, 4-1A, 4-1B). In this plot volcanic deposits are characterised by high titanium and low potassium contents and again do not fall close to the field of

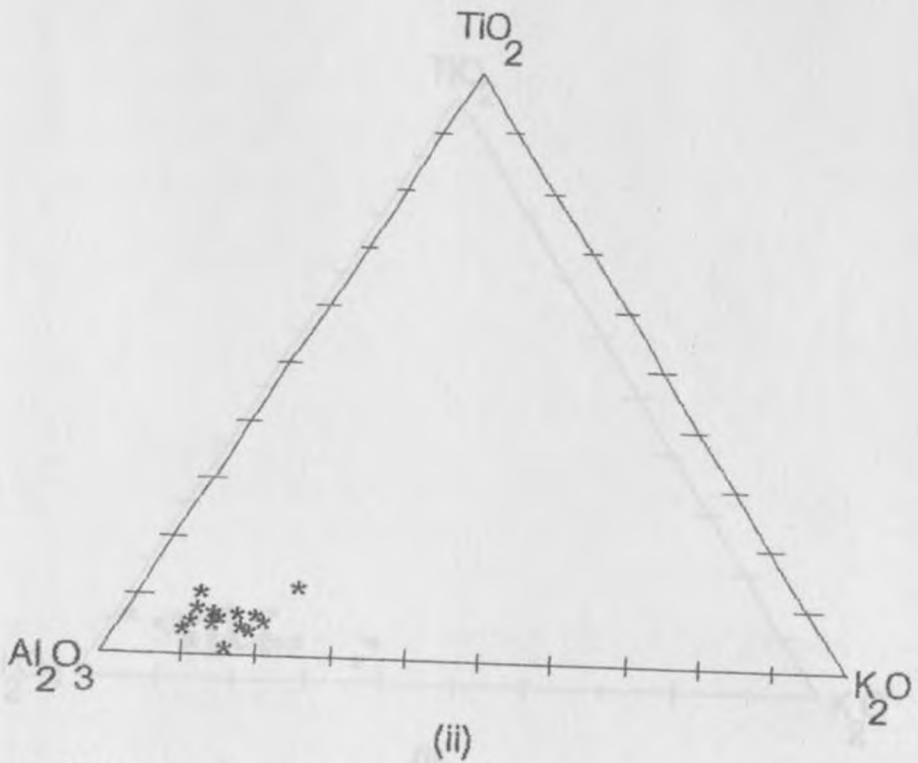
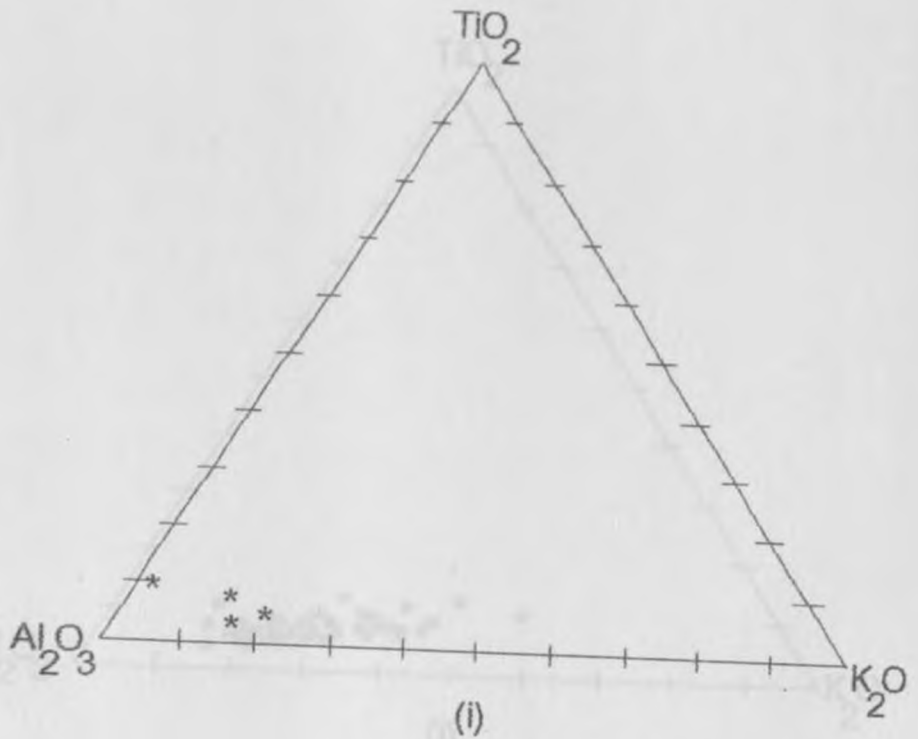


FIG.4-1 $TiO_2 - K_2O - Al_2O_3$ ternary plots of the (i) Soysambu and (ii) Enderit Formations.

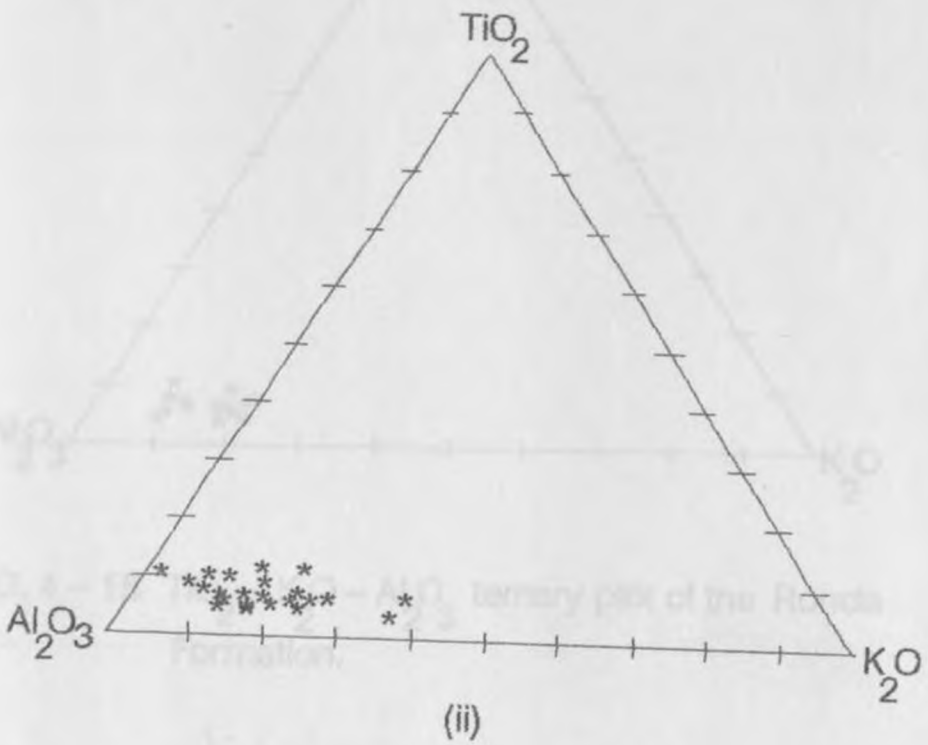
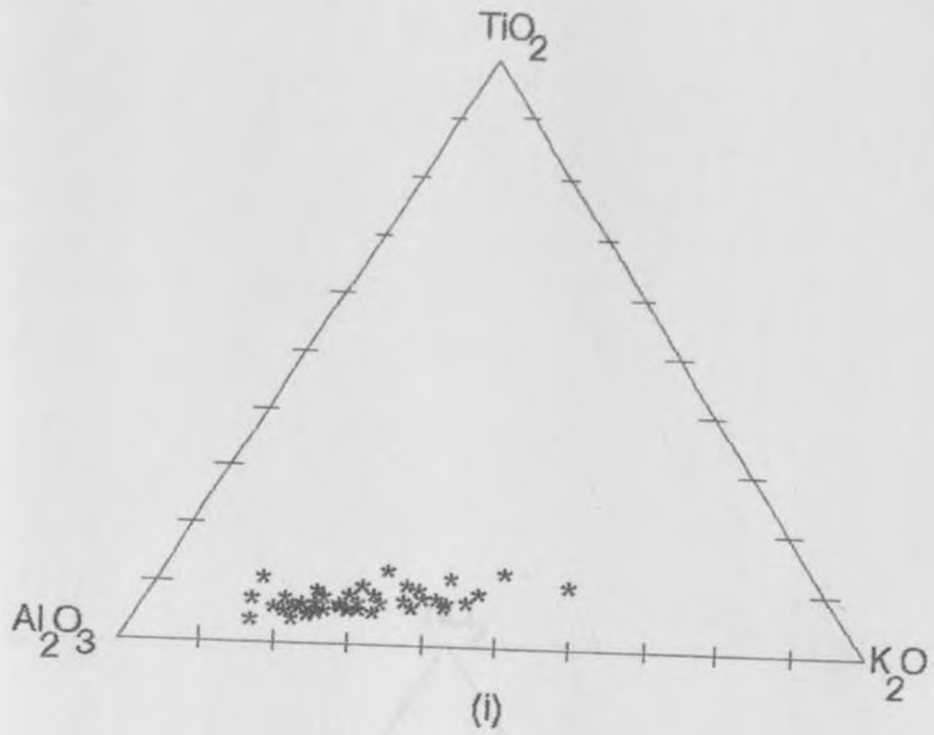


FIG. 4-1A $\text{TiO}_2 - \text{K}_2\text{O} - \text{Al}_2\text{O}_3$ ternary plot of the (i) Kariandusi Formation (ii) Makalia Beds.

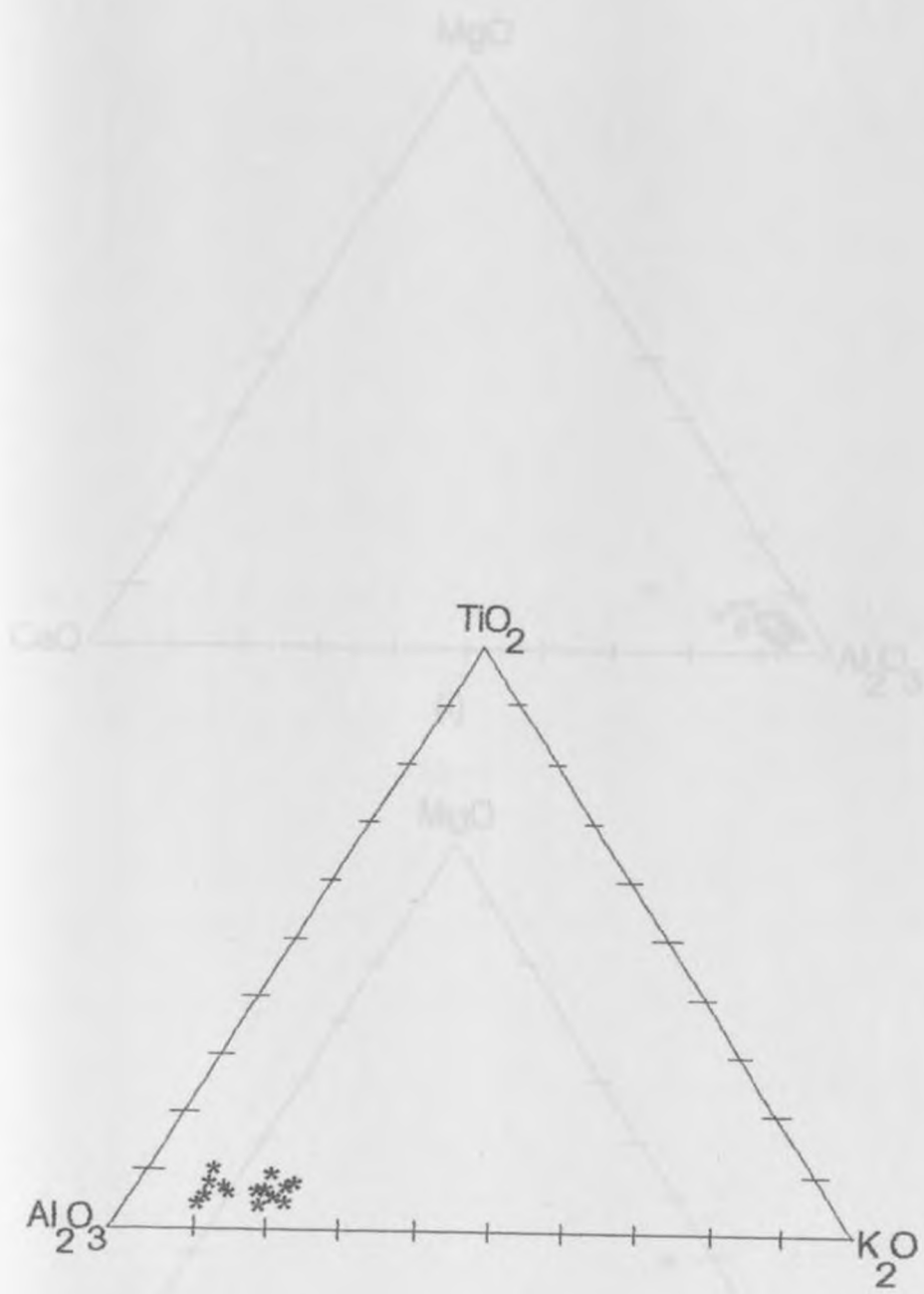


FIG. 4-1B $\text{TiO}_2 - \text{K}_2\text{O} - \text{Al}_2\text{O}_3$ ternary plot of the Ronda Formation.

FIG. 4-2A $\text{MgO} - \text{Al}_2\text{O}_3 - \text{CaO}$ ternary plot of the (i) Mikata beds (ii) Endell Formation

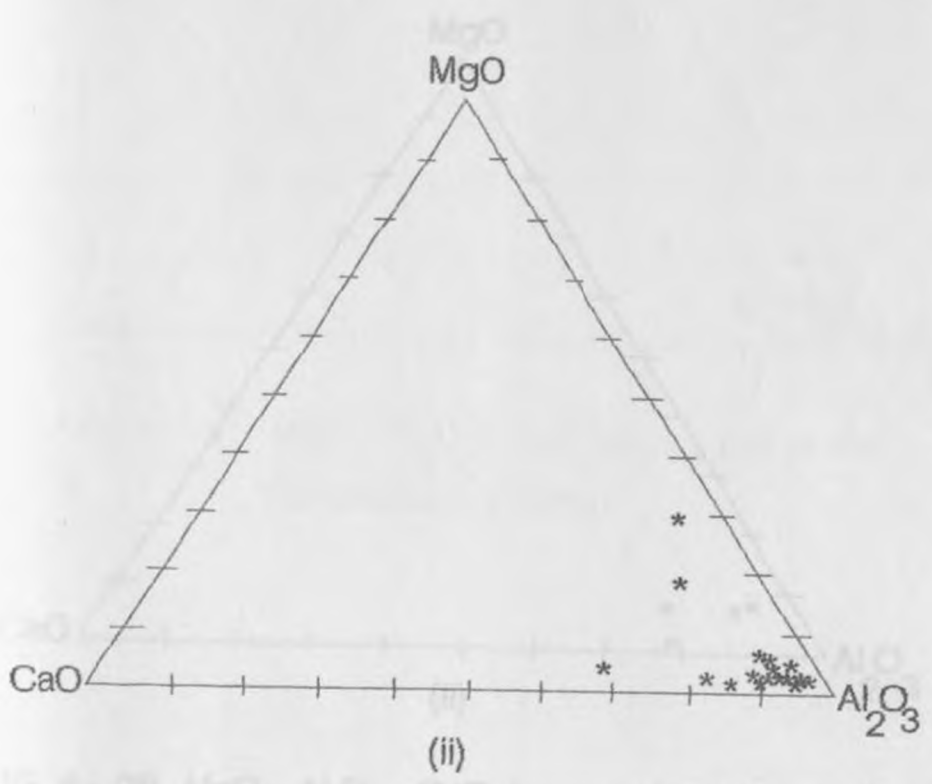
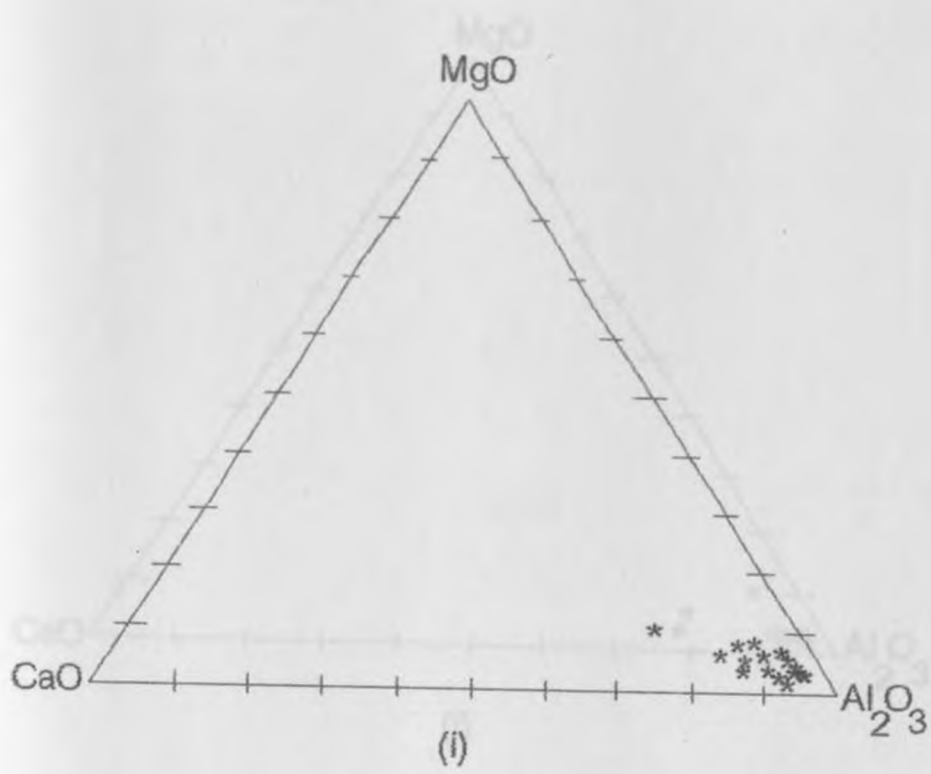


FIG. 4-2A MgO - Al_2O_3 - CaO ternary plot of the (i) Makalia Beds (ii) Enderit Formation

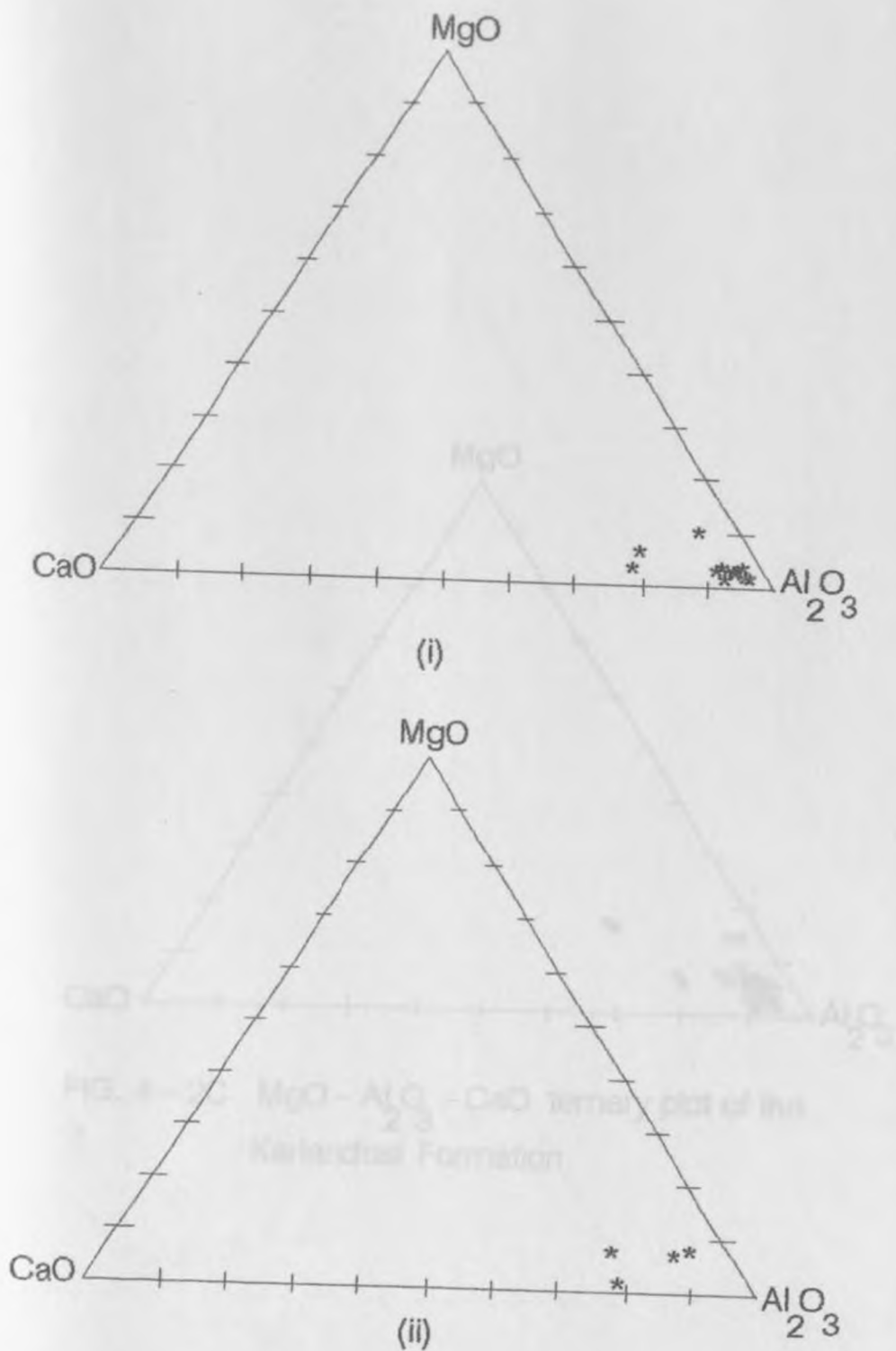


FIG. 4-2B MgO - Al₂O₃ - CaO ternary plot of the (i) Ronda Formation and (ii) Soysambu Formation

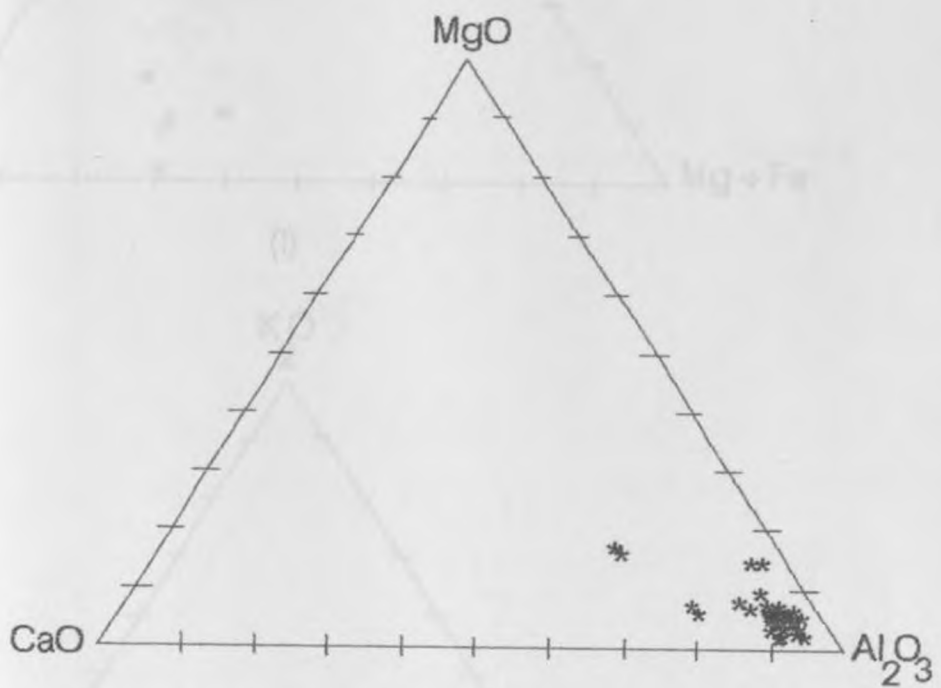
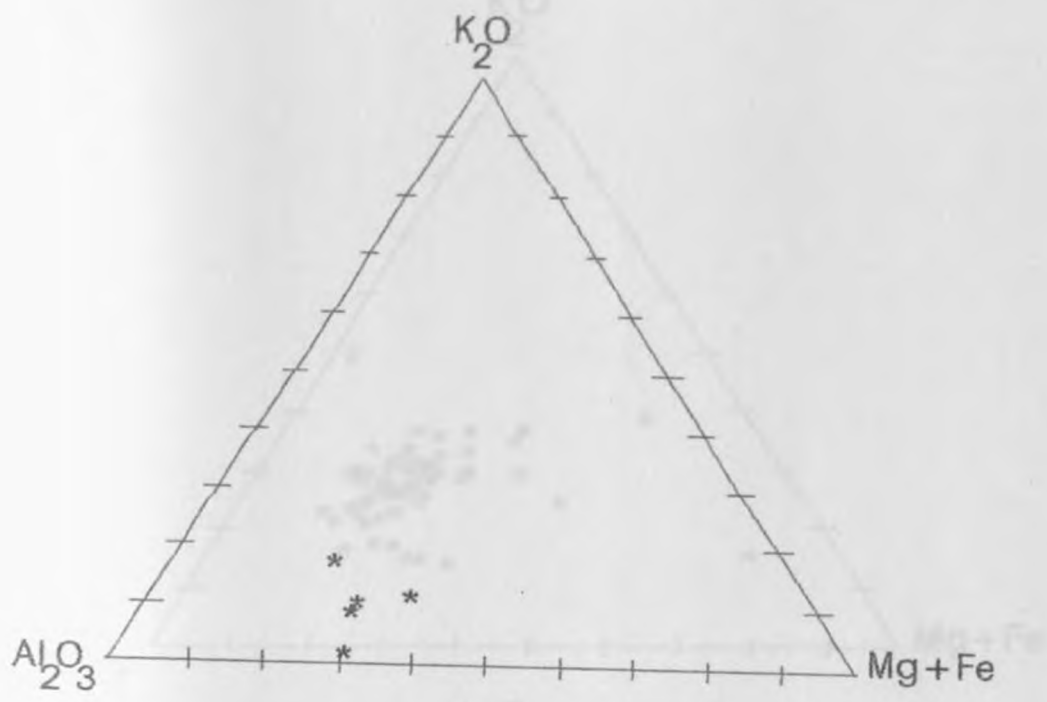
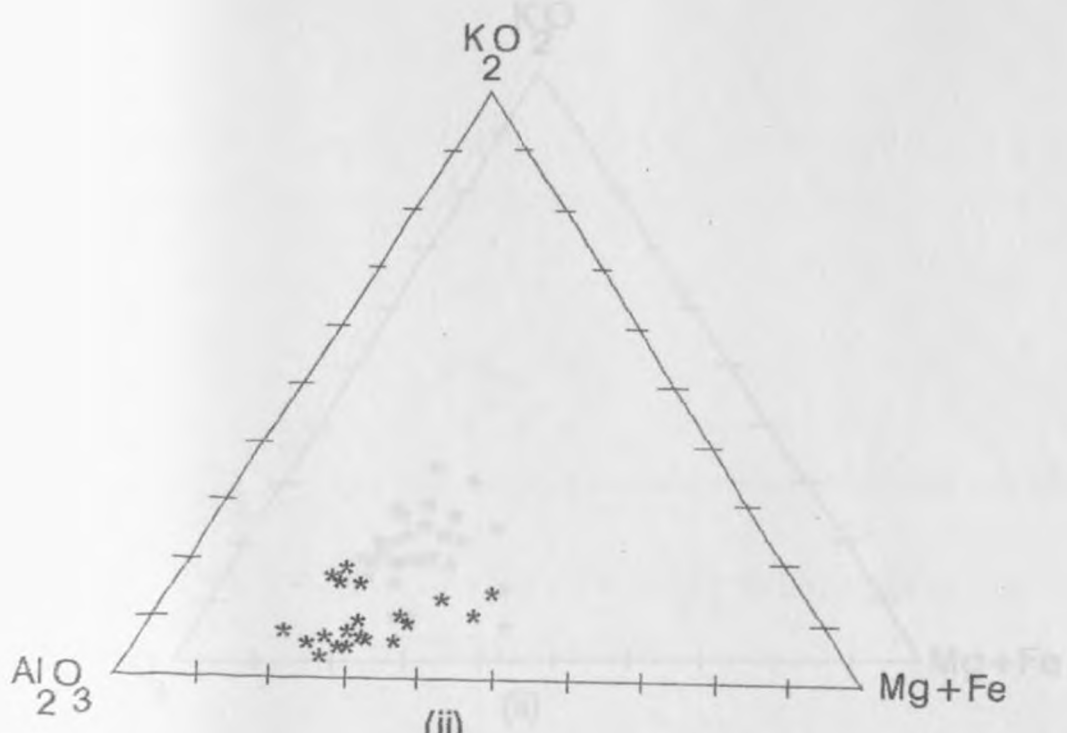


FIG. 4 - 2C MgO - Al₂O₃ - CaO ternary plot of the Kariandusi Formation

(i) MgO - Mg+Fe - Al₂O₃ ternary plot of the
 (i) Kariandusi Formation and (ii) Endell Formation

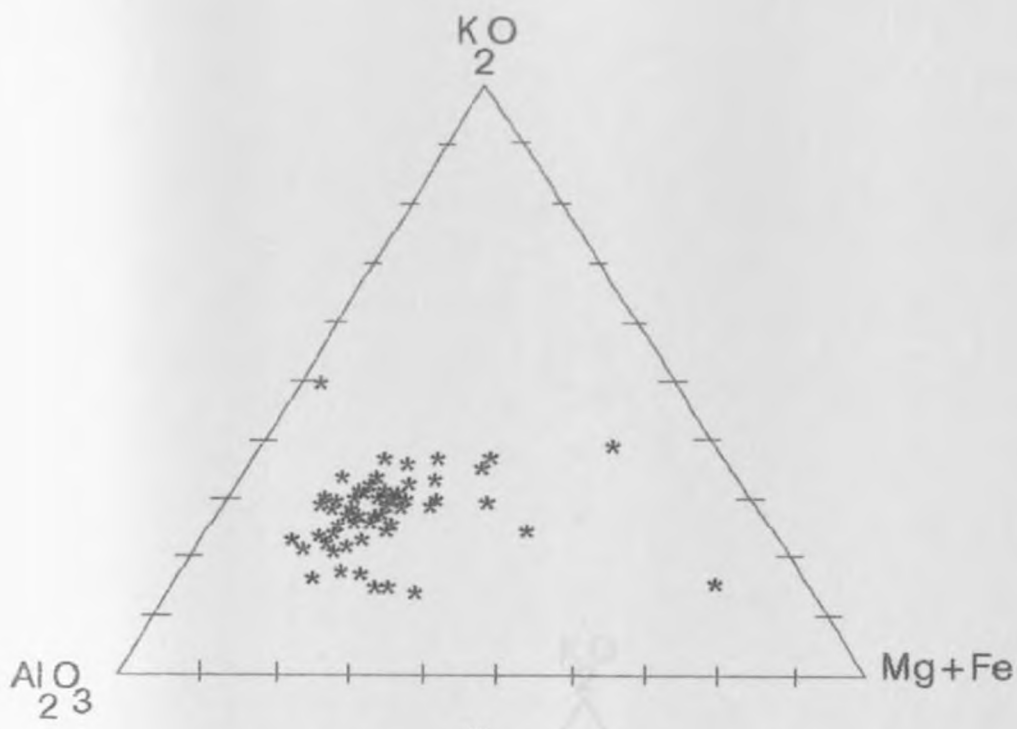


(i)

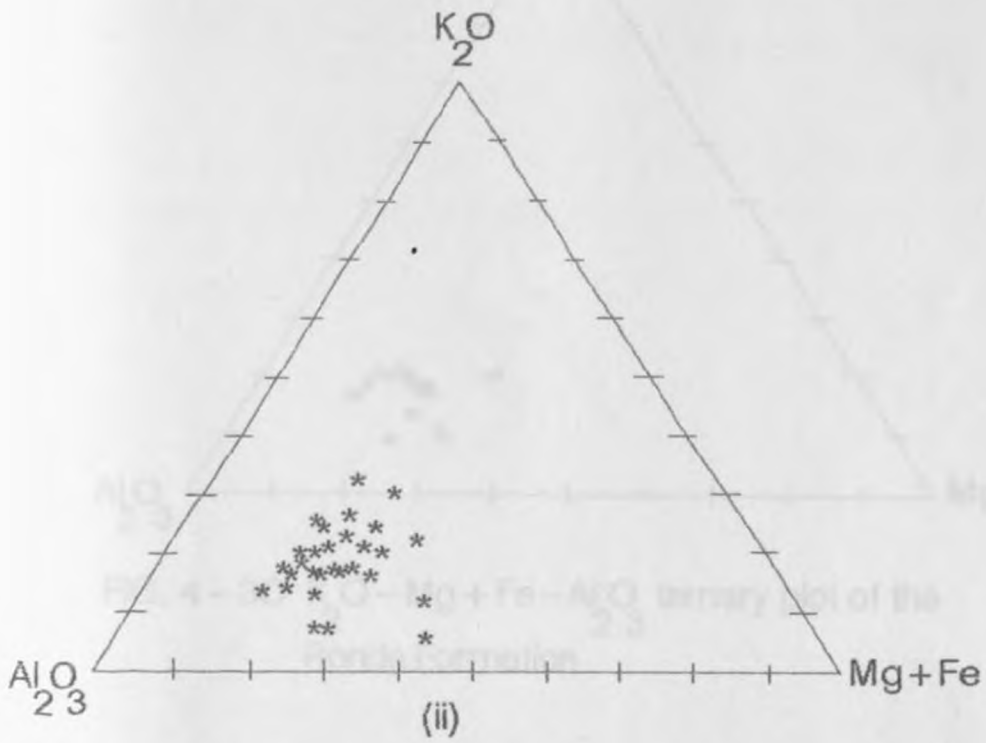


(ii)

FIG. 4 - 3A $K_2O - Mg + Fe - Al_2O_3$ ternary plot of the
 (i) Soysambu Formation and (ii) Enderit Formation



(i)



(ii)

FIG. 4-3B $K_2O - Mg + Fe - Al_2O_3$ ternary plot of the
 (i) Kariandusi Formation and (ii) Makalia Beds.

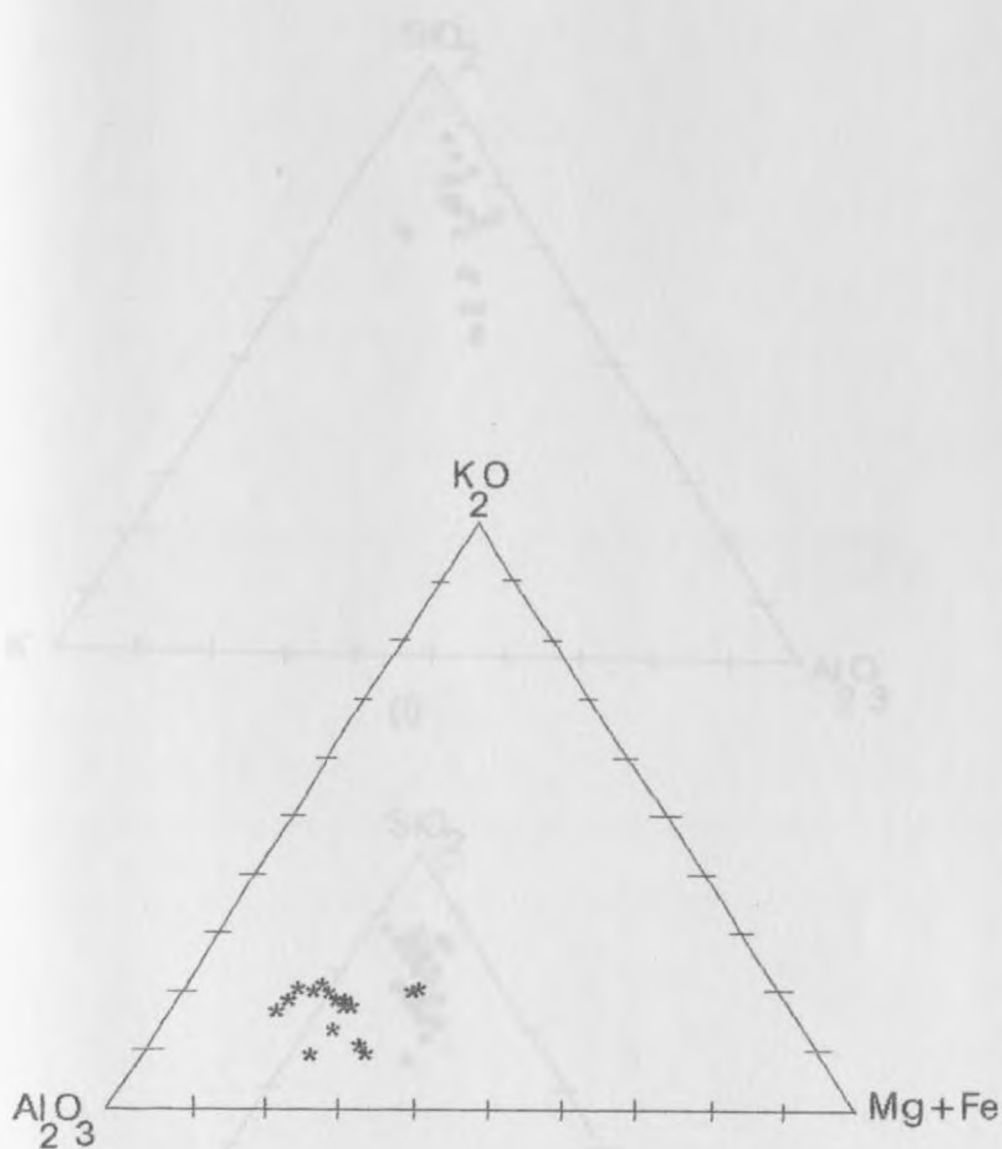


FIG. 4 - 3C $K_2O - Mg + Fe - Al_2O_3$ ternary plot of the Ronda Formation

FIG. 4 - 4A $SiO_2 - Al_2O_3 - FeO + K_2O$ ternary plot of the (i) Makala Beds and (ii) Katerouss Formation

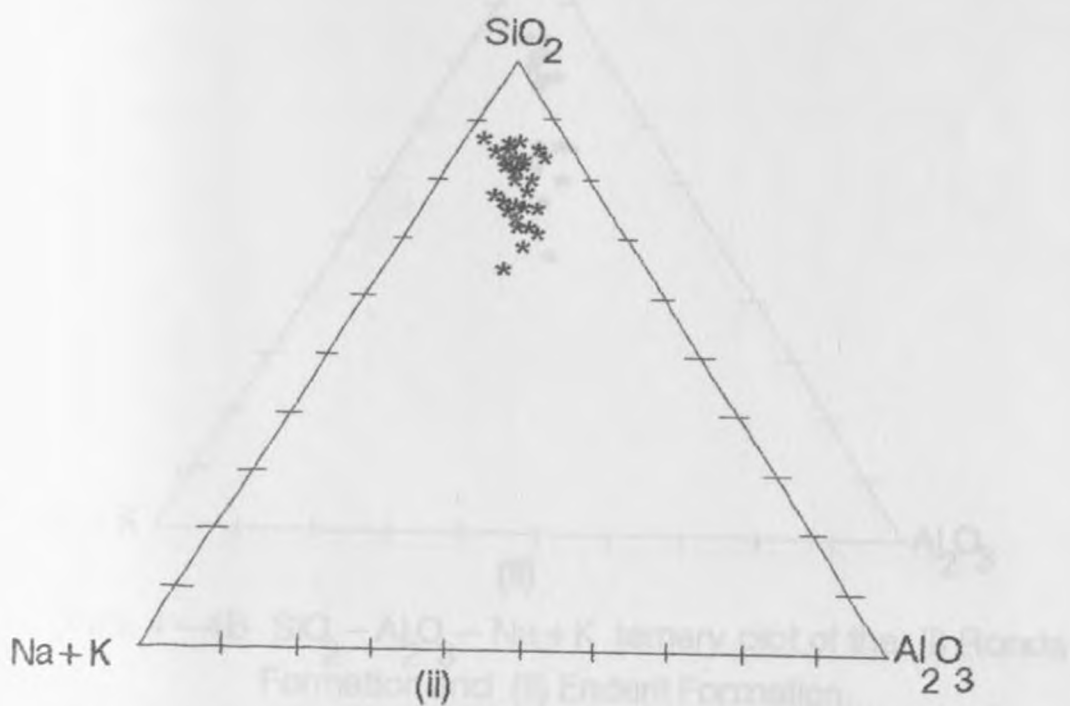
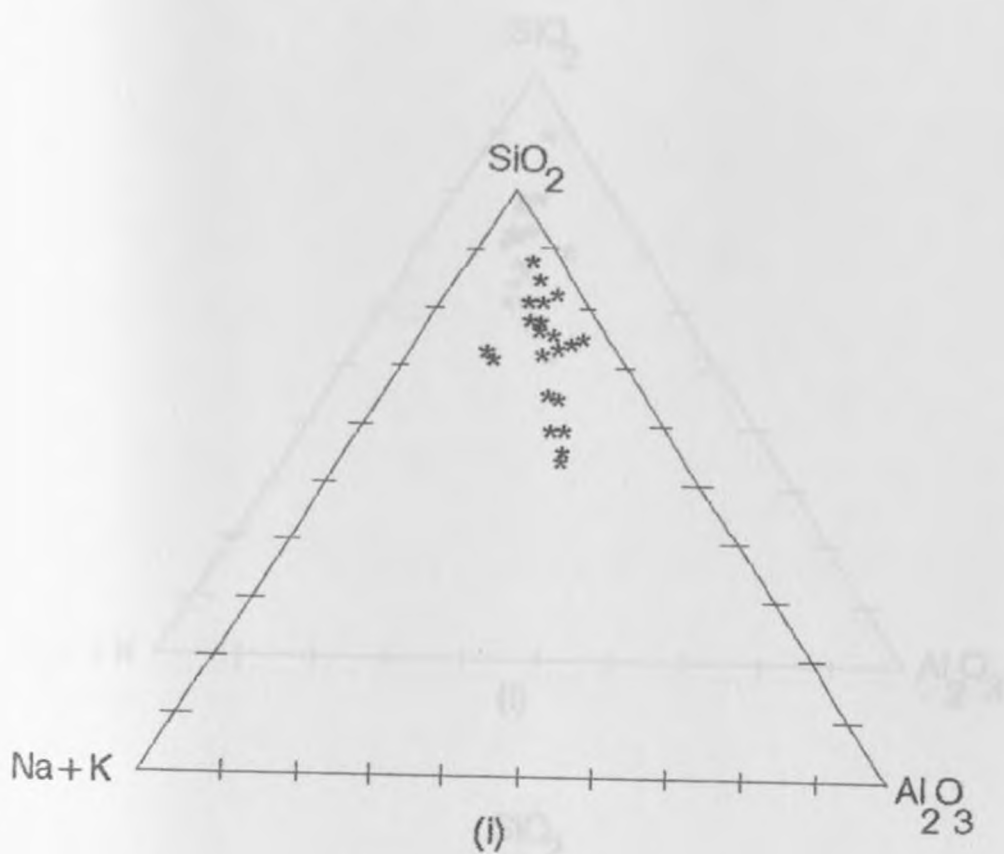


FIG. 4-4A SiO₂-Al₂O₃-Na+K ternary plot of the (i) Makalia Beds and (ii) Kariandusi Formation

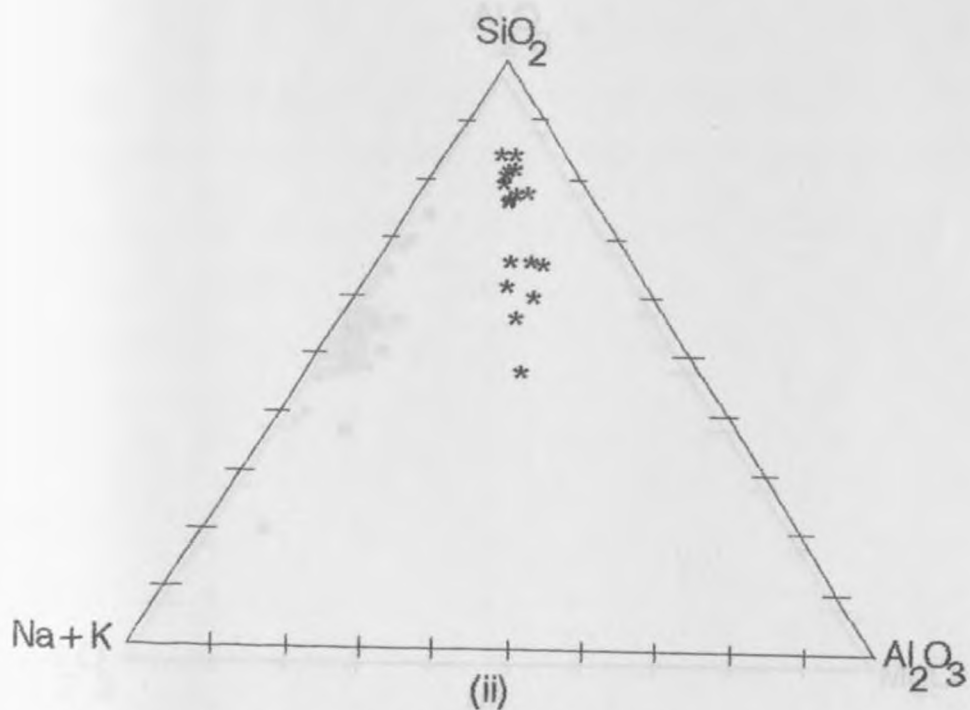
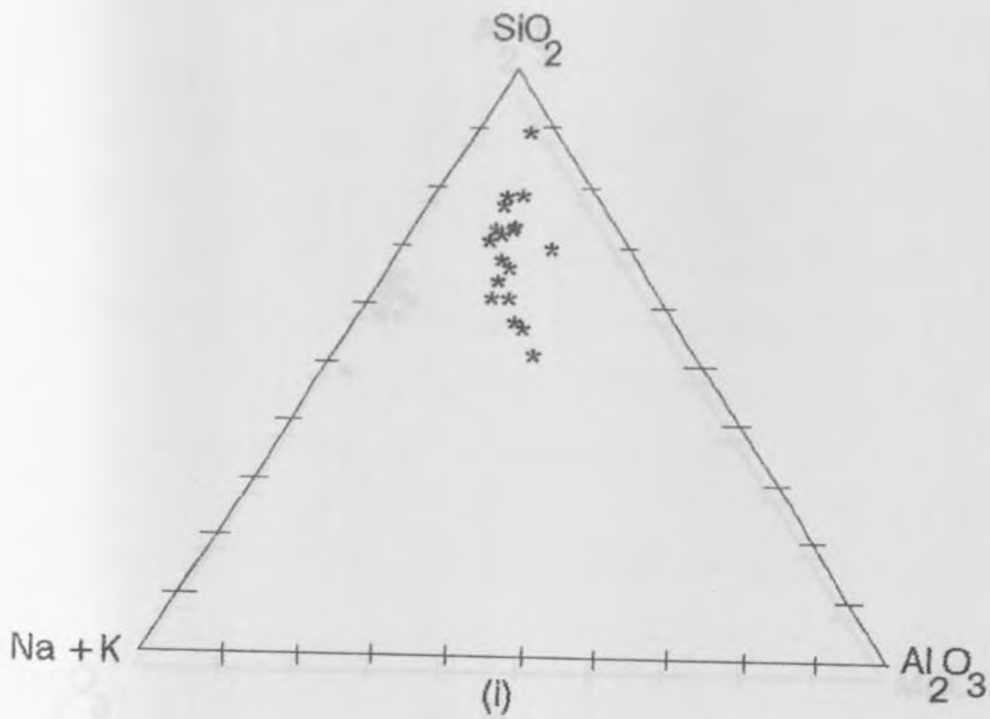


FIG. 4-4B $\text{SiO}_2 - \text{Al}_2\text{O}_3 - \text{Na} + \text{K}$ ternary plot of the (i) Ronda Formation and (ii) Enderit Formation

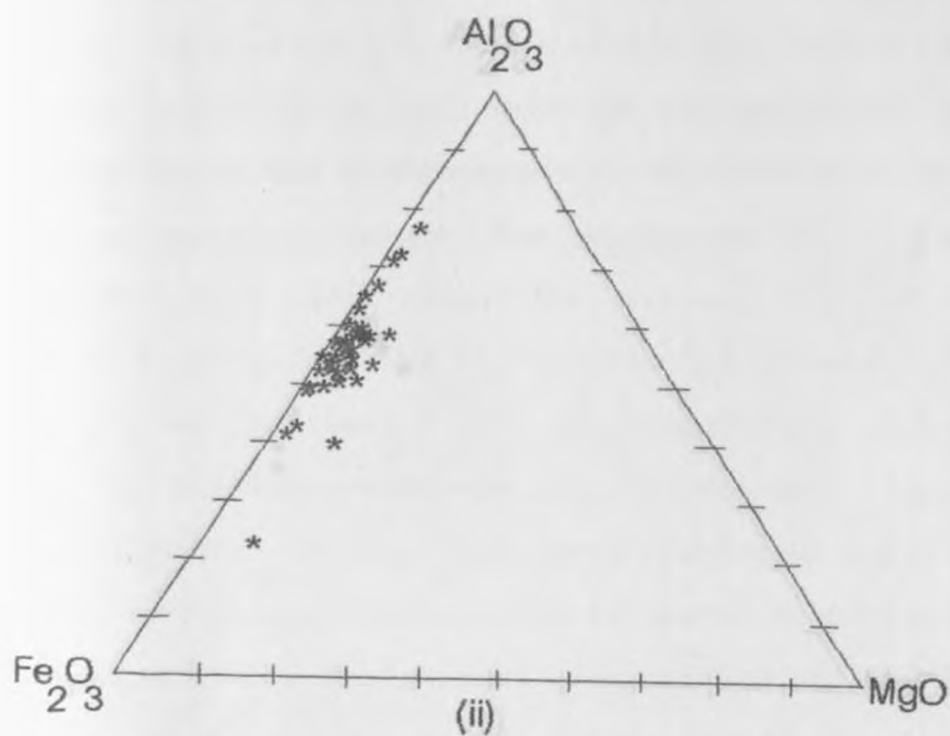
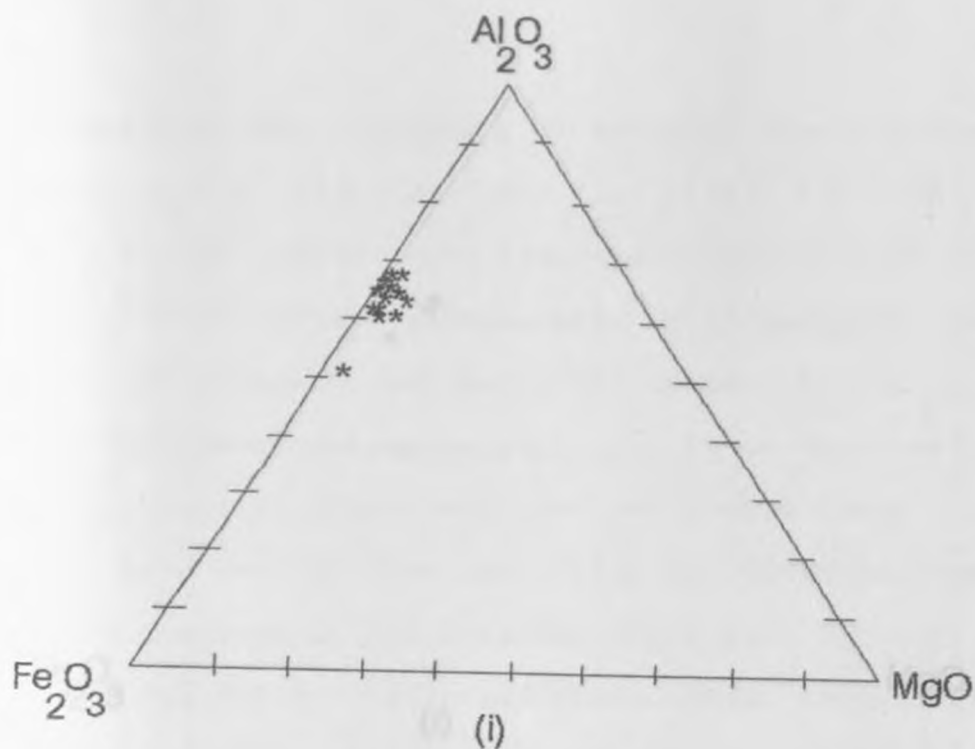


FIG. 4-5A Al_2O_3 - MgO - Fe_2O_3 ternary plot of the (i) Ronda Formation and (ii) Kariandusi Formation

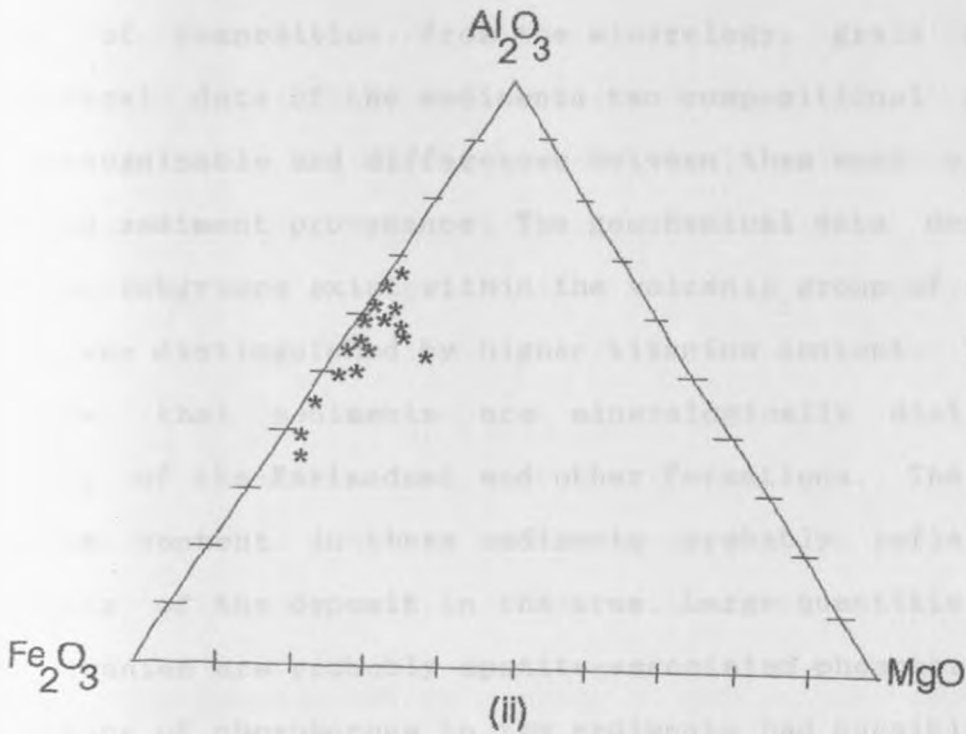
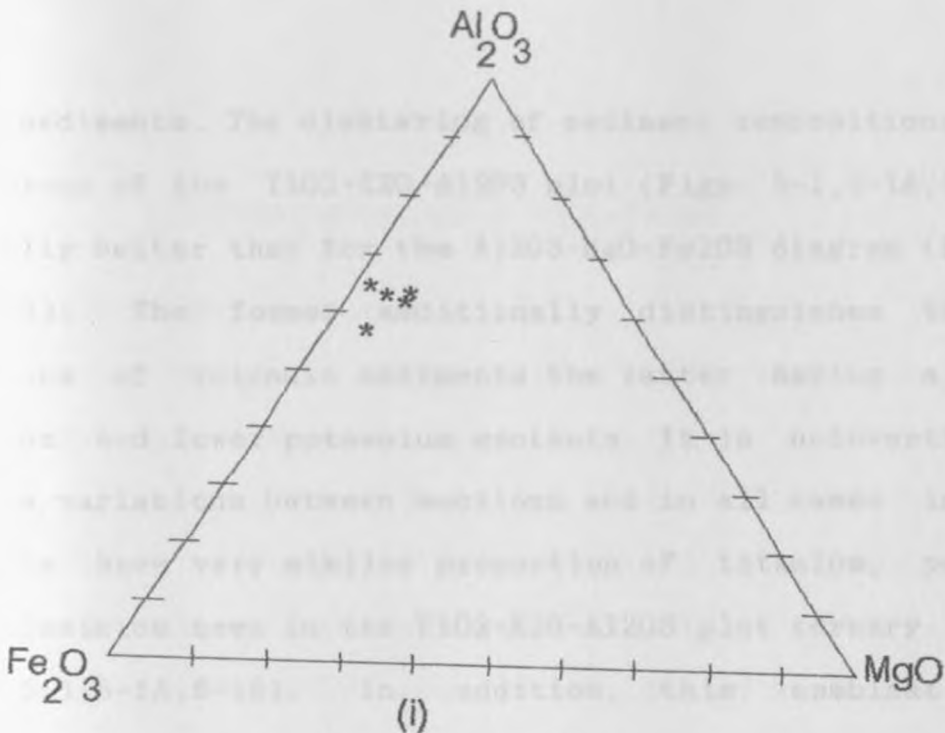


FIG. 4-5B $Al_2O_3 - MgO - Fe_2O_3$ ternary plot of the
 (i) Soysambu Formation and (ii) Enderit Formation.

other sediments. The clustering of sediment compositions within each group of the TiO_2 - K_2O - Al_2O_3 plot (Figs. 5-1, 5-1A, 5-1B) is generally better than for the Al_2O_3 - MgO - Fe_2O_3 diagram (Figs. 5-1I, 5-1J). The former additionally distinguishes the two subgroups of volcanic sediments the latter having a higher titanium and lower potassium contents. It is noteworthy that despite variations between sections and in all cases individual deposits have very similar proportion of titanium, potassium and aluminium seen in the TiO_2 - K_2O - Al_2O_3 plot ternary diagram (Figs. 5-1, 5-1A, 5-1B). In addition, this combination of parameters separate the two Formations by relatively large shifts of composition. From the mineralogy, grain size and geochemical data of the sediments two compositional subgroups are recognisable and differences between them must relate to changing sediment provenance. The geochemical data demonstrate that two subgroups exist within the volcanic group of sediments which are distinguished by higher titanium content. The data indicate that sediments are mineralogically distinct in sections of the Kariandusi and other Formations. The higher titanium content in these sediments probably reflect their proximity of the deposit in the area. Large quantities in all the volcanics are probably apatite-associated phosphorous. The occurrence of phosphorous in the sediments had possible origin in the surrounding volcanic rocks and biological related lacustrine environments.

CHAPTER 5

LITHOSTRATIGRAPHIC FORMATIONS.

5.1 Lithofacies Associations.

The Central Rift is characterised by a wide variety of lithofacies associations documented in both the modern and ancient sedimentary deposits. The lithofacies are characteristic of coarse to fine grained alluvial fan, fluvial, eolian and lacustrine depositional systems. It is a common phenomenon in sedimentary systems that two or more lithofacies may be genetically related and detailed stratigraphic studies have resulted into recognition of numerous lithofacies associations (Miall, 1978; Reineck and Singh, 1986) which can be interpreted as the products of particular depositional environments. The terminology used to describe lithofacies associations here is modified after Reading (Reading, 1978), who used the term "facies" to represent a distinctive rock type that forms under certain conditions of sedimentation reflecting a particular process or environment. A group of facies that occurs together and has a genetic or environmental relationship is hence termed "facies association."

Facies relationships which represent particular depositional environments can be distinguished at a variety of scales of subdivision (Burggraph, 1982; Walker, 1979). Associations which represent large-scale depositional environments (e.g. fluvial

channel or alluvial fan) are termed "major lithofacies associations." The major facies or depositional environments can further be subdivided into minor facies units termed minor lithofacies associations. In the Lakes Nakuru, Elmentaita and Naivasha basins five major lithofacies associations are recognised in the rift sediments. The facies are the (1) lacustrine facies (laminated siltstone, diatomaceous silts and claystones association), (2) deltaic-littoral facies (interbedded sandstone siltstone association), (3) fluvial facies (conglomerate and sandstone association), (4) piedmont, alluvial fan facies (fanglomerates: agglomerate, "conglomerate" pebbly mudstone association) and (5) eolian facies (pyroclastic tuff, volcanic ash, sandstone, siltstone and claystone association).

Some of the above listed major lithofacies associations may consist of several recognisable minor lithofacies associations. The fluvial channel environment, for instance, can be divided into two minor lithofacies associations of lenticular conglomerate and sandstone lithofacies associations. The lenticular conglomerate associations consist of large volcanic clasts (e.g. basalt). The clasts vary from rounded to sub-rounded rocks depending on the distance of transportation from the source. These lenticular conglomerates are interpreted as the product of high-energy channel draining off

alluvial fans of adjacent volcanic highlands. The polymictic-tuff conglomerate and sandstone associations is interpreted as the deposit of a low-energy channel.

5.2 Kariandusi Formation

Kariandusi Formation is subdivided into three lithofacies associations consisting of lacustrine facies, lake-margin facies and fluvial facies. Facies relationships (Fig. 5-1) were reconstructed along north - south cross-section through the Kariandusi Diatomite Mine. The Lake deposits accumulated in Pleistocene perennial lake in the central part of the basin and is particularly well exposed at the Kariandusi diatomite mine. Lake margin sediments were laid down on low-lying terrain intermittently flooded by the lake. Alluvial fan deposits are concealed beneath lake margin facies along the north-western and south-eastern margins of the basin where they possibly interfinger with the lake margin deposits. Lake margin facies outcrop at the Kariandusi Prehistoric Site and those along the Nakuru-Naivasha main road are similar in lithology and within these deposits are found archaeological and palaeontological sites.

5.2.1 Lacustrine facies.

The lake deposits are well exposed at the diatomite mine where they have maximum thickness of 30 m (Plate 2b) but wedges out to less than 3 m near the south-western margin. Lacustrine

North L17 L17A L17B L17C L41L1 L14A L14B L14C L14D L13 14 iv 14 iii L14 ii L14 i South

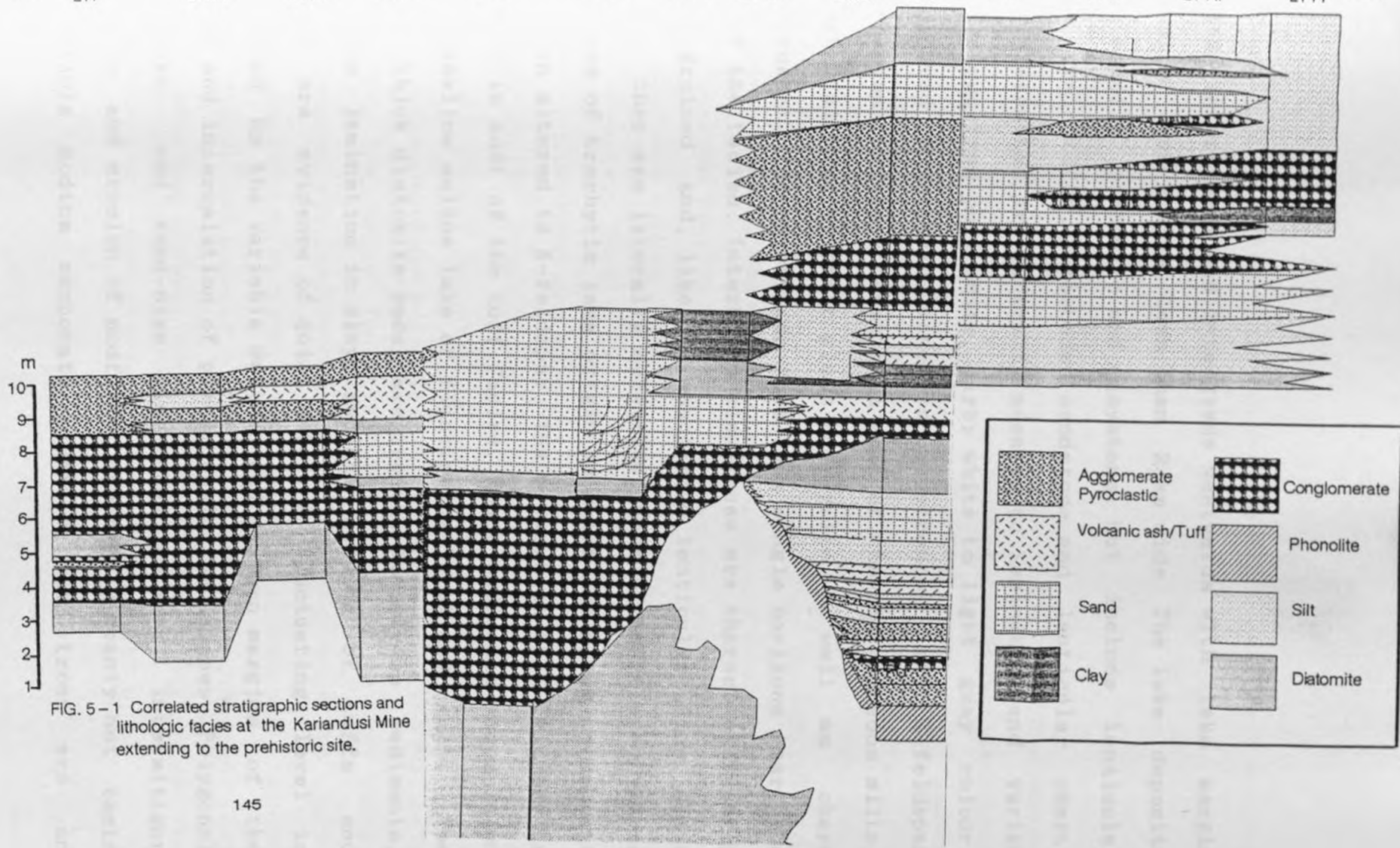


FIG. 5-1 Correlated stratigraphic sections and lithologic facies at the Kariandusi Mine extending to the prehistoric site.

tion of a saline sodium carbonate lake. The chert nodules facies interfinger and intergrade westwards with lake margin deposits over a zone less than 2 km wide. The lake deposits are chiefly diatomite and claystone, but include lenticular fine grain tuffs, interbedded sandstone and lenticular chert. The diatomites are generally massive to laminated and varies in colour from pure white, dirty white to light gray colour. Widespread authogenic minerals occurrence of K-feldspar (potassium feldspar) constitute most of the diatomaceous silts, though altered volcanic glass and pyrite, as well as chert are present. The chert beds form thin single horizons near the top of the facies. Interbedded claystones are characteristically fine grained and, like the associated lenticular fine grain tuffs, they are laterally extensive. Most of tuffs are vitric and are of trachytic lava origin in which the glass component has been altered to K-feldspar. The proportion of K-feldspar is highest in most of the tuff facies. These sediments accumulated in a shallow saline lake of fluctuating level and extent. The white thick diatomite beds are typical lacustrine sediments, and the lamination in clays and even bedding of tuffs and cherts are evidence of quiet water. A fluctuating level is indicated by the variable western and eastern margins of the facies and intercalation of pebbly pumice sandstones. Polygonal mudcracks, and sand-size claystones reflect intermittent exposure and erosion of mudflats. Apparently scanty but casts of soluble sodium carbonate minerals and trona are an

indication of a saline sodium carbonate lake. The chert nodules are of a type associated with deposits of saline sodium carbonate lakes (Eugster, 1967, 1969).

5.2.2 Deltaic-littoral facies.

The lake-margin facies at Kariandusi vary from 2 to 13 m thick, generally interfinger with the lake deposits. These sediments are principally interbedded pumice sandstone, lenticular pumice tuff, reworked diatomaceous claystone, and sandy tuffs. The sandstones are mainly feldspathic and volcanic glass detritus. Granule- and pebble-size volcanic clasts occur extensively on the western side of the basin. These sediments grade eastwards into a section that is dominantly sandy and clay tuff facies. Within the lake margin deposits as in the lake deposits occur beds of uncertain genetic relationship in view of their limited exposure. Claystone and pumice clasts predominate in most of the lake-margin conglomerate facies. Claystones are greyish brown and commonly contain root markings. Reworked diatomite tuffs and diatomaceous silts and tuffaceous sandstones variably constitute the facies. The tuffs are lenticular in the south-west exposures and massive towards the depocentre of the lake. The same pumiceous conglomerates consist of widespread rounded pumice cobbles and generally form a uniform marker horizon bed for correlating several sections (e.g. L14i-L14iv), on the north western and south-western sectors of the basin.

At locality 14iv on the western edge of the Kariandusi basin, the facies is overlain by yellowish brown diatomaceous silt. The sand-size well sorted volcanic silt detritus beneath a homogeneous tuff points to eolian transport. The underlying sequence below tuff in the locality consists of sand conglomerate and only exhibit lacustrine features towards the base. The lake margin deposits contain a few steep-sided stream channels filled with tuffs or conglomerates. The deepest channel is located at the diatomite mine, locality 14. The detritus in this facies is from north-westerly sources. The channels must have been cut by streams flowing southward.

On the Nairobi-Nakuru road cut (Plates 1a, 1b), this facies has both lacustrine and fluvial features indicating that it accumulated on terrain intermittently flooded by lake. The sandstone indicates shallow, wave-agitated lake water and the laminated vitric tuff suggests quiet water, either of lake or floodplain. Lenticular conglomerate and channelling are fluvial features. The depth of stream channel may provide a rough measure of lake level fluctuation. Claystone and reworked diatomite pellets probably reflect erosion of mudflats by wind at a time of low lake level. In view of their large size, the rounded pumice cobbles probably floated southward across the lake to their present location. The lake water flooding the lake margin was less saline than the centre of the basin. Vitric tuffs are extensively altered in the facies and both

authigenic K-feldspar and evidence of soluble salts are lacking. Overall the lake-margin deposits are mainly tuffs and claystone, conglomerate and scanty diatomaceous silts. Palaeosols are weakly developed and many horizons occur over both tuffs and claystones. Where developed they are crumbly variably brown or brownish gray and intensively rootmarked. Palaeosols on tuffs are characterised by vitric tuff of the finest grain weathered to montmorillonite.

Tuffs are dominantly trachytic but included basaltic and andesitic composition. A few tuffs represent single showers of ash that fell on the land surface and were generally reworked only slightly if at all. A massive thick tuff sometimes root marked and containing diatoms in addition to pyroclastic materials is often a product of several eruption in which the ash was developed either in marsh land or on land surface intermittently flooded by lake water. A few tuffs are for most part laminated and are dominantly lacustrine. Limestones occur as coarse concretions cemented together in claystones and were probably precipitated from ground water at shallow depth.

Volcanic detritus accompanied by fragments of bone and pumice clasts are located in the upper unit of locality L13. The clasts are welded tuff derived from adjacent ignimbrite. Conglomerate in the lower unit are chiefly pumice-pebble conglomerate. Fossilised vegetation is indicated by abundant

coarse, generally unbranching vertical root channels and casts. These probably represent shore grasses and reeds. Diatomites and siliceous tuffs in the deposits point to the fluctuating lake level and periodically saline alkaline conditions. The lake-margin facies accumulated in relatively flat terrain that was intermittently flooded and dried in response to changes in the lake level. Originally the lava surface had a local relief which was buried by sediments. Claystone and widespread water laid tuffs were deposited at times of high water level, whereas palaeosols, archaeological sites (e.g. the Kariandusi Prehistoric site), eroded surfaces, and extensive land-laid tuffs represent periods of exposure. Most of the fluctuations may have been relatively short, either seasonal or involving no more than a few tens of years. Apparently streams carried pebbles of tuff over mudflats. The clasts are associated with torrential downpours to the north which led to the transportation of coarse sediment southward over mudflats.

5.2.3 Fluvial facies

In the Kariandusi area fluvial facies consists of well sorted tightly packed, clasts supported pumice conglomerate that form the uppermost portion of the Kariandusi Formation in sections 14, 15 and 17 (Figs. 3-4, 3-6, 3-6A, 3-7, 3-8; 5-1). On the north western side of the basin, stratification is generally lacking but imbrication is common. The matrix consists of

moderately sorted pumice sand-granule-sized particles. The dominantly conglomerate beds of the area are typically ranging between 2 to 8 m in thickness, have erosional bases and fine upward into either lenticular or wedge shaped lithofacies. At the diatomite mine, the fluvial facies is characterised by rounded, well sorted, clast supported pumice conglomerate. Horizontal stratification, trough and planar cross stratification and imbrication are evident in the beds. The beds range from less than 1 to well over 5 m in thickness and typically extend several tens of meters laterally. Toward the south-west and along the Nairobi-Nakuru main road the facies have erosional bases, and some exhibits cyclic crude upward-fining trends. In general however, the grain size changes are abrupt and not systematically predictable within the entire facies.

5.3 Enderit Formation

The Enderit Formation include both the Enderit and Makalia sequences (Plates 6a, 6b, 6c, and 7) and is of special geological interest because of the many lithofacies and environments it represents. Its stratigraphy is generally complex and correlation is difficult in many places. Enderit Formation comprises of six lithofacies representing six major types of depositional environments, including alluvial fan, alluvial plain, lake and lake-margin aeolian and fluvial-lacustrine complex.

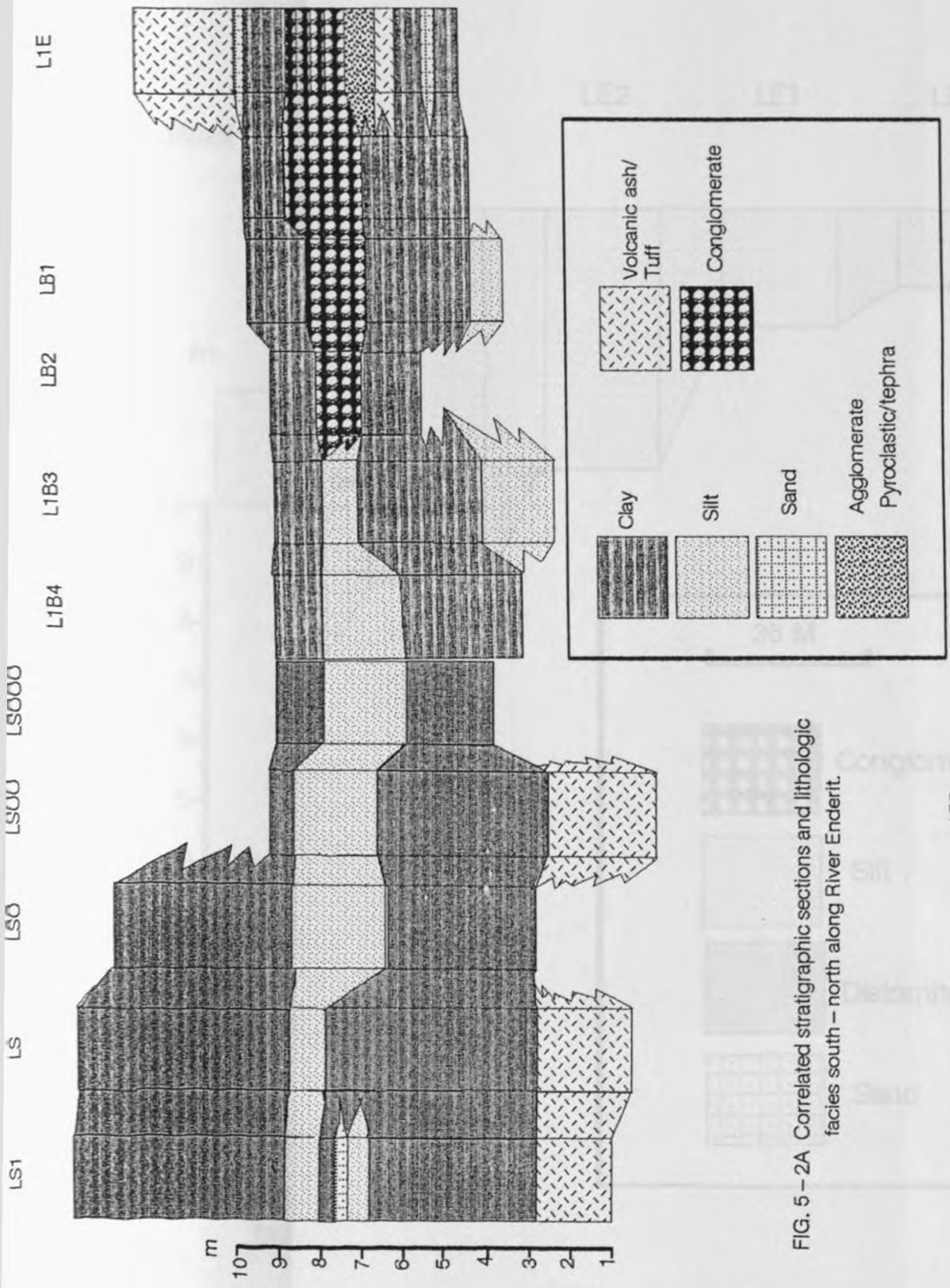


FIG. 5 - 2A Correlated stratigraphic sections and lithologic facies south - north along River Enderit.

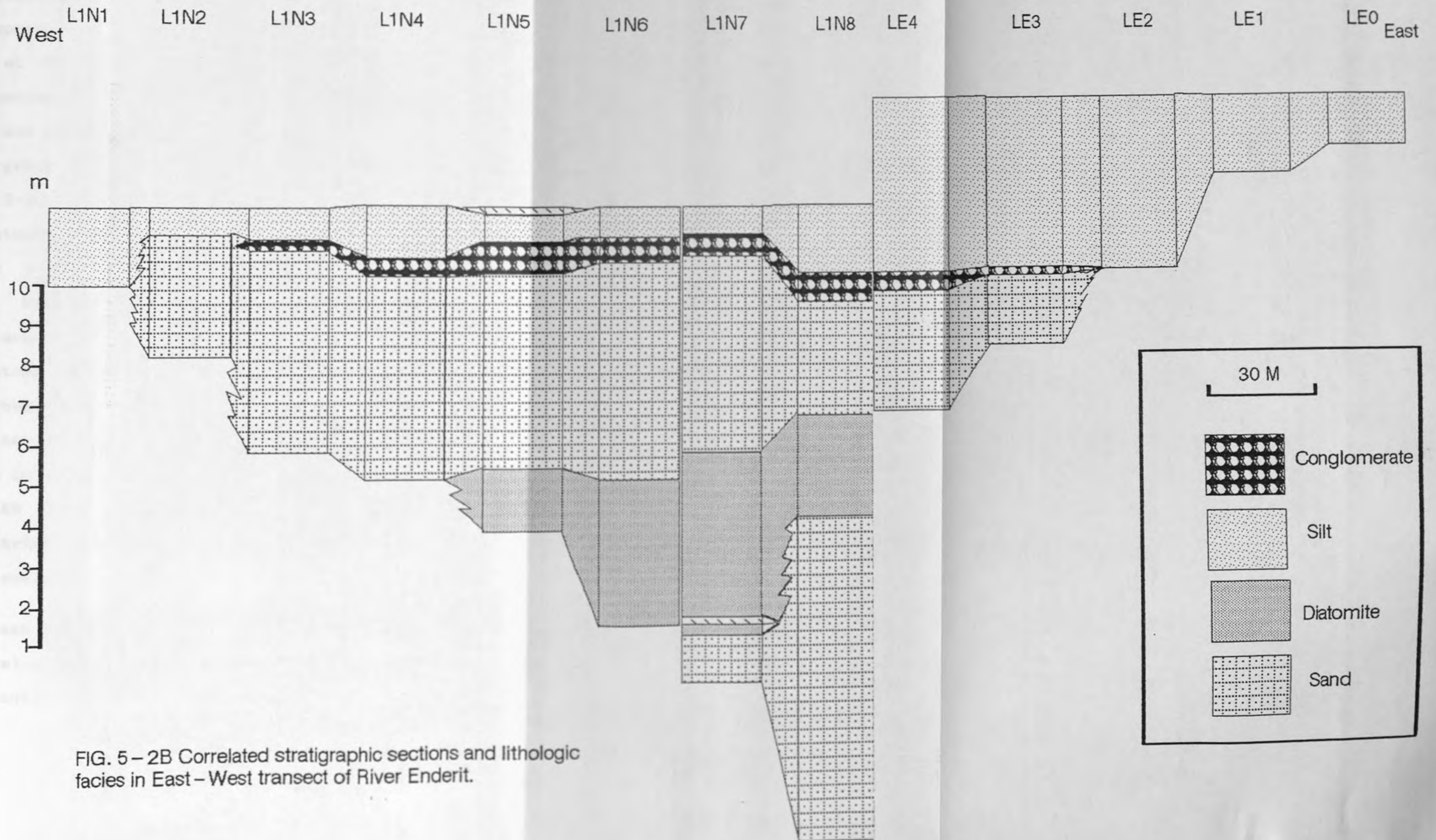


FIG. 5 – 2B Correlated stratigraphic sections and lithologic facies in East – West transect of River Enderit.

5.3.1 Lacustrine facies

The lake deposits border mixed fluvial and lacustrine sediments, termed fluvial-lacustrine deposits. Lake deposits are presently only in a few localities at different stratigraphic levels. In these localities they are most widespread in both the lower sections (Figs. 5-3H, 5-4A; 5-4B) and at the relatively higher levels (Figs. 5-3G, 5-3E, 5-3F). The sediments generally range from 10 cm to 5.4 m in thickness and are predominantly diatomaceous silt and claystones which intergrade with reworked tuffs and sandstone facies (Figs. 5-3A, 5-3C, 5-3E, 5-3F; 5-4A, 5-4B). Both claystones and sandstones consist chiefly of feldspathic detritus derived from older volcanic terrain of the bounding fault scarps to the west. Most of the tuffs are altered chiefly to K-feldspar. To the south of River Enderit, lake deposits pinches out as claystone grades into siltstone. The claystone facies are interbedded with silty and sandy tuffs and can be shades of gray or brown in colour. Tuffs are generally thick evenly bedded and mafic in origin. Except in sections L8H and L8I (Fig. 5-3E) and LEO-LE9 (Figs. 5-3H and 5-3I), where they are thick fluvial-lacustrine deposits (Fig. 5-2B), sandstones are thin laminated and generally widespread.

The lake facies here are mainly claystones and thin laminated diatomaceous silts towards the south. Claystones here are dominantly gray and brown in colour. Desiccation cracks were

noted at few horizons near the eastern margin of the facies (Fig. 5-3G). Some of the easternmost sandstones contain appreciable widespread sands. Lithologically, the sandstone are of two types, well sorted medium grained and ill-sorted coarse grained both consisting of angular to subangular texture dominantly of volcanoclastic detritus (Figs. 5-3H and 5-3I). At Makalia, lacustrine silt facies are well developed toward the south and is exposed over a distance of 1.8 km. The K-feldspar rich volcanic constitute 30 to 70 percent of the detrital pumice silt, the remainder include fine grained calcareous clays, pumice clasts and chert nodules occurring at various levels.

The lake deposits in the Enderit and Makalia areas are considered to have formed in a single lake of fluctuating levels and concomitant decrease in size. The inference here is based lithological similarities of the sedimentary facies which possibly accumulated south extension of proto-Lake Nakuru basin. In the originally vast basin, formed an extensive shallow saline alkaline lake, a precursor of the now much smaller but generally similar in its sediments to the present Lake Nakuru. The lower part comprised of widespread volcanogenic claystones and siltstones. Salinity was possibly highest towards the centre as indicated by widespread trona casts on the fringes of the contemporary Lake Nakuru. Lake

deposits towards margins represent a zone of transitional to the lake-margin environment. The provenance of lensoid trona crusts, although not well understood, involved saline, alkaline solutions with aluminosilicate materials among which volcanic glass was possibly a minor constituent. The major reactants may have been amorphous clay or aluminosilicate gel of the type formed today around hot springs in the Eburru volcanic ridge, and south at Lake Magadi (Eugster and Jones 1968). Saline alkaline lake water is also recorded by chert nodules. Intermittent flooding by fresh water or exposure during low lake levels is indicated by red oxidised beds. Rootmarks and tubules were formed by marshland vegetation, which indicates fresh or brackish water. Although the lake deposits have mineralogical features indicative of saline, alkaline lake water, the associated diatomite deposits point to fresh or brackish water. The lake fluctuated in level as indicated by sandstone intercalations in the claystones. Some areas were exposed as by both oxidised beds and dessication cracks. The coarse angular ill-sorted sandstones strata was possibly derived from the adjacent bounding fault scarp then transported by sheetwash or small streams over exposed mudflats. It is also conceivable that fault movements caused the lake waters to decrease in size by water loss through underlying fractures and subsequent percolation underground to a lower base level in the hydrological system. The subsurface

seepage would reduce the effect of evaporative concentration and hence the lake salinity. Similar hydrological system is reported to provide the principal recharge for the Lake Magadi in the south (Eugster, 1970).

5.3.2 Lake margin facies.

The lake margin facies extend westward and intergrade with alluvial fan and aeolian deposits. The deposits to the west consist of claystone, sandy tuffs calcareous limestone and diatomaceous silts. The more common claystones are principally yellow to brown and commonly contain rootmarks usually of marshland vegetation. Claystones generally have rather little detrital sand. The sand sand-size detritus is chiefly volcanic origin and occasionally contain clasts of tephra. Petrographic study shows that over 15 to 50 percent of the claystones contain small particles of biogenic diatomaceous silt and the rest are volcanoclastics. Thin beds of diatomaceous earth measuring only a few centimetres which are white to cream coloured commonly contain root marks and tubules. With increasing silt, the diatomaceous beds grade into diatomaceous siltstones or claystones which often may constitute the main part of the facies. They form massive cream coloured beds 20 cm to 2.5 m thick that invariably have siliceous rootcasts. The bulk of the biogenic earthy siltstones is in the form of diatomites, although the claystones sometimes

contain a small percentage of diatomaceous earth in addition to detrital silts, sands and pyroclastics.

Tuffs are common in the facies and characteristically form massive rootmarked lenticular to wedge-shaped beds. All reworked pyroclastic tuff and contain particles of obsidian. The most widespread tuffs are fine - to medium-grain eolian tuff. The eolian tuff is lenticular to massive varying from less than 2 cm to 3 m in thickness and exhibits undulating lenticular bedding, a structure that possibly reflects low dunes. The eolian tuff has the texture of a rather well sorted medium grain sand, with clay matrix. The eolian tuff occasionally interfingers with claystone.

Limestone occurs sparsely as thin nodular lenses of chalky-white or pale gray colour. They are finely crystalline and the nodular beds form concretions. A few beds are relatively of soft cream coloured limestone containing admixed clay, diatomaceous silt and tuffaceous detritus. The mineralogical assemblage has a significant degree of geochemical similarity with the beds in Enderit and Makalia areas. Coarse vertical rootmarks suggest marshland vegetation was commonly associated with the facies at both at Enderit and Makalia areas.

5.3.3 Alluvial fan facies.

Alluvial fan facies outcrop along the western margin of both the Enderit and Makalia basins. These deposits are 2 to 6 m

thick at Enderit Drift and they thin abruptly to 1.5 m to the south (Fig. 5-3B. L1C, L1C, LC1, L1C3). Measured sections of the facies are 90 percent pyroclastic deposits, 6 percent claystones, 3 percent conglomerate, and 1 percent sandstone. The pyroclastic deposits are principally reworked tuffs, mainly lapilli tuffs, and ash-flow tuffs. Volcanic pyroclastic together with pumice conglomerates form the entire thickness of the facies at Enderit Drift. Reworked deposits are crudely stratified but are lacking cross-bedding. They consist largely of pumice rich detritus and include clasts of derived from the bordering trachytic and phonolitic lava suites. Many samples contain sand-sized clasts some of which are sub-rounded to rounded granules. Rootmarkings are increasingly widespread and abundant. Conglomerates form lenticular beds, some of which fill incised stream channels. Clast size decreases consistently eastward, and except for rootmarking indicating some grass cover, the alluvial fan deposits are completely void of fossil evidence.

The deposits originated largely from the eroded fault scarps and possibly from explosive eruptions and most of the pyroclastic was redeposited by stream and alluvial fan of very low gradient. Mafic agglomerates and fanglomerates indicate explosive eruptions from central volcanoes such as the Menengai Crater.

5.3.4 Eolian facies

Sediment transport by wind occurred on a significant scale as shown by the high proportion of tuffs and claystones. Eolian deposits form the bulk of the contemporary alluvium cover on the floor of the basins. On the stratigraphic sections these deposits are exposed discontinuously and interfinger westward with claystone of lake margin facies. Although some water reworked lacustrine tuffs are intercalated within the eolian deposits. Measured sections of the facies indicate a dominance of eolian origin with an average 86 percent tuff, 13 percent silt, 2 percent claystone. At least 98 percent of the tuff are wind transported and the rest water-reworked. Eolian tuffs are typically massive or crudely bedded, rootmarked and pale yellowish-brown. In places the tuff is poorly sorted and may contain isolated pebbles of lava or pumice. The pyroclastic is dominantly trachytic and mineralogically similar to the underlying alluvial fan deposits. Clay is common as the dominant matrix material and reworked tuffs were altered at the land surface, penecontemporaneous with deposition. The alteration and limited calcite cementation are easy to recognise in the field and are two of the major criteria for distinguishing eolian tuff facies from the lake margin facies.

Limestones generally form patchy nodular beds of pale gray or yellowish brown colour. Some of them are tuffaceous and grade

into eolian tuffs. Laminated calcrete are however ubiquitous in lake margin eolian facies. Some of the limestones comprise fragments of tuffs in a calcareous matrix. Conglomerates are scanty, whereas claystones are most common in the facies. They are reddish-brown and the sand fraction of the claystone is principally volcanic detrital. Most of the rootmarkings and tubules are indicative of grass or marshland vegetation. The eolian facies consist of wind-worked materials deposited on and adjacent to an alluvial fan. The detritus was later spread by streams. Eolian tuffs have many features in common with the present day deposit of wind worked volcanics on the rift floor and probably have similar origin. The most obvious and common similarities are in grain size sorting and claystone detrital. The eolian tuffs, may like modern deposits, represent the low undulating dune ridges later modified by wind and possibly stabilised by marshland vegetation.

The climate was relatively hot and dry and soluble salts were deposited at the surface by both evaporation and evapotranspiration processes. This is documented by pedogenic limestone and saline sediments. Grassland vegetation is suggested by rootmarkings and the lack of fossils may reflect unfavourable preservation conditions.

5.3.5 Fluvial facies

The fanglomerate facies at Enderit comprises poorly sorted clast supported disorganised pebble - boulder conglomerate. Clasts 0.4-0.5 m in the long dimension are abundant, but primary sedimentary structures and textural trends are absent. Individual beds range from 0.5 to 4 m in thickness and extend several tens of meters laterally. A formal distinction between matrix and framework is difficult to establish because of the poor organisation and textural polymodality of the facies. The unit has erosional bases and sometimes exhibit crude upward fining trends. In general, however, grain size changes are abrupt and not systematic. At Enderit Drift, the facies consists of massive very poorly sorted matrix supported pebble boulder conglomerate. Clasts sizes range from less than 1cm to more than 1 m. Pumice clasts are typically suspended in mudstone matrix. Individual beds display wedged shaped geometry and usually have flat, non-erosional basal contacts. The exposure is confined to narrow gully and its lateral extension was exposed along River Enderit.

This facies overlies alluvial fan facies in the south (Fig. 5-3B), interfinger and intergrade with fluvial-lacustrine deposits over a distance of over 1.2 km. The facies is unconformably overlain by siltstone in the Makalia Beds (Fig. 5-4A) in the west where the fluvial deposits are comprised of 63 percent claystones. Conglomerates occur at various levels

but are most widespread towards the base of the facies. They are lenticular in cross-section and fill narrow channels in places. Clasts range from pebbles to boulders and are principally pumiceous. Few conglomerates in the Makalia area consist largely of trachytic cobbles and boulders. The clasts are apparently mudflow deposits of essentially the same rock type on the Makalia River bed. Pebbles examined under the microscope, have coarse feldspathic groundmass and accessory glass.

5.4 RONDA FORMATION

5.4.1 Deltaic - littoral facies

The Ronda Formation on the north-western edge of Lake Nakuru consist of two main lithofacies namely, lake margin facies and fluvial-lacustrine deposits. The lake-margin deposits are laterally exposed at a distance of nearly 1.2 km westward from the present Lake Nakuru around Ronda sand quarry. These beds are 2.3 to 8.1 m thick, and measured sections are 84 percent tuff, 10 percent clay and 4 percent conglomerate, 2 percent sandstone. Claystones are generally gray or brown, rootmarked and rather sandy. Diatomaceous claystones are extremely scarce. Tuffs are reworked and form lenticular beds, most of which are rootmarked. The pyroclastic is mainly trachytic and resembles the lavas of the Menengai Crater in the north from which it was apparently derived. Volcanic clasts are in some

tuffs and sandstones particularly near the base of the facies. The tuffs are fresh and constitute most of the sandstones which are either chiefly primary or reworked from older deposits. Conglomerates facies consists of mixtures of detrital lava clasts and pumice. No faunal remains are recorded in the Ronda area and scanty rootmarkings are the principal source of ecological information. These suggest that marshland was subordinated in possibly contemporary recent deposits of the area.

5.4.2 Fluvial-lacustrine facies

At the Ronda sand quarry in the north west of lake Nakuru, fluvial-lacustrine are thick, widespread exposed discontinuously around sand quarry at Ronda and along Rivers Njoro and Lamurak close to their deltas into Lake Nakuru. The deposits here are generally 4 to 10 m thick, but wedges out to less than 1m near the western margin where lacustrine deposits exposed on the facies overlies lake margin deposits (Fig. 5-5D, L12A). The basal contact of the fluvial-lacustrine deposits is disconformable on the underlying volcanic but occasionally gradational in places (Fig. 5-5). The deposit has a relatively high pumice sandstones facies comprising about 70 percent of the constituents, the rest 18 percent tuffs or volcanic ash, 8 percent conglomerate, 3 percent diatomaceous siltstone or claystone. There is also very small percentage of trona or evaporite deposits. The sandstone facies is dominantly fluvial

or mixed fluvial lake-margin and lacustrine sediments. Lacustrine facies are lens-shaped siltstone claystone interbeds and interfingers with purely fluvial sediments to the west or pinches out (L23C, Fig. 5-3). Sandstone form at least 75 percent of the facies. The small percentage of tuffs show turbulent flow pattern (Fig. 5-3). Casts and moulds of trona have been found in several places. Sandstones of this facies are characteristically poorly sorted towards the west, and detritus is typically a bimodal mixture of sand and granules.

Eastward the sandstone facies is generally medium-grained, well sorted and the beds vary in thickness from 15 cm to 2 m. The beds may have a wide lateral extent and are commonly laminated, cross-bedded or ripple marked. Rootmarking are common along bed planes in a few places. The sandstones almost entirely consist of volcanic detritus and unconsolidated tuffs.

Claystones are dominantly leucocratic gray, pale brown and resemble the lacustrine clays to the east of the lake in the game park (L2P, Fig. 5-3). Beds of nodules of chert are at various horizons. Conglomerates form lenticular beds and are dominantly pumice pebbles. Fluvial features include cut-and-fill or scour structures and medium scale cross-bedding.

The lacustrine sandstones are well sorted fine- to medium-grained, and laminated or rippled. They may contain interbeds

of pale claystone. The lake margin sandstones are poorly sorted, commonly clay, and sometimes contain coarse pumice sands and trona. The sandstones of mixed and indeterminate origin form a bimodal mixture of fine to medium grained sand from the west and coarse sand and pumice granules from northern sources, possibly from Menengai. Individual beds can be traced for considerable distances where good exposures are available. The structures in the facies commonly show thin, even stratification, cross bedding and sometimes massive beds. The facies often have rootmarks. Sorting varies widely but is generally moderate to good. Scattered pebbles or angular clasts of tuff are in some of the more poorly sorted sandstone beds. Claystones are either lacustrine, fluvial or of eolian origin. Lacustrine claystones are dominantly sand-silt fraction of volcanic origin. Fluvial claystones are at varying levels and are typically brown, rootmarked sandy, and are associated with sandstones and conglomerates of fluvial origin. Claystones of eolian origin are most commonly brown and may or may not have rootmarkings.

Tuffs are characteristically reworked and contaminated with detrital sand and claystone pellets. They may grade into sandstone, commonly in the same bed. As with the sandstones some tuff beds are clearly fluvial whereas others have both fluvial and lacustrine features. All the tuffs are entirely mafic and glassy.

A few tuffs however, have features suggesting deposition in ponded water. They show both even lamination or ripple marking in several places. Clasts of the pumice tuff conglomerates show only slight alteration and can be traced to come from the immediate adjacent volcanic scarps. Most of the tuffs were thus altered shortly after deposition apparently in a saline, alkaline lake water. Conglomerates are typically fluvial and form lenticular beds of cut and fill channels. Clasts are chiefly pumice rocks and the average clast size decreases from west to east.

5.5 Soysambu Formation

5.5.1 Lacustrine facies

Lacustrine facies at Soysambu consist of tabular thick laminated diatomite beds (Plate 4b; Fig. 5-4A). Individual beds of the facies are 5 - 7 m thick. The abundance of organic diatom material produces a delicate lamination. Sandy and silty laminae commonly are present and gives alternating dark gray white banding appearance. Toward its top the facies is interbedded with silt and mottled red mudstone. The upper unit is structureless, poorly sorted and usually exhibit a block fabric. The upper unit of the facies is abundant in the Enderit section where it forms thin beds between conglomeratic and sandy units.

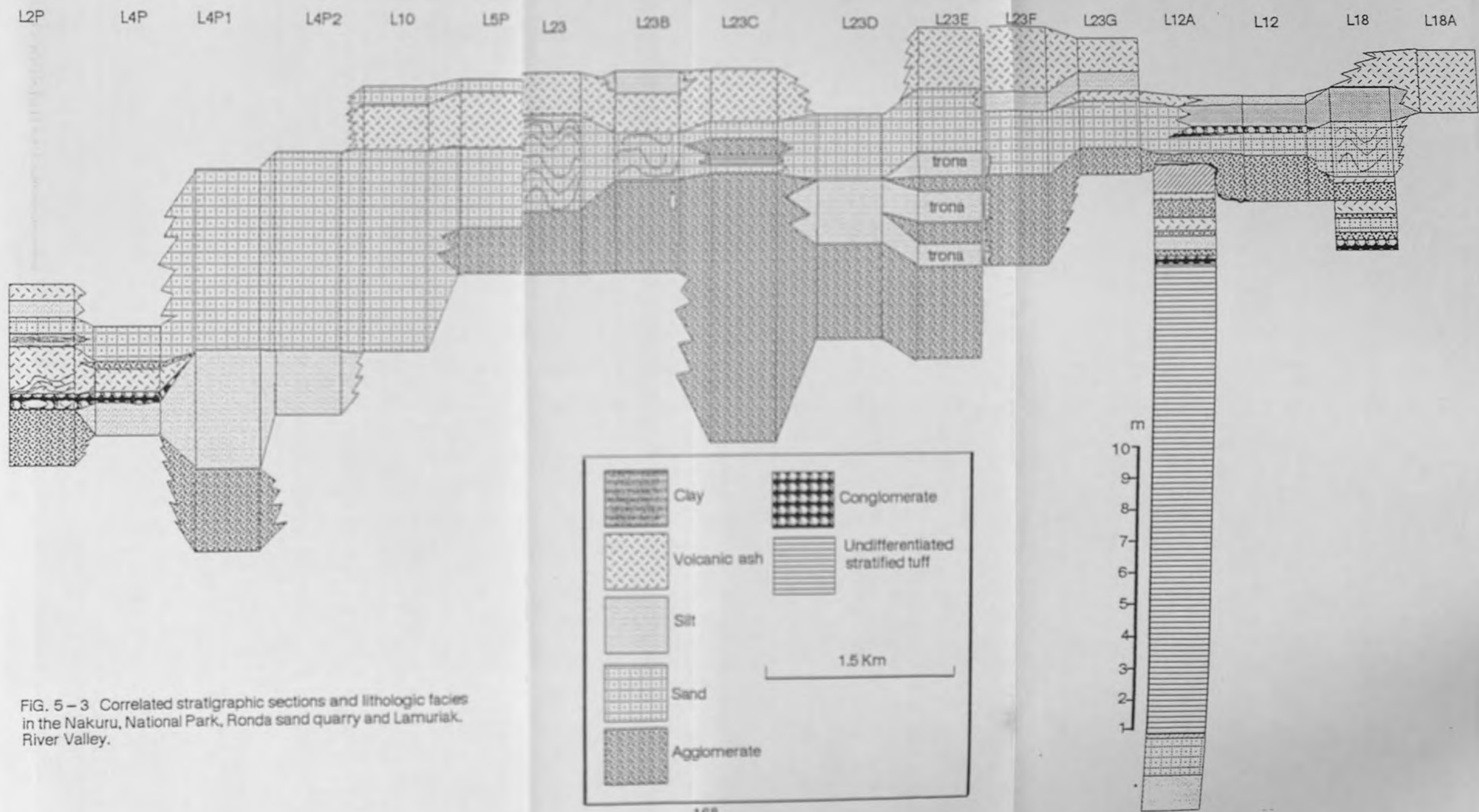


FIG. 5-3 Correlated stratigraphic sections and lithologic facies in the Nakuru, National Park, Ronda sand quarry and Lamuriak, River Valley.

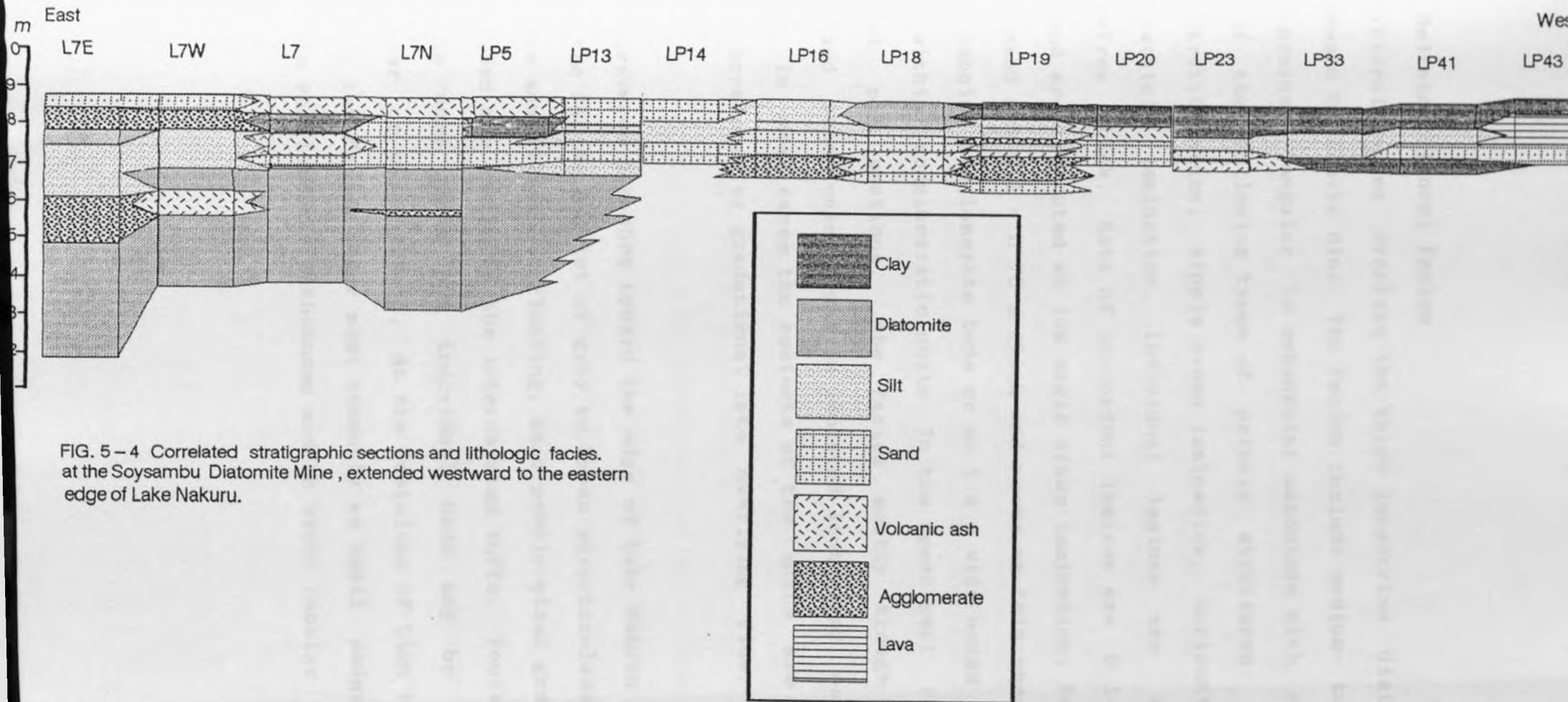


FIG. 5-4 Correlated stratigraphic sections and lithologic facies at the Soysambu Diatomite Mine, extended westward to the eastern edge of Lake Nakuru.

5.5.2 Deltaic littoral facies

The littoral facies overlies the thick lacustrine diatomites at Soysambu Diatomite Mine. The facies include medium- to very coarse-grained, angular to subangular sandstone with one or more of the following types of primary structures: trough cross-stratification, ripple cross lamination, horizontal to subhorizontal lamination. Individual laminae are a few millimetres thick. Sets of concordant laminae are 0.1-0.3 m thick and are truncated at low angle cross-lamination. Beds of pumice sand are 0.1 - 0.75 m thick and occur as thin sheet-like units capping conglomerate beds or as 1-4 m wide wedge shaped units within conglomeratic units. In the upper part of most measured pit sections, the facies mostly trough cross stratified sandstones occur in isolated lenticular sandstone bodies. In most cases the contacts of the units are either sharp, erosional or gradational into overlying finer-grained facies.

In the traverse trenches toward the edge of Lake Nakuru in the west, the facies consist of grey to brown structureless silty sandstone and siltstone. Floating, sand-pebble-sized grains and root traces are common in the intercalated tuffs. Rootmarkings occur in some units and individual beds may be tabular lenticular or wedge-shaped. At the footslope of Lion Hill in the west, the facies occur most commonly as small wedge-shaped units in conglomerate lithosomes and as broad tabular beds a

few decimetres to several metres thick between beds of conglomerate facies.

At the diatomite mine the facies is characterised by 0.1-0.5 m thick beds of massive, fan, very fine to fine-grained sandstone. Individual beds have sharp basal contacts, are tabular and can be traced laterally for several meters. Root traces and small vertical burrows are common. Small ferruginous concretions and ripples are present in some beds. The facies is usually interbedded with caliche limestones facies and in turn overlain by black tuff similar to the tuff above diatomite at Makalia. In conclusion, the embaying margins of the contemporary lake basins in the central rift valley record a complex shifting pattern of fluvial lake-margin and lacustrine environments. The different patterns of sedimentation in the Enderit, Makalia and Ronda in the Nakuru Basin and at Soysambu and Kariandusi areas are most likely due to fault displacement which presumably formed separate depocentres within separate but possible contemporary basins. The facies consists chiefly of fluvial sandstones at the the upper sequence and lacustrine diatomites at the bottom. In most cases the lacustrine deposits interfinger with fluvial detrital sediments and water-table and caliche carbonate rocks. The sandstones were probably deposited by streams at the lake margin and reworked by the lake during periods of rising lake level. There is

evidence for temporary saline, alkaline ponds or small shallow occasionally fresh-water lakes, but none for a relatively stable body of water in any one place. Water-table and caliche carbonate rocks are widespread. Wind was a significant agent in sediment transport of the facies as indicated by claystone tuffs. Presumably much of the associated sand-size volcanic detritus was redeposited by wind.

ENVIRONMENTS AND SEDIMENTARY PROCESSES

6.1 Depositional Environments

The sediment formations in the Central Rift basins represent different depositional environments mainly of volcanic origin. The dominance of volcanoclastics is reflected in the sedimentology and geochemistry of tephra rich lithofacies. The various facies (Chapter 5) can be attributed to different environments including (1) piedmont depositional environment (2) alluvial fan (3) fluvial channel and floodplain environments (4) deltaic distributary channel and interdistributary floodbasin (5) lacustrine environment (lacustrine prodelta and lacustrine littoral).

6.1.1 Piedmont environment.

This environment is restricted to the foot of Kariandusi, Enderit and Makalia fault scarps. It is predominantly comprised of breccias and paraconglomerates. The breccias are composed of poorly sorted angular volcanic cobbles and boulders derived from fault facing basalts, phonolites, trachytes and columnar jointed ignimbrites. The matrix is extremely scanty and limited to pumice granules and sands. The sediments are lenticular sinuous and variable in thickness along fault scarps.

The paraconglomerates constitute a few meters thick deposits of ill-sorted angular volcanic clasts. This facies often extend over few square meters and both breccia and paraconglomerate facies are interpreted as mass flow deposits of high concentration floods. The absence of fine grain matrix and the pervasive framework support suggest that pseudoplastic or viscous dominated debris flows could not have been the principal mechanism of clast transport. The lack of traction sedimentary structures indicates that the depositional flows were not in equilibrium with a typical regime bedforms. Most probably, a dense dispersion of pebbles and cobbles was carried along by a composite fluid phases that comprised limited sandy clay and water. The combined forces each attaining varying degrees of importance during any given flow probably served to transport sediment that composes the facies. Pierson (1980) demonstrated that the traction shear stresses, buoyancy and dispersive pressures all combine to keep clasts moving in hyper concentrated flows (Miall, 1978). Todd (1989) suggested that deposits similar to facies are produced by high density steam flows that derive non-turbulent gravely traction carpets long stream beds. They are mainly deposited by high density viscosity flows along fault scarps subjected to alternating dry and wet season.

6.1.2 Alluvial fan environment

Alluvial fans cover several kilometres along most fault scarps and the foot of steep-sloping volcanic cones on the rift floor. The slopes of most alluvial fans averages about 5° and rarely exceeds 10° . The surface generated by coalescence of several alluvial fans form the gentle rolling ground around the Menengai footslope, and posthumous volcanic cones to the south of Elementaita. The sedimentary body develops either a convex upward cross fan profile or a concave upward radial profile fan. Alluvial fan sediments are characteristically immature and developed relatively close to their volcanic source areas. They indicate high energy unidirectional fluid flows and are typically very poorly sorted with the range in grain sizes reflecting short distances of transport. The facies are dominantly angular conglomerate and variable volcanic rock detritus within a brown silty sand matrix which represents 40 % to 70 % of the bulk volumes. They are characteristically debris flow deposits with very low porosity.

The alluvial facies to the south of Naivasha on the footslope of Mount Eburru consists of relatively thick stratified volcanic granules in a matrix of sand and clay of fairly good porosity. Volcanic sand facies in the area are of various types depending on the grain size or stratification. They range from very coarse to fine grained sand and may exhibit massive or

graded bedding, feldspar rich volcanic detritus. Most fan sequences are recognised by overall coarsening and thickening upward deposits, indicative of relative maturity. The sequences are commonly subdivisible into several subsequences dependent on the depositional locality which may be proximal or distal relative to the depocentre. Proximal environments are characterised by matrix supported paraconglomeratic facies mainly deposited as graded debris flow environments in which sequences generally fine upward. The facies are commonly deposited as single broad major channels along the scarps or volcanic cone footslopes.

Toward the middle part, alluvial fans are characterised by numerous distributary channels radiating outwards. They became sites of rapid sedimentation as channel fills, and braiding rapidly shift laterally across the fan. The distal areas are marked by finer grained sheetlike deposits of less channelised outer fan sediment. The flow laterally deposit extensive bodies of sediments that are quite similar to alluvial plain or lacustrine facies. Elementary sequences exhibit channel fills consisting of a channel lag with orthoconglomerate or coarse-grained volcanic sand grading into cross-bedded or massive medium grained sand, silt and clay. In distal location, alluvial fans grades into either fluvial, littoral lake environments. The sequences generally suggest deposits of possible turbidity current acting in shallow waters. When

alluvial fan do not enter into lacustrine water they grade laterally into alluvial sediments commonly by rivers flowing longitudinally down valleys.

The geometry of alluvial fan sediments depend on the tectonic framework of the basin bounding scarps. At the footslope of the Menengai Crater, in the northern part of Lake Nakuru, the radius of each alluvial fan sediments in plane view varies from 1.5 to 2 km. The thickness is concealed beneath recent alluvium, but possibly range from tens to many hundreds meters. In the south of Elementaita, the geometry is very complex with proximal facies generally overlying more distal facies resulting into a lens-shaped body. Coalescing of adjacent fan produces a series of merging lens-shaped bodies in the Enderit area. Apparently Holocene tectonic faulting and volcanicity formed and superimposed cones on the rift floor. Neotectic subsidence of basin floor and uplift of shoulders due to rejuvenation of faults partly contributed to the development of the fans. The tectonic movements were accompanied by landslide deposits along the fault scarps. On the western flanks of the fault scarps, large cones built by fluvial streams contrast with the small prograding fans with steep slopes in the southern flanks.

6.1.3 Fluvial environment.

The common evidence for fluvial environments are deposits of conglomerates. These depend on the material transported by different rivers which in turn depend on the drainage area. Apart from conglomerates fluvial facies here consist of thin or thick lenticular bodies of granules, pebbles and occasionally cross-bedded volcanic rich deposits. The environment however, has many of the characteristics of fluvial gravels facies that are deposited in modern gravely braided streams (Reineck and Singh, 1986). The upward fining within individual beds probably resulted from waning flow velocity following floods. The characteristic textural bimodality of facies probably resulted from post flood infiltration of open framework gavel by sand or by sieve deposition (Hooks, 1967). The units associated with much thicker beds were deposited in small channel that developed during waning and normal stages on tops and margins of gravel bars.

The erosional bases, lenticular shapes, and upward fining trends in bodies indicate deposition in channels. The association of imbricated crudely horizontally stratified and cross-stratified conglomerate indicate deposition by longitudinal gravel bars and intervening channels (Rust, 1972). Based on the typical thickness of individual channels beds were 1-4 m deep. The generally coarse grain size and poor sorting suggest that deposition primarily occurred during floods.

Reworking of flood sediments by waning and normal stage flows produces the lenses commonly associated with the fluvial environments. The environment is also characterised by a predominance of reworked lacustrine diatomaceous silt, sandy silt beds and thick massive or ripple-marked beds in linear valleys or in close proximity to lake embayments. The latter fluvial deposits, especially clays, represent flood plain deposits or infillings of abandoned channels.

In the Naivasha, Nakuru and Elementaita Basins, fluvial environments occupy relatively moderate surfaces. The fluvial network is largely controlled by tectonic trends especially the north-south fault trend. Generally the coarse fraction of most fluvial deposits are restricted to the upslope zones of the rivers where they are capable of transporting heavy load material. The lower zone is dominated by laminated fine sands and silts in the Elementaita and Nakuru areas. The low energy fluvial environments consist mainly of mudstone and volcanic tuff rich siltstones. These are associated with Pleistocene-Holocene flood plain deposits. Their deposition are controlled by lake level fluctuations in response to climatic and tectonic influences. The extent of fluvial network in the area however, is scanty and the volume of deposit is generally limited in both vertical and lateral geometry. Coarse sediments are restricted to only a few meters wide and high in channels

parallel to the streams.

6.1.4 Alluvial plain environment

The Central Rift lakes exhibit extremely limited alluvial plain facies corresponding to flood plain and deltaic environments in the area. The deltaic plain facies consists of fine to coarse granules, pebbles in a silty clay matrix. Lenticular beds of up to 1 m thick generally exhibit massive or cross-bedded structures (Plates 1a; 5c-5d). The sands are fine to coarse grained feldspar-rich volcanic detrital in argillaceous matrix. The facies are interpreted as deposits of large and small, two- and three- dimensional, subaqueous ripples. Cross stratification sandstone facies may be deposited during the growth, immigration and washout of antidunes and are often associated with waning-flood deposits. In the upper parts of most measured sections the facies was deposited in shallow braided channels.

Alluvial environment facies at Enderit Drift is interpreted as sandy mudflow deposits. The mudflow of alluvial fans commonly bury pre-existing topography with little erosion. Channels may be plugged by mudflow but later reactivated by neotectonic fault effects or hyperconcentrated stream flows (Plates 6a, 6b). This type of process would account for the common wedge-shaped units associated with Enderit facies. The tabular beds of facies represent mudflows that spilled out of the channels

and spread over relatively flat surfaces. Subsequent re-establishment of low vegetation on mudflow surfaces produced root casts and pedogenic mottling. They occasionally contain substantial siltstones interbedded in feldspar-rich sands.

The size of alluvial plain environments in different lake basins are quite variable and consequently their deltaic related facies occupy fairly restricted areas of the total surface of the different lakes. Except a few deltas fed by perennial streams like the Kariandusi River, most of the deltas are built by smaller temporary rivers which bring periodic large quantities of sediments strongly influenced by the intermittent changes of the lake level. To the north of Kariandusi, the deltaic plain consist of conglomerate and coarse sand deposited in small braided channels a few tens of meters long generating elongated lenticular pumice pebbly sand bodies. The delta front was built of fine to coarse sand, silt and clay deposited on a gentle slope. The prodelta is dominated by a fine sedimentation composed of interbedded silt and clay containing numerous feldspars and predominantly lithic volcanic detrital. Scattered delta plains are located on the eastern bank of Lake Elementaita and to the northern end of Lake Naivasha, a small delta plain is located in a bay limited by faults. The deltaic plains exhibit different facies including conglomerate granule sand, silt and clays. The delta front is

often dominated by fine sediments and progrades in response to lake subsidence. The prodelta exhibits alternation of sand silt and clays.

A relatively extensive flood plain is located on the northern end of the Lake Naivasha. This zone is characterised by large alluvial fan and the northern swamp is cut by Rivers Gilgil and Malewa and several radial streams from Mount Eburru on the west, Longonot in the south and Mau Kinangop fault scarps. Alluvial fan facies and flood plain deposits are observed in the delta plain. Both in the delta front and prodelta the sedimentation is dominated by silt, clay and mud with plant debris. The laminated facies are characteristic of low energy environment.

The flood basins of Lakes Nakuru and Elmentaita show a veneer sedimentation. The subaerial delta plain consists of volcanic sands associated with feldspar accessory quartz, lithic fragments, evaporite crusts and the clays are dominated by montmorillonite and kaolinite. There is a considerable variation in thickness with a maximum of 2 m along sections.

6.1.5 Lacustrine environment

The fine grain diatomaceous silt indicate shallow lacustrine environments. The restriction of lacustrine facies to lower levels of the stratigraphic sections at Kariandusi and Soysambu and their association with lenticular beds of fine ash tuffs

suggest that the sediments formed in relatively shallow lakes on the rift floor. The general limited extent of the facies and lack of shoreline facies further indicate that the rift lakes were not extensive and may have simply occupied fault controlled grabens. The lacustrine nature of the deposits are again supported by the tabular geometry of the Pleistocene diatomaceous beds.

Mineralogy of the rift sediments provide much information about the chemical environments of sediments and indirectly about the palaeogeography and climate. Saline alkaline lakes of Nakuru and Elmentaita yield some diagnostic suites of rocks and soluble sodium carbonate minerals of gaylussite ($\text{Na}_2\text{Ca}(\text{CO}_3)_2 \cdot 5\text{H}_2\text{O}$) and trona ($\text{NaHCO}_3 \cdot \text{Na}_2\text{CO}_3$) crust precipitates around lake mudflats (Plate 3b). This is reminiscent of high salinity of the Pleistocene lakes in the area points to the closed rift basins in a possibly semi-arid climate. Unaltered diatomites phytoliths and trachytic glass in lake deposits afford a means of locating areas of relatively fresh water. This is because the opaline silica of diatoms and phytoliths dissolves slowly at a pH of 7 to 9, whereas at pH of 9.5 or more it dissolves rapidly.

Hence, the mineralogical features the sediments in the area indicate that many lacustrine alluvial sediments were often exposed and resulting into surfaces sodium carbonate

concentrated at the surface by evapotranspiration. Mineral reaction in land-laid tuffs likewise document a saline, alkaline soil environments. The more reactive components (nepheline, glass) are altered to produce alkali rich clays, calcite, dolomite among others which cement the deposits. However, that authigenic minerals and silicate reactions can be used as evidence for the surface only if they can be shown to be penecontemporaneous with deposition. Otherwise phyllosilicates, for example can form long after deposition and provide no information about the environment in which sediments were deposited. A penecontemporaneous reactions and sedimentation can be demonstrated in various ways but one of the commonest is to find a clast of altered rock (for example tuff) in a conglomerate only slightly younger than the altered deposit which supplied the clast. If the authigenic minerals in the clasts are altered or abraded at the margins, then the clasts must have been altered before it was eroded and deposited in the conglomerate.

Caliche soils or pedogenic concentrations of calcium carbonate (Plate 4c and 4d) occur throughout the Nakuru, Elmentaita and Naivasha sequence and provide a line of evidence for a semi-arid environment climate in the region during the Pleistocene and Holocene periods. The caliche layers are of various types but the most common and distinctive type is dense, laminated

calcrete typically 1 to 3 cm thick. These calcrete are associated with eolian tuffs, and the calcium carbonate of calcrete originated (from wind-transported particles of older calcite rich volcanic (Dawson, 1964) and by chemical reaction of mafic pyroclastic at the land surface. Calcium carbonate was carried downward in solution and precipitated at a horizon of lower permeability, most commonly palaeosols and layers of cemented tuffs.

6.1.6 Palaeontology and archaeological evidence.

Fossilised remains and organic structures are among the most sensitive indicators of climate and palaeogeography. In the study area however, faunal remains are scarce and are only preserved at one horizon along the new road cut west of Kariandusi. The faunal remains here consist of large Proboscidiens bones and are therefore generally less sensitive environmental indicators. In this area however, if the faunal remains were both abundant and varied they probably would be of value in distinguishing the various depositional environments.

Fossilised leaves are rare, and little is known of the pollen at the Nakuru, Elementaita and Naivasha basins. Root markings are however both widespread and abundant and serve to distinguish savannah grassland from swamp and shore vegetation. Root - markings diagnostic of savannah grassland vegetation are

narrow, finely textured, and branching; swamp and shore vegetation (for example, Typha and some other types of grasses and reeds) is indicated by sub-horizontal rhizomes and by coarse generally unbranching vertical channels and casts. Diatoms apparently bloomed in the shallow Pleistocene lakes in which the tabular lacustrine beds formed. Hominid activities also have a bearing on the geologic interpretation. Undisturbed occupation sites, for example, indicate emergent land surfaces. As for example, lava tools at the Kariandusi prehistoric site on top of the diatomite sequence points to a relatively fresh water lake. The fine grain diatomaceous silt facies are restricted to the lower parts of the Kariandusi and Soysambu sequence. The stratigraphic sections in the two areas and their association with lenticular facies suggest that they were deposited in shallow ponds and lakes on the rift floor. The lack of facies that might be interpreted as shoreline facies suggests that these lakes or ponds were not extensive and may have simply occupied low areas on distal (fault scarp) fan fringes.

6.1.7 Provenance of clastic deposits

Clastic sediments can generally be assigned to specific sources with reference to their composition. Similarly in the central rift valley eruptive sources can be distinguished by the composition of lavas. Sand size or coarse particles are most

diagnostic, but the phyllosilicates or "clay minerals"; of argillaceous rocks may also reflect source areas. Montmorillonite is commonly associated with coarser detritus of volcanic origin. A characteristic weathering product of mafic volcanic rocks in semi-arid climate, and much of that in the Nakuru-Elmentaita and Naivasha basins probably originated in weathering of volcanic rocks. Clay minerals can however be formed or modified after deposition, hence they cannot be interpreted solely in terms of source area. Mixed-layer illite-montmorillonite may, for example be formed by alteration of either illite or montmorillonite.

Particle size reflect the strength of waves and currents and the distance from the source area. Clays for example are the characteristic detrital sediment of a quite pond or lake. Within fluvial and ash fall deposits, particle size normally decrease in a down-current direction. This suggests a northern sediment source for detritus in the Kariandusi Formation which coarsen from north to south. By contrast, the stream laid trachytic deposits of the Enderit Beds coarsen from south to north indicating a southward source. Sorting of particle size reflects the nature of the transporting medium and the activity of waves and currents. Sediments can be sorted rapidly in aqueous currents, hence the sorting of sediments commonly reflect the last current action to move and deposit. Sand deposited on beaches or in shallow water is characteristically

better sorted than deposited in streams at Kariandusi. Deposits of mass movement either as mudflows or ash flows are characteristically unsorted and contain coarse blocks in a fine grain matrix of clay or volcanic ash. Pedogenic processes (for example, roots and burrowing organisms) mix material on the land surface and hence decrease the degree of sorting and stratification. Both ash layers and fluviatile sediments may be "homogenised" by activities of roots and burrowing organisms.

Primary structures are among the most diagnostic features for determining the processes and environment of sedimentation. Those observed in the Nakuru-Elementaita Naivasha basins include stratal thickness, cross-bedding, ripple marks, root markings, mud cracks and channelling (cut-and-fill). Stratal thickness can to some extent be used in estimating time, but its use in the area is complicated by the fact that faulting has resulted in different sedimentation rates for different areas, thus invalidating time estimates based on stratal measurement over large areas. Channel alignment provide extremely useful information for establishing the stream pattern. A channel orientation alone offers two possible directions as for example the north-south Enderit River channel which could represent either a north-flowing or a south-flowing stream. If however, the source for the detritus in the channel is known, the the flow direction is fixed. Variability of channel alignments may

reflect the degree of meandering in a stream. Deposits of meandering streams can be distinguished from those of braided ones by a combination of textural features and sedimentary structures (Selley, 1970, Visher, 1965). The lateral migration in a meandering stream produces a characteristic of grain size and of sedimentary structures. The coarsest detritus is at the base, overlying an eroded surface, and the grain size decreases upward. Similarly the scale, or set height of cross-section bedding decreases upwards and at the top of micro cross-laminated planar bedded fine sandstones may grade into silts and sand of floodplain. The thickness of this sequence if complete is a measure of the stream depth.

The river systems consist of an interlaced network of low sinuosity channels. The deposits are typically composed of sand and gravel, and occasionally silt and clay. Although the distribution between braided and meandering streams can lose significance from a sedimentological point of view in semi-arid climates, where a single river may be braided in some places and meandering in others. Eolian sediments of two types can be recognised in the Nakuru-Elementaita, and Naivasha beds: extensive beds of eolian tuffs and localised concentration of claystones. The large-scale, steeply inclined cross-bedding of eolian deposits is exhibited locally in tuffs. Laterally extensive beds massive eolian tuffs are the dominant type of eolian deposit in the region. The massive eolian tuffs are

CHAPTER 7 CORRELATION

deposited in wind transported pyroclastic mostly of medium sand size, that accumulated on the land surface, generally as thin blanket like deposits. Claystones are in many beds. The modern unconsolidated equivalent of the tuffs is found in the surface layers as detrital sands are commonly associated with claystones. The claystones are almost certainly formed by wind erosion of mudflats, either of floodplain or at the margins of lakes. Ripples and small dune of claystones are reported from tidal mudflats, intermittently dry lake basins of semi-arid and arid regions where efflorescent salt lakes are important in breaking up the surface layers of clay into particles small enough to be transported by wind (Price, Bowler, 1973). Many of the claystones in the Nakuru, Elmentaita and Naivasha area have fluvial and lacustrine features, indicating that they were commonly blown from the mudflats into streams or lakes.

7.1 Chronostratigraphic Correlation

There are no rocks exposed in this central part of the rift valley that are older than Pliocene age. The lacustrine sediments in the area document the fluctuating depositional environments which evolved in the sector of the Rift since about 1.0 million years ago. The oldest lake sediments of Kariandusi Formation on the East of Lake Elmentaita is assigned a date of 0.7 ma. (Strecker, personal communication). The formation is underlain by the Kariandusi trachyte which is dated 0.9 Ma. The early investigations of Leakey, Solomon and Nilsson used archaeological evidence to establish for the central Kenyan Rift lake sediments and the entire East Africa a stratigraphic framework sequence based purely on climatic variations for Pleistocene and Recent lake sediments in the area. The climatic based-stratigraphic sequence equated both the Pleistocene and Holocene lake deposits in the area with the pluvial (wet and cool) periods in Europe (Leakey, 1931). The correlation were neither based on the geology, palaeontology nor did it take into consideration the effects of volcanic and tectonic processes in this sector of the rift. The chronostratigraphic sequence subsequently established was as follows:

Nakuran - Wet period climatic phase c. 850 POST PLEISTOCENE

the deposits before interpreting as WET PERIOD

Makalian - Wet/dry retreat

Gamblian - Upper wet, mid-dry, pause, lower wet UPPER PLEISTOCENE PLUVIAL

Kamasian - Interglacial (lake dried) MIDDLE PLEISTOCENE PLUVIAL

Kageran.

Leakey later subdivided the Kamasian into a Lower and an Upper Kanjeran. The equation of sediments at Kariandusi with those of Marigat (Baringo) was dropped and instead the Kariandusi deposits were equated with the Middle Pleistocene artefact bearing sediments of Kanjeran on the Winam Gulf of Lake Victoria and those of Olorgesailie Formation in the southern Kenya Rift Valley. Their (Nilsson, Leakey and Solomon) recognition that the Nakuru-Elementaita basin sediments reflect climatic fluctuations in East Africa was correct but Leakey's correlation of the deposits with similar deposits outside the central Kenya Rift is unattainable hypothesis. Thus the pluvial related chronostratigraphic correlation received no support (Flint 1959.; McCall 1967 ; Nyamweru 1977) since it was neither founded on palaeontological evidence nor geological data. Even within the rift sector itself, Nyamweru argued that earlier correlations were based on inaccurately measured

altitudes and discontinuous sections and more work needed to be done on the deposits before interpreting sediments in the area entirely in terms of basin wide chronology. Nyamweru (Nyamweru 1969) also indicated that she did not study in detail the sections at Enderit and Makalia in southern part of the Lake Nakuru Basin.

The investigations by the author was therefore partly initiated to establish accurate correlation in the part of the Rift Valley. Both field data and laboratory findings supports Nyamweru's' sentiments and confirms that the sediments in these valleys actually represented short and local phases within the valley with hardly any areal equivalent in the rest of the basin. The geological evidence therefore enhances the interpretation of the sequence and now makes it possible to verify evidence with the aim of establishing the possibility of correlation with other areas in the basin.

7.2 Lithostratigraphic correlation of measured sections.

The basis of lithostratigraphic correlation for the sediment formations in the Lakes Nakuru, Elmentaita and Naivasha basins used in this study was determined by the author during his field investigation of the area. It forms the basic framework for all environmental and tectonic interpretation in this study. The choice of the measured sections in the correlation was dictated by the need to have as complete a coverage of the study area as possible. The recorded sections were therefore

sharp, gradational and unconfusable contacts, the
usually arising from partial removal by
chosen that contained sufficient succession that their
inclusion in the correlation would be significant in terms of
tectonic and environmental interpretation. The correlation in
the field was based on the identification of markers and
continuity of distinct beds and took into consideration that
for sedimentary units to be of practical use as marker beds
they must be laterally extensive, have been deposited in a
brief period of time and should be readily recognisable in the
field (Plate 1b). It is also of advantage if the unit is of
known age either by determinations on the unit itself or by
inference from data derived from the enclosing sediments. Both
the tuff horizons and cyclic lacustrine beds proved locally
useful in the correlation and reconstruction of widely
scattered sedimentary exposures in the area. The sedimentary
history of the area is one of a deltaic complex prograding from
coarse conglomerate on the foot of bounding fault scarps
margins to very fine silts on the rift floor lake beds. The
resulting areal distribution at any specified stratigraphic
level of the depositional environment is complex. Though the
sediments reflect these environmental changes, their obvious
lithological dissimilarity within individual basins and from
basin to basin render most of the deposits recognisable in the
field. The sharply defined basal contact of the obvious marker
sediments and tuffs were taken as isochronous correlation
surfaces. The upper surface of the beds are commonly varied

between sharp, gradational and unconformable contacts, the latter normally arising from partial removal by penecontemporaneous or subsequent erosion. As marker beds, tuff formation are particularly important in that the eruption, transport and deposition of an individual tuff was probably very rapid. Inevitably there must have been sometime required for transport into the basin and dispersal of tuffs within the basins. The time involved is insignificant when compared with the best resolution available from the geophysical dating methods. Though the basal contact of the individual tuffs are diachronous in detail for all practical purposes they can be considered time equivalent throughout the study area. When an individual tuff unit is not present either due to local non-deposition or penecontemporaneous erosion it may be possible to estimate the stratigraphic level at which it should have occurred. This requires identification of a surface which is isochronous with the basal facies of the tuff. The reliability of the position of this surface in the absence of the tuff depends on the selection of time equivalent of approximately time equivalent non - tuffaceous marker beds.

7.2.1 Enderit Formation.

Enderit Formation was divided into several units (Figs. 7:3-1A to 7:3-1D) when it became clear that it represented several depositional events. The author analysed, both the field

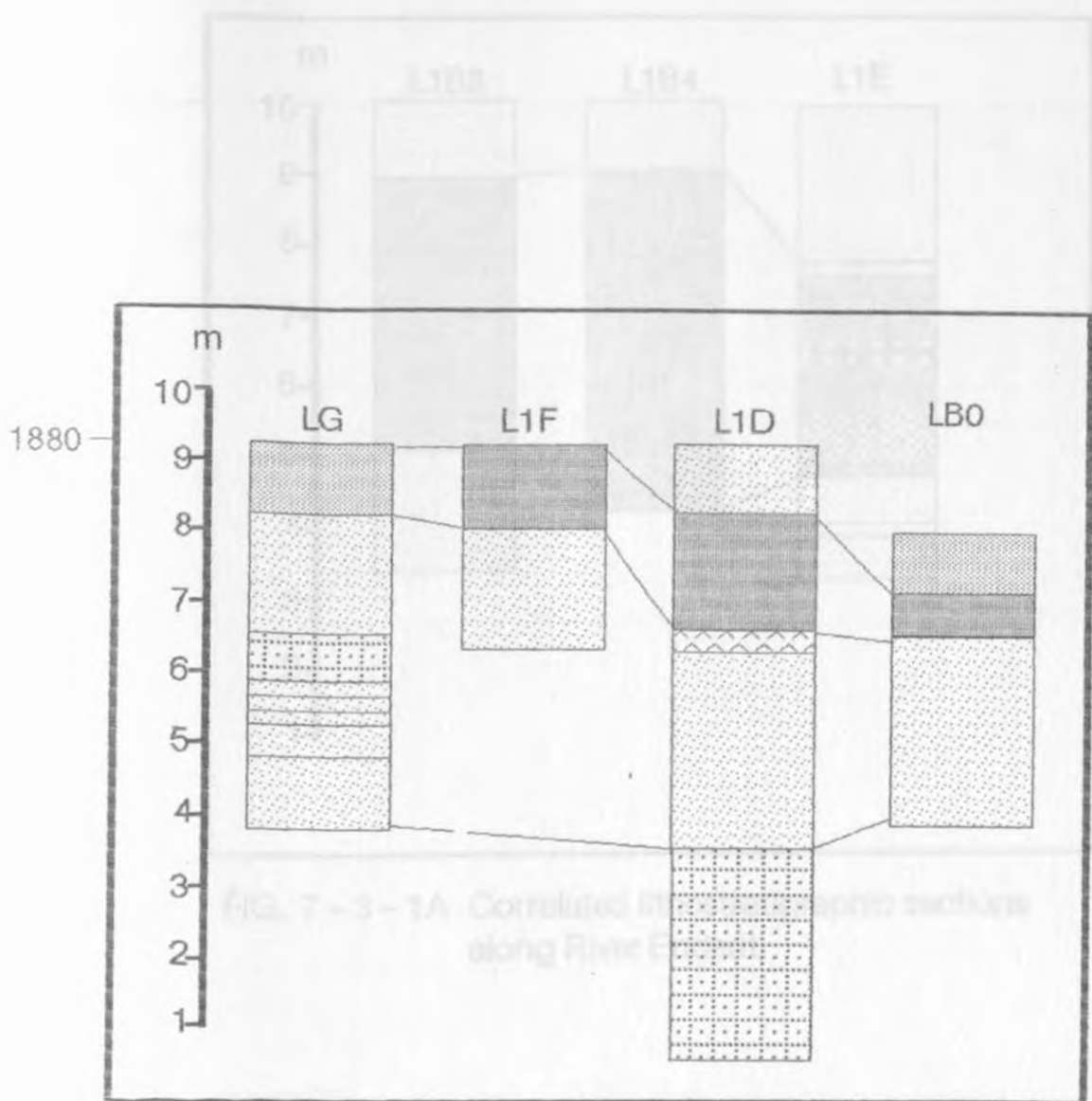


FIG. 7 - 3 - BO Correlated lithostratigraphic sections, River Enderit.

(NB . 1880 is measured altitude in meters, variously indicated for the subsequent lithostratigraphic correlations).

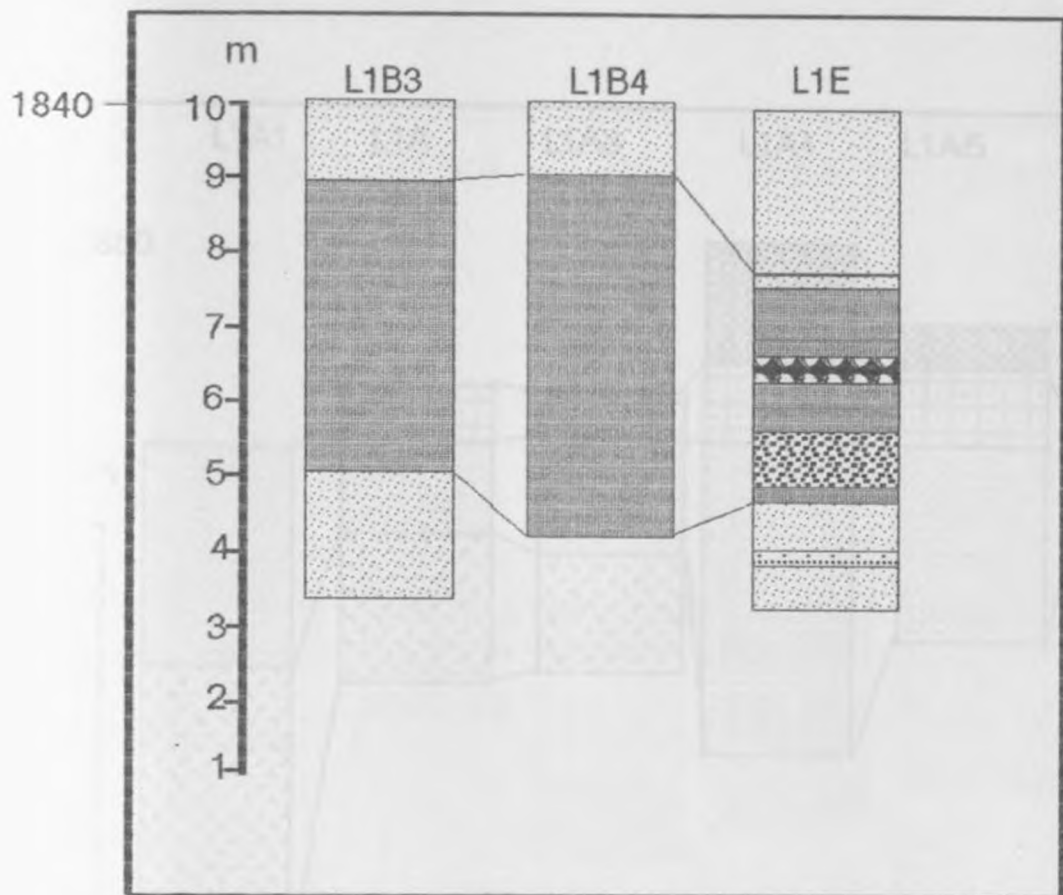


FIG. 7-3-1A Correlated lithostratigraphic sections along River Enderit.

7-1B Correlated lithostratigraphic sections along River Enderit. 197

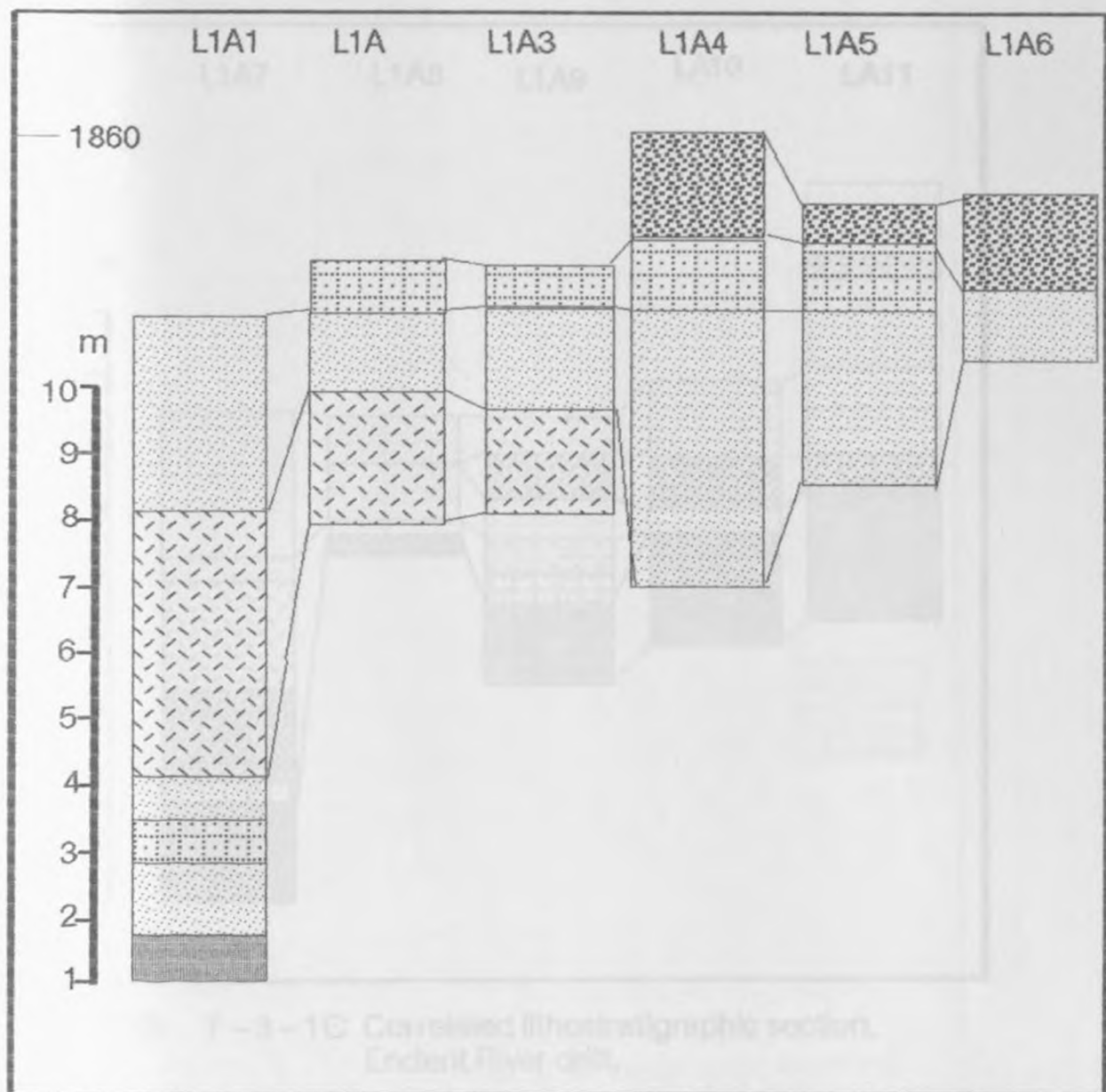


FIG. 7-3-1B Correlated lithostratigraphic sections along River Enderit.

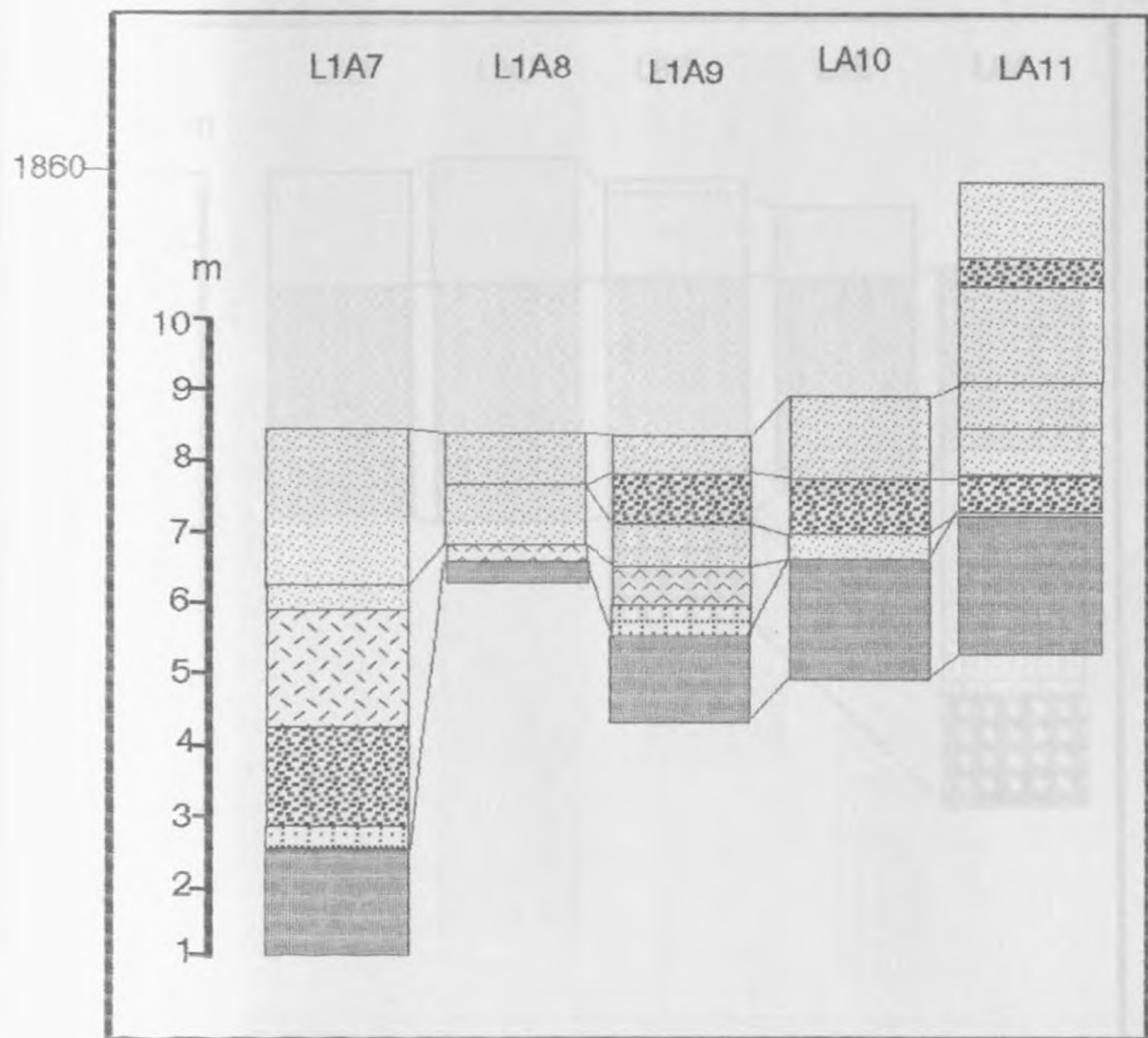


FIG 7-3-1C Correlated lithostratigraphic section,
Enderit River drift.

FIG. 7-3-1D Correlated lithostratigraphic sections
north of Enderit drift

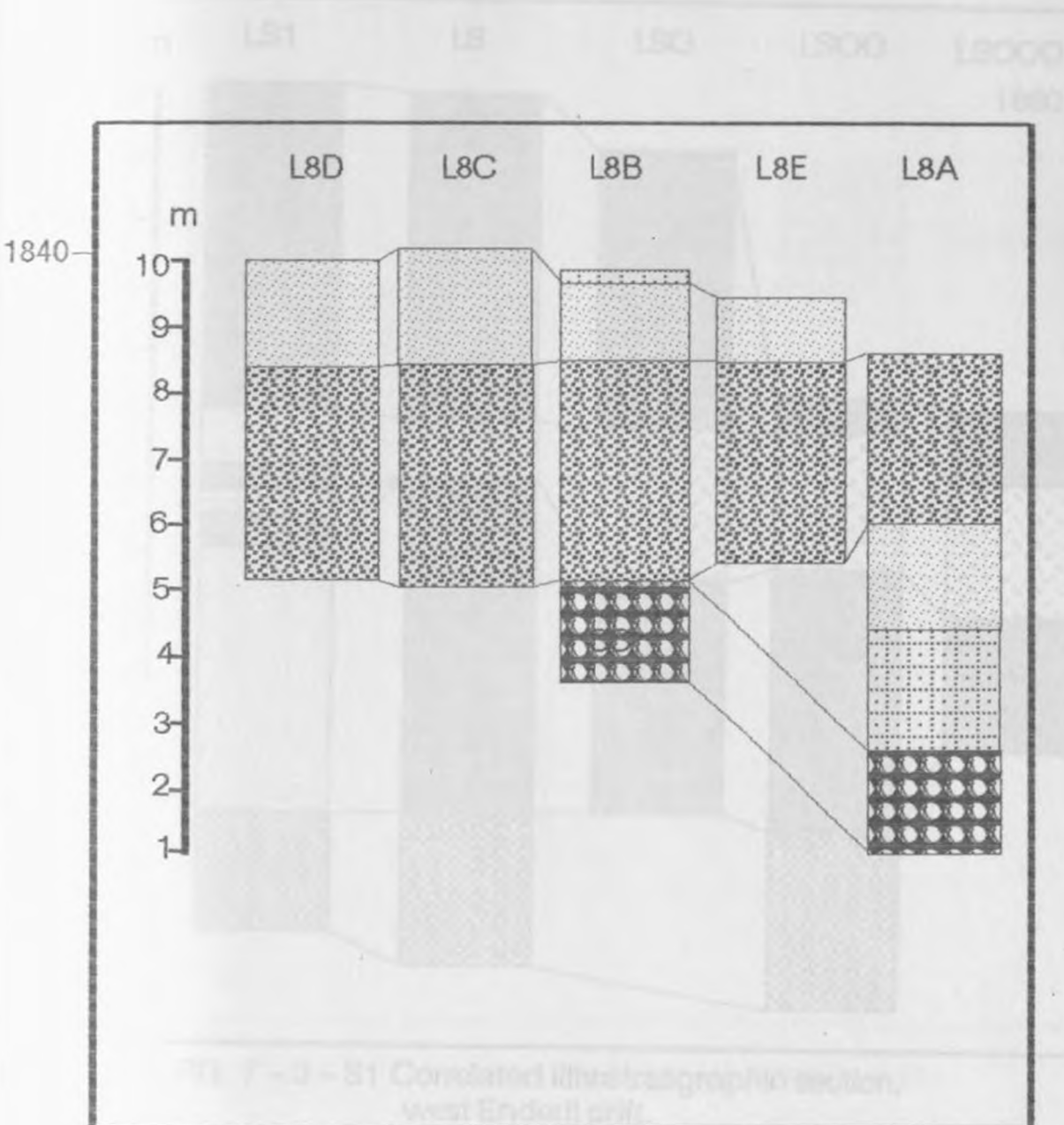


FIG. 7-3-1D Correlated lithostratigraphic sections north of Enderit drift

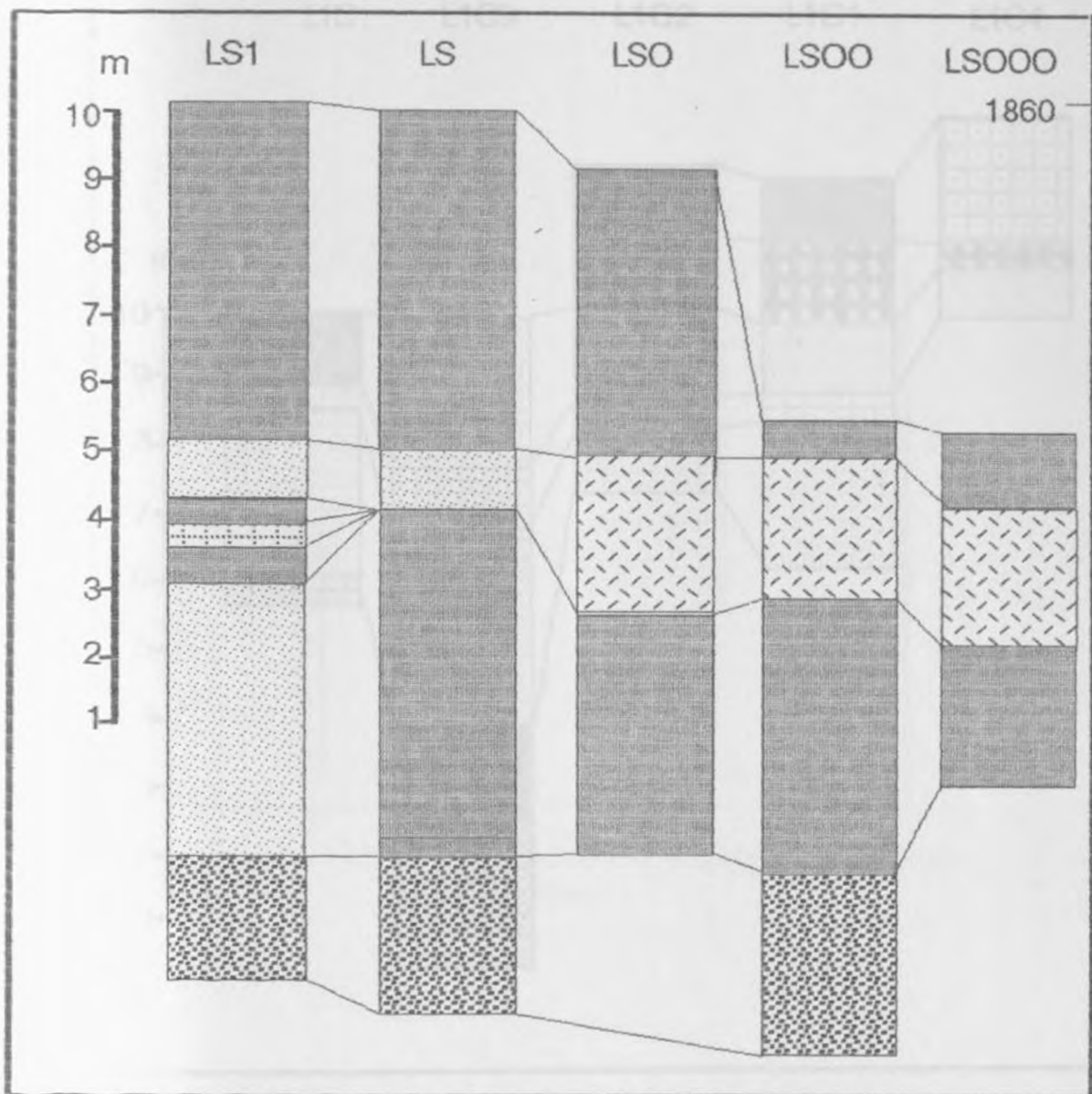


FIG. 7-3-S1 Correlated lithostratigraphic section,
west Enderit drift.

1845

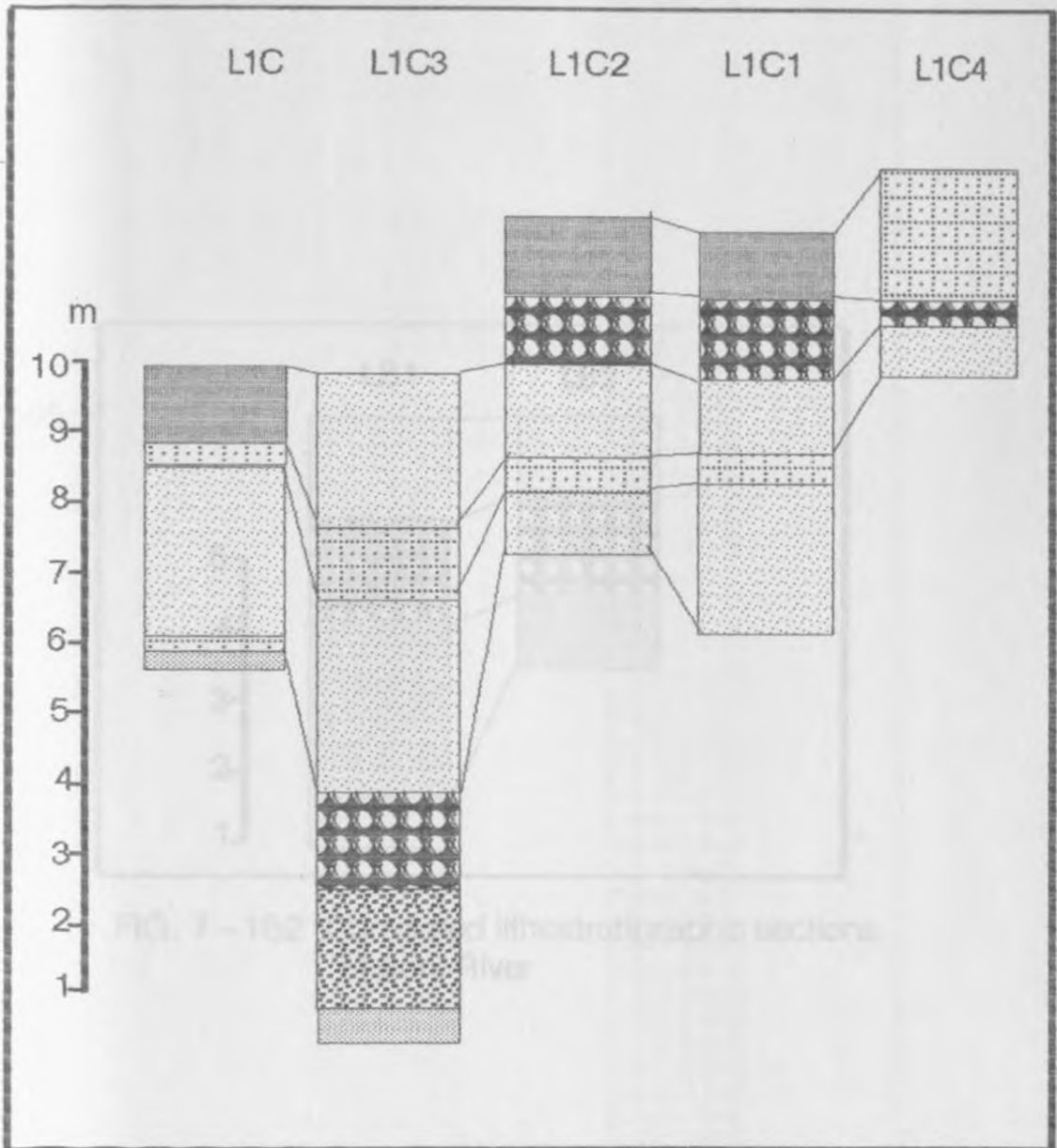


FIG. 7-1C4 Correlated lithostratigraphic section,
Enderit River.

209

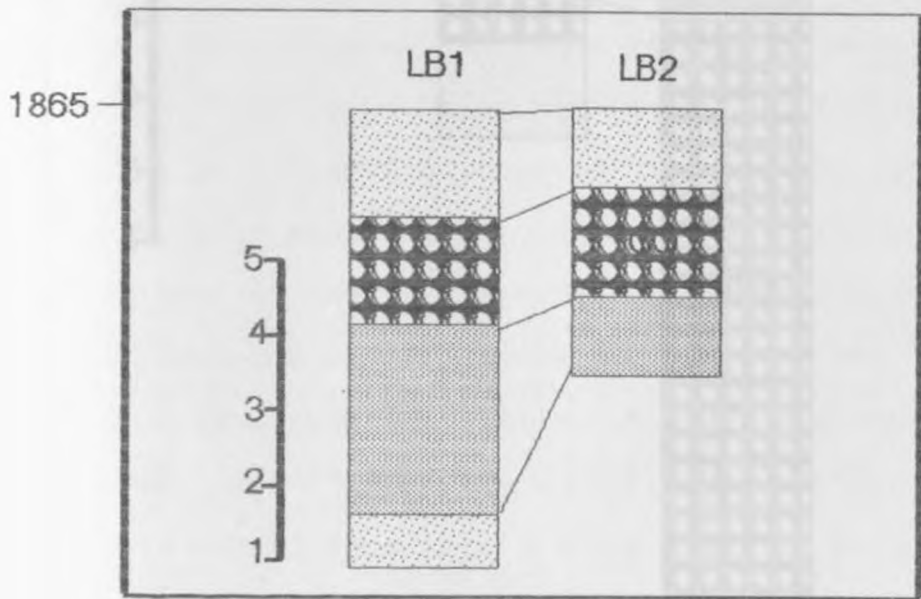


FIG. 7-1B2 Correlated lithostratigraphic sections
Enderit River

203

FIG. 7-1A Correlated lithostratigraphic sections
north of Enderit River drift

204

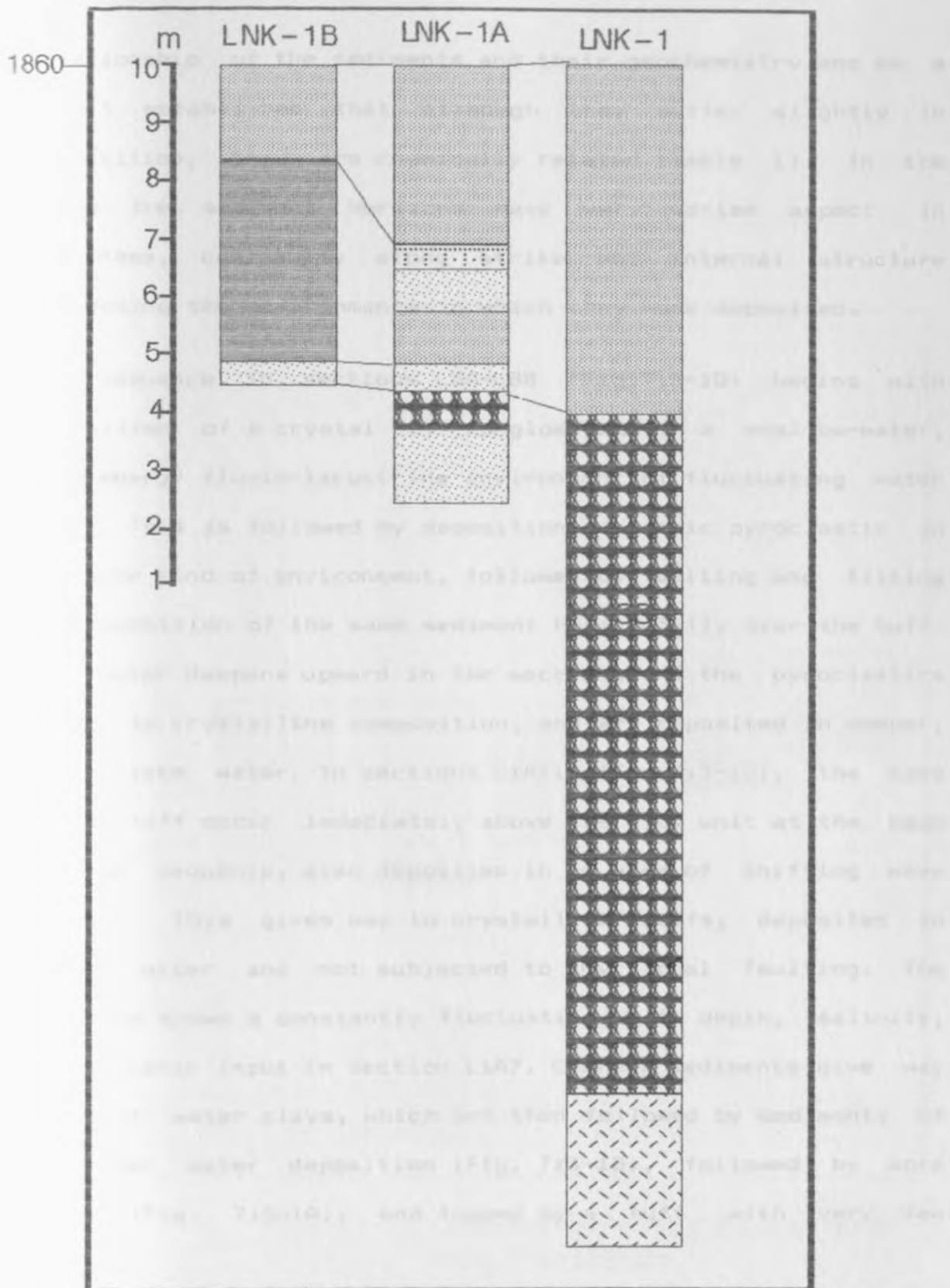


FIG. 7 - NK - 1A Correlated lithostratigraphic sections north of Enderit River drift.

relationship of the sediments and their geochemistry and as a result established that although they differ slightly in composition, they are chemically related (Table 1). In the field the sediment horizons have very varied aspect in thickness, continuity along strike and internal structure reflecting the environments in which they were deposited.

The sequence in sections L8A-L8B (Fig.7:3-1D) begins with deposition of a crystal tuff conglomerate in a shallow-water, high energy fluvio-lacustrine environment of fluctuating water depth. This is followed by deposition of lithic pyroclastic in the same kind of environment, followed by faulting and tilting and deposition of the same sediment horizontally over the tuff. The water deepens upward in the section, and the pyroclastics change to crystalline composition, and are deposited in deeper, quiet lake water. In sections L1A11 (Fig.7:3-1D), the same lithic tuff occur immediately above the clay unit at the base of the sequence, also deposited in an area of shifting wave energy. This gives way to crystalline tuffs, deposited in deeper water and not subjected to any local faulting. The sequence shows a constantly fluctuating water depth, salinity, and volcanic input in section L1A7. Coarser sediments give way to quiet-water clays, which are then followed by sediments of shallower water deposition (Fig. 7:3-1B), followed by more clays (Fig. 7:3-1A), and topped by a tuff with very few

size, which represents a change in type of sand a little
 diastolic activity, accompanied by an increase in the
 size of the lake. The sequence is silt and clay sandstone
 on the top with occasional volcanic ash and minor heavy
 metal (Fig. 7-3-1A, 7-3-1B, 7-3-1C).

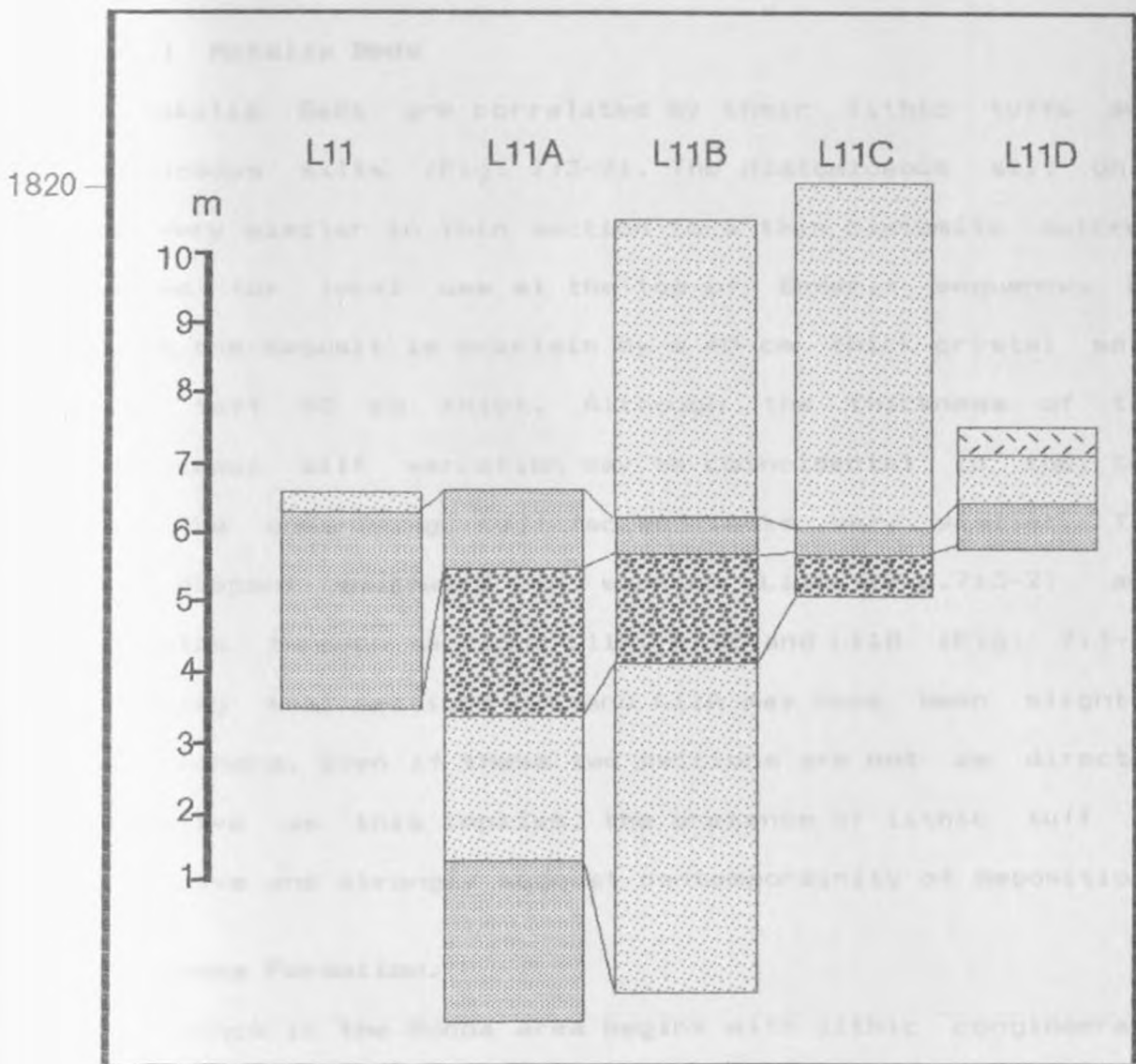


FIG. 7-3-2 Correlated lithostratigraphic sections
 along River Makalia

volcanics, which represents a change to finer or even a hiatus in pyroclastic activity, accompanied by an increase in the salinity of the lake. The sequence is silt and clay dominated towards the top with occasional volcanic ash and minor sandy silt intercalations (Figs. 7:3-1A, 7:3-1B, 7:3-1c).

7.2.1.1 Makalia Beds

The Makalia Beds are correlated by their lithic tuffs and diatomaceous silts (Fig. 7:3-2). The diatomaceous silt unit look very similar in thin section to a thin diatomite outcrop quarried for local use at the top of Enderit sequence. At Enderit the deposit is overlain by a 40 cm thick crystal soft black tuff 40 cm thick. Although the thickness of the diatomaceous silt variation may be coincidental in the two areas the underlying tuff facies looks very similar. The water deepens southward in section L11A (Fig.7:3-2) and fluctuates through sections L11B, L11C and L11D (Fig. 7:3-2) indicating that sections L11 and L11A may have been slightly more inshore. Even if these two sections are not as directly correlative as this implies, the presence of lithic tuff is distinctive and strongly suggest contemporaneity of deposition.

7.2.2 Ronda Formation.

The sequence in the Ronda area begins with lithic conglomerate at the base cyclic pumiceous siltstones, sandstone and claystones tuffs at the Gorge where the ephemeral River Njoro

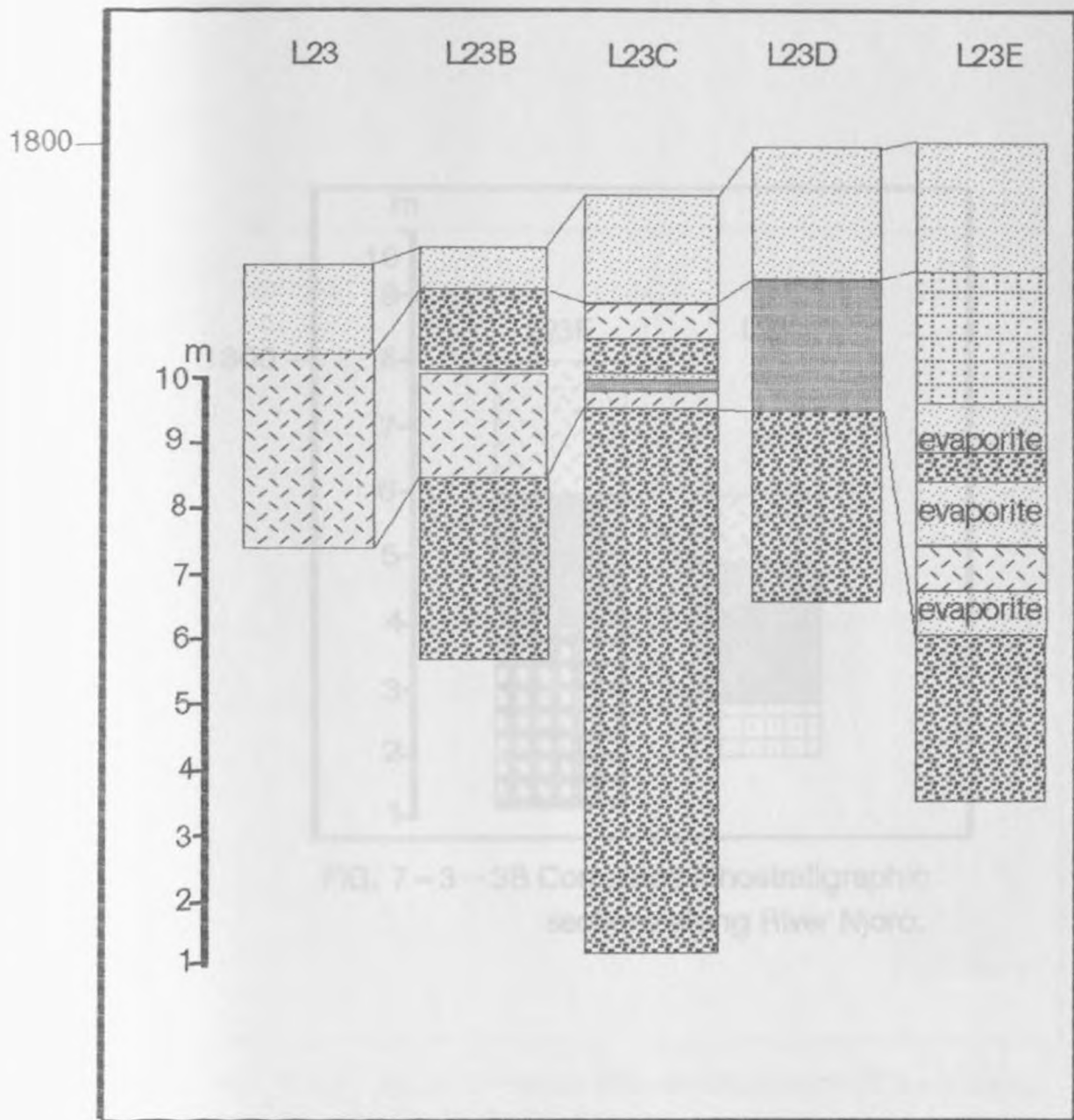


FIG. 7-3-3A Correlated lithostratigraphic sections eastern face in the Ronda sand quarry.

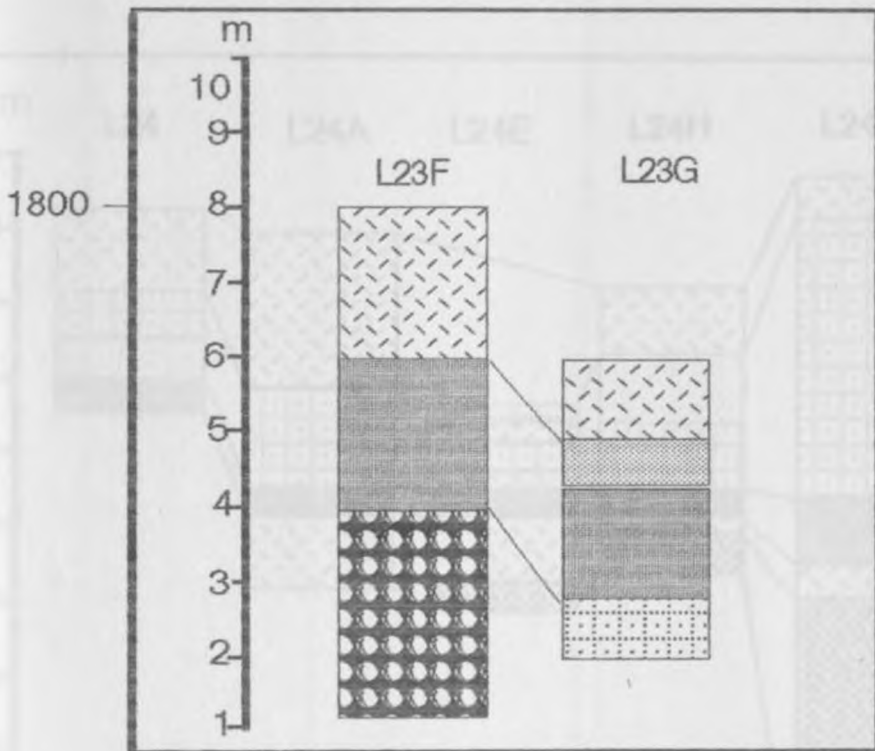


FIG. 7-3-3B Correlated lithostratigraphic sections along River Njoro.

FIG. 7-3-3C Correlated lithostratigraphic sections along River Njoro.

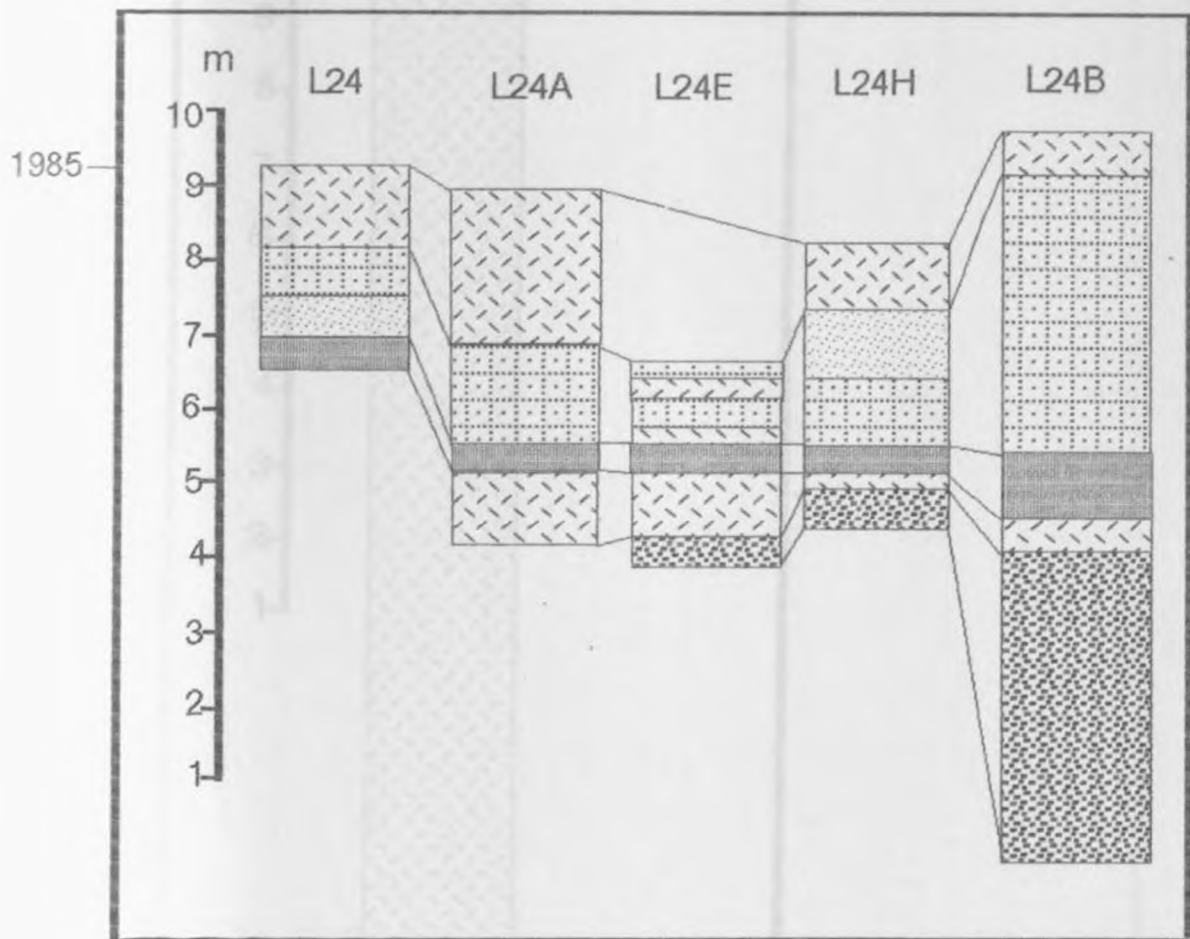


FIG. 7-3-3C Correlated lithostratigraphic sections along River Njoro.

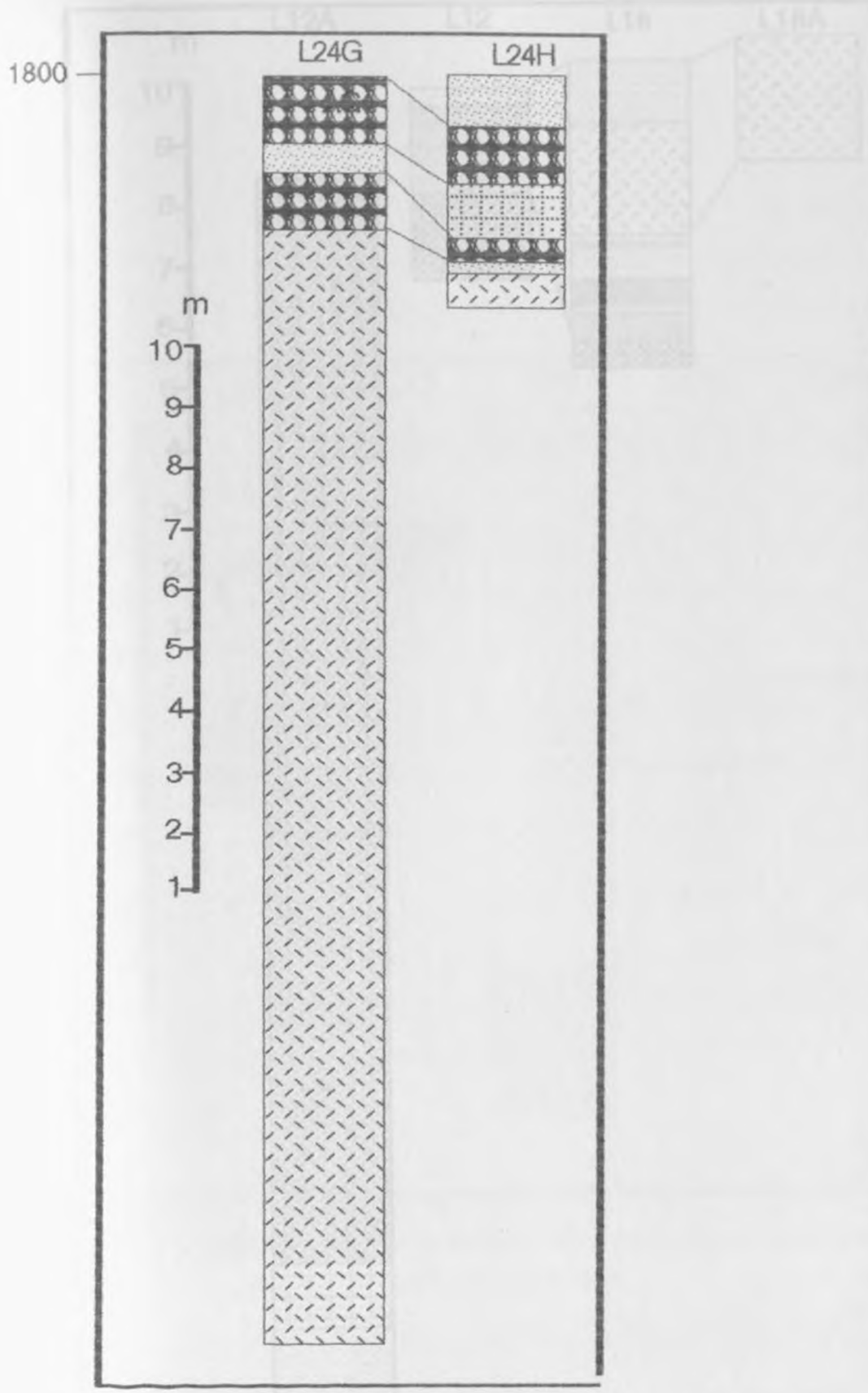


FIG. 7-3-C Correlated lithostratigraphic sections along River Njoro.

7-3-3D Correlated lithostratigraphic sections along the eastern edge of Lake Nakuru game park.

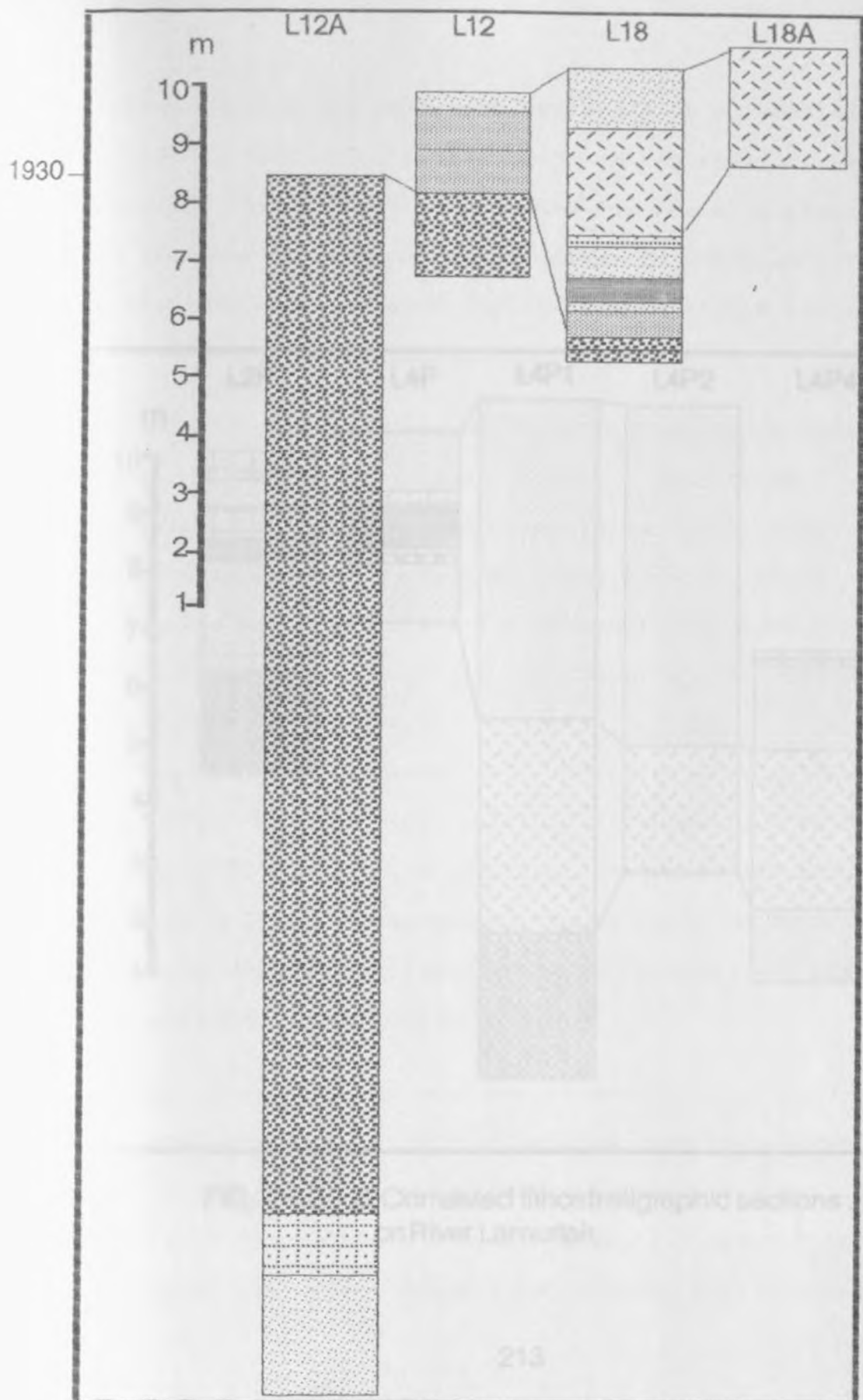


FIG. 7-3-3D Correlated lithostratigraphic sections
north - eastern edge of Lake Nakuru game park.
212

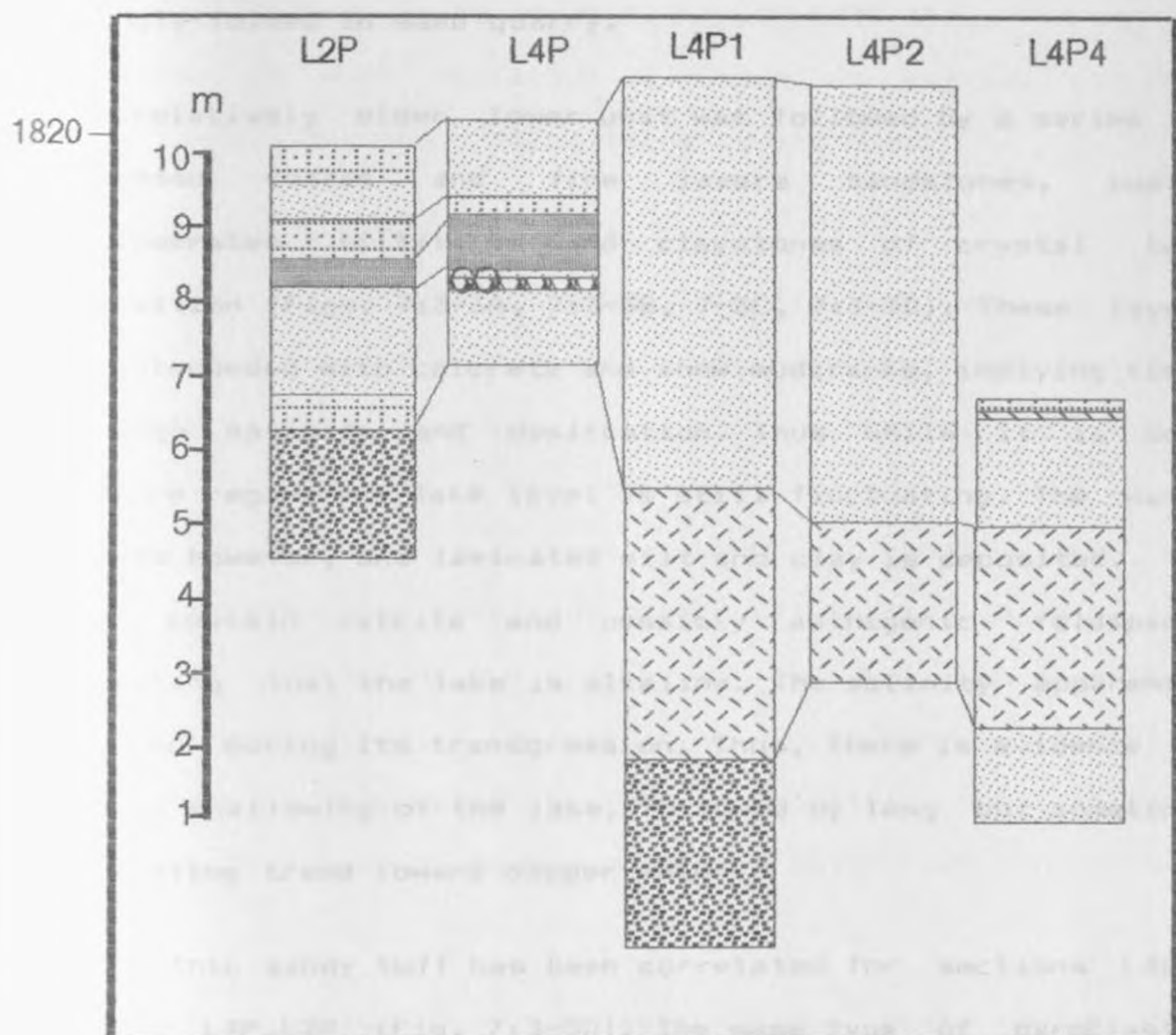


FIG. 7-3-D Correlated lithostratigraphic sections .
on River Lamuriak

enters Lake Nakuru. The unit measures about 30 m, section L12A (Fig. 7:3-3D) entirely pyroclastic in composition and is unconformable marked with a red baked top which distinguishes it from the overlying the Holocene units. On the side of Honey Moon Hill the same sequence is repeated although here it is strongly folded in sand quarry.

The relatively older lower unit was followed by a series of laminated coarse and fine layers sandstones, pumice conglomerates siltstones and claystones of crystal tuff composition (Figs. 7:3-3A, 7:3-3B, 7-3C, 7:3-3D). These layers are interbedded with calcrete and show mudcracks, implying times of high salinity and desiccation. Thus while it is more offshore regime the lake level is still fluctuating. The water deepens however, and laminated silt and clay is deposited. The clay contain calcite and possibly authigenic feldspars, suggesting that the lake is alkaline. The salinity apparently persisted during its transgression. Thus, there is evidence of initial shallowing of the lake, followed by long but sometimes fluctuating trend toward deeper water.

The lithic sandy tuff has been correlated for sections L4P2, LP1, and L4P, L2P (Fig. 7:3-3D). The same type of pyroclastic material is seen in thin section to form the fine clays in the higher part of the sections (Figs. 7:3-3D, 7:3-3C, 7:3-3B) but the sediment differ in composition of their matrix. This is

undoubtedly a reflection of the environment of deposition and not an indication of a new kind of tuff. The fluctuating lake level seen in sections L23-L23E (Fig. 7:3-3A) is also noted in sections L24-L24B (Fig. 7:3-3C), in the long sequence of laminated coarse and fine crystal tuffs. Since it is further offshore, the sediments in sections L23-L23E (Fig. 7:3-3A) do not show as much variation as those in section L24-L24B (Fig.7:3-3D), but the general trend is the same.

7.2.3. Soysambu Formation

The sequence from the Soysambu diatomite mine west of Lake Nakuru were sampled and generally are only short sections. The sediments are crystal tuff with a high concentration of pumice alluvium, that conceals the horizontally-bedded sandy clays. The horizontal alluvium clays mark the uppermost unit on the lacustrine diatomite lake beds. The overlying crystal tuff was probably formed during the retreat of the lake, with some form of transport mechanism concentrating pumice sands. Deposition in water is suggested by the diatomite intercalations, shrinkage cracks in the matrix and some water reworking of the grains.

The pumice tuffs, clays, silts and sands that formed pits sequence is correlated with the sandy clay sections above the diatomite deposit (Fig. 7:3-4) with the clays assumed to be approximately contemporaneous. The sediments are almost

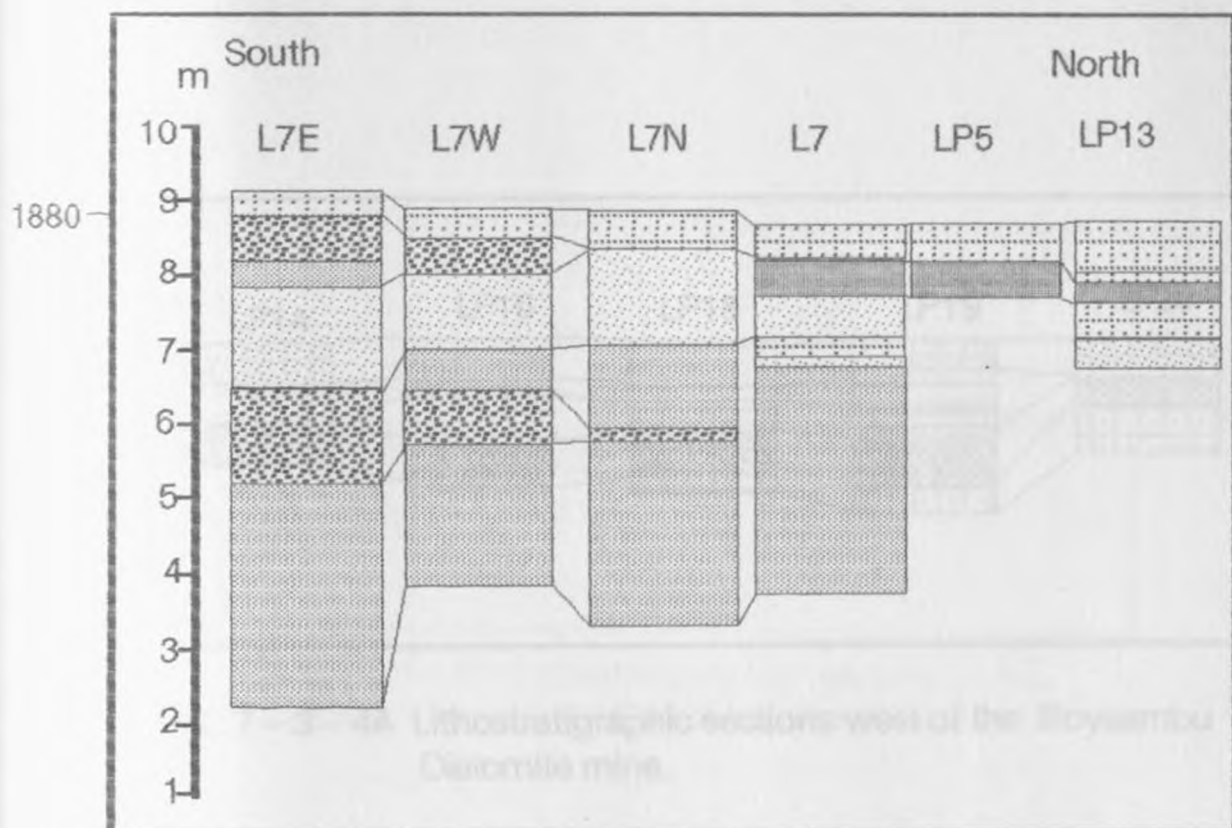


FIG. 7-3-4 Correlated lithostratigraphic sections at the Soysambu Diatomite Mine.

217

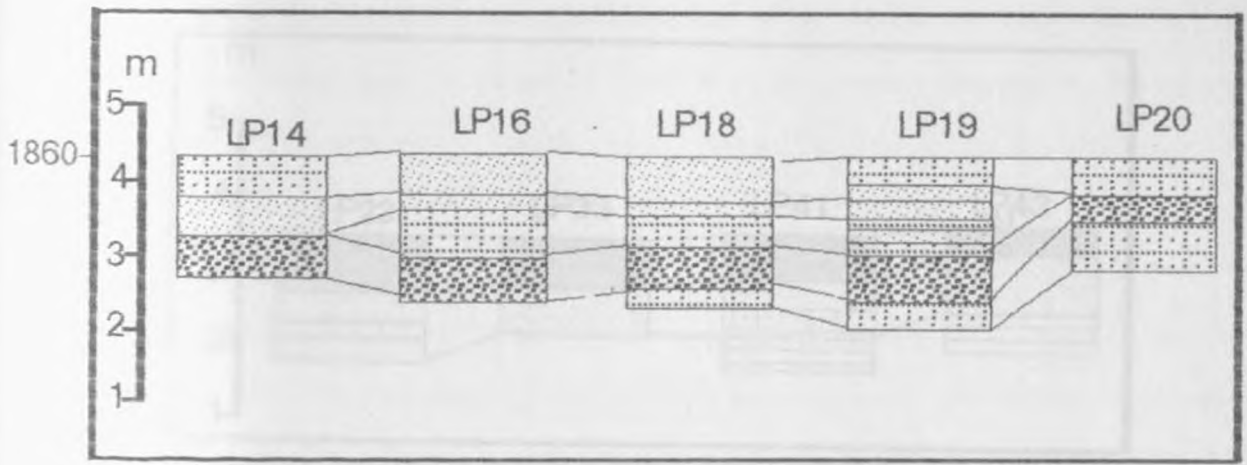


FIG. 7-3-4A Lithostratigraphic sections west of the Soysambu Diatomite mine.

... in lithology with increasing "sandstone" ...
 ... and showing calcareous horizons. These are topped by
 ... clay changing colour from grey, to brown, becoming
 ... more calcareous further up in the section.
 ... of the distal ... unit and the ... sections
 ... as the ... with ...
 ... are considered equivalent.

Caribbean Foreland

The ... of the Caribbean Foreland
 ... in the field on the basis of

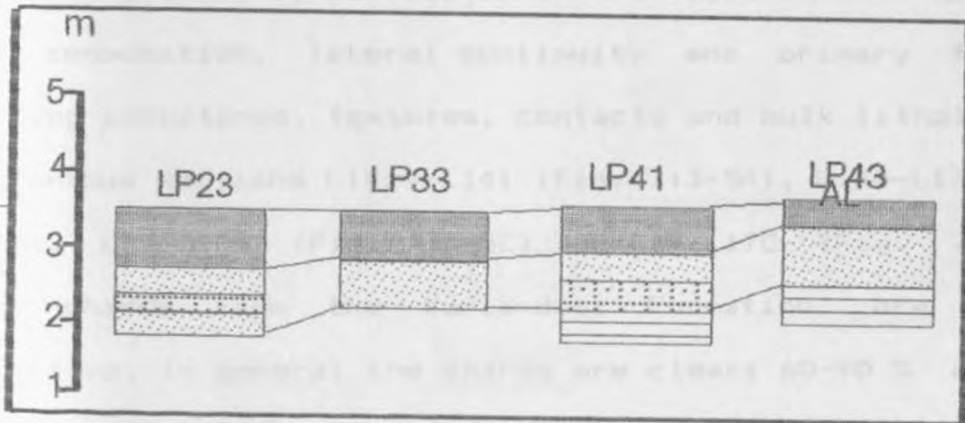


FIG. 7-3-4B Lithostratigraphic sections on the western bounding edge of the Soysambu basin.

identical in lithology with increasing "sandstones" becoming coarser and showing calcrete horizons. These are topped by calcareous clay changing colour from grey, to brown, becoming coarser and more calcareous further up in the section. Correlation of the diatomite mine unit and the pits sections is straightforward as the uppermost tuff and common calcrete intercalations are considered equivalent.

7.2.4 Kariandusi Formation

Both tuffs and diatomaceous silts of the Kariandusi Formation have been physically correlated in the field on the basis of their composition, lateral continuity and primary features including structures, textures, contacts and bulk lithology in the various sections L14iv-L14i (Fig. 7:3-5A), L14A-L13 (Fig. 7:3-5B), L15-L15B (Fig. 7:3-5C) and L17-L17C (Fig. 7:3-5D). Glass shards from the Kariandusi Formation are fairly distinctive. In general the shards are clear: 60-90 % are very light grey. This tuff has pumice clasts of variable compositional trend and may represent eruptive products of different proportions of compositionally variable magma chamber.

At diatomite mine, the Formation however show little variability in both the petrology and geochemistry as shown by the bulk sediment component of pumice and tuffs. This suggests that all sections are genetically related in that the

L14A

L14B

L14C

L14D

L13

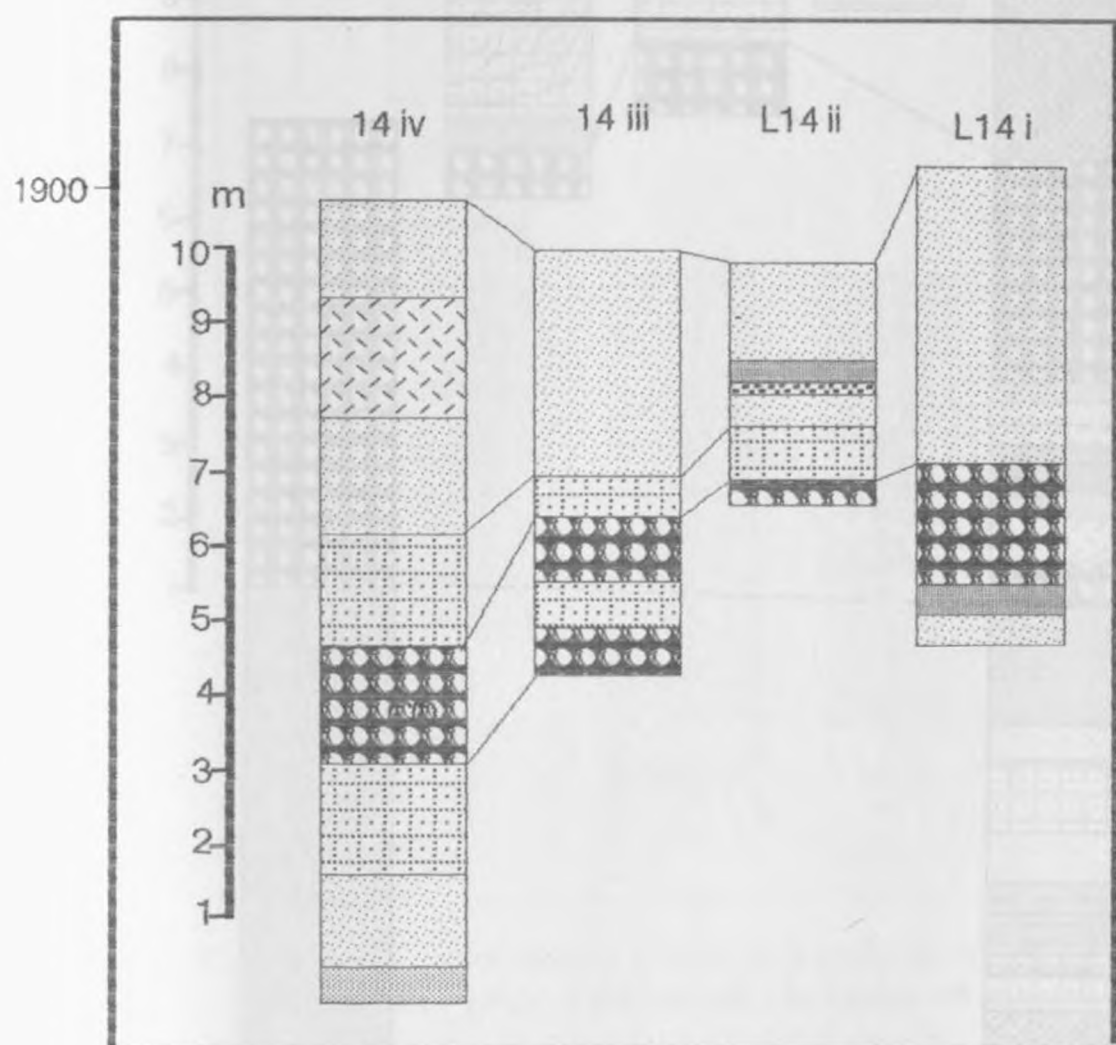


FIG. 7-3-5A Correlated lithostratigraphic sections south of the Kariandusi.

7-3-5B Correlated lithostratigraphic sections north of Kariandusi Dataromilimyo.

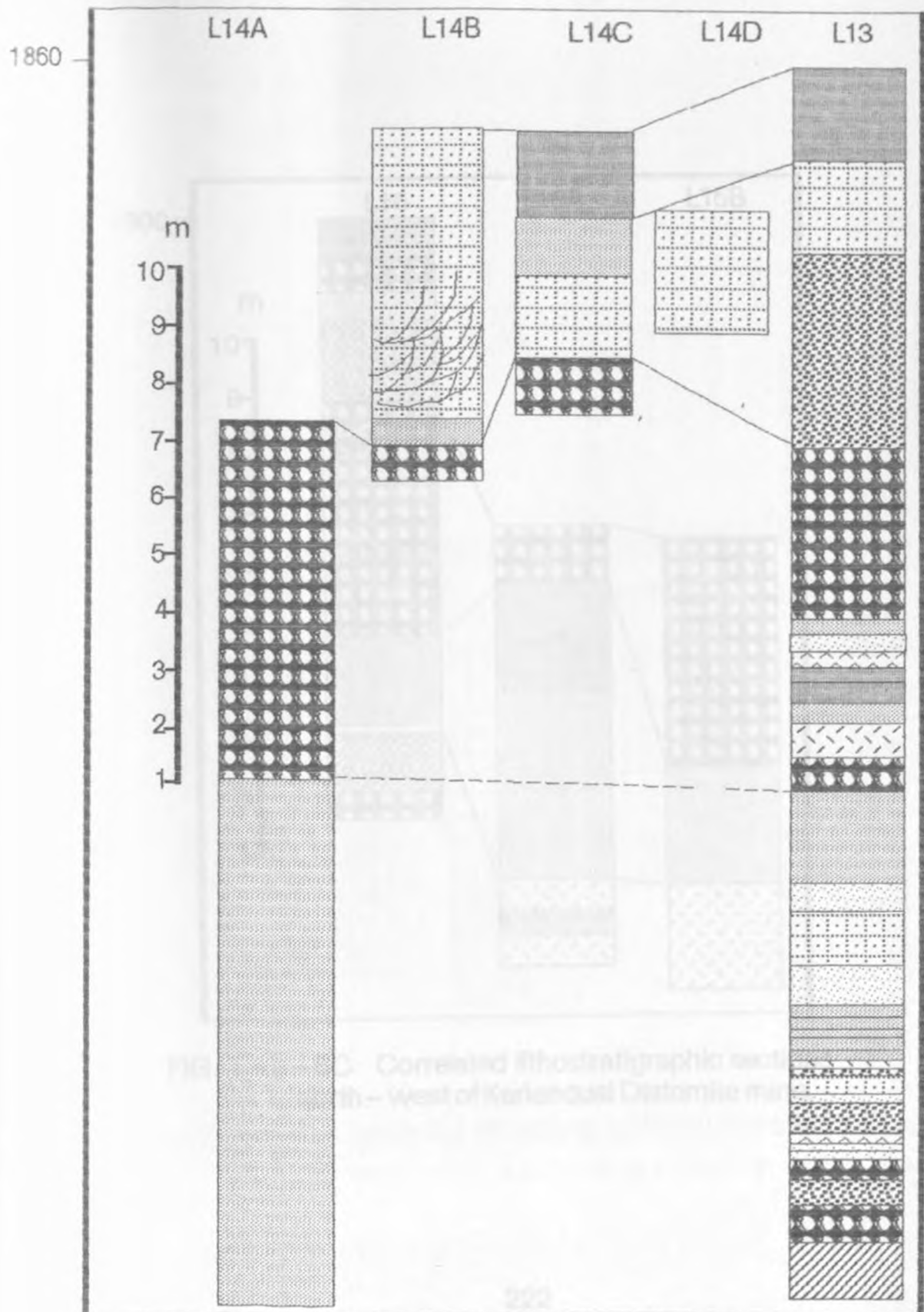


FIG. 7-3-5B Correlated lithostratigraphic sections, north of Kariandusi Diatomite mine.

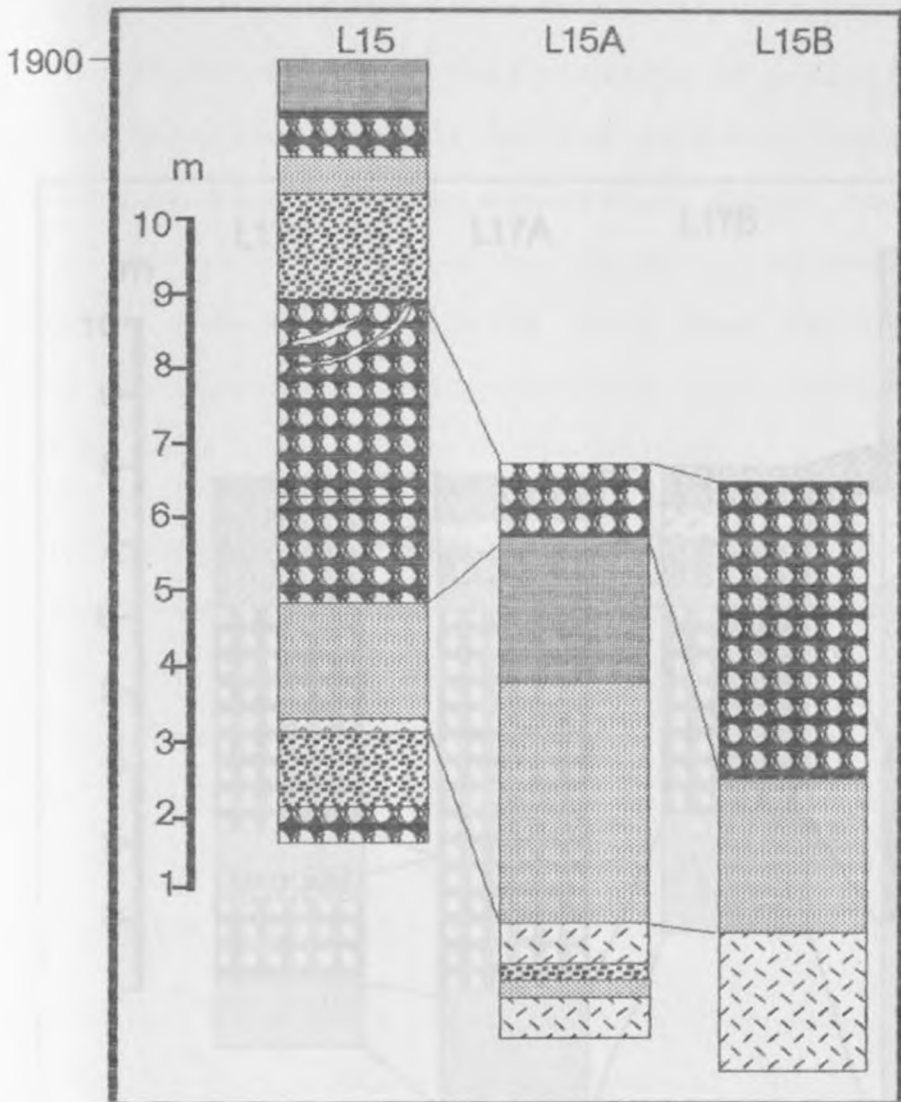


FIG. 7-3-5C Correlated lithostratigraphic sections north-west of Kariandusi Diatomite mine.

7-3-5D Correlated lithostratigraphic sections north-east of Kariandusi mine extending to the Proterozoic Sea.

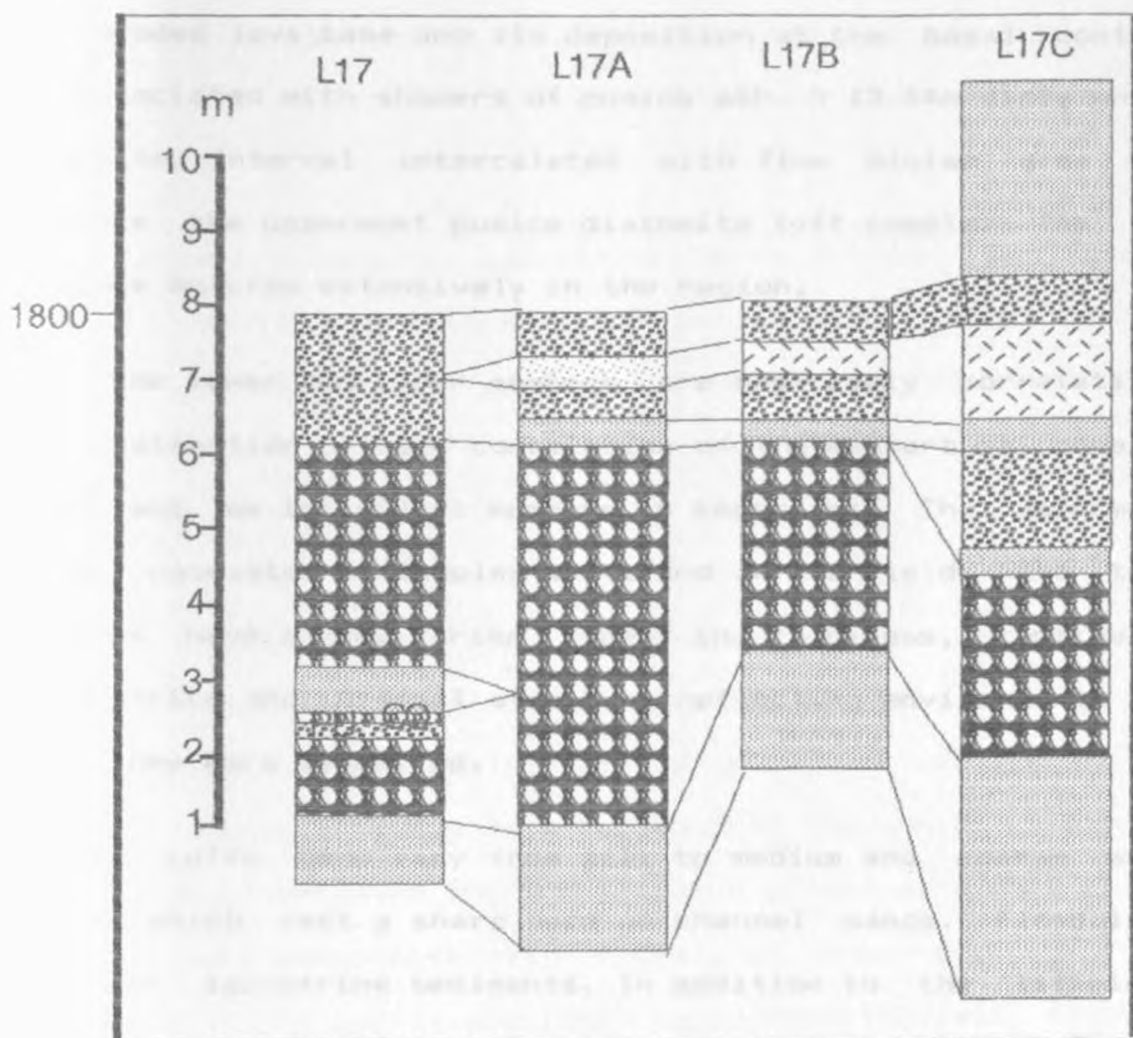


FIG. 7 - 3 - 5D Correlated lithostratigraphic sections north - east Kariandusi mine extending to the Prehistoric Site.

variations fall on well defined compositional trends. Hence the lake beds of the formation at the Kariandusi Diatomite Mine are considered as two separate members. The lower member of the formation at the diatomite mine consists of a 13.1 m thick F (filler variety) white diatomite. The formation has a faulted and eroded lava base and its deposition at the basal contact was associated with showers of pumice ash. A 13.44m dirty white diatomite interval intercalated with fine bluish grey ash separate the uppermost pumice diatomite tuff complex. The top sequence outcrop extensively in the region.

Both the lower and upper members are separately correlative. The distinction between correlation of the members as general units and as individual members is important. The uppermost member consists of complex tuffs and in the field, the tuff horizons have a very varied aspect in thickness, continuity along strike and internal structure reflecting environments in which they were deposited.

Typical tuffs here vary from silt to medium and coarse sand grade, which rest a sharp base on channel sands. Floodplain silts on lacustrine sediments. In addition to the lithology they were correlatable on the basis of their structures. Though small in scale the structures include cross stratification ripple and plain lamination. The volcanic ash associated with the Kariandusi Formation possibly represent airfall volcanic

dust or sheet washed sediment from the landscape either near the source or from local sources. The bulk of the deposits is composed of fragmentary volcanic glass with a limited suite of primary volcanic crystal fragments; sanidine, orthoclase, alkali pyroxene and ilmenite with occasional quartz. Frequent laterally extensive thin clay, silt and pumice sand and diatomites afford useful lateral correlation between sections (Figs. 7:3-5A to 7:3-5D).

Pumice clasts commonly associated with channel and beach littoral complexes are abundant on the alluvial flood plains and are correlatable in most of the sections of Kariandusi Formation. In grain size, the pumice clasts range from granule to boulder gravel. Although there is an apparent diminution in grain size from the basin margin towards the present lake shore, occasional coarser grain entrainment reached quiet zones of the lake bottom. Grain size variation at any locality is often significant reflecting that floating was an important transport mechanism away from the source. The pumice contains phenocrysts of sanidine, orthoclase and alkali-pyroxene, which are sometimes associated with crystals of accessory quartz. The glass of the pumice and their sanidine-orthoclase crystal phenocrysts have special significance as potential material for K/Ar dating studies.

7.3 Geochemical correlation.

The chemical composition of a sedimentary component is distinctive, and the differentiation of sedimentary components results in the separation of associated elements. Typical separations include enrichment of K_2O and Al_2O_3 in finer grained, phyllosilicates-rich fraction and the enrichment of SiO_2 and Na_2O in the coarser-grained, sediment fraction. Fe_2O_3 and MgO are also enriched in the fine fraction, if they are abundant constituents in the phyllosilicates. The chemical compositions of sediment from locations of the Enderit, Makalia, Ronda, Soysambu and Kariandusi therefore provide an important basis for correlating the formations. The chemical variation trends are generally similar. This indicates that locally there was no large scale variation in the environments of deposition and source areas. Chemical variations in the sediments of the Central Kenya Rift basins are primarily dependent upon the mineralogy of the sedimentary rocks. The mineralogy is dependent on the various factors including provenance, relief, weathering, sorting, and negligible diagenesis as most of the sediments are unlithified. These factors are partially dependent on the regional setting of the sedimentary system and the geochemical studies are especially valuable when evaluating the clastic mineralogy of altered sedimentary rocks. Although the mineralogy can be significantly changed by processes associated with burial and

diffusion during diagenesis which may present significant problems when trying to evaluate the composition of a sedimentary rock. Alteration can be especially severe in the phyllosilicates fraction, where matrix recrystallization can obliterate all direct evidence detrital phyllosilicates, since phyllosilicate fraction is especially sensitive to the hydraulic effects associated with winnow and scour. However, this change may not necessarily affect the bulk chemical composition and in the largely unconsolidated rift sediments its effect is insignificant. In addition the low reactivity and solubility of common silicate minerals, reduce the potential advective transport and further limits potential chemical changes in sedimentary systems. Different combinations of common sedimentary minerals may result in similar chemical compositions, and single chemical analysis can rarely be used to discriminate and infer the clastic mineralogy of a sediment. Thus it is possible to use chemical variations in sedimentary rock suites to infer the composition in fractionable solids in sediments, and the processes by which these deposits were formed. The samples chosen from the sections indicate that the series of tectonic events here produced various distinct basins and volcanic ash.

7.3.1 Sediment chemistry variation trends.

The entire rift sediments contain relatively low SiO_2 and have low Si/Al and Na/K ratios. These are possibly

consequences of low quartz content and high plagioclase content of the highly immature rift sediments. High Na/K and Na/Al ratios are commonly associated with mineralogically immature sands and greywacke (Pettijohn, 1957; Crook, 1974). The K-feldspar in the formations is detrital in origin relatively coarser and suggests sedimentary suite of different sources.

Chemical variations in the sedimentary suites (Figs. 7-1A to 7-1C) suggests that the concentration of K₂O is well correlated to the concentration of Al₂O₃ in the Enderit and Ronda deposits (Fig. 7-1B). The correlation is however only fair in Ronda (Fig. 7-1E) negligible in Makalia (Fig. 7-1B) but non-existent in the Soysambu (Fig. 7-1A) deposits and a negligible negative correlation is reflected in the Kariandusi deposits (Fig. 7-1A). The SiO₂ and Al₂O₃ are well correlated and the SiO₂ - Al₂O₃ chemical variation trend extrapolates towards aluminium enrichment in the Enderit, Makalia (Fig. 7-2B), and Soysambu (Fig. 7-2A). The SiO₂ rich samples are also more coarsely grained, quartz poor sediments. Each trend forms a line that connects the compositions of illite and quartz. Thus indicating that illite and quartz do not behave as two hydraulically differentiable, monomineralic sedimentary components. K-feldspar does have K₂O and Al₂O₃ in the proper ratio to produce these trends. Much of the K-feldspar has sharp, euhedral outlines suggesting probable authigenic origin or a detrital

phase from neighbouring sources. Unstable detrital grains would only survive in environments of little intense chemical weathering.

Although differentiated there are very poor correlations of K_2O with Al_2O_3 at Makalia, Soysambu and Kariandusi. Poor correlations among alkali elements reflect the abundant presence of detrital K-feldspar and plagioclase. The quartz/K-feldspar, plagioclase ratios were evidently highly variable and may be considered typical for an immature sediment containing abundant rock fragments and diffusion of K^+ has little effect on the bulk composition of an accumulating sediment. The finer-grained samples apparently contain the higher concentrations of K_2O and Al_2O_3 and lower concentration of SiO_2 . This would support the interpretation that finer-grained illite was possibly sorted from coarse grained quartz during sedimentation. The rift sediments contain considerably high sodium. These sedimentary rocks contain detrital alkali feldspar and are evidently derived from the neighbouring volcanic rocks. Except for the Enderit and Ronda Formations, the $K_2O-Al_2O_3$ trend do not pass near zero percent K_2O and Al_2O_3 and the $SiO_2-Al_2O_3$ does not pass near 100 percent SiO_2 . The lack of axial intercepts suggests that the coarser - grained sedimentary components contained very little SiO_2 and was dominated by feldspar. One special quality of the linear trend that passes through the origin is that a constant ratio must

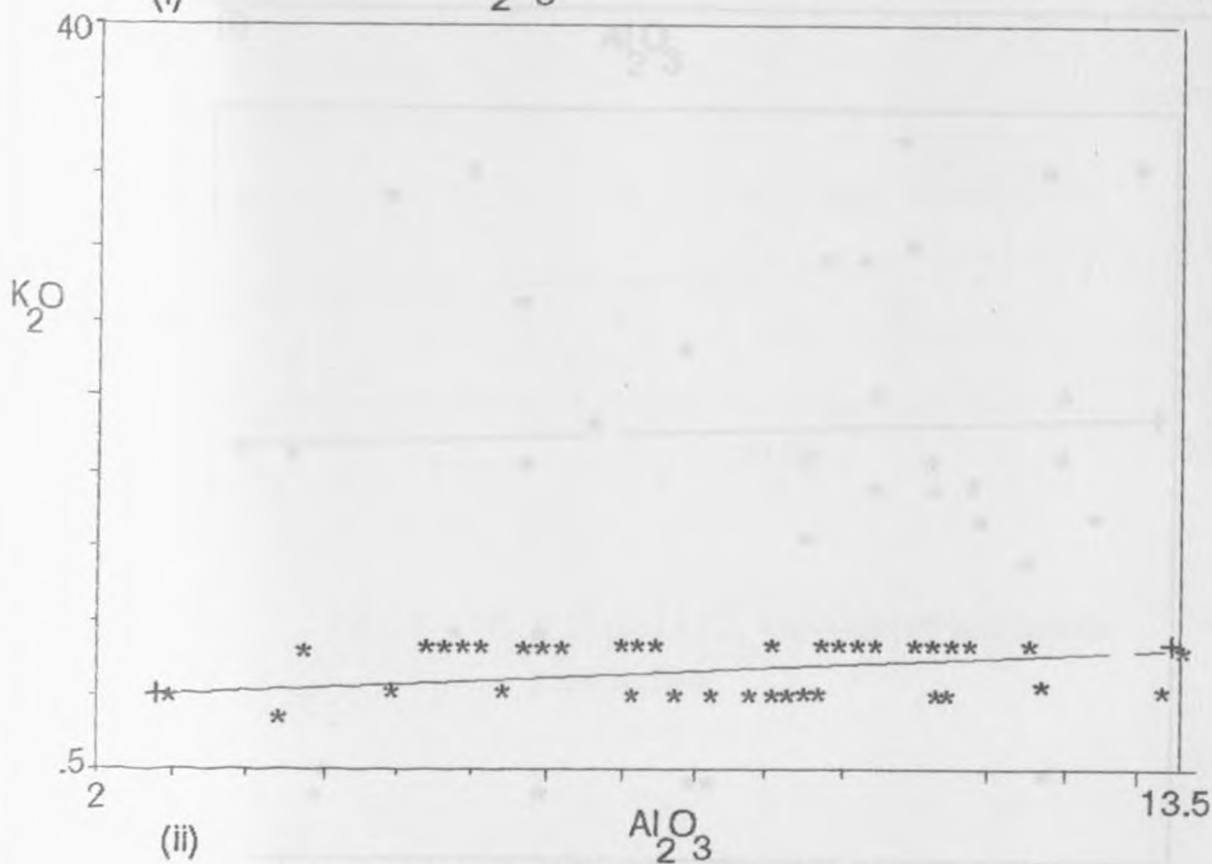
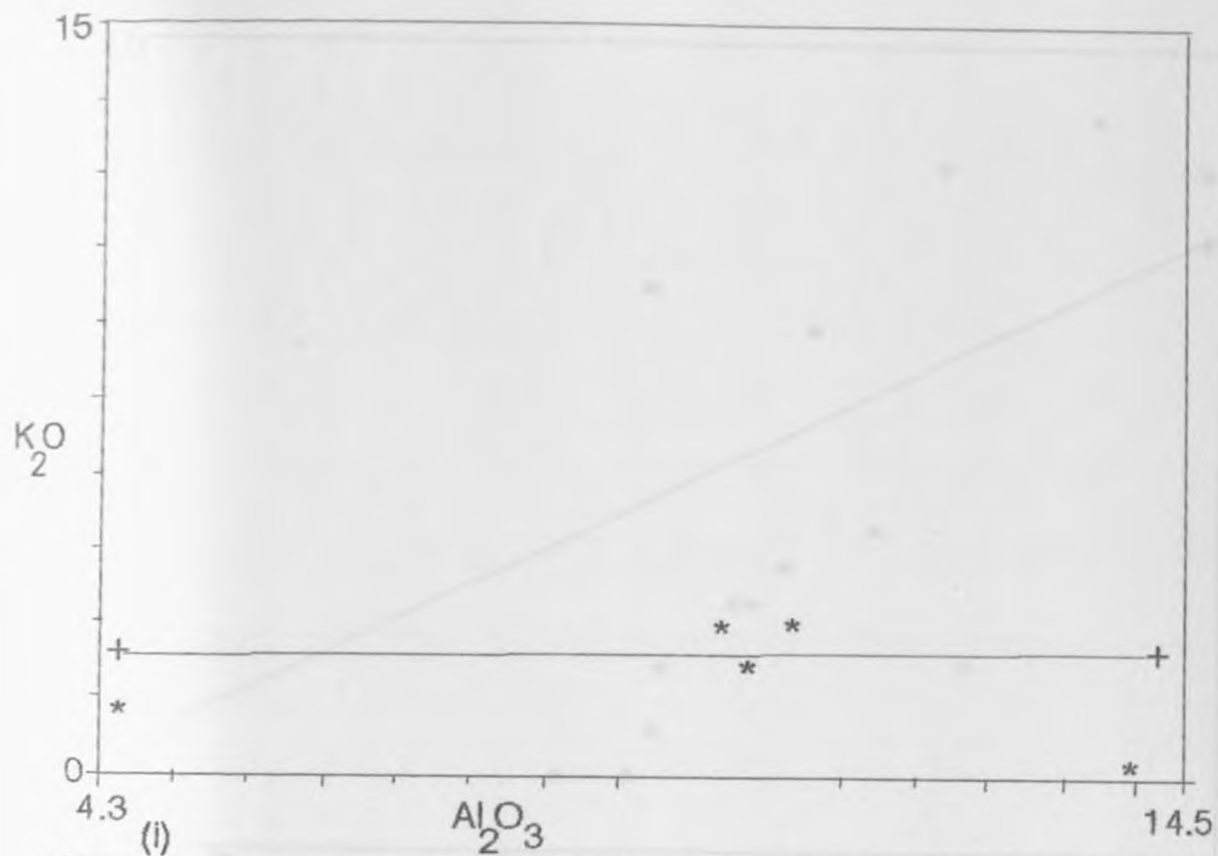


Fig. 7 - 1A K_2O and Al_2O_3 variation of sediments from
 (i) Soysambu and (ii) Kariandusi.

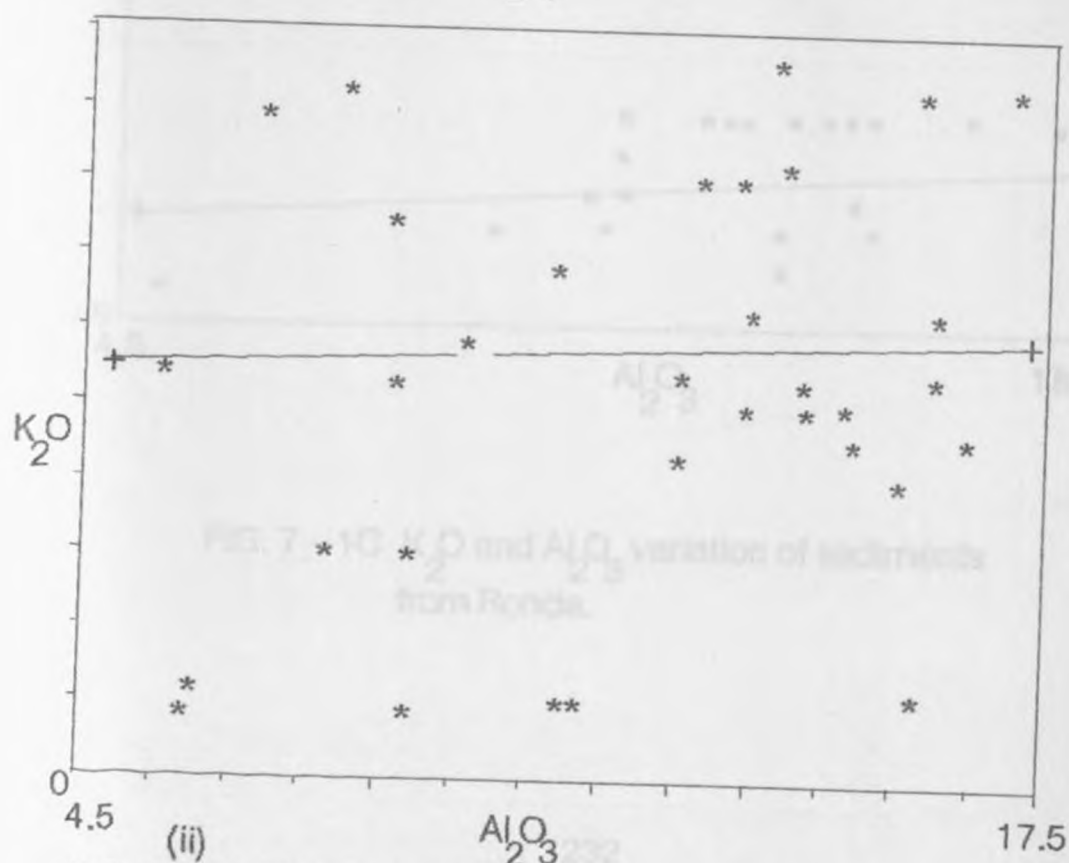
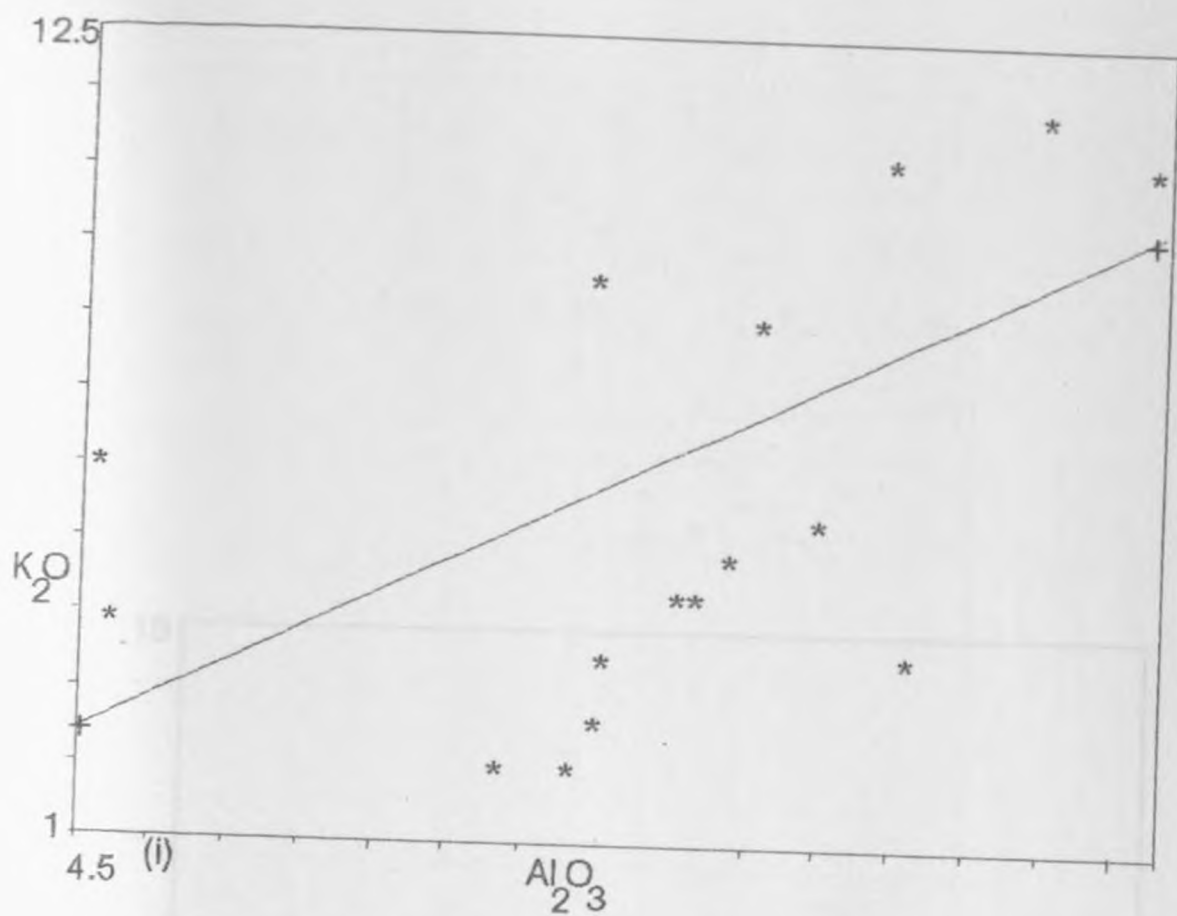


FIG. 7-1B K_2O and Al_2O_3 variation of sediments from (i) Enderit and (ii) Makalia.

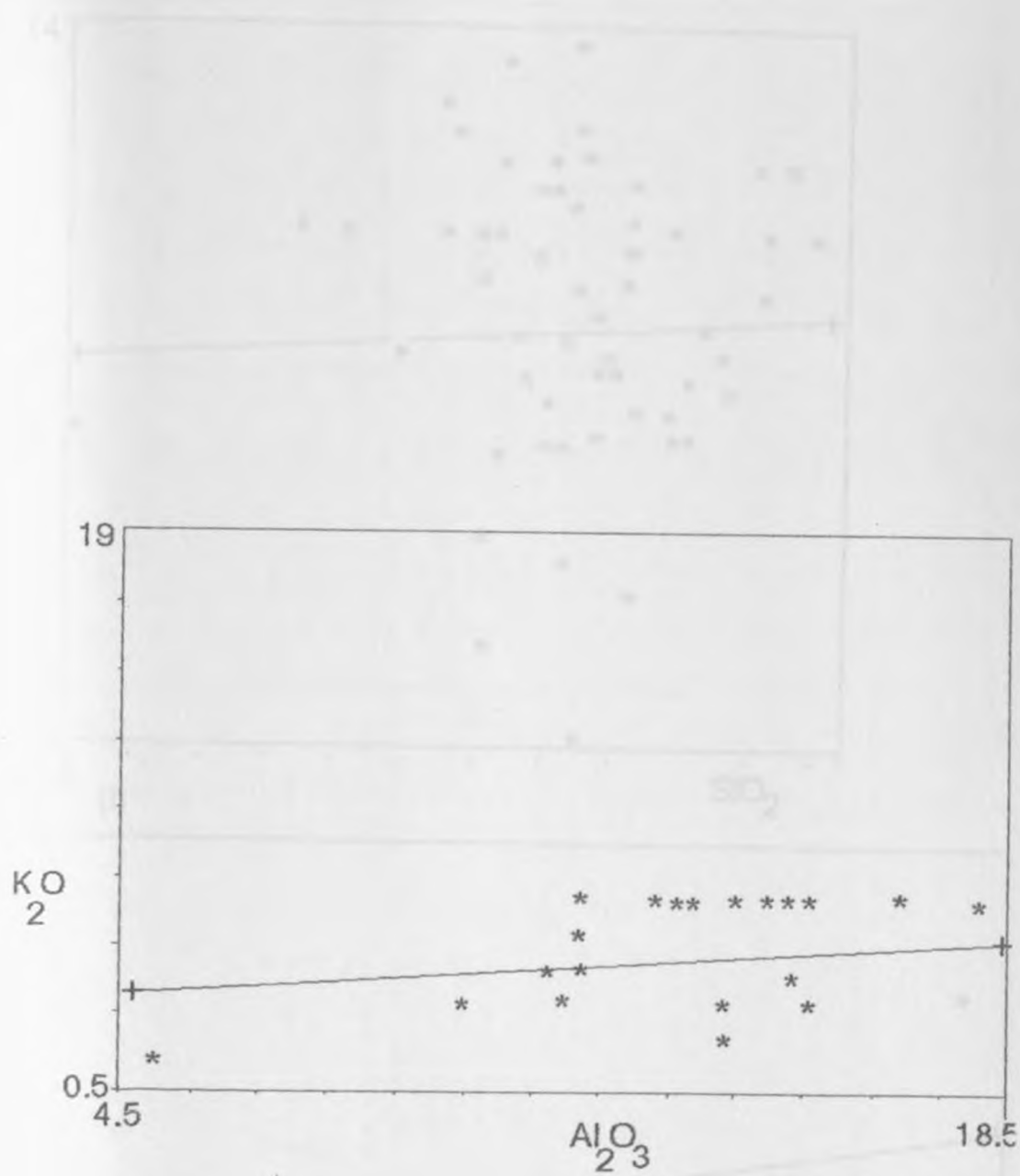


FIG. 7-1C K_2O and Al_2O_3 variation of sediments from Ronda.

(ii) SiO_2 232

FIG. 7-2A Al_2O_3 and SiO_2 variation in sediments from (i) Karanikal and (ii) Goyambur

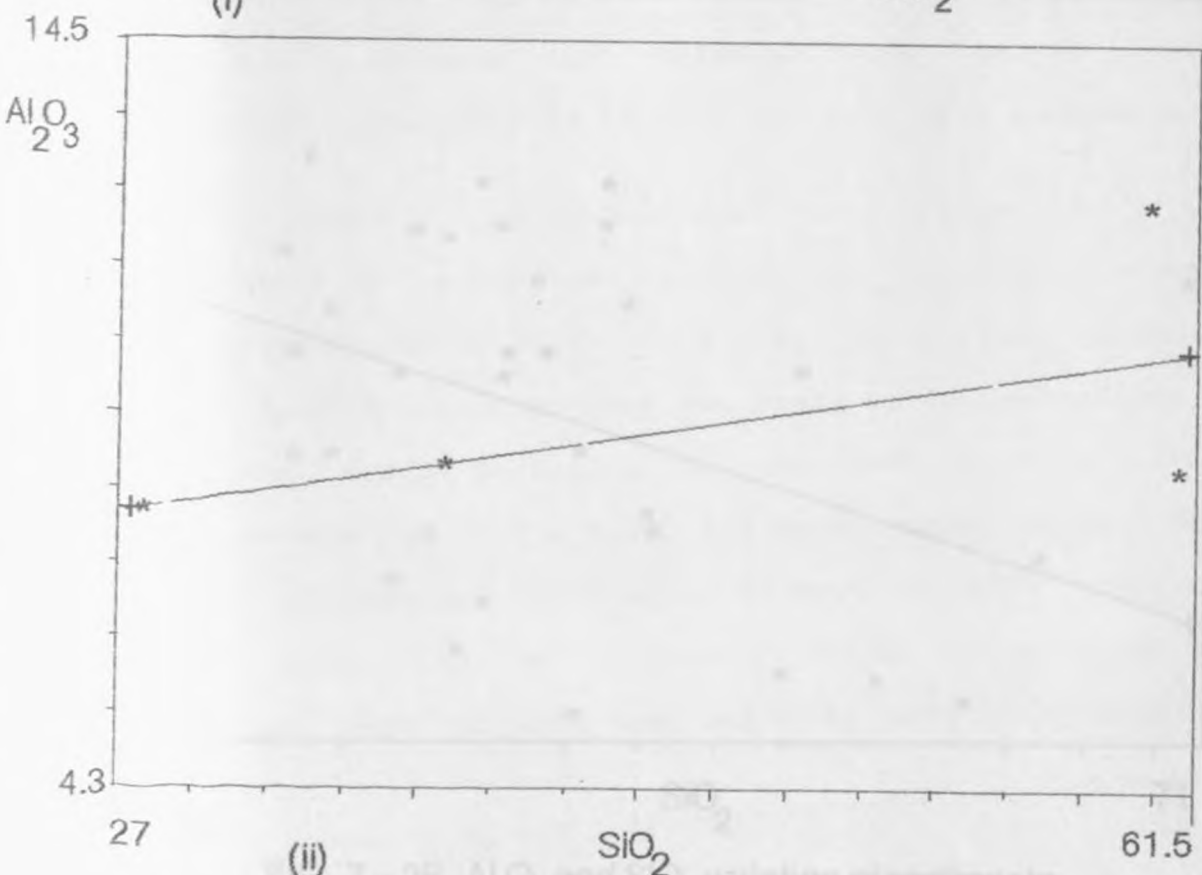
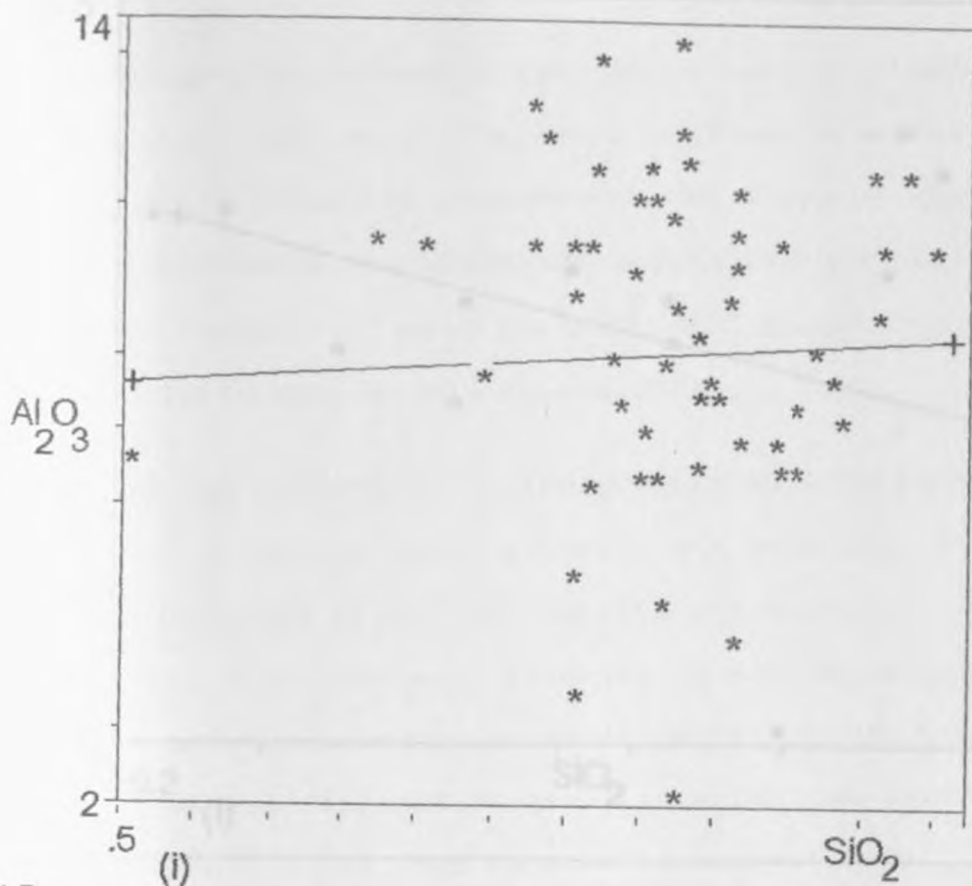


FIG7 - 2A Al_2O_3 and SiO_2 variation in sediments from (i) Kariandusi and (ii) Soysambu

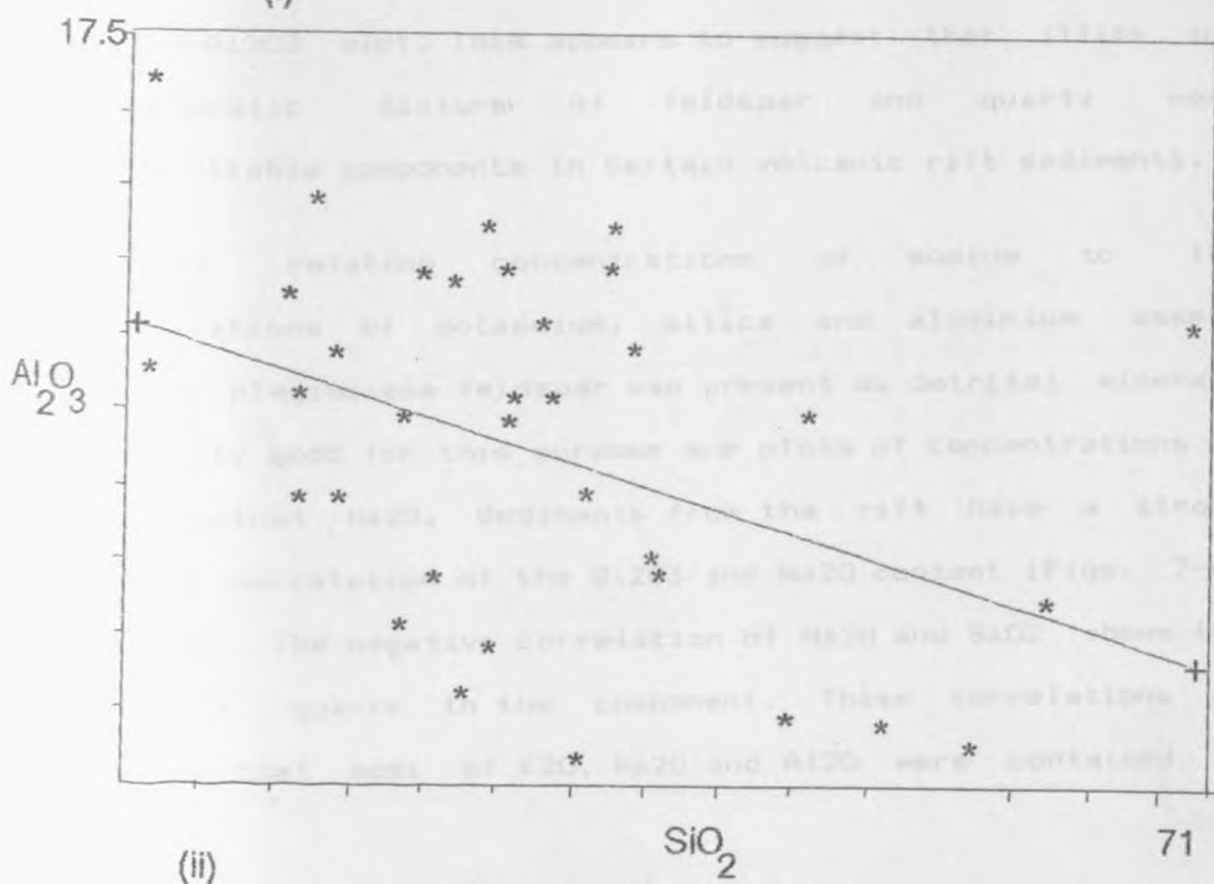
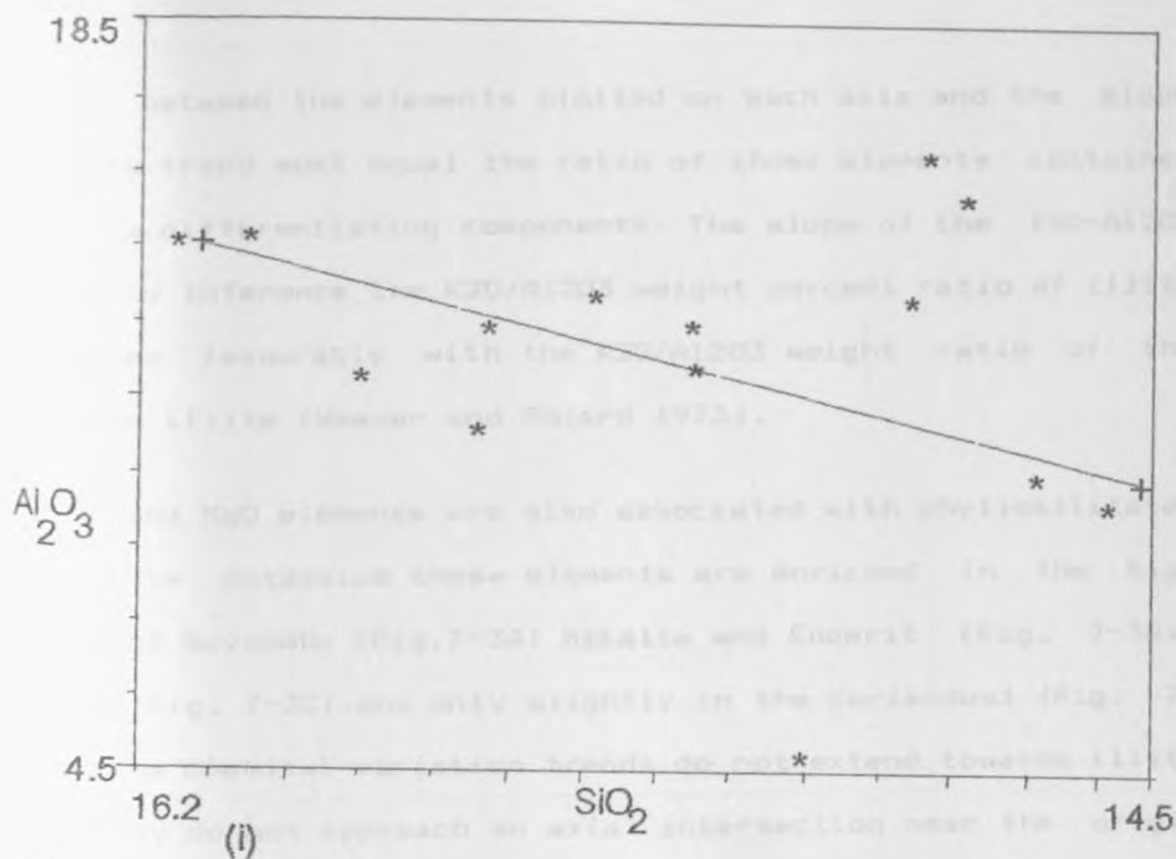


FIG. 7-2B Al₂O₃ and SiO₂ variation of sediments from (i) Enderit and (ii) Makalia.

exist between the elements plotted on each axis and the slope of the trend must equal the ratio of those elements contained in the differentiating components. The slope of the $K_2O-Al_2O_3$ trend by inference the K_2O/Al_2O_3 weight percent ratio of illite compares favourably with the K_2O/Al_2O_3 weight ratio of the average illite (Weaver and Polard 1973).

Fe_2O_3 and MgO elements are also associated with phyllosilicates and like potassium these elements are enriched in the high Al_2O_3 of Soysambu (Fig. 7-3A) Makalia and Enderit (Fig. 7-3B), Ronda (Fig. 7-3C) and only slightly in the Kariandusi (Fig. 7-3A). The chemical variation trends do not extend towards illite as they do not approach an axial intersection near the origin of $K_2O-Al_2O_3$ plot. This appears to suggest that illite and polymineralic mixture of feldspar and quartz were differentiable components in certain volcanic rift sediments.

Diagrams relating concentrations of sodium to the concentrations of potassium, silica and aluminium assess whether plagioclase feldspar was present as detrital mineral. Especially good for this purpose are plots of concentrations of SiO_2 against Na_2O . Sediments from the rift have a strong negative correlation of the SiO_2 and Na_2O content (Figs. 7-4A and 7-4B). The negative correlation of Na_2O and SiO_2 shows the lack of quartz in the component. These correlations do suggest that most of K_2O , Na_2O and Al_2O_3 were contained in

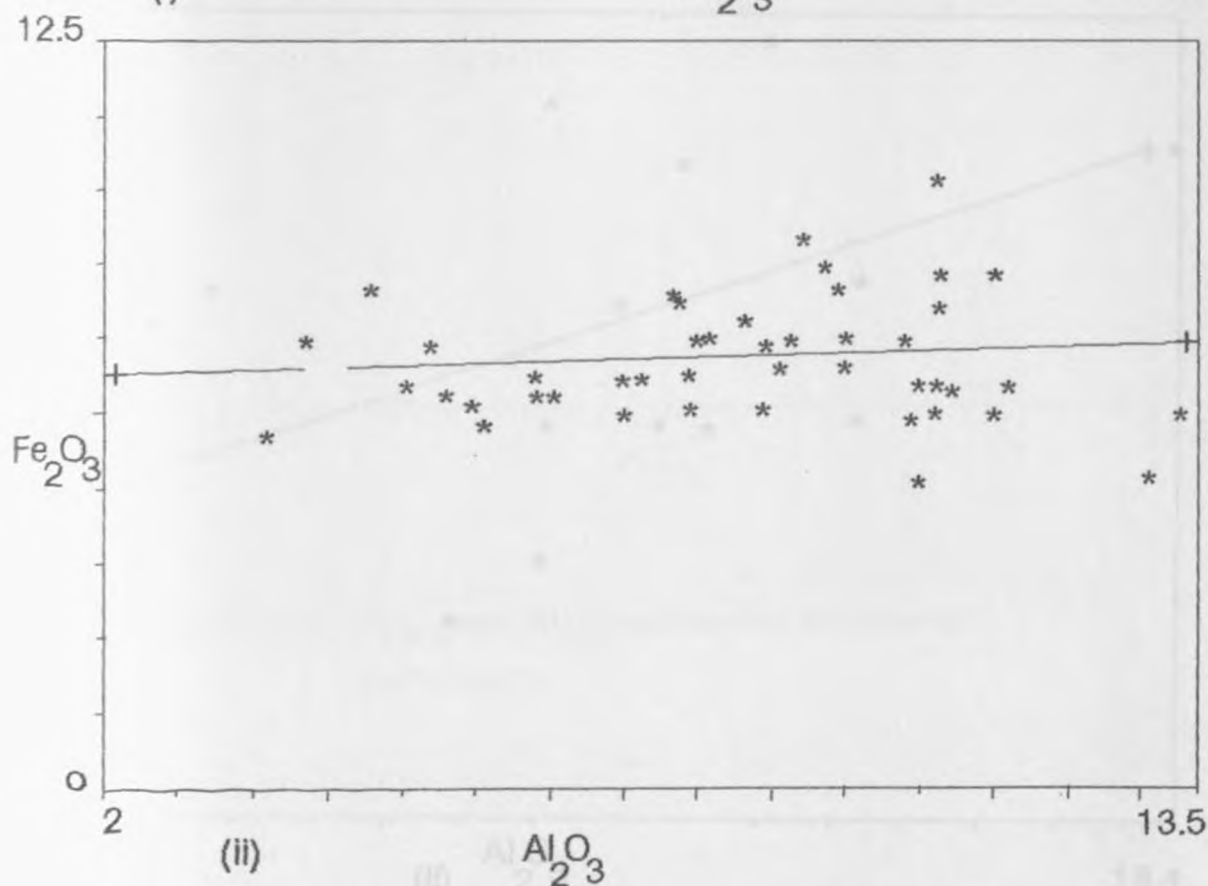
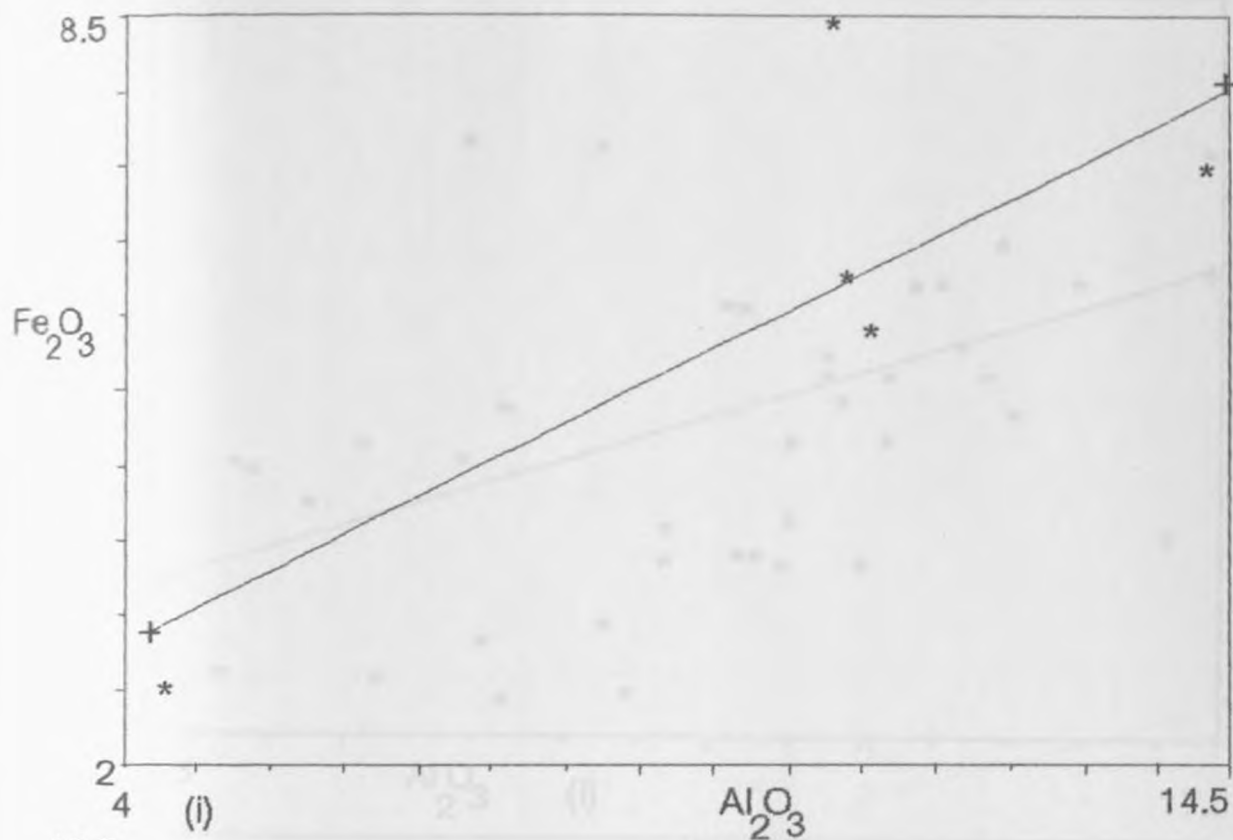


FIG.7 - 3A Fe_2O_3 and Al_2O_3 variation in sediments from (i) Soysambu and (ii) Kariandusi.

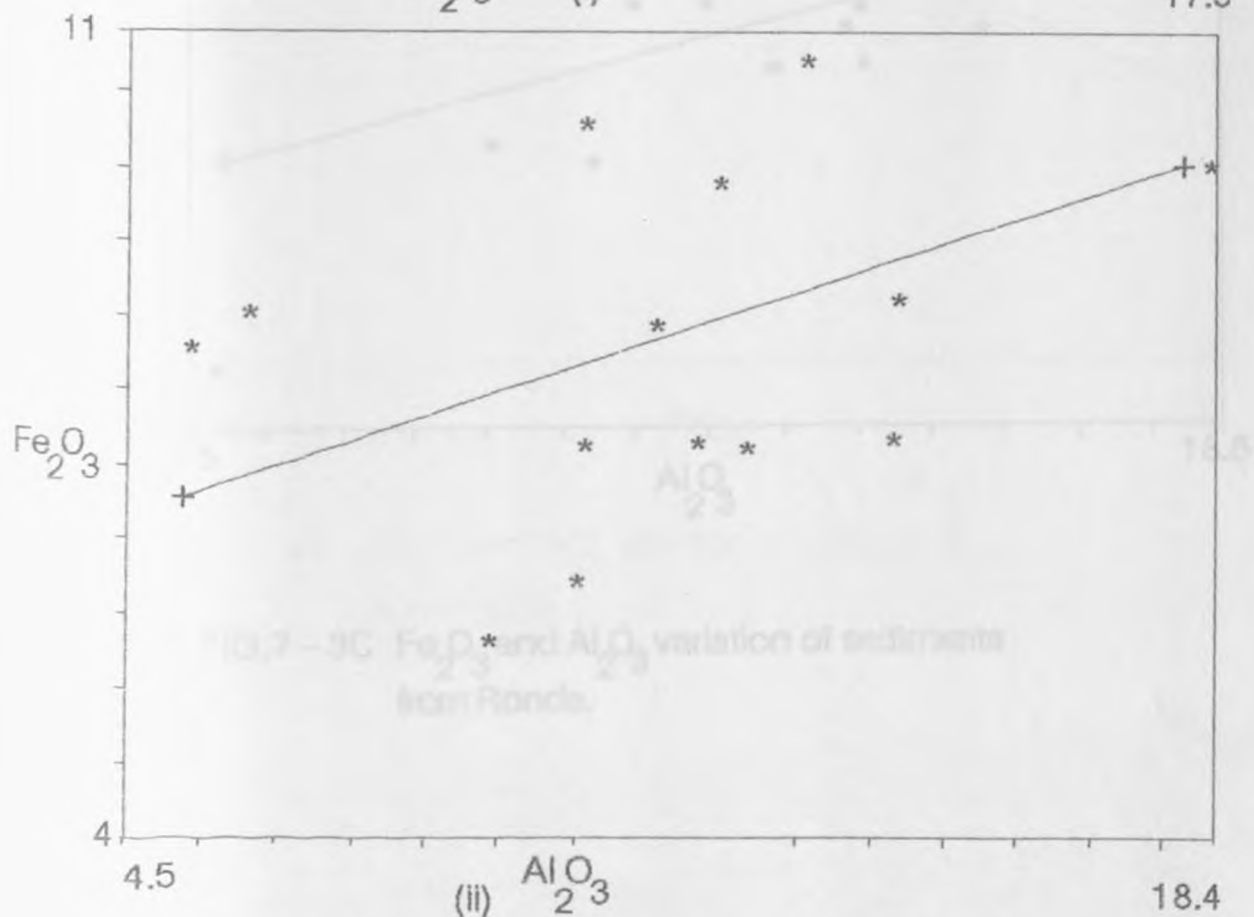
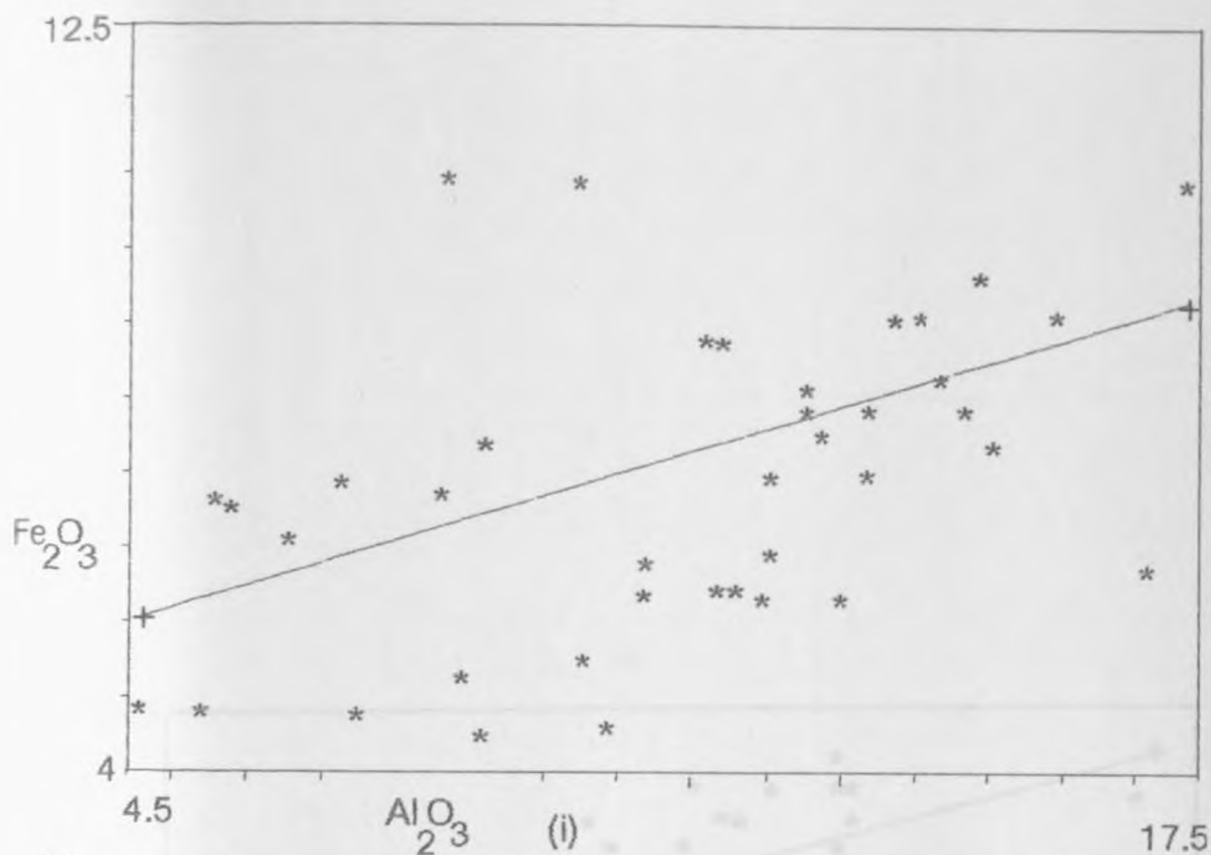


FIG. 7-3B Fe_2O_3 and Al_2O_3 variation in sediments from (i) Makalia and (ii) Enderit

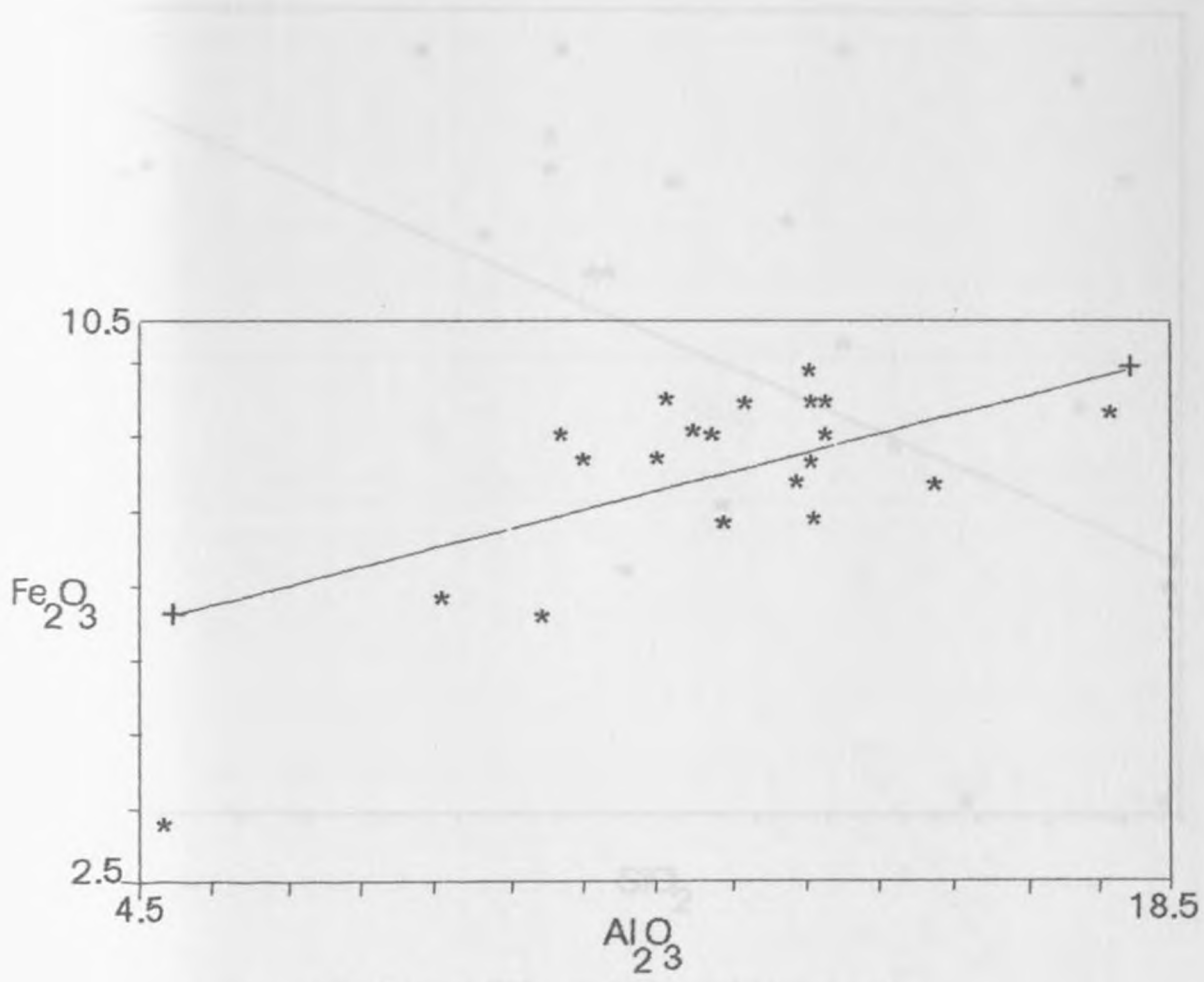


FIG.7 - 3C Fe_2O_3 and Al_2O_3 variation of sediments from Ronda.

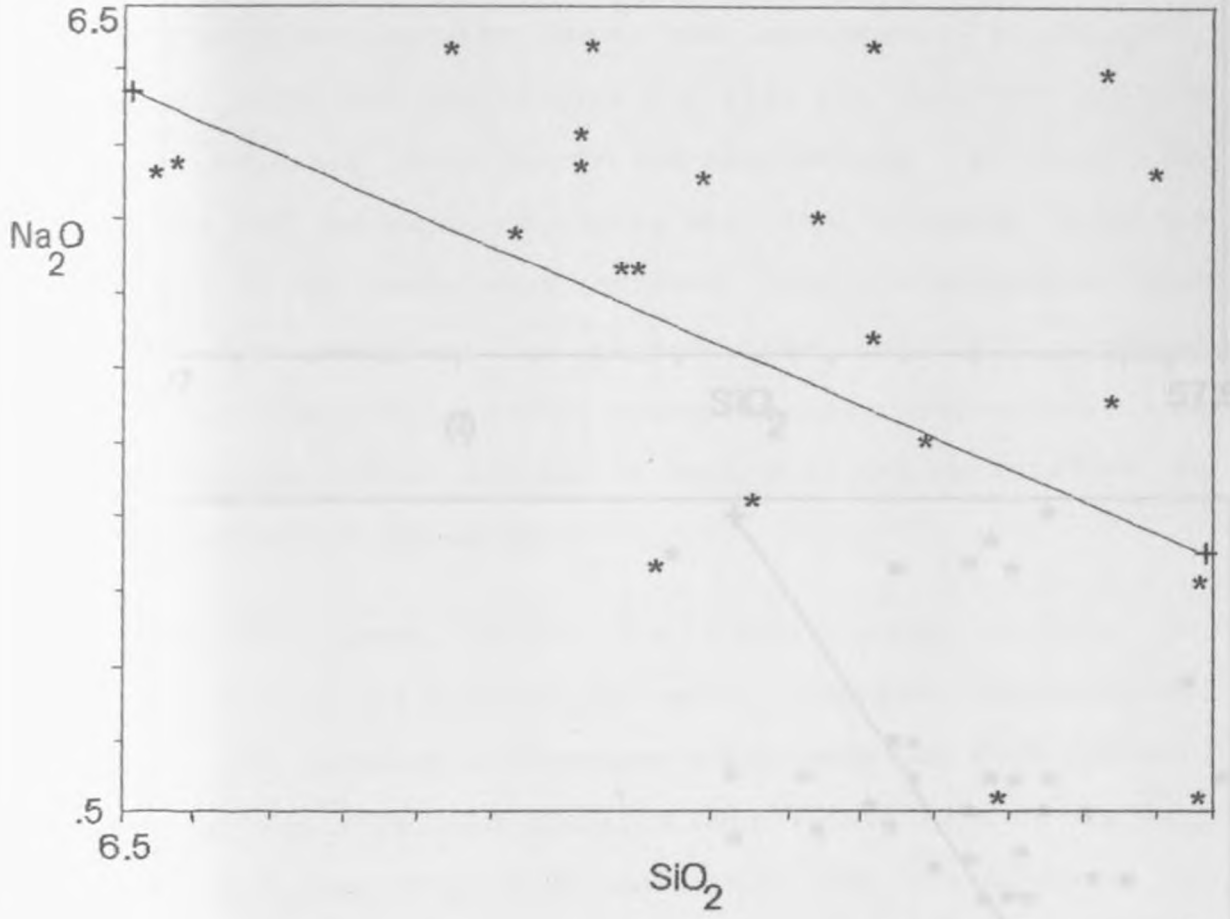


FIG. 7 - 4A Na₂O and SiO₂ variation of sediments from Ronda.

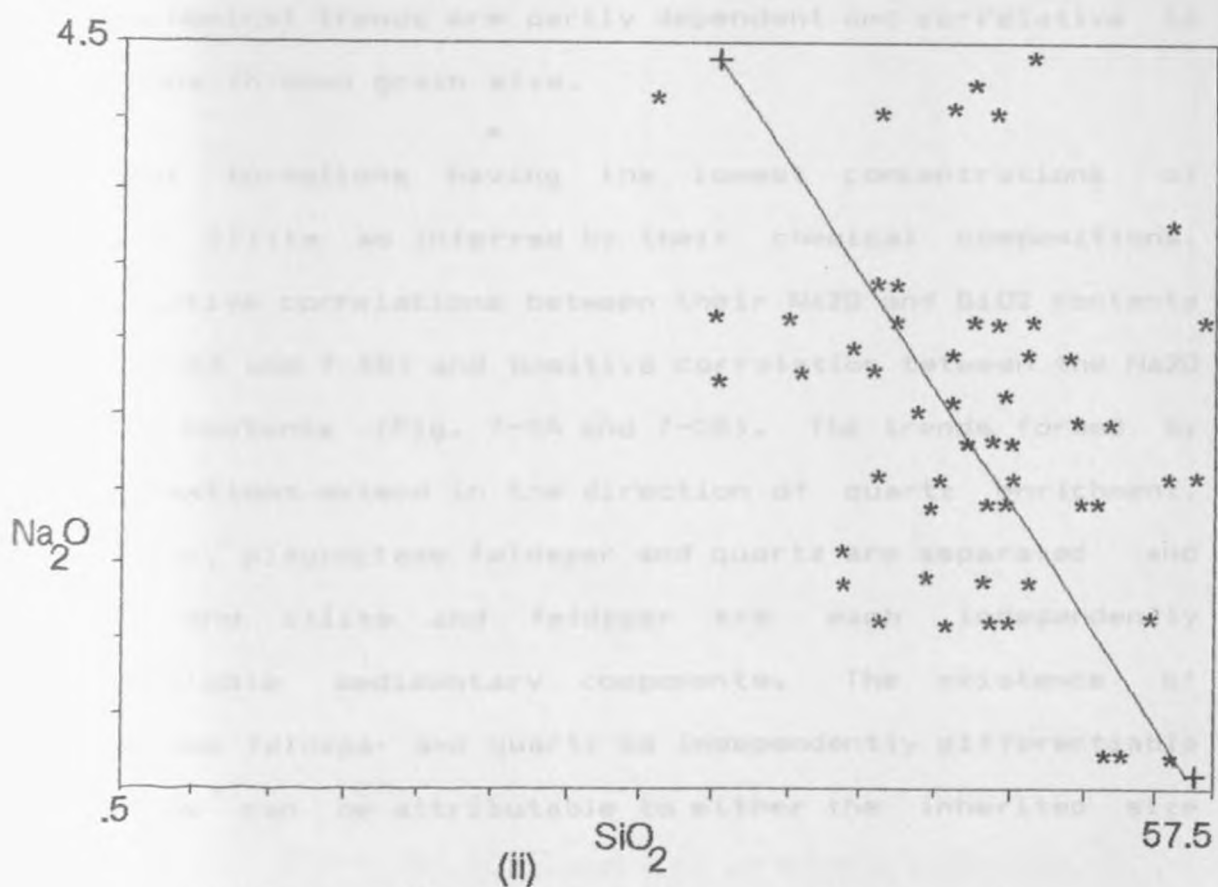
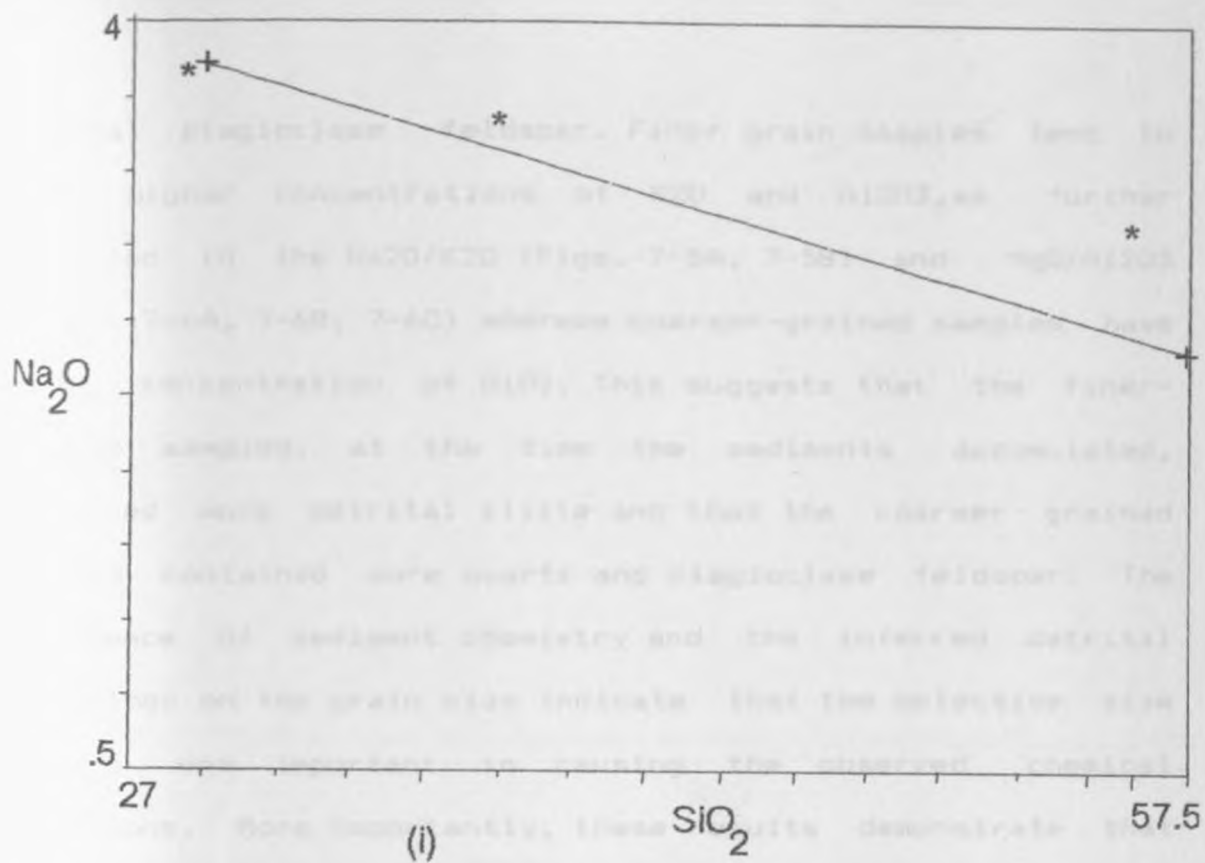


FIG. 7 - 4B Na_2O and SiO_2 variation of sediments from Soysambu and Kariandusi.

detrital plagioclase feldspar. Finer grain samples tend to have higher concentrations of K_2O and Al_2O_3 , as further evidenced in the Na_2O/K_2O (Figs. 7-5A, 7-5B) and MgO/Al_2O_3 (Figs. 7-6A, 7-6B, 7-6C) whereas coarser-grained samples have higher concentration of SiO_2 . This suggests that the finer-grained samples, at the time the sediments accumulated, contained more detrital illite and that the coarser grained samples contained more quartz and plagioclase feldspar. The dependence of sediment chemistry and the inferred detrital mineralogy on the grain size indicate that the selective size sorting was important in causing the observed chemical variations. More importantly, these results demonstrate that the geochemical trends are partly dependent and correlative to variations in mean grain size.

The four formations having the lowest concentrations of detrital illite as inferred by their chemical compositions, have negative correlations between their Na_2O and SiO_2 contents (Figs. 7-4A and 7-4B) and positive correlation between the Na_2O and K_2O contents (Fig. 7-5A and 7-5B). The trends formed by the formations extend in the direction of quartz enrichment. Apparently, plagioclase feldspar and quartz are separated and quartz and illite and feldspar are each independently differentiable sedimentary components. The existence of plagioclase feldspar and quartz as independently differentiable components can be attributable to either the inherited size

FIG 7-5A Na_2O and K_2O variation in sediments

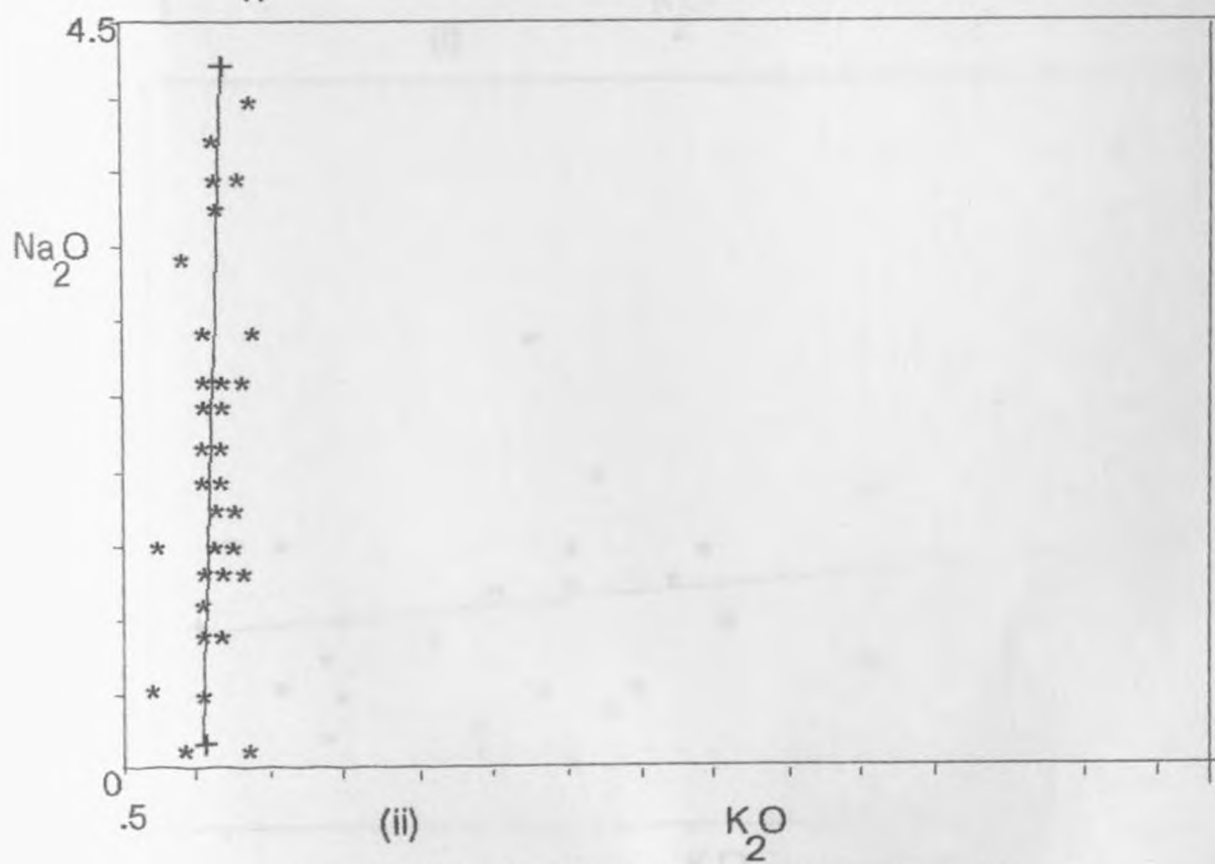
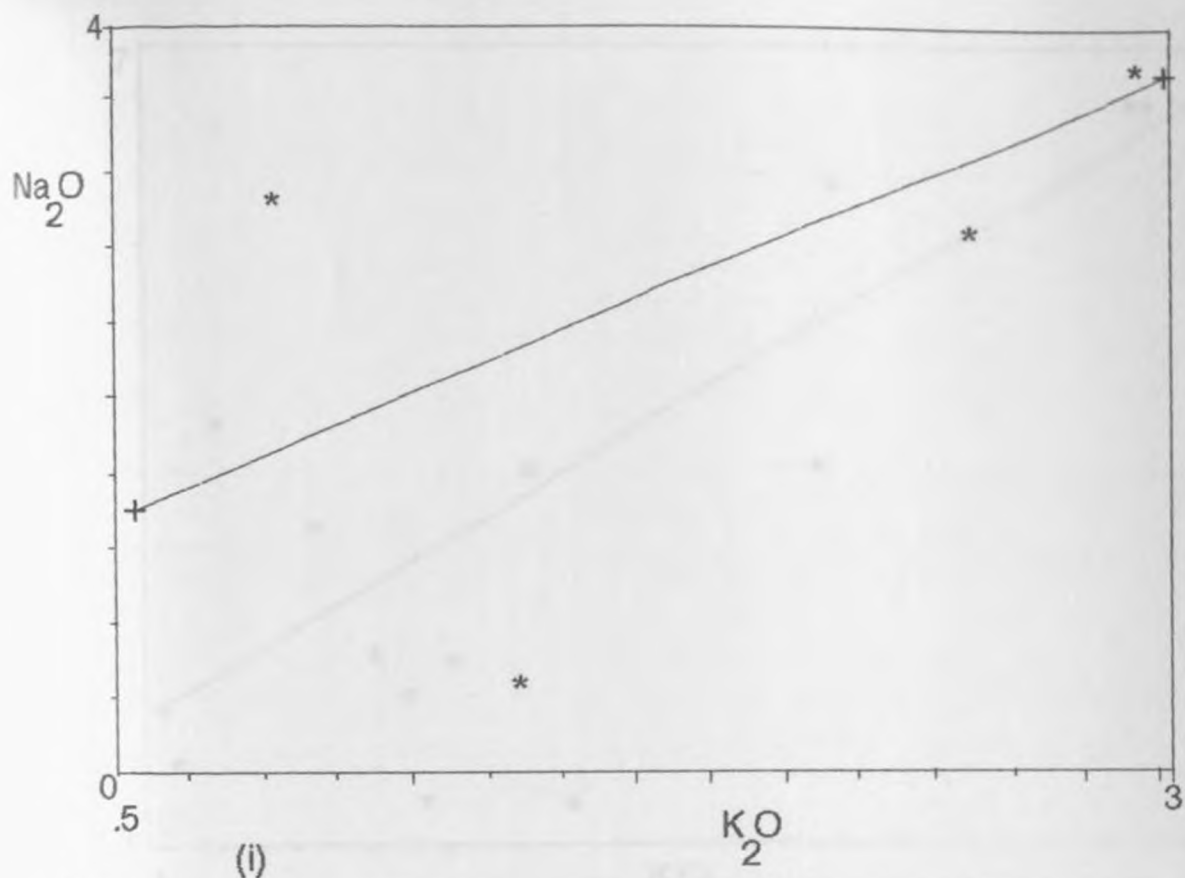


FIG 7 - 5A Na_2O and K_2O variation in sediments from (i) Soysambu and (ii) Kariandusi.

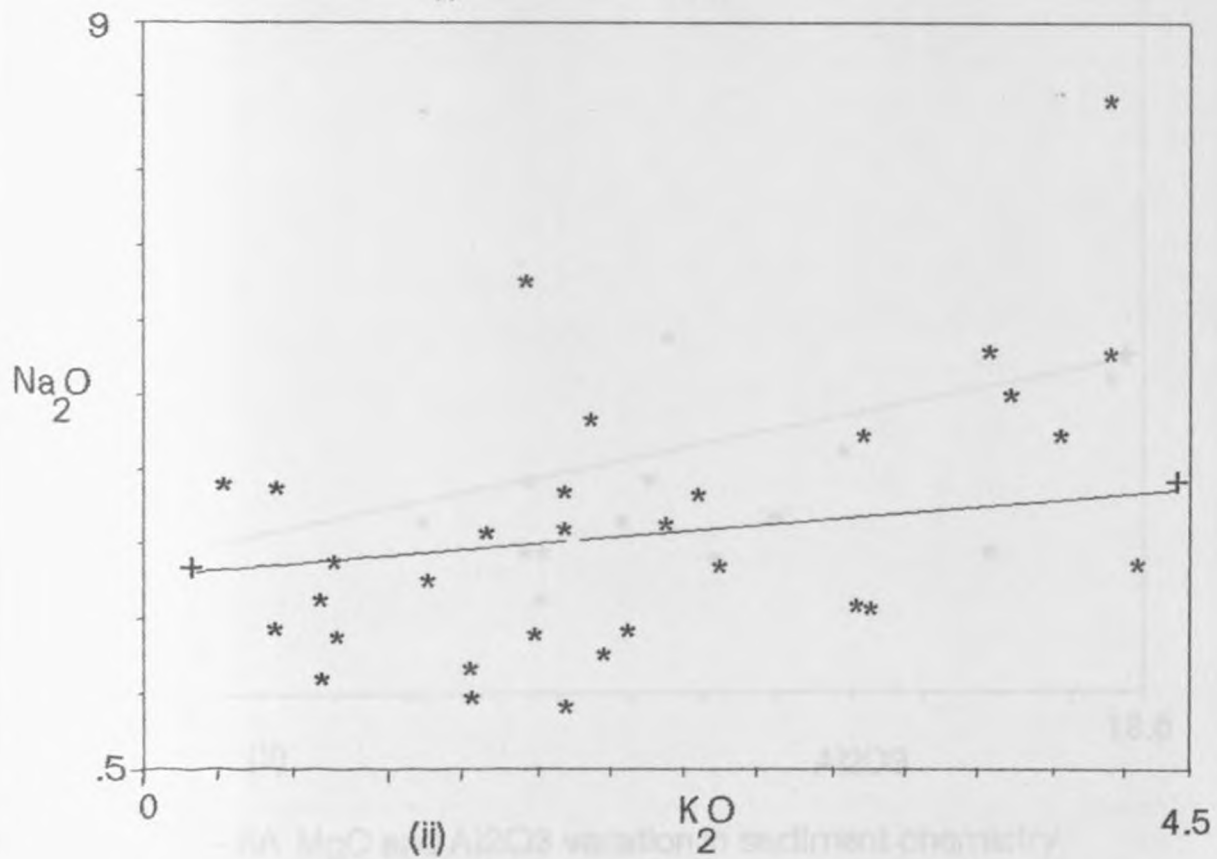
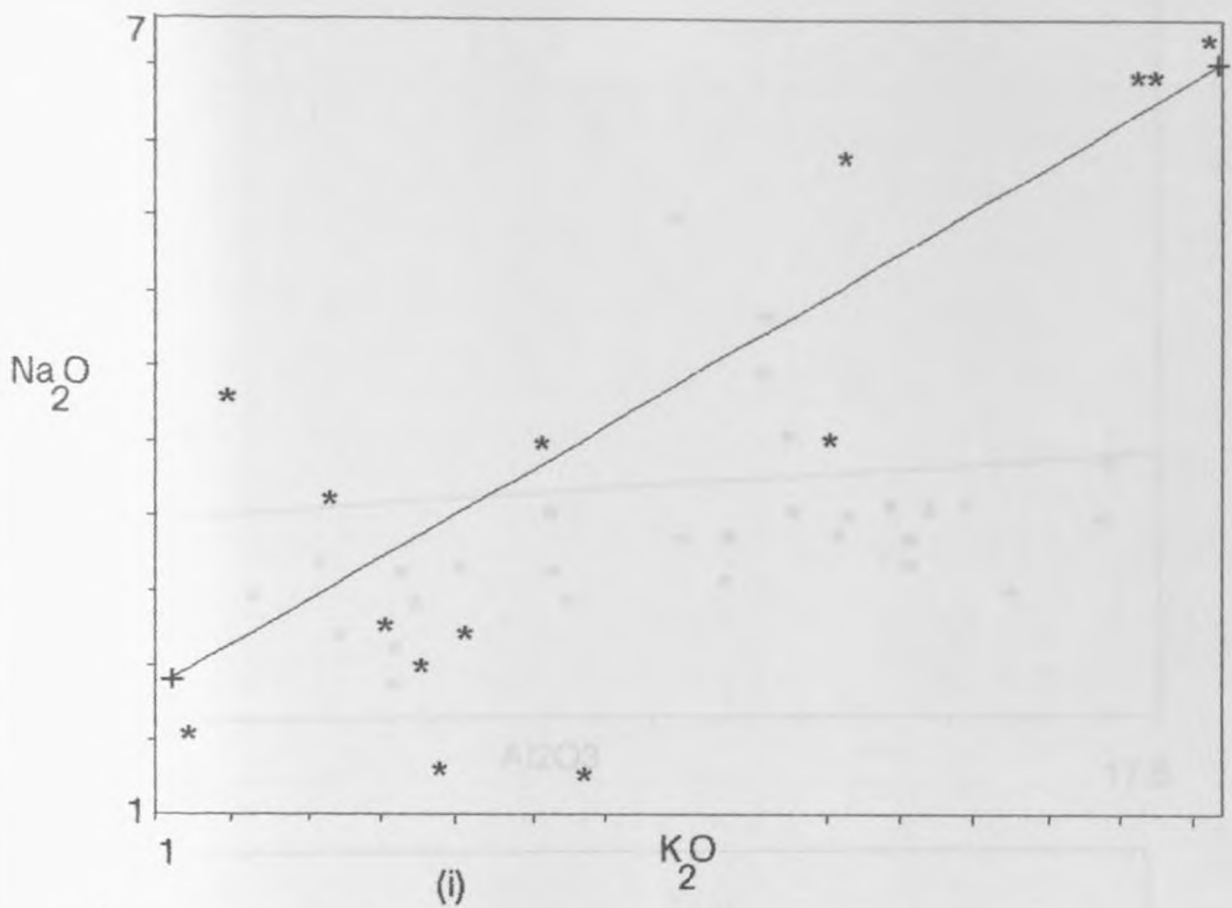


FIG. 7-5B Na_2O and K_2O variation in sediments from (i) Enderit and (ii) Makalia.

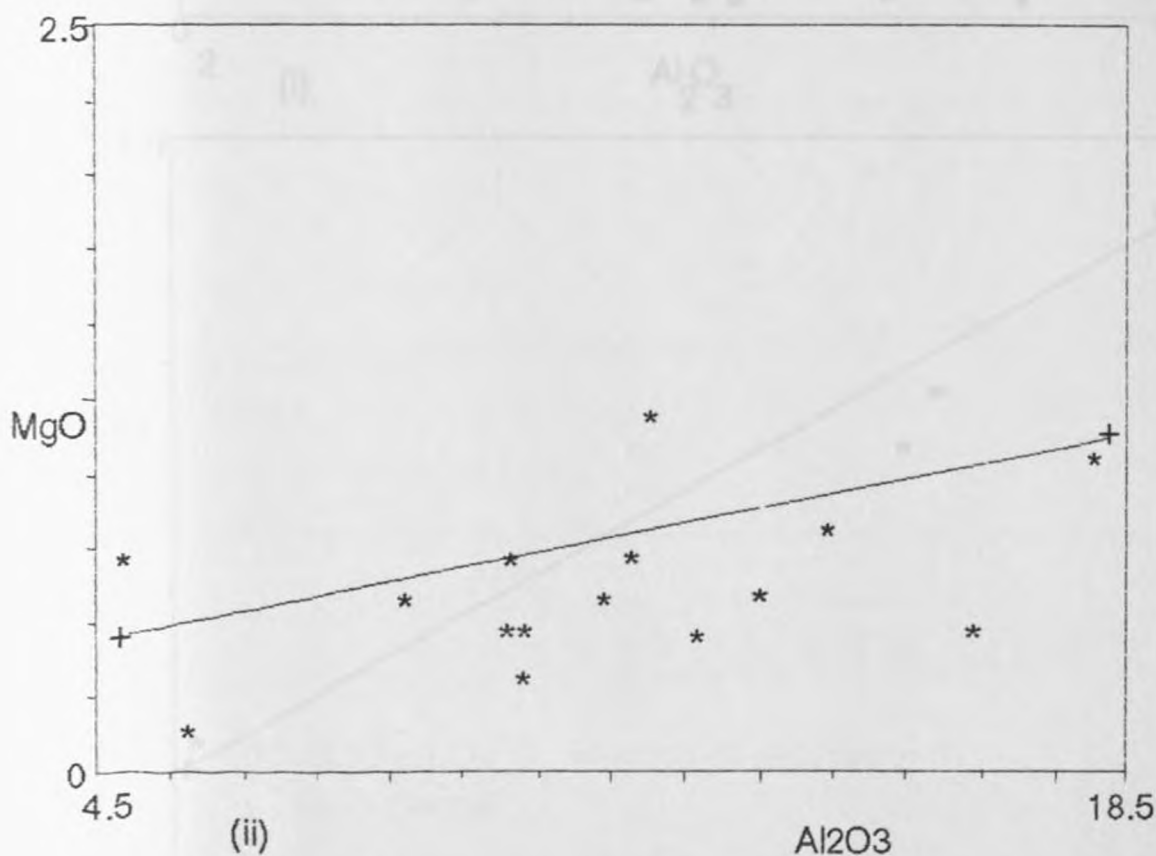
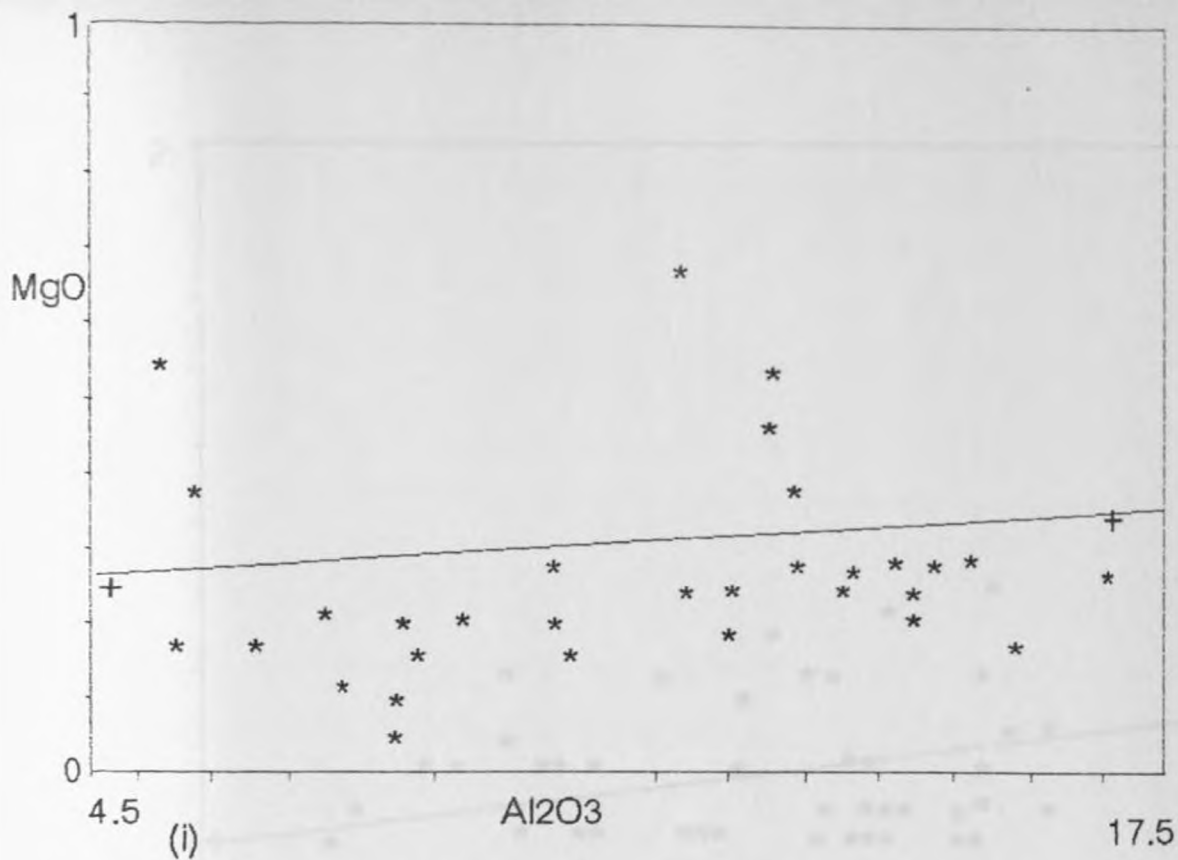


FIG.7 – 6A MgO and Al₂O₃ variation in sediment chemistry from (i) Makalia and (ii) Enderit

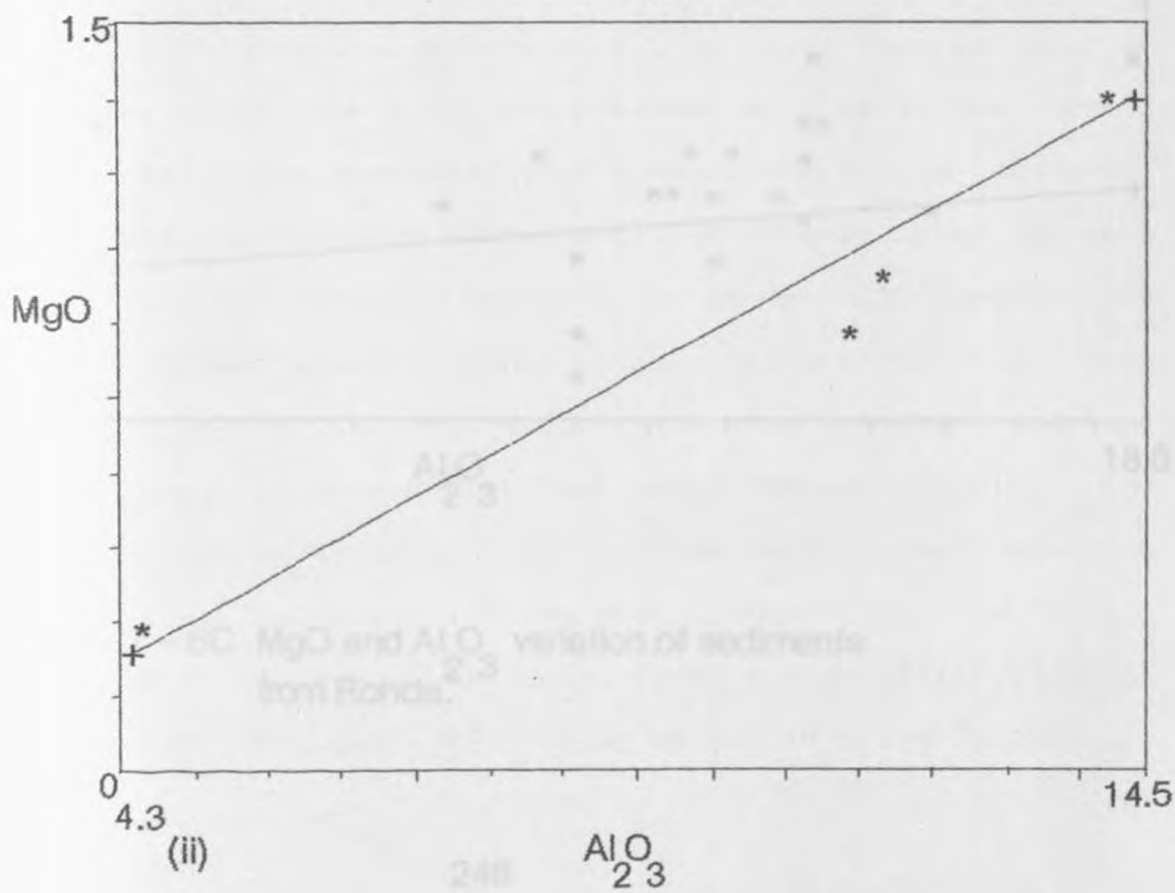
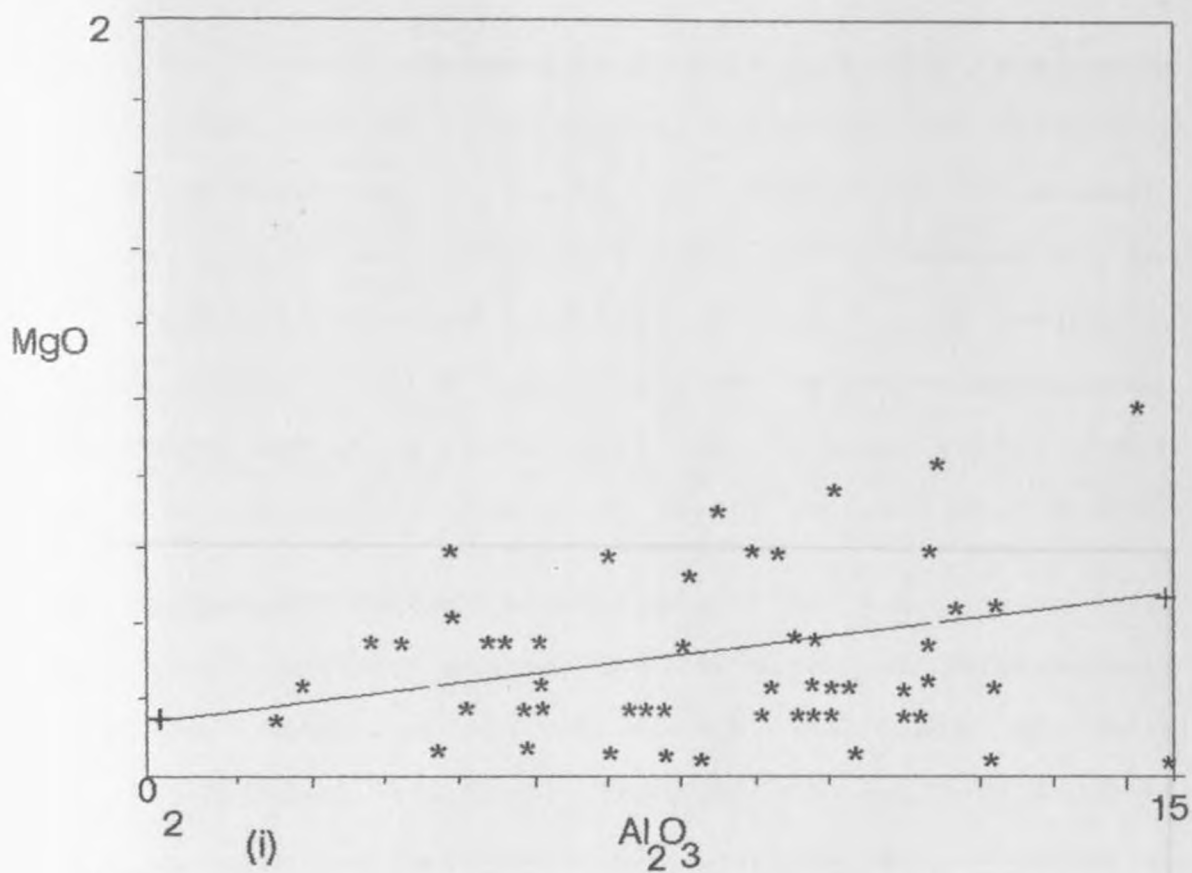


FIG. 7 - 6B MgO and Al_2O_3 variation in sediments from (i) Kariandusi and (ii) Soysambu

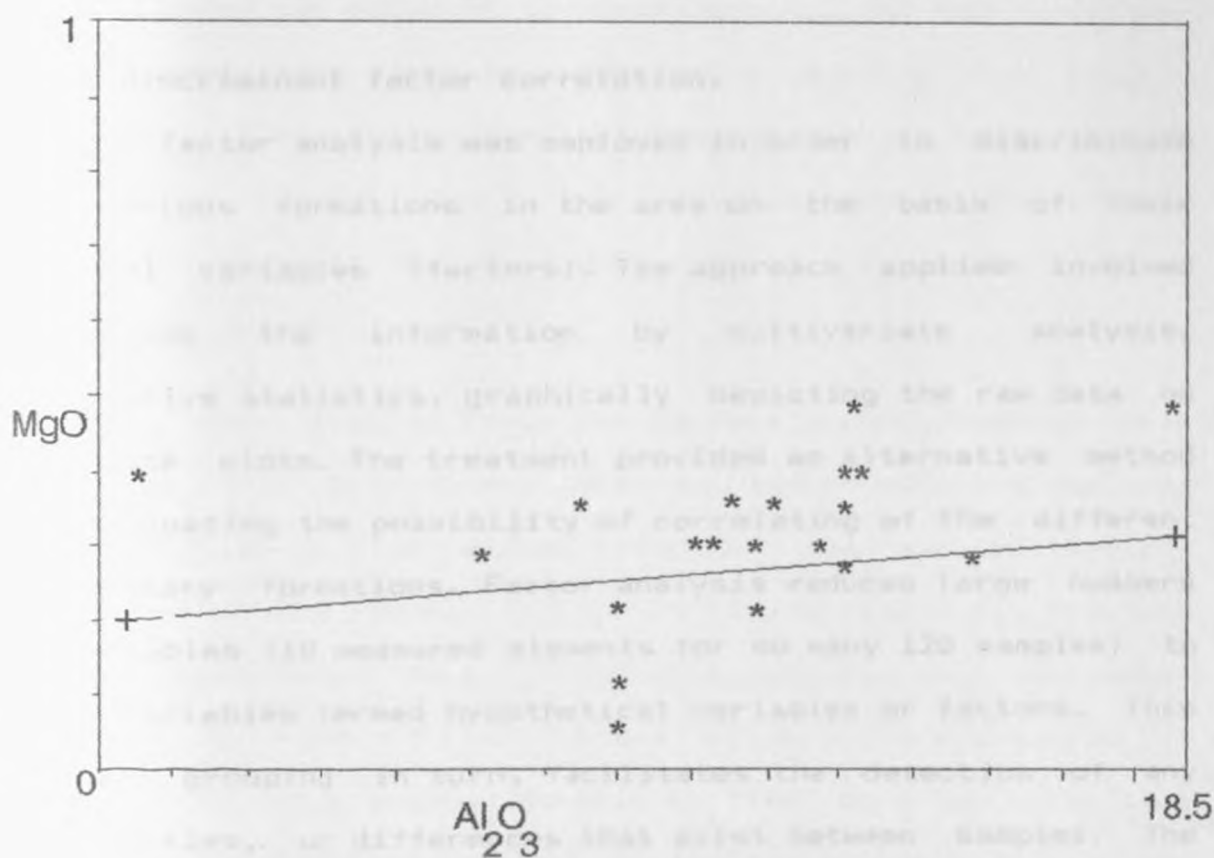


FIG. 7-6C MgO and Al₂O₃ variation of sediments from Ronda.

distribution from the sediment sources or selective comminution and enrichment in the finer grained fraction of relatively unstable feldspar as a result of weathering, transport, deposition and in situ abrasion (Odom, 1975). Because of the short transport and rapid deposition of these rift sediments there was probably little opportunity for selective comminution of feldspar, and it is likely that the feldspar/quartz ratio varied as a function of grain size in the sediment source area.

7.3.2 Discriminant factor correlation.

Q-mode factor analysis was employed in order to discriminate the various formations in the area on the basis of their chemical variables (factors). The approach applied involved processing the information by multivariate analysis, descriptive statistics, graphically depicting the raw data on bivariate plots. The treatment provided an alternative method of evaluating the possibility of correlating of the different sedimentary formations. Factor analysis reduces large numbers of variables (10 measured elements for so many 120 samples) to fewer variables termed hypothetical variables or factors. This smaller grouping in turn, facilitates the detection of any similarities, or differences that exist between samples. The use of factor analysis to interpret sedimentological data has been applied successfully by many authors and is widely recognised (Imbrie and Van Andel, 1964; Klovan 1966; Harbaugh and Merriam 1968; Beal 1970; Allen et al. 1971, 1972; Dal Cin

1976; Gardener et al. 1980; Miesch 1980; Anwr et al. 1984).

The Q-mode Fortran program used in this study was developed by Davis (1986). The application of this multivariate statistical techniques to sedimentary rocks have been reported by several authors (Imbrie 1963; Klovan 1966, 1975; and Drappean 1973, Fay personal communication). The program designed for flexible usage options was employed to normalised all the ten variables on a range from zero to one. After scaling the program normalises the data so that the sum squares in each row is unity. The Q-mode program was performed separately on the geochemical data of the Soysambu, Enderit, Kariandusi, Ronda Formations and Makalia Beds.

Rotated factor loading (from the varimax factor loading) were generated at 5% significant level and the results are depicted by tabulation to discriminate separately the four sedimentary formations in the Central Kenya Rift basins (Table 6). For this purpose normalised factor components were plotted on binary diagrams to test if this would allow discrimination of sediments of the different basins. As final step the normalised factor components were plotted on two components or bivariate diagrams to provide a basis of correlating the different sedimentary formations.

TABLE 6 DISCRIMINANT FACTOR ANALYSIS (F-TEST)

	1-27	28-43	44-61	62-115	116-120
	MAK	END	RON	KAR	SOY
MAK	-		<1%	<<1%	
END		-	5%	<<1%	
RON	1%	5%	-	<<1%	1%
KAR	<1%	<<1%	<<1%	-	<1%
SOY			5%	<<1%	-

F- test at 5% for significant difference between sediments of MAK = Makalia, END = Enderit, RON = Ronda, KAR = Kariandusi, SOY = Soy-sambu.

- Indistinct difference between samples
- | Insignificant difference between samples
- 1% Significant difference between samples
- <1% Highly significant difference between samples
- <<1% Very high significant difference between samples.

The binary diagrams show excellent differentiation of the Enderit Formation from the Kariandusi Formation (Figs. 7-8A, 7-8B). The geochemical discriminant score plots distinctly separate Enderit and Ronda Formations. The plots of the discriminant scores provide good to excellent discrimination between the different formations. The Enderit Formation and the Makalia Beds are however, undifferentiated by discriminant factor scores (Fig. 7-8C), thus the two constitute the Enderit Formation. The lack of discrimination of the Enderit and Makalia areas are possibly attributed to periodic basin overlap consequently grouping the facies from two distinct depositional environments. The detrital would then be subjected to reworking and redistribution from one environment to the other. This mixing of unconsolidated particles by fluvial and alluvial lacustrine on the delta plain is recorded by presence of reworked aggregates. Evidence for lateral reworking is also borne out by physical correlation of top tuff sequences of the Enderit and Makalia areas.

Of the four formations the Enderit and Ronda Formation bivariate diagrams show only moderate to extremely good discrimination (Fig. 7-8D). Although the two formations are geographically located on the extreme northern and southern parts of contemporary Lake Nakuru basin, the discriminant plots from the two formations are broadly on separate fields with minimal overlap between them.

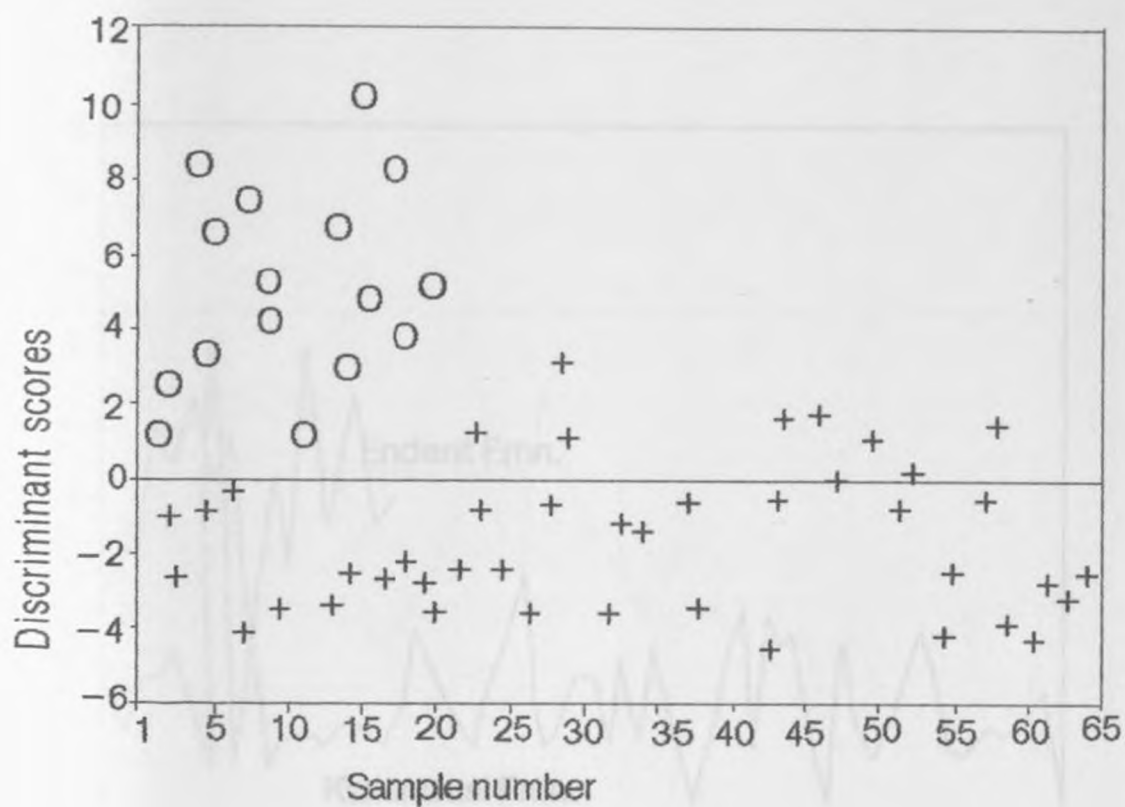


FIG. 7-8A Bivariate discriminant scores plot of Enderit Formation (O) Kariandusi Formation (+).

FIG. 7-8B Bivariate discriminant diagrams of Enderit vs Kariandusi Formations.

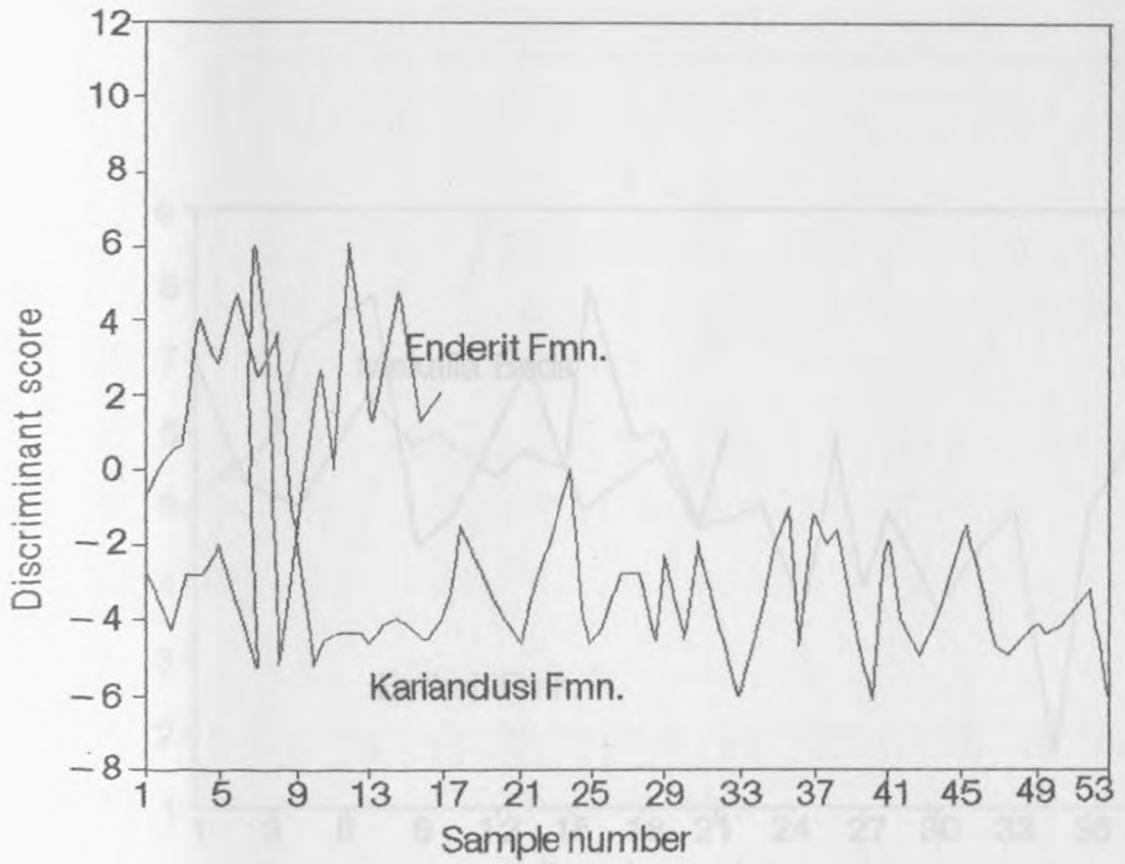


FIG. 7-8B Bivariate discriminant diagrams of Enderit vs Kariandusi Formations.

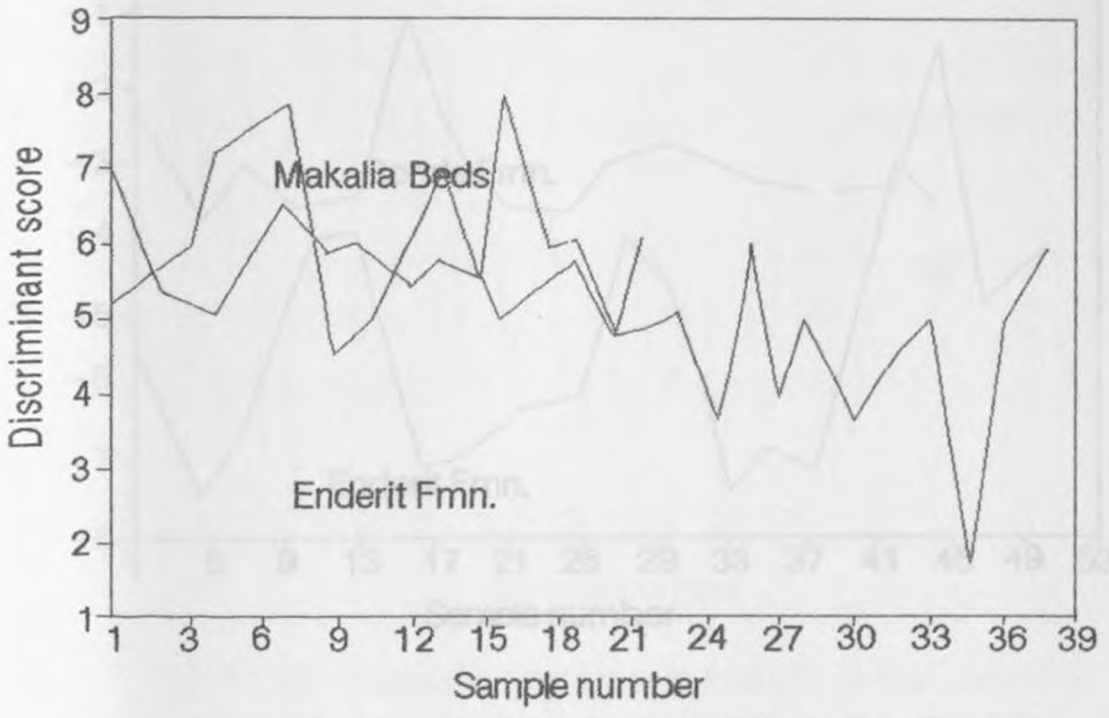


FIG 7-8C Bivariate discriminant diagrams of Enderit vs Makalia deposits.

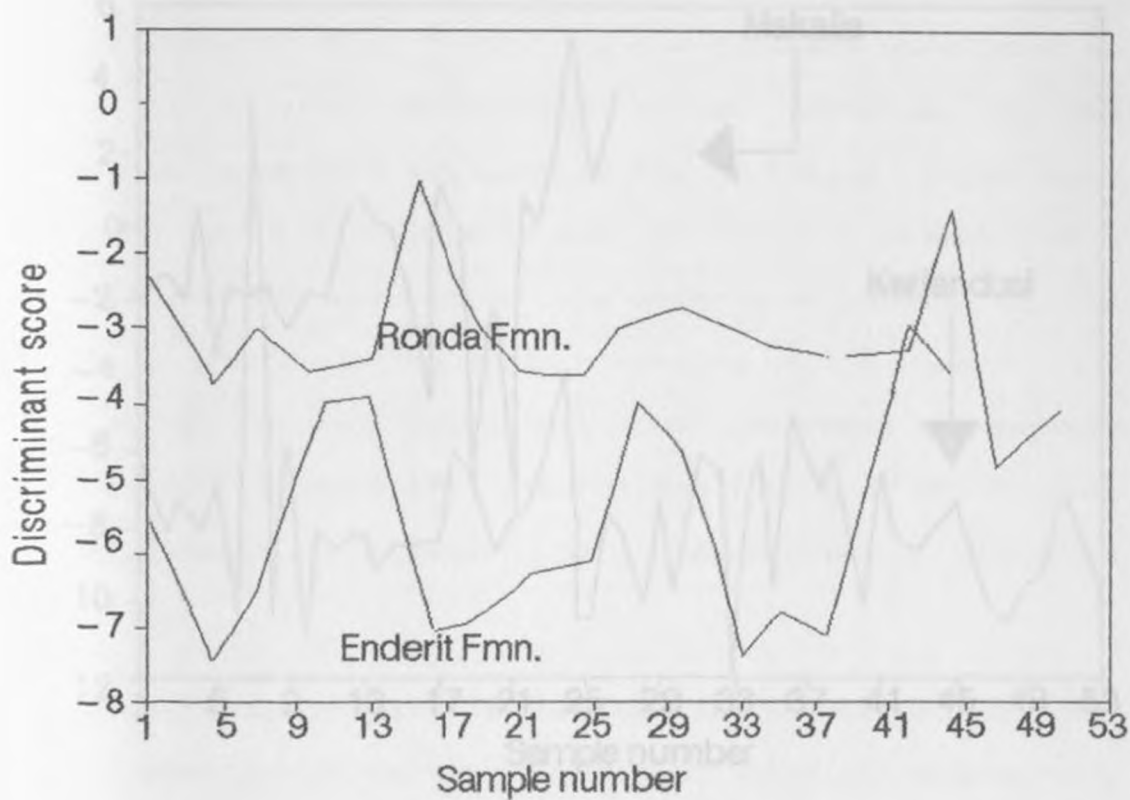


FIG. 7 – 8D Bivariate discriminant plots of Enderit vs Ronda Formations.

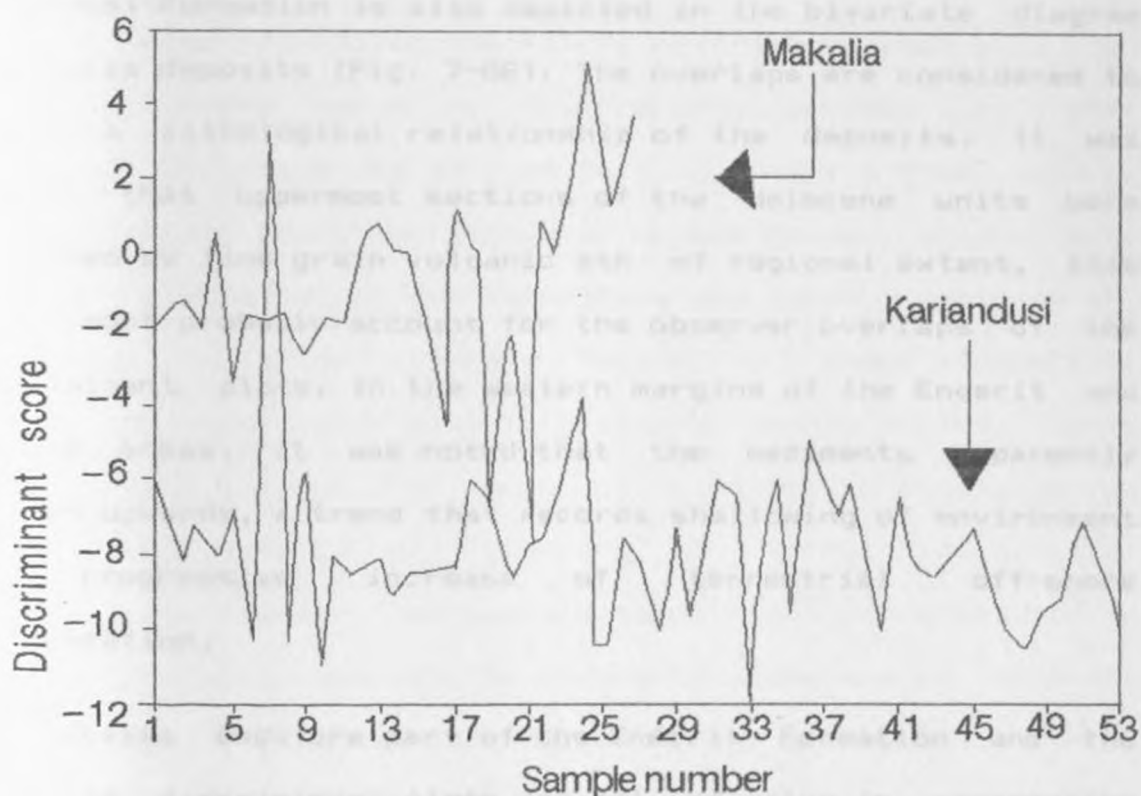


FIG. 7-8E Bivariate diagrams of Makalia vs Karaindusi Formations showing good discrimination of the deposits

The Enderit and Kariandusi Formations show good bivariate discriminant plots (Figs. 7-8A, 7-8B) segregating the two formations. Also noteworthy from the bivariate plot is a thin possibly wind blown ash extension from the Kariandusi Formation into the Enderit field. A similar extension from the Kariandusi Formation is also depicted in the bivariate diagram of Makalia deposits (Fig. 7-8E). The overlaps are considered to record a lithological relationship of the deposits. It was evident that uppermost sections of the Holocene units were dominated by fine grain volcanic ash of regional extent, this would most probably account for the observer overlaps of the discriminant plots. In the western margins of the Enderit and Makalia areas, it was noted that the sediments apparently coarsen upwards, a trend that records shallowing of environment and progressive increase of terrestrial off-shore sedimentation.

The Makalia Beds are part of the Enderit Formation and the bivariate discriminant plots are only of value in segregating the former from the Ronda, Soysambu and Kariandusi Formations (Figs. 7-8E and 7-8F). Although the discriminant plots and the geochemical fields of the formation very weakly coincide with those of the Kariandusi (Fig. 7-8E) and Ronda (Fig. 7-8F) Formations. However, examination of the field data and the geochemical results do not indicate an apparent single basin. Of the four formations, the Ronda Formation comprises the

highest mean value of aggregate pumice and extremely little diatomaceous beds. . The bivariate plots of geochemical combinations are only of fair characterisation (Fig. 7-8H). The bivariate plots of the formations are evidently distinct from those of the Kariandusi and show no overlap. The field occupied by the Ronda Formation are fairly restricted and only few bivariate plots serve to discriminate samples of this formations and these are only of fair to moderate good values: Soysambu versus Kariandusi; Enderit versus Ronda. Also of some value of discriminating the formations are plots combining the percentage of major elements. Samples of these formations plotted on major oxide bivariate diagram occupy varied fields and are more diverse. The above petrological characteristics record the effects of reworking of terrestrial-alluvial deposits by fluvial, eolian and lacustrine processes in a variety of environments. The bivariate plots are of moderate to good value for firmly discriminating the geochemical fields between the Makalia Beds versus Kariandusi Formation and the Ronda Formation versus Makalia Beds (Figs. 7-8E and 7-8F). However, field examination of the deposits from the point of view of their obvious lithology reveal no relationship among the formations. The non-existence of relationship or overlap features are interpreted as a record of unique tectonically controlled depocentres in separate areas of the rift.

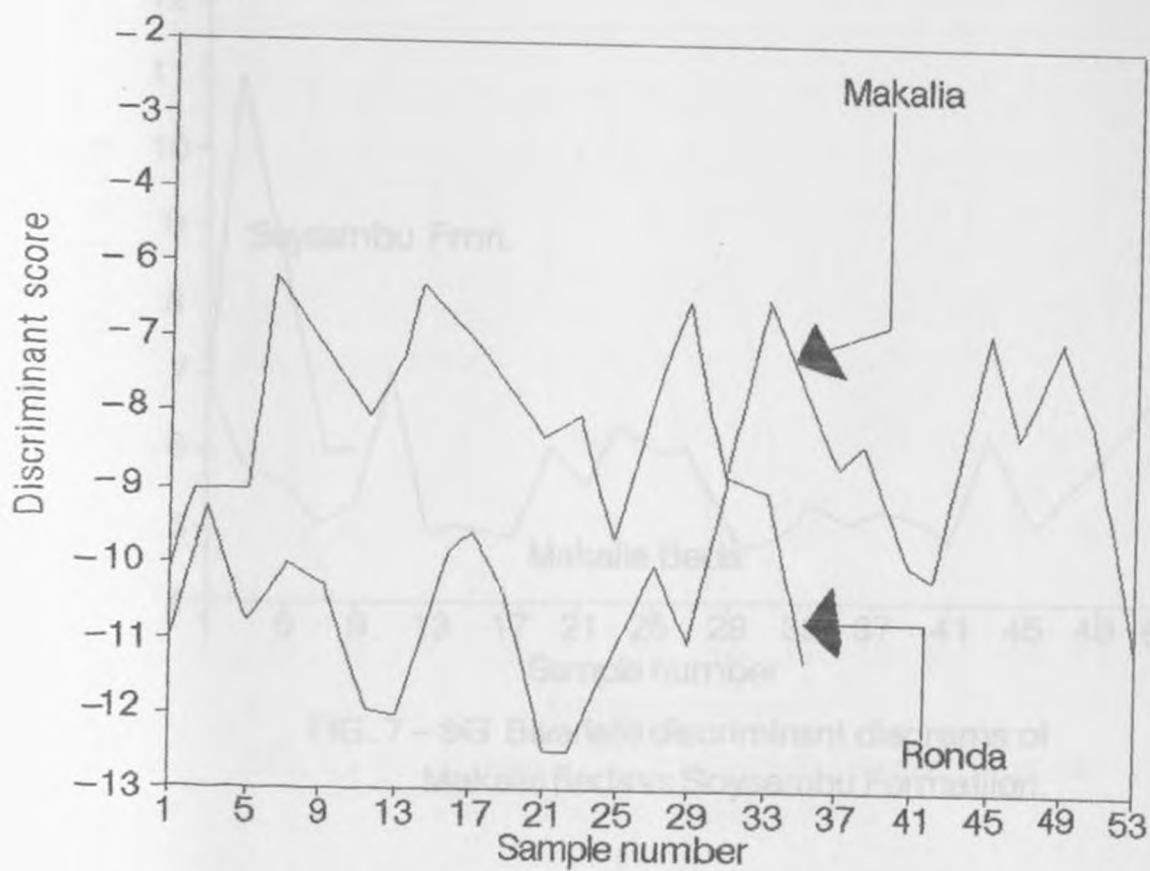


FIG. 7-8F Bivariate discriminant diagram of Makalia vs Ronda sediments.

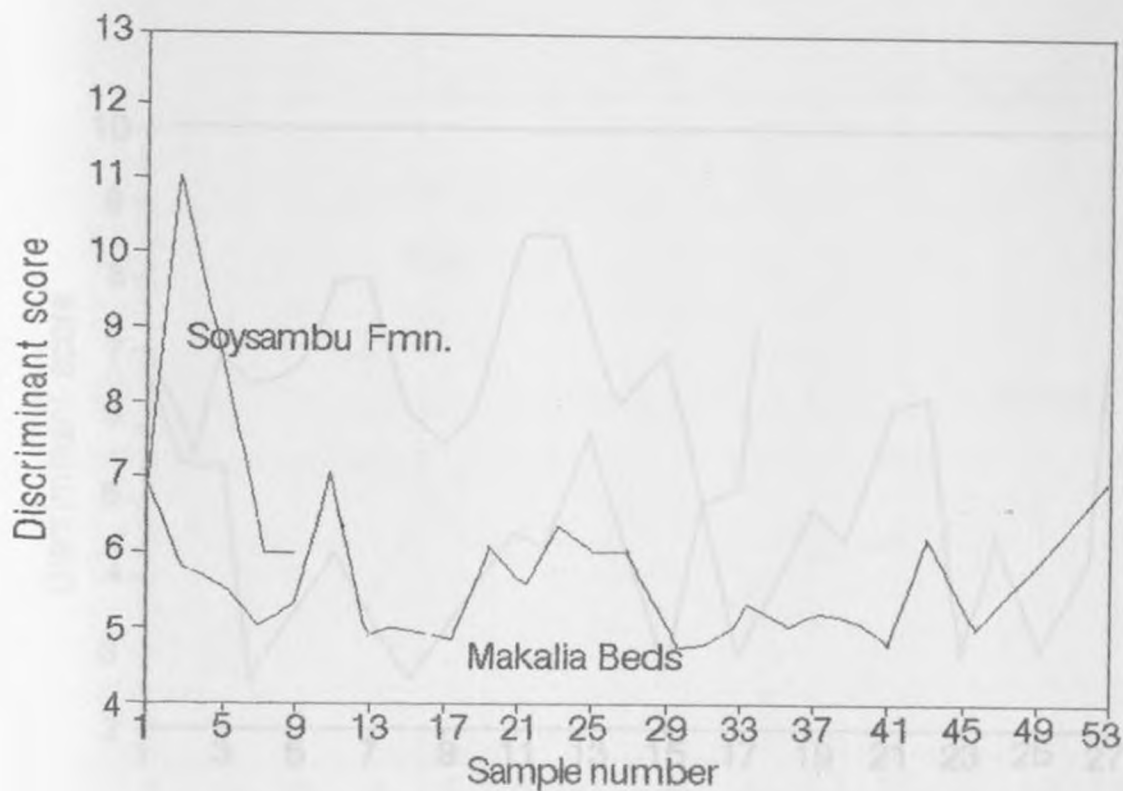


FIG. 7-8G Bivariate discriminant diagrams of Makalia Beds vs Soysambu Formation.

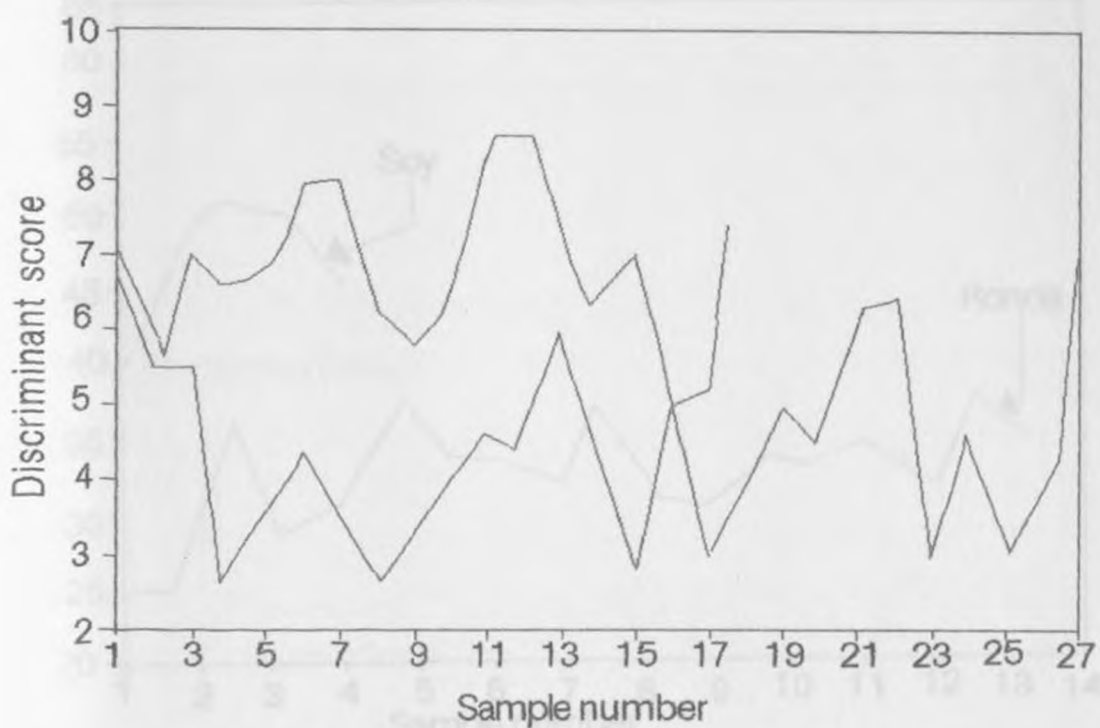


FIG. 7 – 8H Bivariate discriminant diagrams of Ronda Formation vs Makalia Beds.

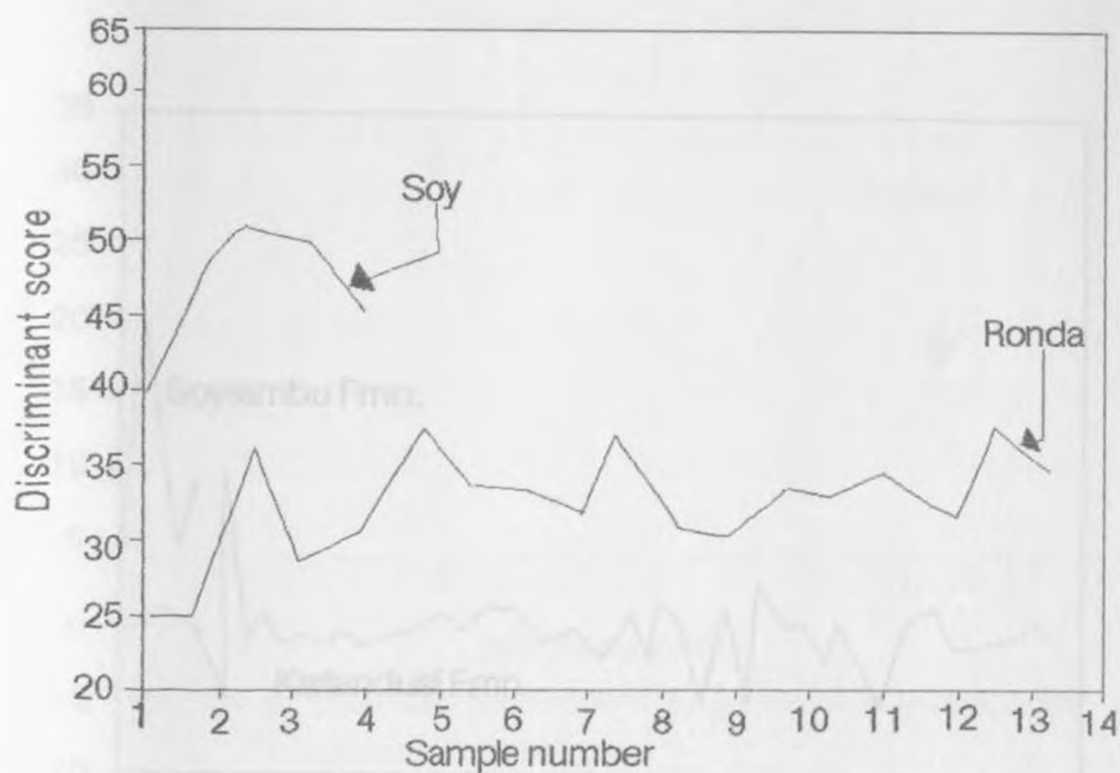


FIG 7 – 8J Bivariate discriminant diagrams of Soysambu vs Ronda Formations.

FIG. 7 – 8K Bivariate discriminant diagram of Soysambu vs Kadandusi Formations.

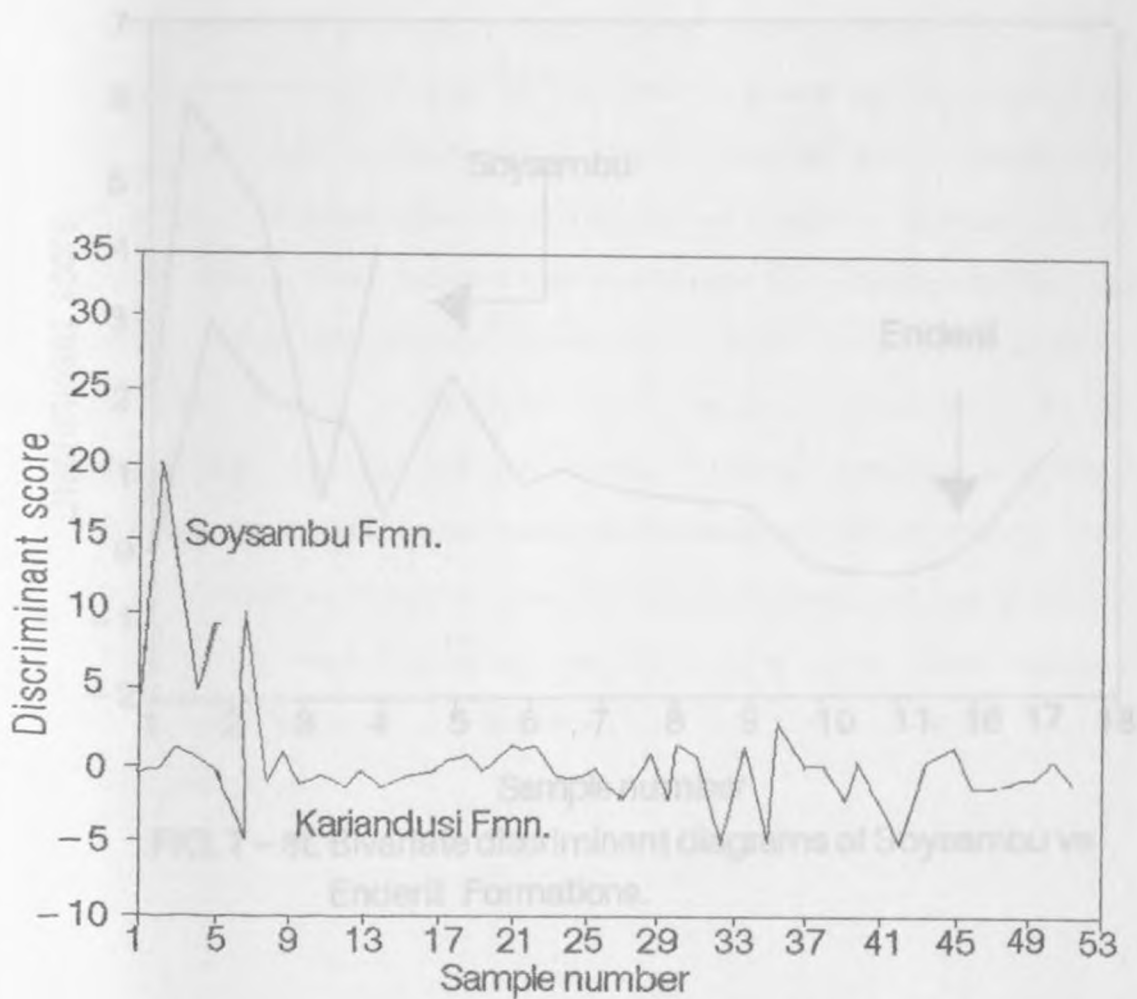


FIG. 7 - 8K Bivariate discriminant diagram of Soysambu vs Kariandusi Formations.

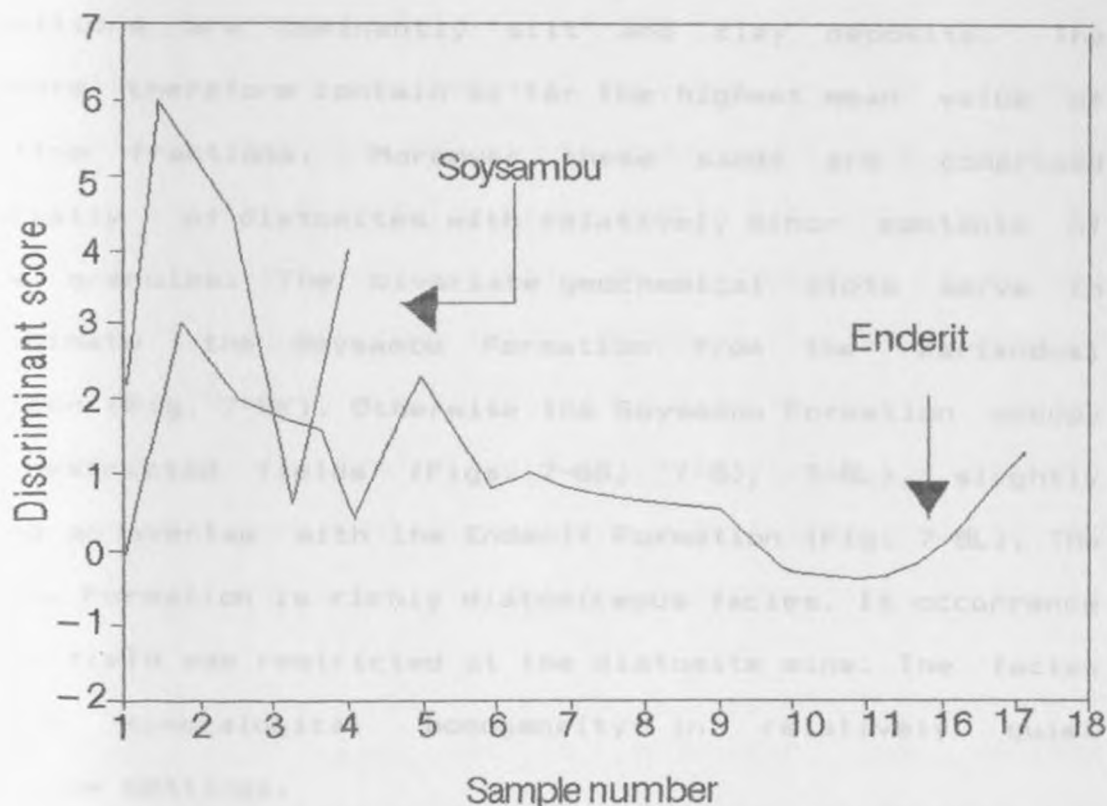


FIG. 7 - 8L Bivariate discriminant diagrams of Soysambu vs Enderit Formations.

Fields occupied by the geochemical variables of the Soysambu Formation are more restricted on their plots against the Makalia Beds (Fig. 7-8G) Ronda Formation (Fig. 7-8J) and the Kariandusi Formation (Fig. 7-8K). Both the Soysambu and Kariandusi Formations are similar in lithology and their compositions are dominantly silt and clay deposits. The sediments therefore contain by far the highest mean value of the fine fractions. Moreover these sands are comprised essentially of diatomites with relatively minor contents of pumice granules. The bivariate geochemical plots serve to discriminate the Soysambu Formation from the Kariandusi Formation (Fig. 7-8K). Otherwise the Soysambu Formation occupy very restricted fields (Figs. 7-8G, 7-8J, 7-8L), slightly showing an overlap with the Enderit Formation (Fig. 7-8L). The Soysambu Formation is richly diatomaceous facies. Its occurrence in the field was restricted at the diatomite mine. The facies indicate mineralogical homogeneity in relatively quiet lacustrine settings.

CHAPTER 8

SUMMARY AND CONCLUSIONS.

8.1 Lithostratigraphic correlations .

The primary objective of this research was to work out the lithostratigraphy of sedimentary outcrops in the Nakuru, Elmentaita and Naivasha Basins. This was relatively easy at Kariandusi in the Elmentaita Basin due to the occurrence of some fairly continuous sections of diatomaceous beds and mineralogically distinctive tuffs. Although the stratigraphic sequences have been more difficult to establish in the complex fluvial sediments of Enderit and Makalia Rivers in the southern edge of the Nakuru Basin, it has been almost impossible in the Naivasha basin where natural surface outcrops are virtually absent.

The second major goal was to establish the various depositional environments from the associated lithofacies in the Nakuru, Elmentaita and Naivasha Basins. This was based on the premise that the rift sediments in the area were primarily lacustrine in origin which, formed in tectonically defined related sedimentary basins. The study assumed that this part of the rift offered possibilities for a regional lithostratigraphical correlation and environmental interpretation advanced by Leakey's, Solomon's and Nilsson's investigations which established the region climatic change based

chronology for the area (Leakey, 1956). The author's findings established that the sedimentary formations represent a wide variety of scattered depositional environments. Both physical correlation and environmental interpretation remains localised in well exposed sections. However, the geochemical correlation of tuffs and associated sediments may offer an alternative potential for a wider and regional correlation of rift sediments. Limited exposures within and outside the basins particularly in the Naivasha Basin proved to be the principal obstacle to a fully satisfactory inter-basinal correlation.

The Enderit and Makalia sequences are stratigraphically and geochemically established to represent a single formation, named the Enderit Formation. This formation was possibly contemporaneous but not part of the transgressive Ronda Formation in the north-western part of lake Nakuru. The sections at Kariandusi are correlated within their lower and upper members. The sequence in sections at both Kariandusi and Soysambu indicate a trend towards more deeper water, followed however, by a fluctuating shallower lake level. These correlate well within their individual depocentres in the Kariandusi and Soysambu Formations. The increase towards the top of volcanic material appears fairly similar in the two areas. At Ronda there is substantial increase of tephra in the content of the lower sediments which become finer as a fairly shallow, saline basin with fluctuating margin playa environment

develops to the east. The correlations as presented in the stratigraphic sections may have limitations but are considered fairly logical as supported by further geochemical data.

B.2 Major element variation trends.

Whereas physical lateral field correlation between basins are not always possible, this study has demonstrated that suites of siliciclastic rock commonly show geochemical variations that result from sediment sorting processes. The variations in unlithified Pleistocene sediments, are vital to sedimentologists for the understanding clastic sedimentary processes, and are considered to be due to mineral distribution formed during and shortly after deposition. The chemical variation trends are useful means of depicting possible relationships and can be frequently modelled as mixtures of independently differentiable sedimentary components. However, the differentiation and the consequent separation of constituent elements may not occur in all sedimentary systems. For example the suite of sediments derived from immature volcanic terrains may not contain fine grained phyllosilicates and will have different chemical distributions. Clastic suites with abundant phyllosilicates and other potentially differentiable sedimentary minerals may also lack coherent chemical trends if differentiation does not occur during sediment transport and deposition. The absence of K- feldspar

as an independently differentiable mineral for instance, simply reflect the scarcity of detrital K-feldspar in the terrains from which many of the sediments are derived.

The deposits of the Nakuru, Elmentaita and Naivasha Basins are purely volcanic sediment and do not contain detrital mica. The absence of illite as a differentiable sedimentary component is demonstrated by the low values of K₂O and poor correlation of K₂O-Al₂O₃ trend (Fig. 6-1A, 6-1B). Significantly the concentration of K₂O remain low despite the abundant presence of potentially reactive volcanic debris. This suggests that the diffusion of K⁺ has little effect on the bulk composition of an accumulating sediment.

8.2.1 Q-mode analyses.

The Q-mode analysis shown on the graphic plots identify and discriminate the Kariandusi, Soysambu, Enderit and Ronda Formations as separate and distinct sedimentary entities. However, evaluation of all the geochemical data presented graphically on bivariate plots show that the variables are not of equal value for discriminating lithofacies associated with the various formations. In any case factorial Q-mode analyses focuses on some of the more significant petrological attributes. While this treatment of data mask some of the significant variables, it nevertheless provides a means for adequate discrimination of the four formations. The results

broadly concur with the more visually obvious petrological characters (including sedimentary structures, textures and overall lithology) that showed marked differences existing between the formations. The graphic treatment of the raw data as a whole allows us to relate the late Pleistocene and Holocene facies for purposes of stratigraphic correlation in the study area. Correlation of sediments between sections can also be achieved as shown between Enderit and Makalia where field data support the laboratory results, i.e. tuffs in the two separate areas are correlated on the basis of lithology and geochemical composition. A correlation of sections based on geochemical components as well as major or most obvious feature including sedimentary structures, gross texture, colour and lithology is potentially useful as basin analytical tools in the rift sedimentology.

8.3 Depositional systems

The suites of facies in the Central Kenya Rift valley clearly indicate deposition in lacustrine and non-lacustrine systems. At Kariandusi in the Elmentaita Basin, occur excellent exposures of lacustrine strata that were deposited on a faulted trachyte. This lacustrine complex is probably equivalent to the Soysambu Formation at Soysambu diatomite mine. Locally the Formation onlap underlying coarse fanglomerate on the western edge of the bounding fault scarp. The diatomite beds and equivalent fine grained deposits support the interpretation of

...in the south of water, but it is mainly controlled
a lacustrine origin. The distribution and association of the
facies suggest that they varied considerably with time and
geographical location on the rift floor. On the basis of
lithofacies separate depocentres have been distinguished in the
Nakuru, Elmentaita and Naivasha Basins. The general environment
of deposition from these sediments reflect fairly shallow,
alkaline lake with some sediments being deposited in higher
energy near-shore regimes, or shallow hypersaline playas.

The Kariandusi diatomite mine revealed extensive prograding
fluvial lacustrine complex, strata predominantly composed of
diatomite and pumice sands. Exposures of the upper portion
sections in areas around Enderit contain pumice ash facies that
may correlate to the Makalia in the north-west. There is
conclusive evidence of both alluvial and fluvial deposition.
The composition of the sediments varies from lithic pyroclastic
material in matrix of calcite or limonite to pyroclastics
deposited in similar matrix. The matrix composition was
presumably controlled by the pH of the lake, although this
could have been influenced by an influx of magnetite dust or
volcanic ash. The composition of the minerals seen in thin
section, on the other hand indicate primarily volcanogenic
origin. Thus, a change in the percentage of volcanic rocks in a
sample indicates a change in the lithic pyroclastic material
being spewn out. The composition of the sediments may depend to

some degree on the depth of water, but it is mainly controlled by the type of pyroclastic material.

Eolian sediments have been found to occur widely in the sequence and are emphasised in environmental interpretations. Most common are the tuffs redeposited by wind and modern eolian sedimentation of volcanic ash in the region. In general, volcanic ash occur in association of fairly shallow fluctuating lake sediments. The pyroclastic lithic tuffs are stratified and often intercalated with lacustrine diatomites in the sections. A chert bed precipitated to the south of Kariandusi in section 17, indicate that the lake was fairly saline. The water deepens at the Kariandusi diatomite mine but toward the top, the lake level fluctuates and mixed sediments are deposited. To the north section 14 shows less drastic fluctuations, tectonic adjustment and stream incision while to the south, a playa environment marked by desiccation developed. The water continues to deepen towards was intermittently marked by erosional disconformity.

The lakes made a substantial transgression and horizontally bedded diatomaceous silts are deposited. The continuing salinity of the lakes is indicated by the calcite and some authigenic feldspar in the silts. Volcanic activity is still important as evidenced by the presence of sanidine in the clay. Finally upon retreat of the lake, a rather coarse tuffs were

deposited, probably with some degree of transport and these tuffs today overlie older sediments. The Lake margins constantly fluctuated, except possibly during the intermittent deposition of the intercalated clays. In the entire basins the volcanic activity continued unabated throughout the sequence, this volcanic activity certainly had an effect on the alkalinity of the lakes, the extent of calcite formation in the sediments, and hence substantial influence in the groundwater chemistry, even though Lakes Kariandusi on the one hand and the present Naivasha were possibly much less saline. The existing radio-carbon dates of the lacustrine deposits (Chapter 2) are inconclusive. However in general, they suggest that most of the rift sediments are less than 700, 000 years old. The lower boundary of the Kariandusi sequence may correspond to this age. The evidently later basalt on the southern part of Lake Naivasha are dated c 400, 000 years old. It is beyond the scope this work to narrow down these dates, but perhaps better faunal correlation, detail palaeomagnetic and radiometric data will offer an alternative cross-check. In general the sediments are of Middle Pleistocene, with the top of the sequence probably less than 400,000 years old.

8.4 Conclusions.

The present investigation reaffirms and shows that in basin lithostratigraphic analysis, descriptive statistics and factorial analysis applied to numerous samples and a large pool of sedimentological data serve to distinguish the various sedimentary formations (lithofacies) in the Central Rift Valley. The approach is particularly valuable for it indicates that the recognition and discrimination of some of these facies for late Pleistocene to Holocene age can be realised. Moreover since the quantitative approach serves to better define facies, the method then also opens the door for more reliable correlations of surface sections. The author anticipates that the approach used in the current investigation will provide an application tool in basin analysis and contribute to future successful lithostratigraphic studies and paleoenvironmental understanding of sections in other parts of the Rift Valley. A detailed sampling survey of superficial deposits collected from different major modern lake environments is clearly needed. Analysis of sedimentary textures and compositions obtained from the subsurface and near surface cores would most likely allow for palaeoenvironmental interpretation and predictions of future environmental changes. In conclusion the present thesis can be viewed as case history in stratigraphic development of rift sedimentary basins. Several sections are included to make the main points understandable. The sections are a discussion

of principles and methods of environmental interpretation and a summary of the lithostratigraphic correlation.

The Kenya Rift lake sediments are potential field archive for the understanding of the palaeoenvironment, palaeoclimatic changes, structure developments and Quaternary geology of East Africa. It is the author's hope that the results of facies analysis and sediment correlation in the Nakuru, Elmenteita and Naivasha basins will provide primary data and framework for future environmental investigations of other rift related basins. The results in this study indicate that alluvial, fluvial, eolian and lacustrine palaeoenvironmental conditions existed during the deposition of Ronda, Enderit and Kariandusi, Soysambu Formations in the Nakuru, Naivasha and Elmenteita Basins.

REFERENCES

- Allen, G. P., Castaing, P. C. and Klingebiel, A. 1971. Preliminary investigation of the surfacial sediments in the Cap-Breton Canyon (South France) and the surrounding continental shelf. *Mar. Geol.* 10, M27-M32.
- Allen, G. P., Castaing, P. C. and Klingebiel, A. 1972. Distinction of Elementary sand populations in the Gironde estuary (France) by R-mode factor analysis of grain-size data. *Sedimentology* 19, 21-35.
- Anwar, Y. M., El Askary, M. A. and Frihy, O. E. 1984. Reconstruction of sedimentary environments of Rosetta and Damietta promontories in Egypt based on textural analysis. *Jour. Afr. Earth Sci.* 2, 17-29.
- Baker, B. H. 1970. The structural pattern of the Afro-Arabian rift system in relation to plate tectonics: Royal Soc. London *Philos. Trans.*, Ser. A, v. 267, p. 383-391.
- Baker B. H. 1986. Tectonic and volcanism of the southern Kenya Rift valley and its influence on rift sedimentation. In *Sedimentation in the African Rifts*. Geological Society Special Publication No. 25, pp. 75-84. Eds. Frostick L.E et al.

Baker, B. H., Crossley, R. and Goles, G. G. 1978. Tectonic and magmatic evolution of the southern part of the Kenya rift valley. In: Neumann, E. R. and Ramberg, I. B. (eds) *Petrology and Geochemistry of Continental Rifts*. D. Reidel Publishing Co., Holland, p. 29-50.

Baker, B. H. and Mitchell, J. G. 1976. The Volcanic stratigraphy and geochronology of the Kedong -Olorgesailie area and the evolution of the southern Kenya rift valley, *Jour. Geol. Soc. London*, v. 132, p. 467-484.

Baker, B. H. and Mohr, P. A., and Williams, L. A. J. 1972. Geology of the eastern rift system of Africa, *Geol. Soc. Am. Spec. Paper* 136, 67 p.

Baker, B. H. and Wohlenberg, J. 1971. Structure and the evolution of the Kenya rift valley, *Nature*, v. 229, p. 538-542.

Beal, A. O. 1970. Textural differentiation within the fine sand grade. *Jour. Geol.* 30, M1-M7.

Bellieni, G., Justin Vincentin, E., Zanettin, B., Picirillo, E.M. 1981. Oligocene transitional tholeiitic magmatism in northern Turkana (Kenya): comparison with coeval Ethiopian volcanism. *Bull. Volc.* 44, 411-427.

- Bhatia, M. R. 1983. Plate tectonics and geochemical composition of sandstones, *Jour. Geol.*, v. 91, p. 611-627.
- Burggraf, D. R., Jr., and Vondra, C. F. 1982. Rift valley facies and palaeoenvironments: An example from the East African Rift System of Kenya and southern Ethiopia. *Zeitschrift für Geomorphologie* 42: 43-73.
- Cooke, H.B.S. 1957. Observations relating to Quaternary Environments in East and Southern Africa. Annex Vol. LXXI., *Proc. Geol. Soc., South Africa.*
- Crook, K. A. 1974. Lithogenesis and geotectonics: the significance of compositional variation in flysch arenite (graywackes), in Dott, Jr., R. H. and Shaver, R. H., eds., *Modern and ancient Geosynclinal Sedimentation*, Soc. Econ. Paleontologists Mineralogists Spec. Paper No. 19, p. 304-310.
- Crossley, R. 1980. Structure and volcanism in the S. Kenya rift. In: *Geodynamic Evolution of the Afro-Arabic Rift System*. Acad. Nazionale dei Lincei, Rome, p. 89-98.
- Crossley, R. and Knight R.M. 1981. Volcanism in the western part of the Rift Valley in southern Kenya. *Bull. Volc.* 44, 117-128.
- Dal Cin, R. 1976. The use of factor analysis in determining beach erosion and accretion from grain-size data. *Mar. Geol.* 20,

95-116.

- Davis, J. C. 1986. *Statistics and Data Analysis in Geology*, (end.) John Wiley, New York.
- DeCelles P.G., M.B.Gray, K.D. Ridgway, R.B. Cole, D. A. Pivnik, N. Pequera and P.Srivastava, 1991. Controls on synorogenic alluvial fan architecture, Beartooth conglomerate (Palaeocene) Wyoming and Montana. *Sedimentology* 1991, 38, No.4, 567-590.
- Dickinson, W. R., and Suczek, C. A. 1979. Plate tectonics and sandstone compositions, *Am. Assoc. Petroleum Geologists Bull.* v. 63, p. 2164-2182.
- Dott, R. H., Jr. 1964. Wacke, graywacke and matrix - what approach to immature sandstone classification?: *Jour. Sed. Petrology*, v. 34, p.625-632.
- Drapeau, G. 1973. Factor analysis: how it copes with complex geological problems. *Math. Geol.* 5, 351-363.
- Eugster, H. P. 1967. Hydrous sodium silicates from Lake Magadi Kenya, precursors of bedded chert. *Science* 157, 1177-80.
- Eugster, H. P. 1969. Inorganic bedded cherts from the Magadi area, Kenya. *Contrib. Mineral. Petrol.* 22, 1-31.
- Eugster, H.P. 1970. Chemistry and origin of the brines of Lake Magadi, Kenya. *Spec. Paper Mineral Soc. Am.* 3, 215-35.

- Eugster, H. P. and Jones, B. F. 1968. Gels composed of sodium aluminium silicate, Lake Magadi, Kenya. *Science* 161, 160-164.
- Fairhead, J. D. and Girdler, R. W. 1972. The seismicity of the East Africa rift system. *Tectonophysics*, Vol. 15, p. 115-122.
- Fairhead, J. D., Mitchell, J. G. and Williams, L. A. J. 1972. New K/Ar determinations on rift volcanicity of S. Kenya and their faulting. *Nature* 238, 66-69.
- Findlater, I. C. 1978. Isochronous surfaces within the Plio-Pleistocene sediments east of Lake Turkana. In: Bishop, W. W. (ed.) *Geological Background to fossil man*. Scottish Academic Press, Edinburgh, p. 415-420.
- Fitch, F.J., Hooker, P.J., and Miller, J. A. 1976. $^{40}\text{Ar}/^{39}\text{Ar}$ dating of KBS Tuff in the Koobi Fora Formation, East Rudolf, Kenya. *Nature*, Vol. 263, p. 740-744.
- Fitch, F. J., and Miller, J. A. 1976. Conventional potassium-argon and argon-40/argon-39 dating of volcanic rocks from East Rudolf; In Coppens, Y., Howell, F. C., Isaac, G. L., and Leakey, R. E. F., eds., *Earliest man and environments in the Lake Rudolf Basin*. University of Chicago Press, Chicago, p. 123-147.

- Flint, R.F. 1959. On the Basis of Pleistocene Correlation in East Africa. *Geol. Mag.* Vol. XCVI, p. 265-284.
- Folk, R. L. 1968. *Petrology of Sedimentary Rocks*. Hemphills, Texas.
- Folk, R. L. and Ward, W. C. 1957. A study in the significance of grain size parameters, *Jour. Sed. Petrology*, v. 27, p. 3-26.
- Friedman, G. M. 1958. Determination of sieve-size distribution from thin section data for sedimentary petrological studies. *Journ. Geol.* 66, 394-416.
- Gardener, J. V., Dean, W. E. and Vallier, T. L. 1980. Sedimentology and geochemistry of surface sediments, outer continental shelf, South Bering Sea. *Mar. Geol.* 35, 299-329.
- Garrels, R. M. and Mackenzie, F. T. 1971. *Evolution of Sedimentary Rocks*: New York, W. W. Norton, 397 p.
- Gregory, J. W. 1896. *The Great Rift Valley*. London.
- Gregory, J. W. 1900. Contributions to the Geology of British East Africa. *Quart. Journ. Geol. Soc.*, Vol. LVI, pp. 205-222.
- Gregory, J. W. 1921. *The Rift Valleys and Geology of East Africa*. London.
- Harbaugh, J. W. and Merriam, D. F. 1968. *Computer applications in Stratigraphic analysis*. John Wiley, New York.

- Herron, M. M. 1987. Future applications of elemental concentrations from geophysical logging: Nuclear Geophysics, v. 1, p. 197-211.
- Imbrie, J. and Van Andel, T. H. 1964. Vector analysis of heavy-mineral data. Geol. Soc. Am. Bull. 75, 1131-1156.
- Jones, W. B. and Lippard, S.J. 1979. New age determinations and the geology of Kenya rift-Kavirondo rift junction, W. Kenya. Jour. Geol. Soc. 136, 693-704.
- King, B. C. 1978. Structural and Volcanic evolution of the Gregory Rift Valley. In: Bishop W. W. (ed) Geological Background to Fossil Man. Scottish Academic Press, Edinburgh, p. 29-54.
- King, B. C. and Chapman, G. R. 1972. Volcanism of the Kenya rift valley. Phil. Trans. R. Soc. London 271A, 185-208.
- King, B. C. and Williams, L.A.J. 1976. The East African Rift System. In: Drake, C. L. (ed) Geodynamics: Progress and Prospects. American Geophysical Union, Washington, p. 63-74.
- Klovan, J.E. 1966. The use of factor analysis in determining depositional environments from grain-size distributions. Jour. Sed. Petrol. 36, 115-125.

- Klovan, J.E. 1975. R- and Q-mode factor analysis. Concepts in Geostatistics, McCammon, R. B. (ed.), p. 21-69. Springer, New York.
- Kottlowski, F.E. 1965. Measuring stratigraphic sections: Holt, Rinehart and Winston, New York, p. 1-253.
- Leakey, L.S.B. 1931. The stone age cultures in Kenya Colony, Cambridge.
- Leakey, L.S.B. 1936. Stone Age Africa, Oxford and London.
- Leakey, L.S.B. 1950. The Lower limit of the Pleistocene in Africa. Proc. Int. Geol. Congress XVIII, Session, London.
- Mboya, B. 1983. The genesis and tectonics of the N. E. Nyanza rift valley, Kenya. Journ. Afr. Earth Sci. Vol. 1, No. 314, p. 315-320.
- McCall, G. J. H. 1957. Menengai Caldera Kenya Colony, Proc. Section I, XXth Inter. Geol.
- McCall, G. J. H. 1967. Geology of the Nakuru - Thomson's Falls Lake Hannington Area. Geol. Survey of Kenya, Report No. 78.
- McCall, G. J. H., B. H. Baker, and J. Walsh, 1965. Late Tertiary and Quarternary sediments of Kenya Rift Valley. Paper Read at Symposium No. 29, Wenner-Gren Foundation for Anthropological Research, Vienna.

- McConnell, R. B. 1972. Geological development of the rift system of eastern Africa, *Geol. Soc. Amer. Bull.*, Vol. 83, p. 2549-2572.
- McKenzie, D. P., Davies, D. and Molnar, P. 1970. Plate tectonics of the Red Sea and East Africa: *Nature*, Vol. 226, p. 243-248.
- Miall, A. D. 1978. Lithofacies types and vertical profile models in braided river deposits: A summary in Miall, A.D., ed., *Fluvial sedimentology*: Canada Society of Petroleum Geologists Memoir 5, p. 597-604.
- Miall, A. D. 1986. *Principles of Sedimentary Basin Analysis*, Springer-Verlag, p. 490.
- Miesch, A. T. 1980. Scaling variables and interpretation of eigenvalues in principal component analysis of Geological data. *Math. Geol.* 3, 12, 523-538.
- Middleton, G. V. 1960. Chemical composition of sandstones: *Geol. Soc. America Bull.*, v. 71, p. 1011-1026.
- Nilsson, E. 1929. Preliminary Report on the Quarternary Geology of Mount Elgon and some parts of the Rift Valley. *Geol. Foren. Forhandl.*, Vol. 51, pp. 253-261.

- John, F. J. 1975. Sedimentary Basins. Harper and Row.
- Nilsson, E. 1935. Traces of Ancient changes of Climate in East Africa. *Sartryck un Geografiska Annaler*, Stockholm, pp. 1-21.
- John, F. J., Foster, F. A., and Piper, B. 1972. *Sand and Siltstone*. New York, Springer-Verlag, 416 p.
- Nilsson, E. 1940. Ancient Changes of Climate in British East Africa and Abyssinia. *Artryck Geografiska Analer*, Stockholm, pp. 1-79.
- Nyambok, I. O. 1985. Evolution of the East African Rift System with special emphasis on the central rift of Kenya, a new model. *Kenya Journal of Science and Technology Series A*, 1985, Vol. 6, no. 2, p. 83-90.
- Papezik, V. S. 1965. Geochemistry of some Canadian anorthosites: *Geochim. Cosmochim. Acta*, v. 29, p. 673-709.
- Pettijohn, F. J. 1943. Archean sedimentation: *Geol. Soc. America Bull.*, v. 54, p. 925-972.
- Pettijohn, F. J. 1963. Chemical composition of sandstones excluding carbonate and volcanic sands, in *Data of Geochemistry* (6th ed.): U.S. Geol. Surv. Prof. Paper 440-S, 9 P.
- F. L. 1975. Framework geology and chemical composition of continental margin - type sandstones. *Geology*, 3:27-30.

- Pettijohn, F. J. 1975. Sedimentary Rocks. Harper and Row, New York, 718 p.
- Pettijohn, F.J., Potter, P. E., and Siever, R. 1972. Sand and Sandstone. New York, Springer-Verlag, 618 p.
- Reading, H. G. 1978. Facies. p. 4 - 14. In H. G. Reading (ed.) Sedimentary environments and facies. Elsevier, New York. Vol. 92 p. 205-226.
- Reineck H.E. and Singh, I.B. 1986. Depositional sedimentary environments. With reference to Terrigenous Clastics. 2nd ed. Springer-Verlag. p. 1-416. Geology, v. 14, p. 209-201. Geologisches Institut, Universität Karlsruhe, Federal Republic of Germany.
- Roser, B. P., and Korsch, R. J. 1986. Determination of tectonic setting of sandstone -mudstone suites using SiO₂ content and K₂O/Na₂O ratio: Jour. Geology, v. 5 p.635-650. Geol. Surv. Canada, Paper 85, 80 p.
- Rust, B. R. 1972. Pebble orientation in fluvial sediments: Journal of Sedimentary Petrology , Vol.42, p. 384-388.
- Saggerson, E. P. and Baker, B. H. 1965. Post-Jurassic erosion surfaces in eastern Kenya and their deformation in relation to rift structure. Jour. Geol. Soc. 121, 51-72.
- Schwab, F. L. 1975. Framework mineralogy and chemical composition of continental margin - type sandstones. Geology, v. 3, p. 487-490.

- Selley, R. C.** 1982. An Introduction to Sedimentology : New York, Academic Press, 417 p.
- Shakleton, R.M.** 1955. Pleistocene Movements in the Gregory Rift Valley. Geol. Runds. Bd. 43, Heft 1, p. 257-263.
- Smith, N. D.** 1974. Sedimentology and bar formation in the Upper Kicking Horse River, a braided outwash stream. Jour. Geol., Vol. 82 p. 205-223.
- Strecker, M.R., Blisniuk, P.M., Eisbacher, G.H.** 1990. Rotation of extension direction in the central Kenya Rift. Geology, v. 18 p. 299-302. Geologisches Institut, University Karlsruhe. Federal Republic of Germany.
- Thompson, A. O. and Dodson, R. G.** 1963. Geology of the Naivasha area. Rep. Geol.Surv. Kenya 55, 80 p.
- Thomson, J.** 1885. Through Masai Land. London.
- Washbourn - Kamau, C. K.** 1971. Late Quaternary Lakes in the Nakuru - Elmenteita basins, Kenya. Geographical Journal, 137 p. 522-533.
- Weaver, C. E., and Pollard, L. D.,** 1973. The Chemistry of Clay Minerals. Amsterdam, Elsevier, 213 p.

Wentworth, C. K. 1922. A scale of grade and class terms of clastic sediments. Jour. Geol. 30, 377-392.

Williams, L.A.J. 1970. The Volcanics of the Gregory Rift Valley, East Africa. Bull. Volc. 34, 439-65.

Williams, L.A.J. 1978. The Volcanological development of the Kenya Rift. In: Neumann, E. R. and Ramberg, I. B. (eds) Petrology and Geochemistry of Continental Rifts. D. Reidel Publishing Co., Holland, p. 101-121.

Williams, L.A.J. and MacDonald, R. and Leat, P. T. 1983. Magmatic and structural evolution of the central part of the Kenya Rift. In: Proceedings of the Regional Seminar and Geothermal Energy in Eastern and Southern Africa. UNESCO-USAID, p.61-7.